

DATING OF ALTERATION AT THE RADOMIRO TOMIC PORPHYRY COPPER
DEPOSIT, NORTHERN CHILE BY THE HIGH PRECISION $^{40}\text{Ar}/^{39}\text{Ar}$ METHOD.

Gregory Blaine Pemberton

Submitted in Partial Fulfilment of the Requirements
for the Degree of Bachelor of Science, Honours
Department of Earth Sciences
Dalhousie University, Halifax, Nova Scotia
April 1997

Distribution License

DalSpace requires agreement to this non-exclusive distribution license before your item can appear on DalSpace.

NON-EXCLUSIVE DISTRIBUTION LICENSE

You (the author(s) or copyright owner) grant to Dalhousie University the non-exclusive right to reproduce and distribute your submission worldwide in any medium.

You agree that Dalhousie University may, without changing the content, reformat the submission for the purpose of preservation.

You also agree that Dalhousie University may keep more than one copy of this submission for purposes of security, back-up and preservation.

You agree that the submission is your original work, and that you have the right to grant the rights contained in this license. You also agree that your submission does not, to the best of your knowledge, infringe upon anyone's copyright.

If the submission contains material for which you do not hold copyright, you agree that you have obtained the unrestricted permission of the copyright owner to grant Dalhousie University the rights required by this license, and that such third-party owned material is clearly identified and acknowledged within the text or content of the submission.

If the submission is based upon work that has been sponsored or supported by an agency or organization other than Dalhousie University, you assert that you have fulfilled any right of review or other obligations required by such contract or agreement.

Dalhousie University will clearly identify your name(s) as the author(s) or owner(s) of the submission, and will not make any alteration to the content of the files that you have submitted.

If you have questions regarding this license please contact the repository manager at dalspace@dal.ca.

Grant the distribution license by signing and dating below.

Name of signatory

Date



Dalhousie University

Department of Earth Sciences

Halifax, Nova Scotia

Canada B3H 3J5

(902) 494-2358

FAX (902) 494-6889

DATE April 15, 1997

AUTHOR Gregory Blaine Pemberton

TITLE DATING OF ALTERATION AT THE RADOMIRO TOMIC PORPHYRY COPPER
DEPOSIT, NORTHERN CHILE BY THE HIGH PRECISION $^{40}\text{Ar}/^{39}\text{Ar}$ METHOD.

Degree BSc Convocation May Year 1997

Permission is herewith granted to Dalhousie University to circulate and to have copied for non-commercial purposes, at its discretion, the above title upon the request of individuals or institutions.

THE AUTHOR RESERVES OTHER PUBLICATION RIGHTS, AND NEITHER THE THESIS NOR EXTENSIVE EXTRACTS FROM IT MAY BE PRINTED OR OTHERWISE REPRODUCED WITHOUT THE AUTHOR'S WRITTEN PERMISSION.

THE AUTHOR ATTESTS THAT PERMISSION HAS BEEN OBTAINED FOR THE USE OF ANY COPYRIGHTED MATERIAL APPEARING IN THIS THESIS (OTHER THAN BRIEF EXCERPTS REQUIRING ONLY PROPER ACKNOWLEDGEMENT IN SCHOLARLY WRITING) AND THAT ALL SUCH USE IS CLEARLY ACKNOWLEDGED.

i

Dating of Alteration at the Radomiro Tomic Porphyry Copper Deposit, Northern Chile by the High Precision $^{40}\text{Ar}/^{39}\text{Ar}$ Method.

Pemberton, Greg

Department of Earth Sciences, Dalhousie University, Halifax, Nova Scotia B3H 3J5, Canada

The Radomiro Tomic (RT) porphyry copper deposit is located approximately 8-10km north of the Chuquicamata mine and 245km northeast of the port city of Antofagasta. Estimates place the deposit at over 800 million tonnes of ore with an average grade of 0.59% Cu (mostly supergene ore) and a mine life of 22 years. RT does not outcrop as the entire deposit is buried beneath Miocene piedmont gravels up to 200m in thickness and has been known only from drillcore and limited underground workings. Stripping is now underway and the mine is due to start operating in 1997 as a new separate division of CODELCO, the Chilean national copper mining company.

The deposit is hosted within an intrusive body of quartz monzodiorite composition that is approximately lower to middle Oligocene in age and was emplaced within the regional N-S trending Domeyko Fault system. This system is spatially associated with all the major porphyry deposits in northern Chile.

High precision, stepwise degassing $^{40}\text{Ar}/^{39}\text{Ar}$ dating was conducted at Dalhousie University to determine the ages of the potassic, argillic and quartz-sericite alteration assemblages at Radomiro Tomic. K-feldspar, biotite and sericite grains were hand picked from six drillcore samples representing the three hydrothermal alteration zones. Results are suggestive of potassic and argillic alteration assemblages having an average age of $32.6 \pm 0.3\text{Ma}$ as part of an initial hydrothermal event. As well, a younger hydrothermal event was dated to $31.8 \pm 0.3\text{Ma}$ from quartz-sericitic alteration minerals. Age differences among the potassic and argillic alteration minerals (K-feldspar and biotite) having high or low closure temperatures are not detectable, are indicative of rapid cooling following emplacement of the host porphyry. ^{39}Ar degassing plateau patterns combined with X-ray diffraction analyses on the K-feldspar samples also support the scenario of a rapid decrease in temperature to less than 150°C in the order of hundreds of thousands of years, rather than millions, following each hydrothermal event.

A full suite of ancillary data was generated on the dated samples establishing the close similarity of the petrology, mineralogy and chemistry to samples of similar alteration types from Chuquicamata.

Key Words and Phrases: Radomiro Tomic, porphyry copper deposit, Chile, argon dating, geochronology, hydrothermal, alteration, potassic, argillic, quartz-sericitic, Chuquicamata

Table of Contents

| | | |
|------------|--|----|
| | Abstract | i |
| | Table of Contents | ii |
| | List of Figures | iv |
| | List of Tables | v |
| | Acknowledgements | vi |
| | | |
| Chapter 1. | Introduction | 1 |
| | 1.1 General Statement | 1 |
| | 1.2 Project Scope | 1 |
| | 1.3 Regional History | 3 |
| | 1.4 Mining statistics and methods | 5 |
| | 1.5 Geologic setting | 7 |
| | 1.6 Porphyry copper deposit models | 9 |
| | 1.7 Proposals for the genesis of Radomiro Tomic | 11 |
| | | |
| Chapter 2. | Whole-Rock Samples and Methods | 15 |
| | 2.1 Introduction | 15 |
| | 2.2 Sample descriptions | 19 |
| | 2.3 Whole-rock chemistry | 26 |
| | 2.3.1 Introduction | 26 |
| | 2.3.2 Methods | 27 |
| | 2.3.2.1 XRF Whole-rock analysis | 27 |
| | 2.3.2.2 Atomic absorption spectrometry | 28 |
| | 2.3.2.3 Titration analysis and measurement of H ₂ O content | 28 |
| | 2.3.2.4 Trace level rare earth analysis | 29 |
| | 2.3.3 Discussion and interpretation | 29 |
| | 2.3.3.1 Rock type | 30 |
| | 2.3.3.2 Tectonic setting | 32 |
| | 2.3.3.3 Alteration effects | 32 |
| | 2.3.3.4 Rare earth elements | 37 |
| | 2.3.4 Productive vs unproductive porphyry copper deposits | 37 |
| | 2.3.5 Conclusions | 39 |
| | | |
| Chapter 3. | Dated Minerals and Methods | 42 |
| | 3.1 Introduction | 42 |
| | 3.2 Mineral separation | 42 |
| | 3.3 Supporting X-ray diffraction analysis | 43 |
| | 3.4 XRD results on dated minerals | 44 |
| | 3.5 Perthitic textures, K-feldspar origin and the validity of using K-feldspar for ⁴⁰ Ar/ ³⁹ Ar dating | 53 |
| | 3.6 Triclinicity tests and cooling rates of potassium feldspars | 55 |
| | 3.7 Electron microprobe methods | 56 |
| | 3.8 Electron microprobe results | 58 |

Table of Contents

| | | |
|-------------------|--|------------|
| Chapter 4. | 40Ar/39Ar Dating | 70 |
| 4.1 | Argon dating theory | 70 |
| 4.2 | 40Ar/39Ar theory | 73 |
| 4.2.1 | Potassium feldspar results | 74 |
| 4.2.2 | Biotite results | 78 |
| 4.2.3 | Sericite results | 81 |
| 4.3 | Mineral pairs from DDH3439 samples | 82 |
| Chapter 5. | Conclusions and Future Work | 91 |
| 5.1 | Conclusions from whole-rock chemistry and mineralogy | 91 |
| 5.2 | 40Ar/39Ar dating | 92 |
| 5.3 | Evidence for two sericite types | 95 |
| 5.4 | Proposed genesis | 97 |
| 5.5 | Future work | 99 |
| References | | 100 |
| Appendices | | |
| A | Whole-rock geochemical data | A1 |
| B | XRD powder diffractograms and peak lists | B1 |
| C | Electron microprobe data | C1 |
| D | Argon plateaus and datasheets | D1 |

List of Figures

| Table # | Figure Name | Page |
|-------------------|---|-------|
| Figure 1.1 | Location map of northern Chile | 2 |
| Figure 1.2a-b | Panoramas of the RT and Chuquicamata deposits | 4 |
| Figure 1.3 | Summary of geologic evolution of the Antofogasta region | 8 |
| Figure 1.4 | Onion-skin' porphyry copper deposit model | 12 |
| Figure 1.5 | Vertical zonation in a porphyry copper deposit | 13 |
| Figure 2.1 | Planview of Radomiro Tomic deposit | 16 |
| Figure 2.2 | 10750N cross-section | 17 |
| Figure 2.3 | 9500N cross-section | 18 |
| Figure 2.4a-b | Photographs of Cu-1001 and Cu-999 | 21 |
| Figure 2.5a-b | Photographs of Cu-1002 and Cu-1011 | 23 |
| Figure 2.6a-b | Photographs of Cu-1010 and Cu-1006 | 25 |
| Figure 2.7 | Zr/TiO ₂ vs Nb/Y discrimination diagram | 31 |
| Figure 2.8 | Na ₂ O+K ₂ O vs SiO ₂ discrimination diagram | 33 |
| Figure 2.9 | Tectonic setting 1 (spider diagram) | 34 |
| Figure 2.10 | Tectonic setting 2 (Rb vs Y+Nb) | 35 |
| Figure 2.11 | Na ₂ O v K ₂ O discrimination diagram | 36 |
| Figure 2.12 | Rare earth element diagram | 38 |
| Figure 2.13 | Productive vs unproductive intrusions | 40 |
| Figure 3.1a-b | XRD analysis of Cu-999K | 44 |
| Figure 3.2a-b | XRD analysis of Cu-999Bi | 46 |
| Figure 3.3a-c | XRD analysis of Cu-1001K and Cu-1001Bi | 47 |
| Figure 3.4a-c | XRD analysis of Cu-1002K and Cu-1002Bi | 49 |
| Figure 3.5a-b | XRD analysis of Cu-1006K | 51 |
| Figure 3.6a-b | XRD analysis of Cu-1010K | 52 |
| Figure 3.7a-b | XRD analysis of Cu-1011 | 53 |
| Figure 3.8 | Perthitic texture | 54 |
| Figure 3.9 | Triclinicity tests | 57 |
| Figures 3.10-3.19 | Electron microprobe images and analyses | 60-69 |

List of Tables

| Table # | Name | Page |
|----------------|---|-------------|
| Table 1.1 | Mine statistics for Radomiro Tomic and Chuquicamata | 5 |
| Table 2.1 | Sample location information | 19 |
| Table 2.2 | Samples used for comparison from Chuquicamata | 27 |
| Table 3.1a-c | Averaged electron microprobe data | 59 |
| Table 4.1 | Summary of $^{40}\text{Ar}/^{39}\text{Ar}$ dates for RT | 74 |

Acknowledgements

I would like to thank my supervisors, Milton Graves of Cuesta Research Ltd. and Dr. Marcos Zentilli for all of the help and encouragement that they provided throughout the duration of my project.

I am grateful to Patricio Cuadra, chief mine geologist for CODELCO, Division RT for advising on sample selection and providing access to company documentation. As well, my thanks go out to Dr. Peter Reynolds and Keith Taylor of the Argon Lab, Gordon Brown from the thin section lab and Bob Mackay at the microprobe lab for all of their assistance..

I often sought the advice and assistance of graduate students Lexie Arnott, Nick Wilson and Darryl Lindsay who were always more than willing to help out and I am indebted to them as well.

Finally, the person who deserves the bulk of my gratitude is my wife Carolyn, who for four long years has been my main source of inspiration.

Chapter 1

Introduction

1.1 General Statement

The Radomiro Tomic (RT) porphyry copper deposit is located in northern Chile approximately 8-10km north of the giant Chuquicamata deposit, and 250km northeast of the port city of Antofagasta (see Figure 1.1). Radomiro Tomic (known also as Chuqui Norte) is one of a series of porphyry copper deposits that make up a late Eocene-Oligocene (31-41Ma) metallogenic belt in the Andes mountain range parallel to the Pacific coast of Chile. The development of this metallogenic belt was the result of a non-collisional, subduction-related, volcanic and plutonic orogeny known as the Andean tectonic cycle (Camus, 1997 and MaksaeV, 1990).

1.2 Project Scope

The purpose of this project was to determine the age or ages of hydrothermal alteration and hypogene mineralization of the Radomiro Tomic porphyry copper deposit. Six drill core samples of different locations within the deposit were dated using $^{40}\text{Ar}/^{39}\text{Ar}$ stepwise degassing techniques. X-ray diffraction, electron microprobe, whole rock chemistry, transmitted and reflected light microscopy techniques were used to aid in the interpretation of the geochronological data generated from potassium bearing mineral separates. From similar work to the south at the Chuquicamata deposit, it has been shown

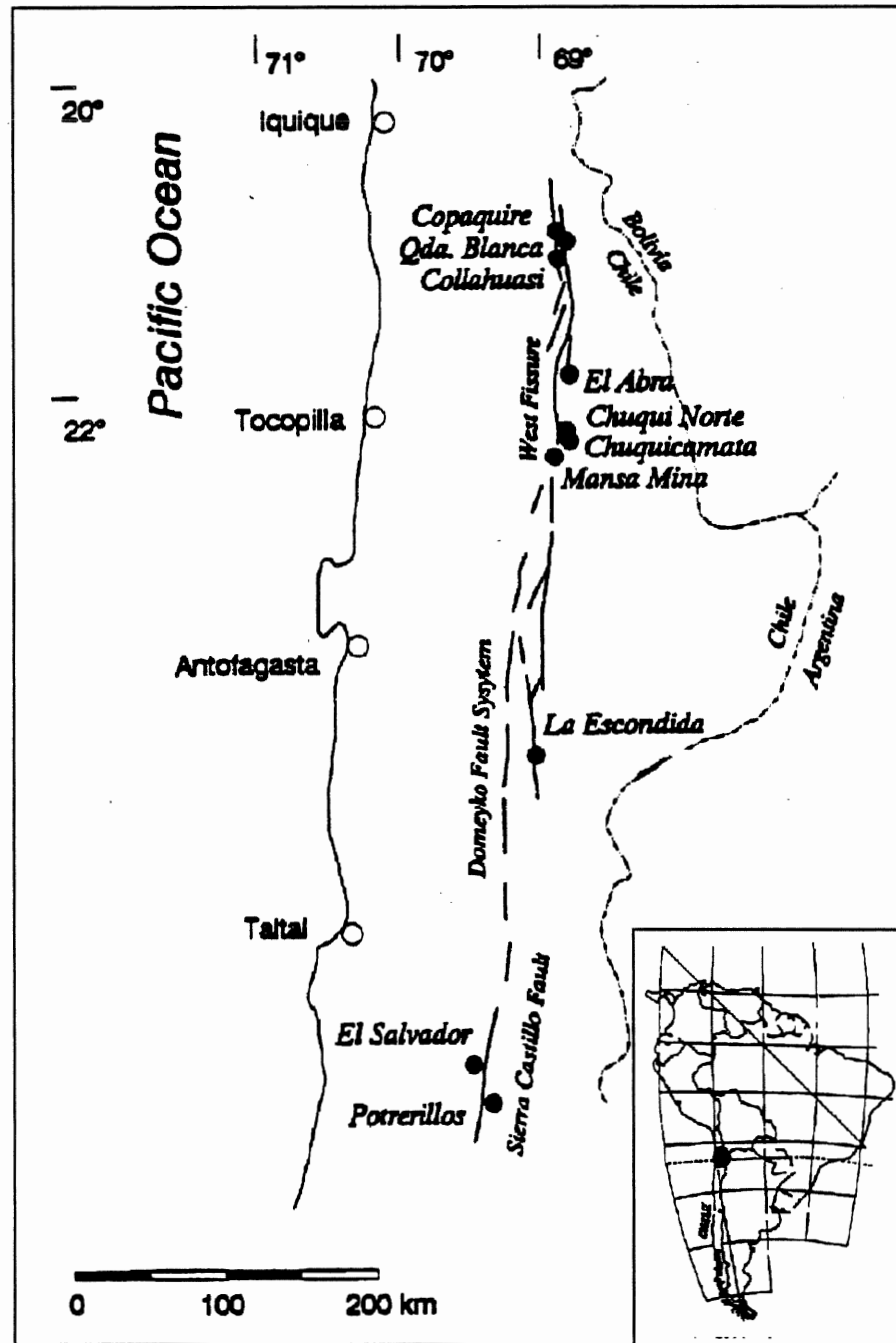


Figure 1.1 Map of northern Chile showing Radomiro Tomic (shown here as Chuqui Norte) and Chuquicamata. Note the N-S trending Domeyko regional fault system, the local expression of this system at RT is known as the West Fissure or Falla Oeste. The insert shows a map of South America with a black circle over northern Chile (after Maksaev, 1990).

that accurate dating methods should allow the isolation of discrete events in the history of the Radomiro Tomic deposit and the correlation of the timing of such events to regional stratigraphy.

The project also compared the $^{40}\text{Ar}/^{39}\text{Ar}$ dating and geochemistry results from the Radomiro Tomic samples to similar data from previous studies done at Chuquicamata (Reynolds et al., 1997). Four samples from Chuquicamata were chosen as representatives of alteration rock types closely corresponding to altered rock at Radomiro Tomic.

1.3 Regional History

The mining history of this area is centred around the Chuquicamata porphyry copper deposit. Radomiro Tomic is a blind deposit buried beneath more than 150m of gravel and was only discovered in the late 1970's (see Figure 1.2a). Native copper and turquoise had been extracted for ornamental use from surface deposits at Chuquicamata since about 2400 years ago by the Atacameño Indians (Peña and Lillo, 1927). Although mining developed rapidly after the arrival of the Spaniards, major exploitation of the Antofagasta region did not begin until the Chile Exploration Company consolidated the property at Chuquicamata in 1913. The Anaconda Copper Mining Company purchased the rights to Chuquicamata in 1923 and retained control for over fifty years (Zentilli et al, 1994). In 1971, large Chilean copper mines were nationalized and put under the control of the Corporacion del Cobre de Chile (CODELCO), the Chilean national copper mining company.

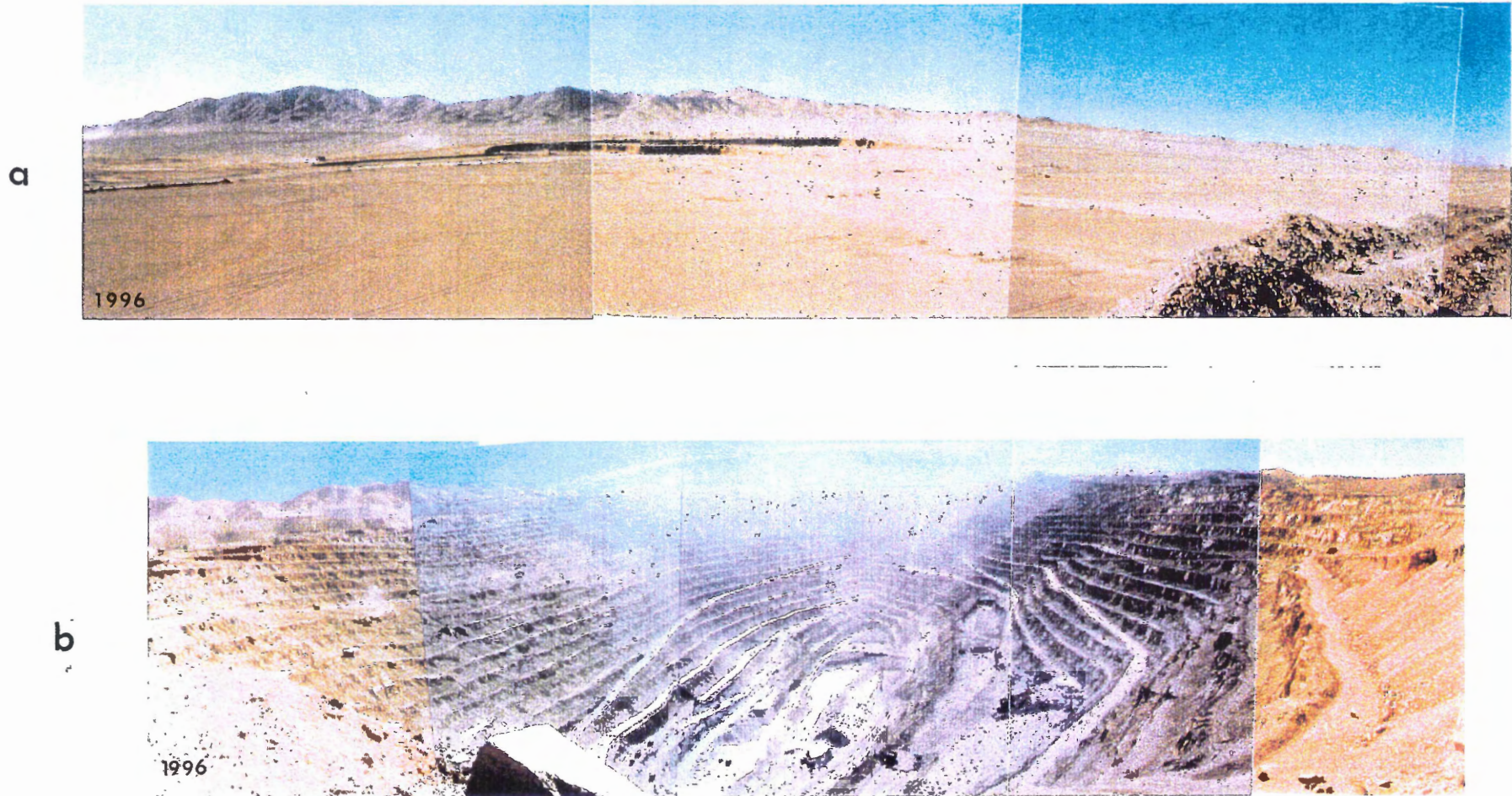


Figure 1.2 a) Panoramic photograph of the RT deposit looking due east at the Chuquicamata hills which represents Mesozoic basement rock. The Chuquicamata open pit is about 8-10km distant at the right (south) of the photograph. 20m high benches can be seen in centre of the photograph where excavation of the Miocene gravels has begun. b) The Chuquicamata open pit looking north toward RT from the south rim. Each bench is 20m in height and the pit is almost 1km deep.

Radomiro Tomic was discovered during the post-nationalization period by CODELCO geologists and has recently been made a fully separate division of CODELCO. Production is due to start in late 1997 or early 1998.

1.4 Mining Statistics and Methods

Chile hosts one of the largest concentrations of copper mineralization on earth accounting for more than 50% of all the copper metal known to date along the circum-Pacific rim basin. Estimates are stated for resources plus reserves of over 340 million tonnes of fine copper metal (Camus, 1997).

Throughout this report, the similarities between Radomiro Tomic and Chuquicamata will be emphasized. However, it is important to note that in terms of the scale of mineral resources, Chuquicamata is much larger.

Table 1.1 Mine Statistics for Radomiro Tomic and Chuquicamata (Cuadra, 1996)

| | <u>RT</u> | <u>Chuqui</u> |
|-------------------|------------------|----------------------|
| Production | est.>150,000tpy | 637,000tpy |
| Reserves | 800Mt | 3000Mt |
| Ore grade | 0.59 wgt% Cu | 0.89 wgt% Cu |

Types of Ore Copper oxides and halides, supergene and hypogene sulphides at both

As seen in Table 1.1, Chuquicamata has three times the probable yearly production of Radomiro Tomic and well over three times the ore reserves of RT. However, the estimates from Radomiro Tomic are constantly being revised upward as the startup date approaches and more detailed data from a more comprehensive drilling program become available. Reserves at Radomiro Tomic could approach 1000Mt. After the gravels capping the deposit are removed, a zone of oxidised ore approximately 200-300m thick will be encountered. The ore grade of this zone averages 1.0 weight percent copper in the form of copper halides, oxides, carbonates and sulphates. Common oxidised copper minerals include atacamite $[\text{CuCl}_2]$ and malachite $[\text{Cu}_2(\text{CO}_3)(\text{OH})_2]$. The cost per pound to produce copper from oxidized ore is less than for supergene sulphide ore which will be encountered when the oxidised zone is depleted. The supergene sulphide ore minerals include covellite $[\text{CuS}]$ and digenite $[\text{Cu}_{1.8}\text{S}]$. Beneath the supergene ore zone, hypogene ore minerals (bornite $[\text{Cu}_5\text{FeS}_4]$ and chalcopyrite $[\text{CuFeS}_2]$) are found.

Radomiro Tomic will be mined by open pit methods similar to those methods used at Chuquicamata (see Figure 1.2b). Mining of the oxidised ore zone will involve dissolution of the oxides, halides, sulphates and carbonates. The next step will include placing electrodes into the resulting solution and electrically plating the cathodes with extremely pure copper metal.

When the supergene ore zone is encountered, ore extraction will involve crushing the ore and using floatation cell techniques to generate copper concentrates. Floatation methods use detergents of compositions specifically designed to adhere to the surfaces of specific minerals. The finely crushed ore is mixed into vats containing the detergents

where mineral-rich grains will be caught in the froth floating on the top of the vat. The concentrated ore and froth is then removed. The purity of the copper concentrates using floatation techniques is not as high as with dissolution methods but subsequent refining and smelting of the copper sulphide minerals are used to further isolate copper metal.

1.5 Geologic Setting

Radomiro Tomic is located within the Domeyko Cordillera and is associated with a hypabyssal intrusive body of granodioritic to monzodioritic composition with hydrothermal alteration dated to Lower Oligocene. Emplacement of the porphyry system occurred near the end of a period of volcanic-plutonic activity known as the Incaic tectonic event (Late Eocene-Early Oligocene) (see Figure 1.3). The intrusion (Porfido Este) was emplaced in Paleozoic and Mesozoic basement rocks within a system of north-south trending regional transcurrent faults known collectively as the Domeyko Fault system. Falla Oeste (or the West Fissure) and Falla Mesabi are two major components of this system that bracket the Radomiro Tomic and Chuquicamata deposits. The Mesabi and Falla Oeste faults systems are likely to have localized intrusion and hydrothermal activity during Eocene-Oligocene time and likely focused volcanic activity and plutonism within the Domeyko Cordillera at transtensive fault jogs (Maksaev and Zentilli, 1988). The Mesozoic basement metasediments, and igneous rocks related to former stratovolcanoes were then eroded exposing the deeper sections of the porphyry which are characterized by

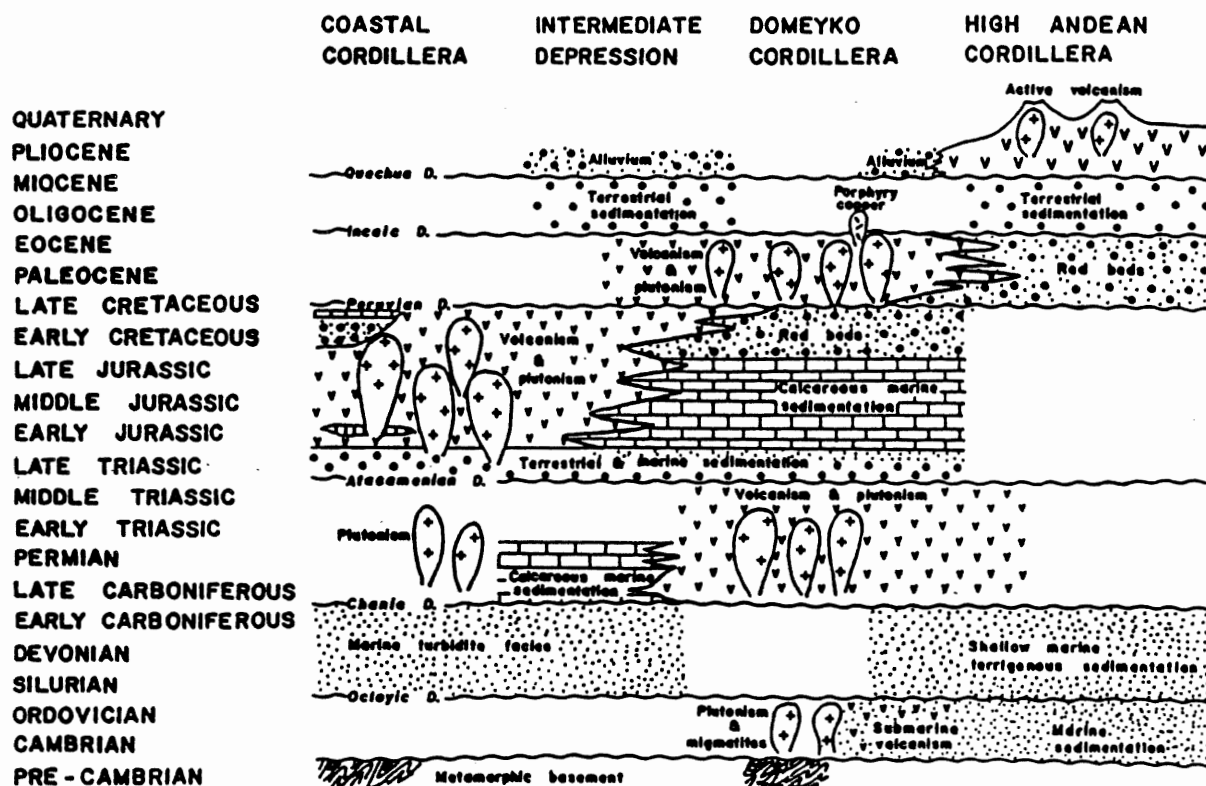


Figure 1.3 Diagram summarizing the general geologic evolution of the Antofagasta Region: western slope of the Central Andes (not to scale). Note the Incaic period of deformation related to the development of porphyry copper systems in the Oligocene (after Makshev, 1990).

potassic alteration (Maksaev, 1990).

Supergene oxidation and enrichment processes in northern Chile were active between about 34 and 14Ma (early Oligocene to middle Miocene; Berggren et al., 1985). Supergene processes consist of a downward vertical and lateral migration of copper in secondary solutions creating a secondary enrichment blanket with ore grades over two to three times the protore grade and also in extended stratabound exotic copper ore bodies (Camus, 1997). A period of hyperaridity set in at 14Ma preserving the supergene enriched blankets from erosion. The most likely cause of the onset of climatic desiccation was the evolution of the Altiplano-Puna plateau which created a rain-shadow effect (Alpers and Brimhall, 1988), a similar event to the evolution of the Tibetan Plateau (Ruddiman and Kutzbach, 1989).

The uppermost section of the deposit has been buried beneath pediment gravels since the mid to upper Miocene (Cuadra et al, 1994). This aggradation of gravel also helped in preserving the deposit.

1.6 Porphyry Copper Deposit Models

Porphyry deposits are large tonnage, low grade mineral deposits with metal assemblages that may include copper, molybdenum, gold and silver. It is generally accepted that many porphyry ore deposits consist of upright cylinders of coaxially distributed zones of alteration and mineralization centred on a felsic, porphyry stock

(Sillitoe, 1973). The origin of these deposits is related to the emplacement of intermediate to felsic porphyritic intrusions at hypabyssal depths (2-5km). These intrusions are most commonly found at current or paleo-convergent plate margins (Titley and Beane, 1981; Sawkins, 1990).

These shallowly emplaced plutons undergo hydraulic fracturing with the onset of cooling and crystallization. Anhydrous minerals generally form first from the melt and do not consume H₂O in the process, resulting in an increase in the water content of the residual melt until fluid pressure overcomes lithostatic pressure (Phillips, 1973). When fluid pressure exceeds lithostatic pressure and rock strength, fracturing and brecciation will occur. The fracturing of the rock allows the vapour and fluids to escape and also creates a zone of relatively high permeability within which a hydrothermal convection cell may form. With the fracturing of the rock, pressure decreases which reduces the solubility of the metals being transported by the vapour and fluids. Copper tends to be several hundred times more concentrated in the vapour phase of a magma than in the residual melt. As pressure decreases metals are precipitated as sulphides along the fractures and veinlets. It is in this manner that up to 60% of the mineralization in a porphyry deposit can be deposited in the characteristic veinlet network of the porphyry stock within a period of under 5,000 years (Sondergeld and Turcotte, 1979).

The energy driving the hydrothermal convection cell comes from the cooling pluton itself. The cooling of a pluton under conditions such as these is thought to be under 100,000 years (Roedder, 1976).

The combination of high permeability due to fracturing along with large amounts

of high- to moderate-temperature fluids circulating through the fractures is responsible for mineralization and alteration of the rock. Alteration is the process of chemical exchange between host rock and circulating fluids. Alteration terms and patterns used in this project are based on the 'onion-skin' model (see Figure 1.4) first developed by Lowell and Guilbert (1970). Potassic alteration occurs at the highest temperatures, 350-550°C, (Rose and Burt, 1979) generally, just below magmatic temperatures. This type of alteration occurs in conjunction with the initial hydraulic fracturing and the release of magmatic waters.

Although there is some controversy over the relationship between porphyry copper deposits and volcanism, several examples exist such as El Teniente, Los Bronces, Potrerillos, El Salvador, La Escondida and Collahuasi that show related volcanic features. Most other porphyry deposits that lack obvious volcanic features have been eroded more deeply, eliminating the link to any preserved surficial expression of the system (Alfaro, 1997). Sillitoe (1973) created a model for vertical zoning in a porphyry deposit which showed an 8km high system that included a pluton at the lowermost levels and a related comagmatic pile at the uppermost level (see Figure 1.5). This comagmatic pile is theorized to constitute a stratovolcano.

1.7 Proposals for the Genesis of Radomiro Tomic

Three basic hypotheses can be formed to explain the genesis of Radomiro Tomic

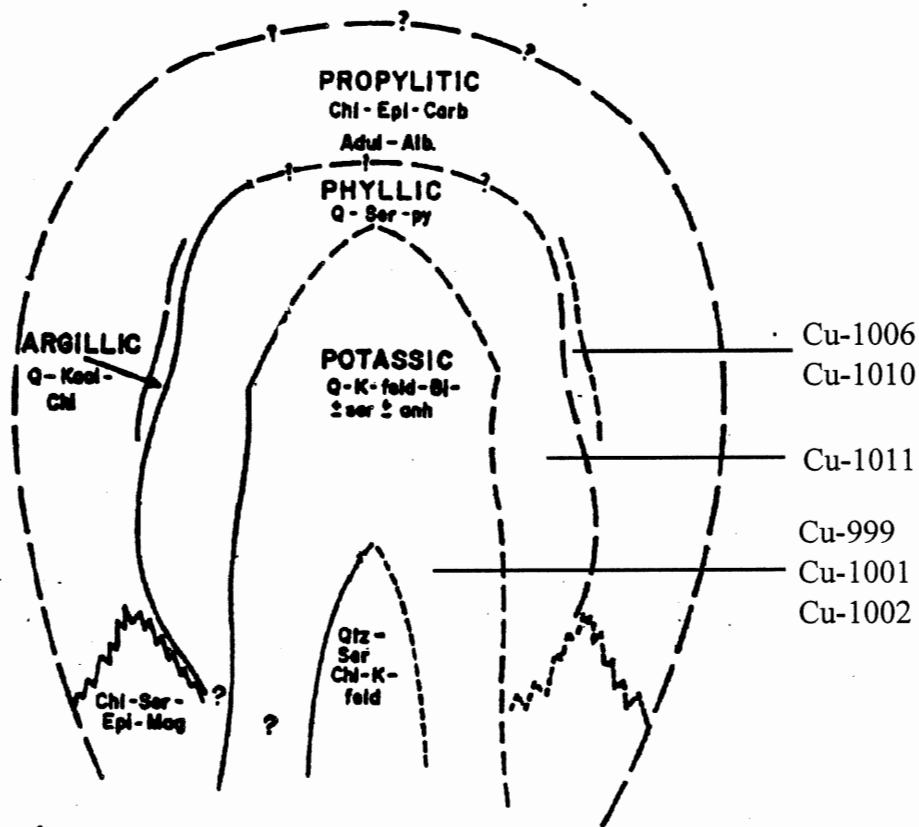


Figure 1.4 This is the 'onion skin' porphyry deposit model (after Lowell and Guilbert, 1970). The cross-section shows the likely positions within the model of the dated samples used in this project according to alteration assemblages. This model is based on the San Manuel - Kalamazoo deposit in Arizona.

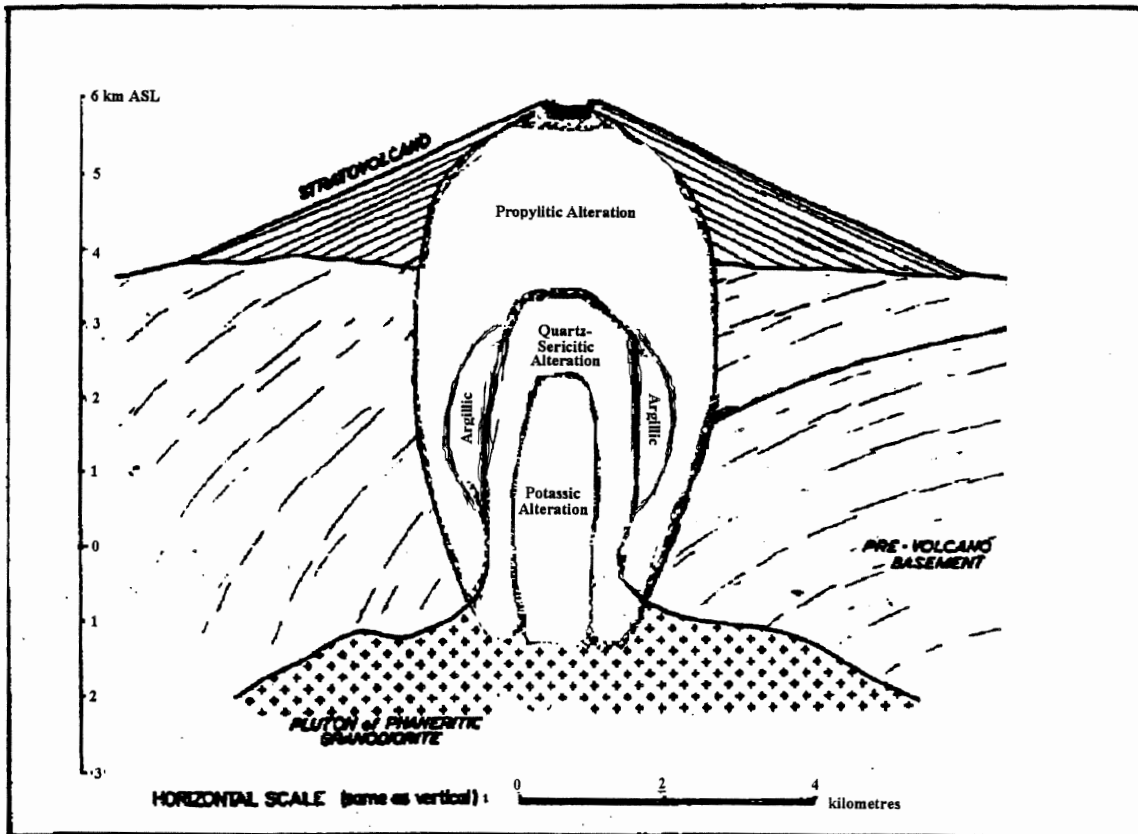


Figure 1.5 Model of a simple porphyry copper deposit (after Sillitoe, 1973) showing its sub-volcanic position intermediate to plutonic and volcanic environments. Alteration zoning is based on the Lowell and Guilbert model. Vertical and horizontal scales are approximate.

relative to Chuquicamata (see Figures 1.6a-c): (1) a formation process resulting from the emplacement of an individual magma body separate from the one responsible for the formation of Chuquicamata; (2) formation as part of the original Chuquicamata deposit, after which it separated, due to faulting and was transported to its current location; (3) that the magma body, which initiated the formation of Radomiro Tomic, was actually an extension of the pluton that formed the Chuquicamata porphyry.

Although the primary focus of this thesis was on determining the age of different alteration events at Radomiro Tomic, the $^{40}\text{Ar}/^{39}\text{Ar}$ and chemistry data generated in this project may help resolve the origin of Radomiro Tomic.

Chapter 2

Whole-Rock Samples and Methods

2.1 Introduction

Radomiro Tomic drill core samples were selected at the Chuquicamata core library by Dr. Marcos Zentilli with the advice of Patricio Cuadra, Chief Mine Geologist at Radomiro Tomic. Two sampling trips were made one on July 14, 1995 and the other on July 5, 1996. From this collection six specimens were selected containing potassium bearing minerals suitable for $^{40}\text{Ar}/^{39}\text{Ar}$ dating (see Table 2.1) for the determination of ages for alteration/mineralization (thermal events) at Radomiro Tomic. The drillcore samples come from the 9500N and the 10750N sections (see Figures 2.1-2.3). The coordinate system used at Radomiro Tomic is based on a reference point to the south at Chuquicamata.

Three of the samples chosen (Cu-999, Cu-1001, and Cu-1002) came from drillcore DDH3439 (see Figures 2.1 and 2.2) and produced good potassium feldspar and biotite specimens at the 40-60mesh level. The mineralogy of these samples is characteristic of potassic alteration. X-ray powder diffraction was used to verify the mineralogy of these samples and proved that the K-feldspar $[\text{KAlSi}_3\text{O}_8]$ is orthoclase and that the biotite $[\text{K}(\text{Mg,Fe,Ti})_3\text{Al}_2\text{Si}_6(\text{OH,O,F,Cl})_2]$ is indeed biotite.

Cu-1006, Cu-1010 and Cu-1011 from drillcore DDH1513 (see Figures 2.1 and 2.3) were originally selected for argon dating of sericite $[\text{KAl}_3\text{Si}_3\text{O}_{10}(\text{OH,F})]$, but the X-ray diffraction results proved that what was thought to be sericite was predominantly kaolinite $[\text{Al}_2(\text{Si}_2\text{O}_5)(\text{OH})_4]$. Cu-1006 and Cu-1010 contained large sub-euhedral K-feldspar crystals with a

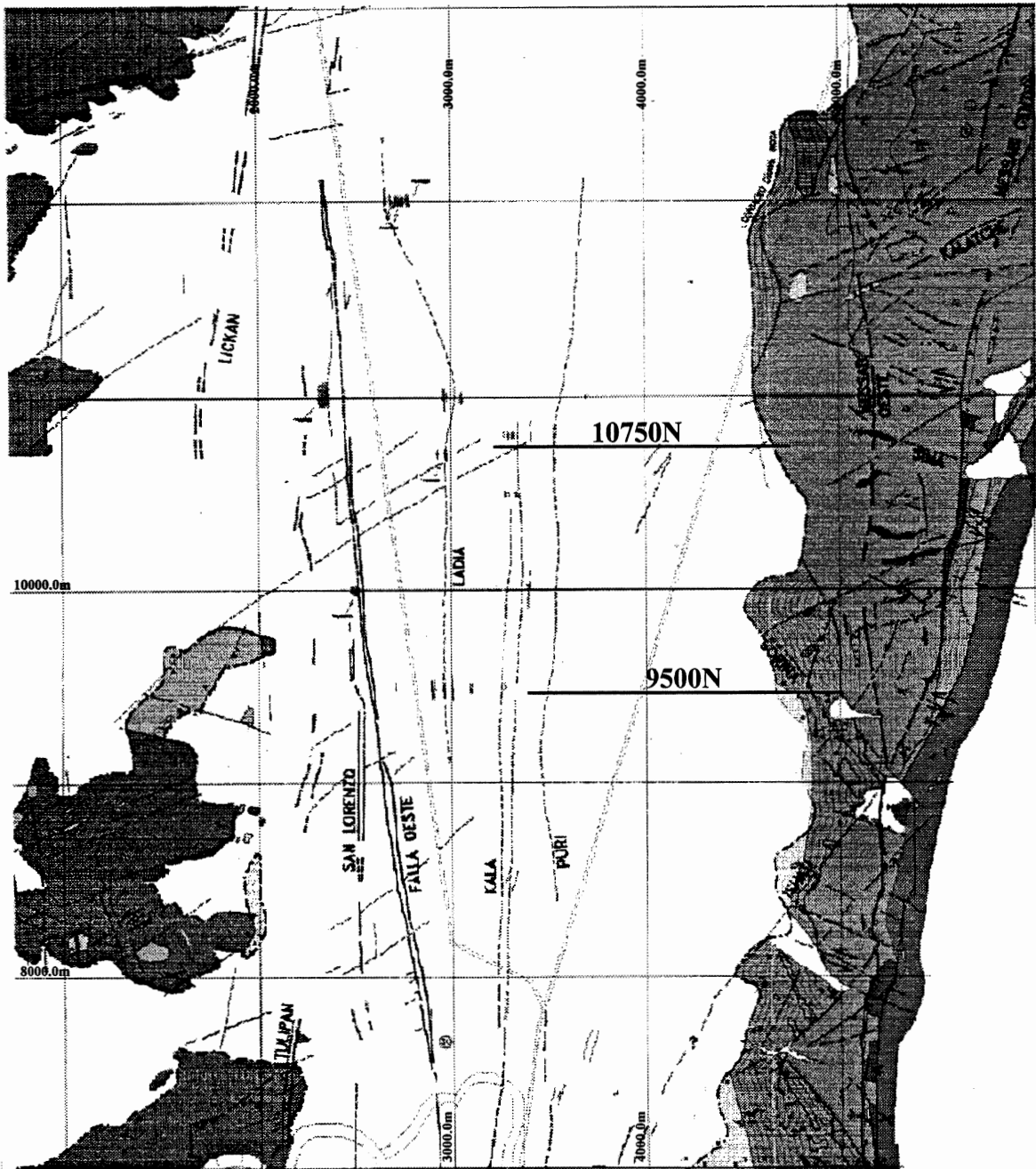


Figure 2.1 Planview of the Radomiro Tomic deposit showing the locations of the cross-sections in Fig.2.2 and 2.3. The grid is 1km x 1km and coordinates are measured north from a reference point at the Chuquicamata deposit. The Mesozoic Chuquicamata hills, seen in Fig.1.2a, are on the right of the diagram and represent basement rock. RT does not outcrop due to a cover of gravel which dominates the centre of the map. Note the N-S trending faults of the Domeyko Fault system, most important is Falla Oeste also known as the West Fissure (after Cuadra et al., 1994).

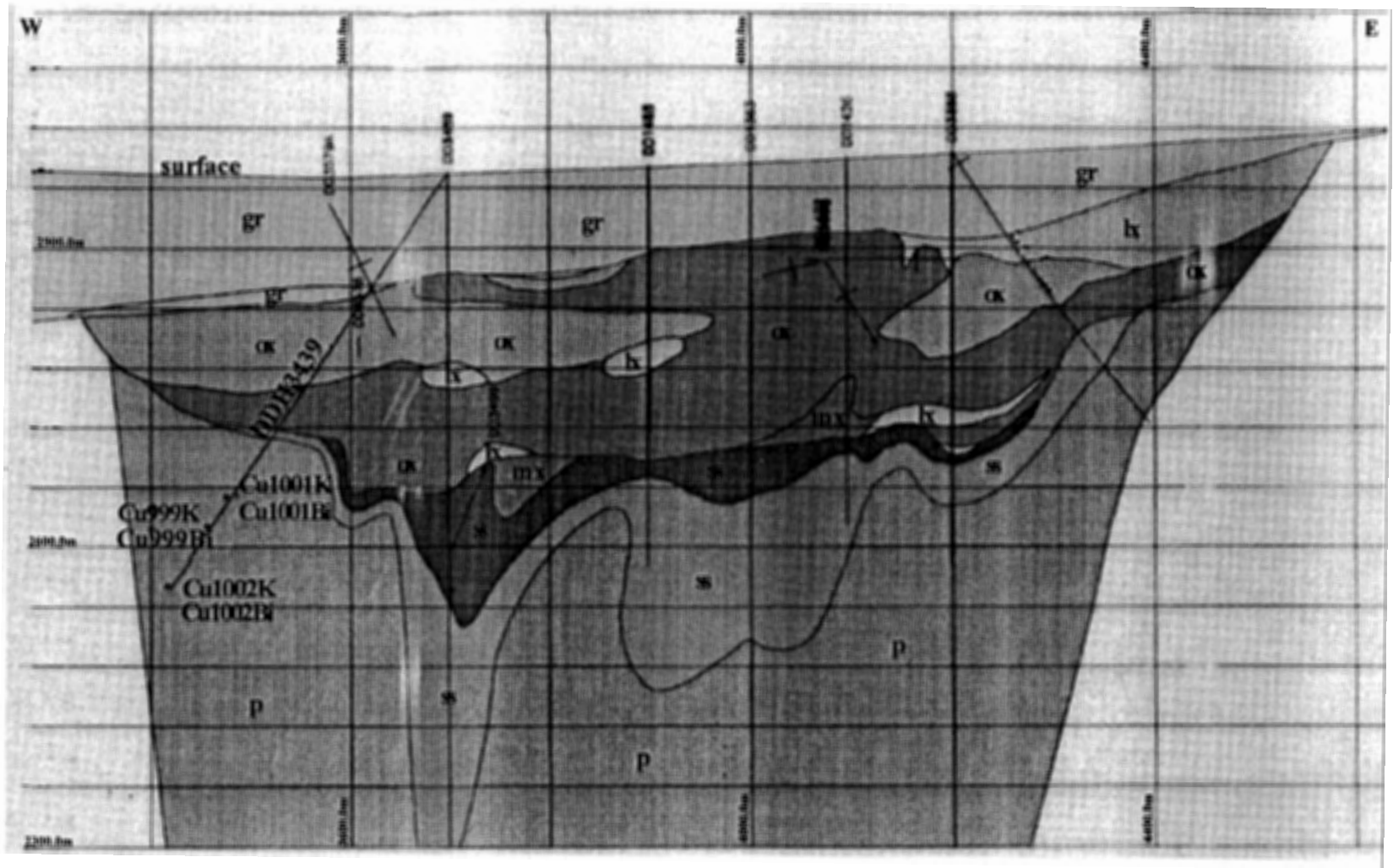


Figure 2.2 Locations of dated samples on the 10750N section. Zones, from top to bottom, are gravels (gr), oxidized minerals (ox), leachate zone characterized by goethite and hematite (lx), supergene sulphides (ss) and a region of mixed oxides and supergene sulphides (mx). The outer zone (p) shows the extent of the porphyry. Surface is approximately 3000m above sea level (after Cuadra et al., 1994).

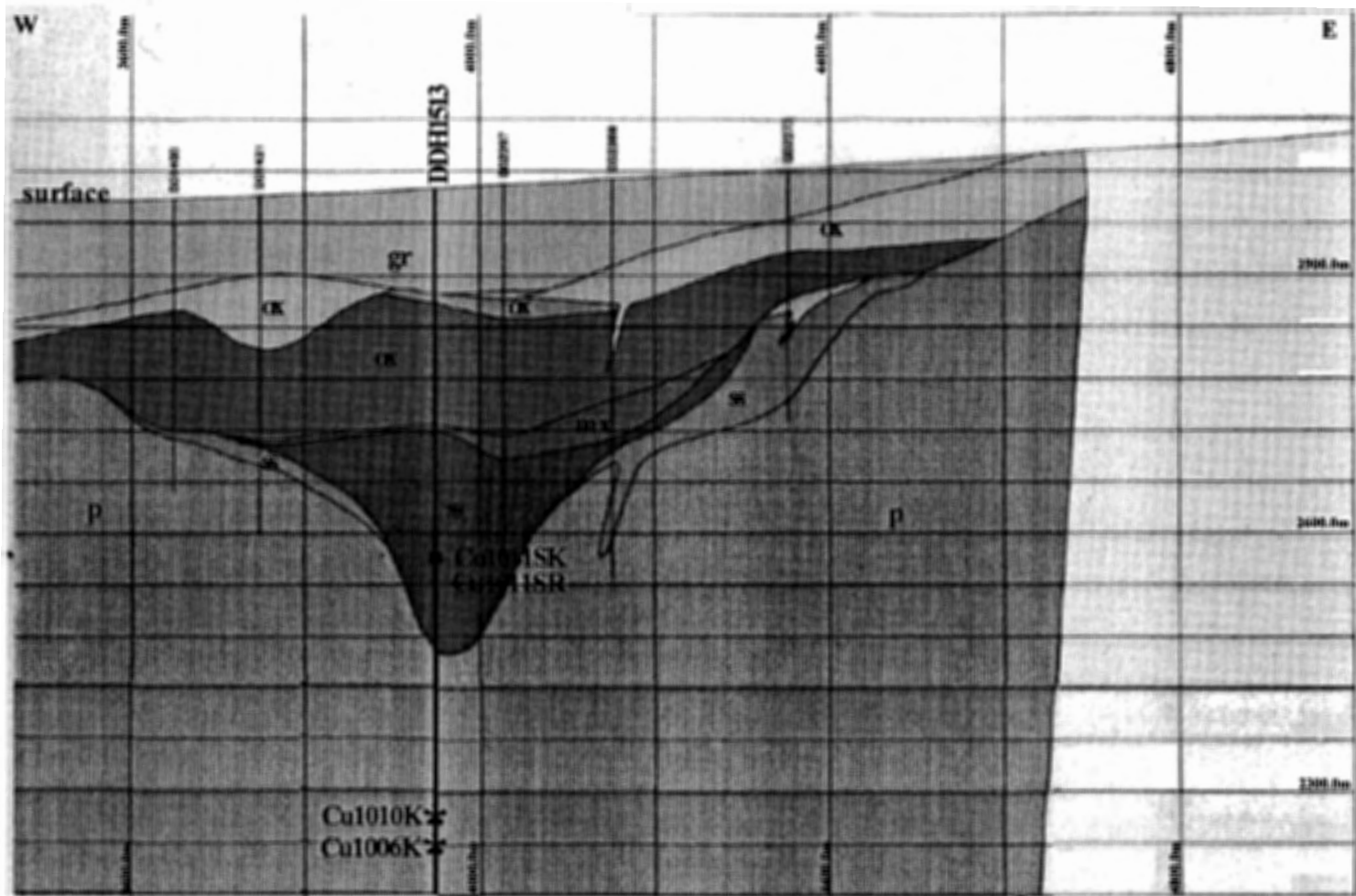


Figure 2.3 Locations of dated samples on the 9500N section. Zones, from top to bottom, are gravels (gr), oxidized minerals (ox), supergene sulphides (ss) and a region of mixed oxides and supergene sulphides (mx). The outer zone (p) shows the extent of the porphyry. Surface is approximately 3000m above sea level (after Cuadra et al., 1994).

grainsize on the order of 1-3mm which were selected for dating. The final sample, Cu-1011SK, was determined to contain sericite through X-ray powder diffraction and by the pattern of argon gas emission during step-wise degassing.

Table 2.1 Sample Location Information (coordinates are based on the mine grid in Fig.2.1)

| Lab# | Field# | Drill Core | Depth (m) | Grid N (m) | Grid E (m) | elev. (m) |
|-----------|----------|------------|-----------|------------|------------|-----------|
| Cu-999K | Z660-95 | dd3439 | 424.58 | 10774 | 3460 | 2624 |
| Cu-999Bi | Z660-95 | dd3439 | 424.58 | 10774 | 3460 | 2624 |
| Cu-1001K | Z662-95 | dd3439 | 389.85 | 10771 | 3479 | 2652 |
| Cu-1001Bi | Z662-95 | dd3439 | 389.85 | 10771 | 3479 | 2652 |
| Cu-1002K | Z663-95 | dd3439 | 501.08 | 10778 | 3419 | 2561 |
| Cu-1002Bi | Z663-95 | dd3439 | 501.08 | 10778 | 3419 | 2561 |
| Cu-1006K | Z667-95 | dd1513 | 763.72 | 9500 | 3950 | 2238 |
| Cu-1010K | Z671A-95 | dd1513 | 730.00 | 9500 | 3950 | 2272 |
| Cu-1011SK | Z671B-95 | dd1513 | 428.80 | 9500 | 3950 | 2573 |
| Cu-1011S | Z671B-95 | dd1513 | 428.80 | 9500 | 3950 | 2573 |

2.2 Sample Descriptions

Observations were made from hand specimen and polished thin section for the purpose of identifying potassium bearing minerals. All petrology for this project was done using polished thin sections that were suitable for electron microprobe analysis as well. Opaque minerals were confirmed during the mineral separation stage, by reflected-light microscopy or electron microprobe analysis.

DDH3439

Cu-1001 (see Figure 2.4a) is a section of 2" diameter drillcore composed of plagioclase crystals (55%), potassium feldspar (35%), quartz (5%) and biotite (5%). K-feldspar crystals are grains >1cm in size with perthitic texture (see section below on the significance of perthitic texture) containing minor quartz, biotite and sodic-plagioclase $[\text{NaAlSi}_3\text{O}_8]$ inclusions. Plagioclase occurs as large, zoned crystals (1-3mm in size) that are slightly sericitized. Cu-1001 contains books of biotite (1mm grains) with only slight chloritization at the edges. Sub-millimetre size quartz grains appear interstitially and as inclusions in the larger K-feldspar crystals. Opaque minerals include magnetite $[\text{Fe}_3\text{O}_4]$, ilmenite $[\text{FeTiO}_3]$ and rutile $[\text{TiO}_2]$. Ilmenite and rutile appear to have replaced euhedral (calcic?) amphibole crystals $[\text{NaCa}_2(\text{Fe},\text{Ti},\text{Mg})_5\text{Al}_2\text{Si}_6(\text{OH},\text{F},\text{Cl})_2]$. There is also pyrite $[\text{FeS}_2]$ and a very minor amount of chalcopyrite. Covellite and digenite appear as rims on the chalcopyrite grains. These rims probably represent supergene enrichment processes although the rims may also represent a second phase of hypogene mineralization associated with the possible younger hydrothermal event dated at 31.8Ma by sericite Cu-1011SR. The dominant accessory mineral is apatite $[\text{Ca}_5(\text{PO}_4)_3(\text{F},\text{Cl},\text{OH})]$ which seems to be closely associated with biotite. This sample has characteristics typical of potassic alteration.

Cu-999 (see Figure 2.4b) is a section of 2" diameter drillcore composed of plagioclase crystals (55%), potassium feldspar (25%), quartz (10%) and biotite (10%). K-feldspar crystals are grains 2-4mm in size with perthitic texture (see section below on the significance of perthitic texture) containing inclusions of sodic-plagioclase. Plagioclase occurs as large, zoned crystals (1-3mm in size) and is slightly sericitized. Cu-999 contains books of biotite (1mm grains) with only

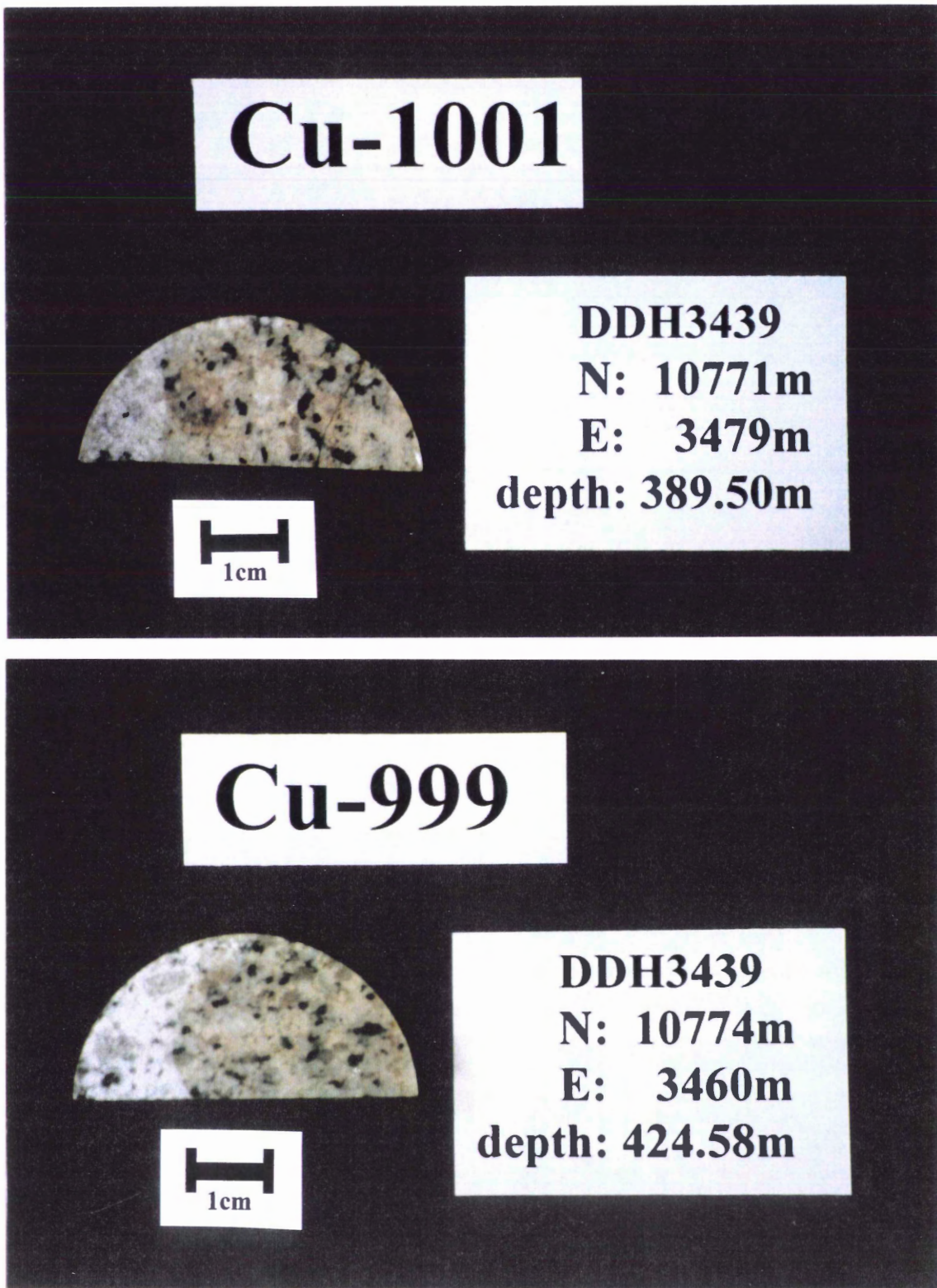


Figure 2.4 a) Sample Cu-1001 is a potassically altered sample composed primarily of zoned plagioclase, perthitic K-feldspar and smaller amounts of slightly chloritized biotite and quartz. b) Cu-999 has a composition similar to that of Cu-1001.

slight chloritization at the edges. Sub-millimetre size quartz grains appear interstitially and as inclusions in the larger K-feldspar crystals. Opaque minerals include magnetite, ilmenite and rutile. Again, ilmenite and rutile appear as pseudomorphs having partially replaced amphibole. Other opaque minerals include pyrite and a very minor amount of chalcopyrite. The dominant accessory minerals are apatite which seems to be closely associated with biotite and amphibole, which in turn, appears to be partially replaced by iron-titanium oxides. This sample has characteristics typical of potassic alteration although the presence of amphibole would suggest that the intensity of alteration was low.

Cu-1002 (see Figure 2.5a) is a section of 2" diameter drillcore composed of plagioclase crystals (55%), potassium feldspar (30%), quartz (10%) and biotite (10%). K-feldspar crystals are grains 2-4mm in size with perthitic texture (see section on the significance of perthitic texture) containing sodic plagioclase. Plagioclase occurs as large, zoned crystals (1-3mm in size) and is slightly sericitized. Cu-1002 contains books of biotite (1mm grains) with only slight chloritization at the edges. It appears that the biotite grains are also oriented to a slight degree which may define a planar fabric. Sub-millimetre size quartz grains appear interstitially and as inclusions in the larger K-feldspar crystals. Opaque minerals include magnetite, ilmenite and rutile which appear as pseudomorphs having completely replaced amphibole. Chalcopyrite and bornite are present. The dominant accessory mineral is apatite which seems to be closely associated with biotite. This sample has characteristics typical of potassic alteration.

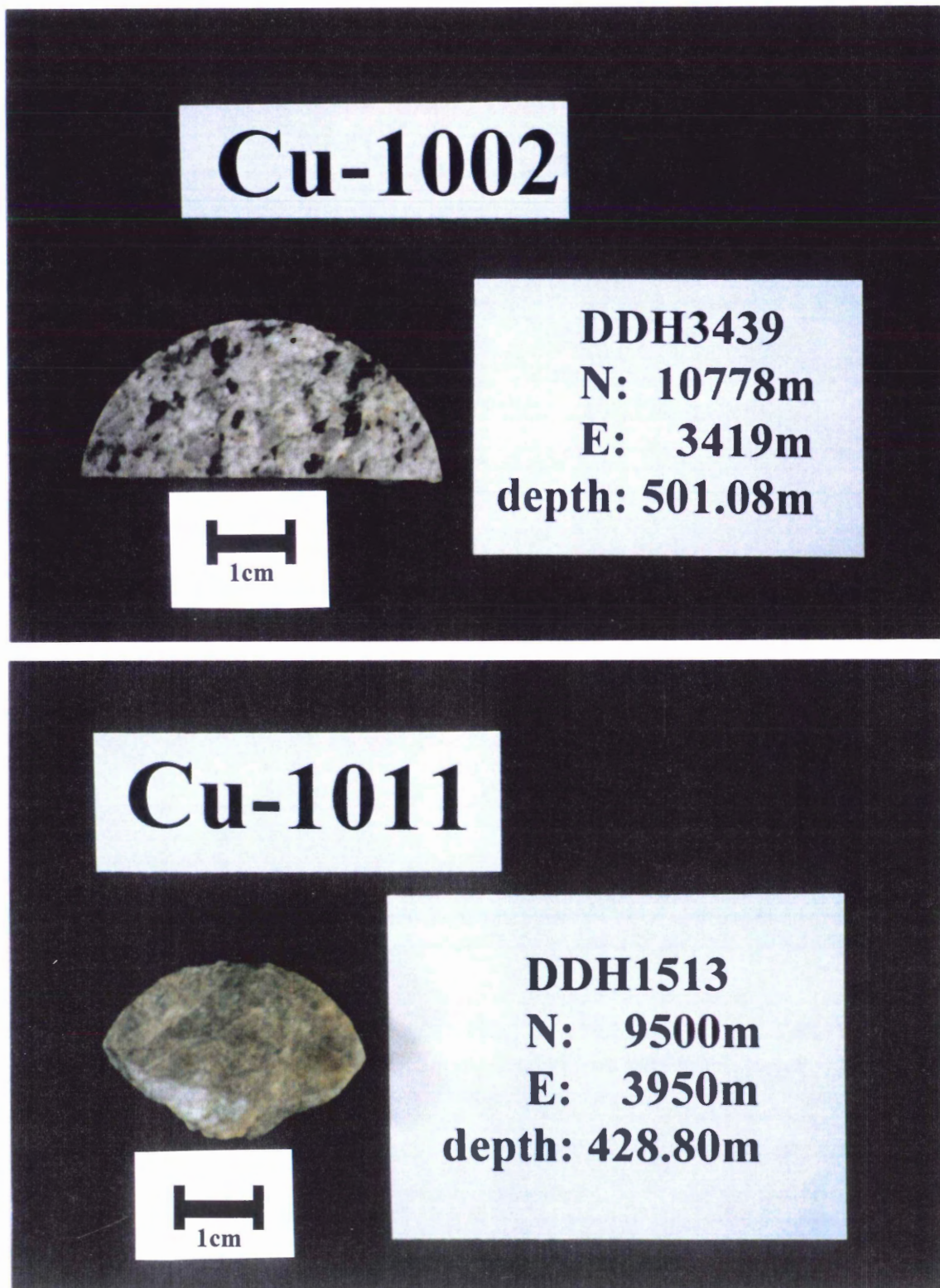


Figure 2.5 a) Sample Cu-1002 is a potassically altered sample composed primarily of zoned plagioclase, perthitic K-feldspar and smaller amounts of slightly chloritized biotite and quartz. It is similar in most respects to both Cu-999 and Cu-1001 except that it contains partially replaced hornblende. b) Cu-1011, from DDH1513 is a quartz-sericitically altered sample containing almost entirely quartz and sericite.

DDH1513

Cu-1011 (see Figure 2.5b) is a 2" diameter section of drillcore composed of sericite (75%) and quartz (25%). The quartz appears as sub-millimetre grains and sericite is yellow-green and extremely fine grained. As determined from X-ray powder diffraction, the sericite is a mixture of muscovite and clays. Opaques are present in very minor quantities and are almost entirely covellite and digenite. This sample is characteristic of quartz-sericitic alteration.

Cu-1010 (see Figure 2.6a) is a 2" diameter section of drillcore composed primarily of light green kaolinite (45%) which appear as pseudomorphs of earlier plagioclase crystals, 1mm grains of quartz (35%), 1mm grains of K-feldspar (15%) and sericite (5%) which appears as small patches within the kaolinite and are visible with the aid of a microscope. Opaques are mainly chalcopyrite. Cu-1010 contains the most chalcopyrite of any of the thin sections surveyed. This sample is characteristic of argillic-type alteration.

Cu-1006 (see Figure 2.6b) is a 2" diameter section of drillcore composed primarily of light green kaolinite (50%) which appear as pseudomorphs of earlier plagioclase crystals, 1mm grains of quartz (25%), 1mm grains of K-feldspar (20%) and sericite (5%) which appears as small patches within the kaolinite. This sample is characteristic of argillic-type alteration.

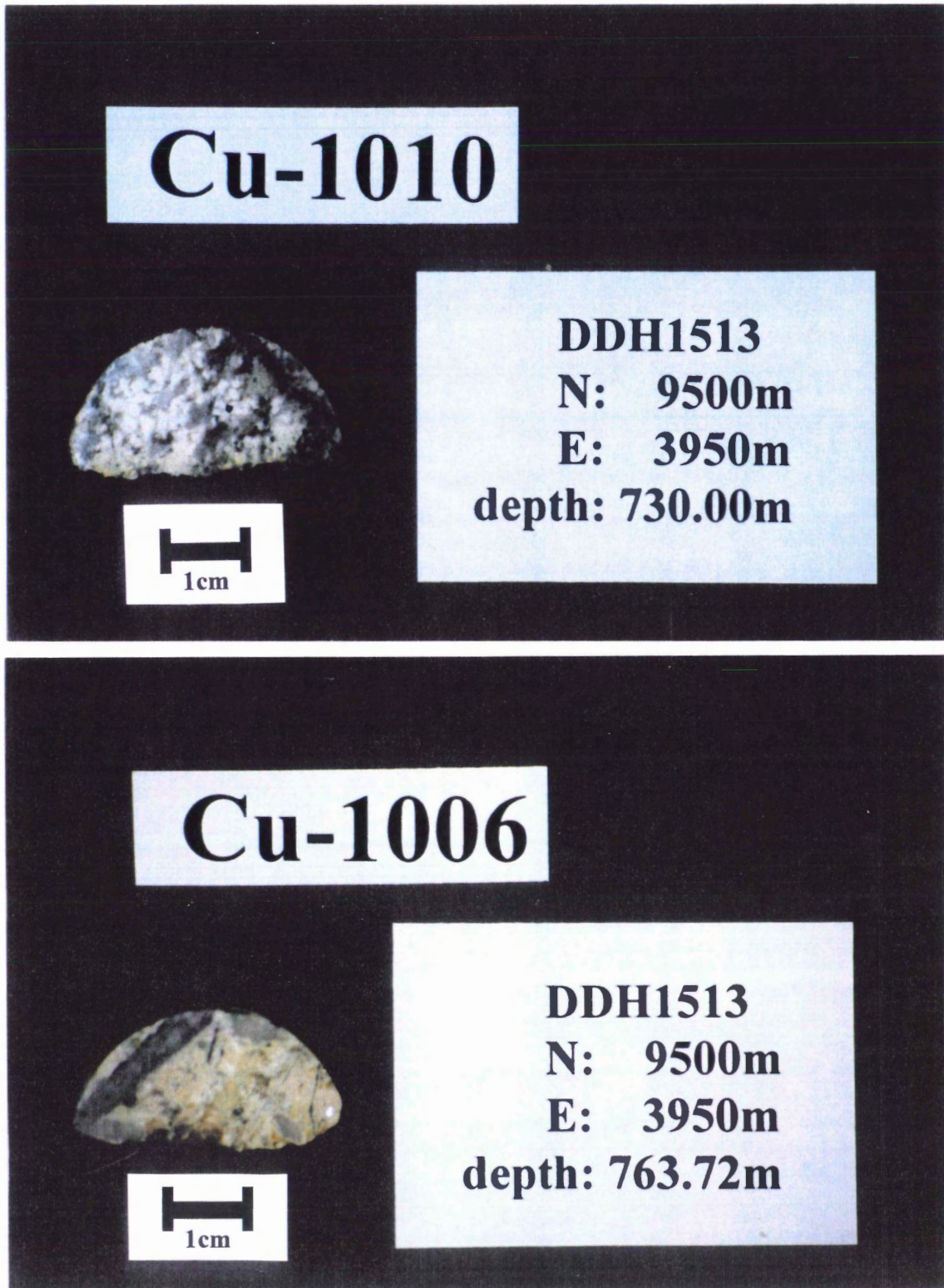


Figure 2.6 Samples a) Cu-1010 and b) Cu-1006 are argillically altered samples composed primarily of kaolinite, K-feldspar, quartz and small amounts of sericite. Cu-1006 also has a cross-cutting quartz-molybdenum vein.

2.3 Whole-rock Chemistry

2.3.1 Introduction

The six samples chosen for $^{40}\text{Ar}/^{39}\text{Ar}$ dating (Cu-999, Cu-1001, Cu-1002, Cu-1006, Cu-1010 and Cu-1011) were sent to Chemex Labs Limited, Vancouver, British Columbia for chemical analysis. Chemical analysis was done in order to help generate a more complete characterization of the dated samples and allow conclusions to be drawn about the petrogenesis of the samples. Tectonic settings and pre-alteration rock types can sometimes be determined from samples that have been highly altered. Chemistry of similar samples from the Chuquicamata deposit (Cu-093, Cu-510, Cu-512, and Cu-513; see Table 2.2) were available from previous studies and have been used in order to provide a comparison of the two deposits.

All of the samples are hydrothermally altered to some extent. Major element analyses with mineralogy and petrology were used to characterize this alteration with respect to standard patterns of porphyry copper deposit alteration zones as proposed by Lowell and Guilbert (1970). More immobile elements, especially trace elements, were used to help see through the alteration effects, make a determination of the original rock type and petrogenesis of the samples.

Table 2.2 Samples used for comparison from Chuquicamata.

| Sample# | Location | Alteration Type |
|---------|------------------------|-----------------|
| Cu-093 | ddh3472: depth 602.60m | quartz-sericite |
| Cu-510 | Banco 1: N360 E3750 | propylitic |
| Cu-512 | Banco L3: N3100 E3180 | potassic |
| Cu-513 | Banco M3: N400 E3450 | argillic |

Each sample from Radomiro Tomic consisted of a 1-2cm³ section. The samples were prepared in a way to generate the most information about the original rock type. As most of the samples have undergone silicification through veining, sections of the samples were chosen to minimize vein content. As well, weathered surfaces were removed. The samples were crushed to 150 mesh (100 micron) grainsize by Chemex using a chrome steel ring mill.

2.3.2 Methods

2.3.2.1 XRF Whole-rock Analysis

X-ray fluorescence spectroscopy was used to determine the higher concentration elements which are reported as oxides, included were Al₂O₃, CaO, Cr₂O₃, Fe₂O₃, K₂O, MgO, MnO, Na₂O, P₂O₅, SiO₂ and TiO₂. The amounts of Rb, Sr, Nb, Zr, and Y were also measured by the same technique. The method involves fusing a powdered sample and then creating a glass disk from the

melt. In this technique, electrons strike a target (such as Mo or Au) resulting in the release of X-rays. This primary source of X-rays irradiates a secondary target which is the sample. This irradiation causes the sample to produce secondary X-rays). The fluorescent X-rays have characteristic energies unique to the source element that emitted them. The number of X-rays produced is proportional to the concentration of the element responsible for emission. Therefore this method provides both the identity of an element and the concentration of that element.

2.3.2.2 Atomic Absorption Spectrometry

The amount of copper in each sample was determined by Atomic Absorption Spectrometry, also by Chemex. In AAS, the material is first put into solution which allows elements in their atomic form to be placed in the path of a beam of light, of a wavelength that causes the atoms to absorb light energy and enter an excited state. The intensity of the beam of light is reduced due to this absorption and the amount of reduction can be correlated to the concentration of the element by comparing the results to absorption in known calibration standards. The element can be identified from the wavelength of light required for excitation to occur.

2.3.2.3 Titration Analysis and Measurement of H₂O Content

FeO was measured by titration analysis by combining FeO in solution with a reacting

species of known concentration. Typically with titration analysis a chemical indicator signals the end of the reaction by changing colour when the FeO present has completely reacted. The volume of FeO is calculated based on the volume of reactant consumed in order to completely react the FeO. Sulphur is measured by Leco titration, a procedure similar to that performed for FeO. H₂O content is measured simply by weighing the sample, drying it and weighing again and then calculating the difference between the two masses.

2.3.2.4 Trace Level Rare Earth Analysis

Rare earth elements (Ce, Dy, Er, Eu, Gd, Ho, La, Lu, Nd, Pr, Sm, Tb, Tm and Yb) were measured by plasma mass spectrometry. In this method the sample is introduced, in solution, into a plasma stream which heats the sample to 8000°C. At this temperature the ions that are generated from the sample are removed to a mass spectrometer where they are separated and collected by their mass to charge ratios. This ratio is unique to each element and is used for identification of the element. This method is useful for elements, such as the rare earth elements that occur in very small amounts (ppm level) and are difficult to separate from one another by other methods.

2.3.3 Discussion and Interpretation

Results are reported in Appendix A. An interpretation of the data is summarized below.

2.3.3.1 Rock Type

The $Zr/TiO_2 * 0.0001$ vs Nb/Y discrimination diagram (Winchester and Floyd, 1977) in Figure 2.7, clearly defines the Radomiro Tomic samples and two of the Chuquicamata samples as trachyandesitic which is the extrusive equivalent to quartz monzodiorite. The Zr/TiO_2 ratio acts as an index of differentiation while Nb/Y ratio shows alkalinity.

The distribution of mobile major elements demonstrates the importance of alteration and mineralization effects on these rocks. The Na_2O+K_2O vs SiO_2 diagram in Figure 2.8, a standard discrimination diagram used to determine rock type, plots the samples from Radomiro Tomic and Chuquicamata as rhyolitic in composition, the extrusive equivalent to granite. This silica-rich determination of rock type is primarily the result of silicification (mostly due to dense quartz veining) which is part of alteration processes typical of porphyry copper deposits and obscures the original composition. The two samples that plot outside the rhyolite zone, Cu-1011 and Cu-093 (this sample plots outside the boundaries of the discrimination diagram; $Na_2O = 0.01$, $K_2O = 2.90$, $SiO_2 = 77.34$), have undergone quartz-sericite alteration. This alteration process increases the silica content by increasing the amount of quartz and reduces the sodium content through the sericitization of plagioclase. The samples, therefore, plot outside of the rhyolite zone boundaries in a region on the diagram higher in silica which is consistent with the effects of this type of alteration. Thus the use of the $Zr/TiO_2 * 0.0001$ vs Nb/Y discrimination diagram to determine rock type is more appropriate than discrimination diagrams that involve SiO_2 because it involves less mobile elements allowing it to see through the alteration processes.

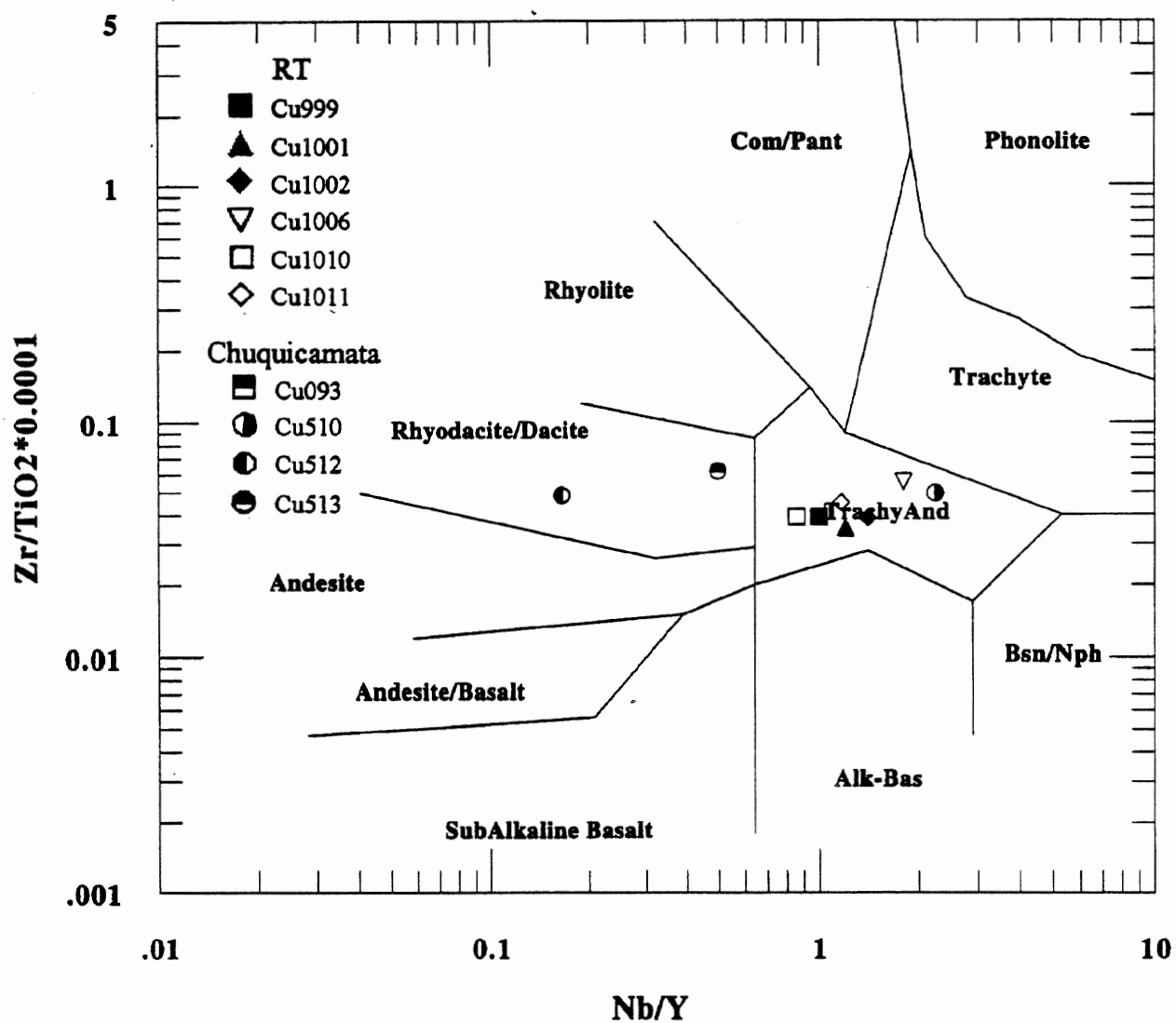


Figure 2.7 $Zr/TiO_2 * 0.0001$ vs Nb/Y discrimination diagram (from Winchester and Floyd, 1977) defines the original rock type of the RT samples and two of the Chuquicamata samples as trachyandesites (extrusive equivalent to quartz monzodiorite). It is debatable which term is better suited to these rocks due to their formation in a subvolcanic environment as seen in the Sillitoe model found in Fig. 1.5. In this diagram Zr/TiO_2 acts as an index of differentiation while Nb/Y serves as an index of alkalinity.

2.3.3.2 Tectonic Setting

Typically, volcanic arc granites are enriched in K, Rb, Ba, Th, Ce and Sm relative to Ta, Nb, Hf, Zr, Y and Yb. Pearce et al. (1984) used a comparison of patterns made from these element values normalized to a hypothetical ocean ridge granite in order to categorize samples into four main tectonic settings. These categories were ocean ridge granites (ORG), volcanic arc granites (VAG), within plate granites (WPG) and collision granites (Syn-COLG). Figure 2.9 shows that the RT samples and two of the Chuquicamata samples have patterns similar to those considered as being typical Chilean volcanic arc granites by Pearce (see insert in Figure 2.9).

It is also possible to discriminate between tectonic settings with only Rb, Y and Nb (see Figure 2.10). The Rb/Y+Nb discrimination diagram (Pearce et al, 1984) clearly defines the RT and Chuquicamata samples sets as volcanic arc granites. Pearce considers these three elements to be the most effective for this purpose.

2.3.3.3 Alteration Effects

The $\text{Na}_2\text{O}/\text{K}_2\text{O}$ diagram in Figure 2.11 shows two distinct groupings that separate the samples that have undergone extensive alteration from those that are relatively unaltered. Cu-1006, Cu-1010 show argillic alteration and Cu-1011 shows quartz-sericite alteration. Cu-999, Cu-1001, and Cu1002 are from the potassic alteration zone. From the diagram it can be concluded that Na becomes depleted with an increasing degree of alteration. The least altered samples are from the potassic alteration zone, but have less potassium than the most altered samples. The

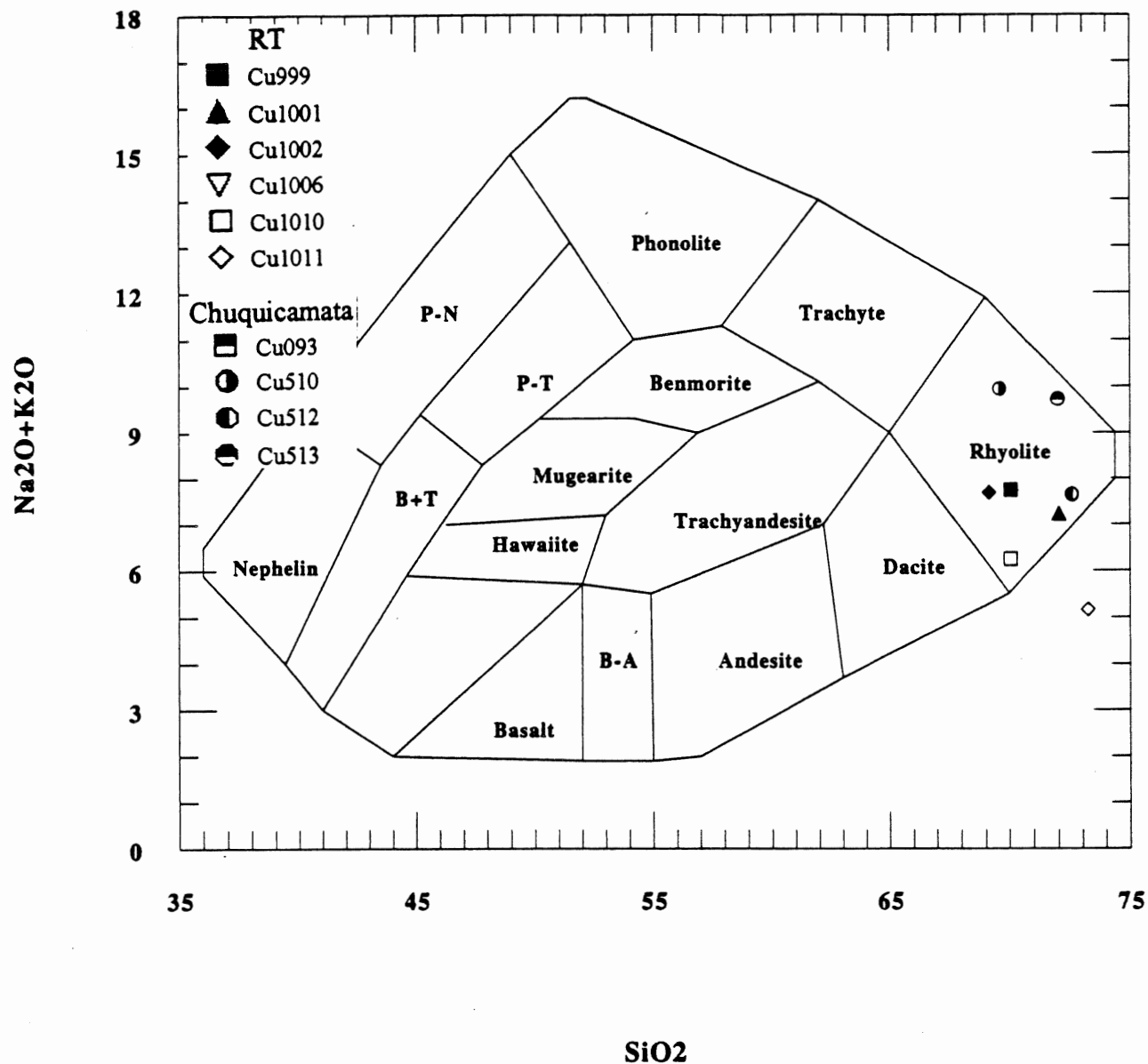


Figure 2.8 The sample set plots within the rhyolite (granite) zone when using the Na₂O+K₂O vs SiO₂ discrimination diagram. This diagram actually represents alteration rather than original rock type. Silica and potassium content increase with increasing degrees of alteration which changes sample set rock type from quartz monzodioritic to granitic. The two samples that plot outside of the rhyolite zone, Cu-1011 and Cu-093 (this sample plots outside of the boundaries of the discrimination diagram and is not shown; Na₂O = 0.01, K₂O = 2.90 and SiO₂ = 77.34), have undergone quartz-sericitic alteration. This type of alteration increases SiO₂ by increasing the amount of quartz and reduces the sodium content through the sericitization of plagioclase. (after Cox et al., 1979).

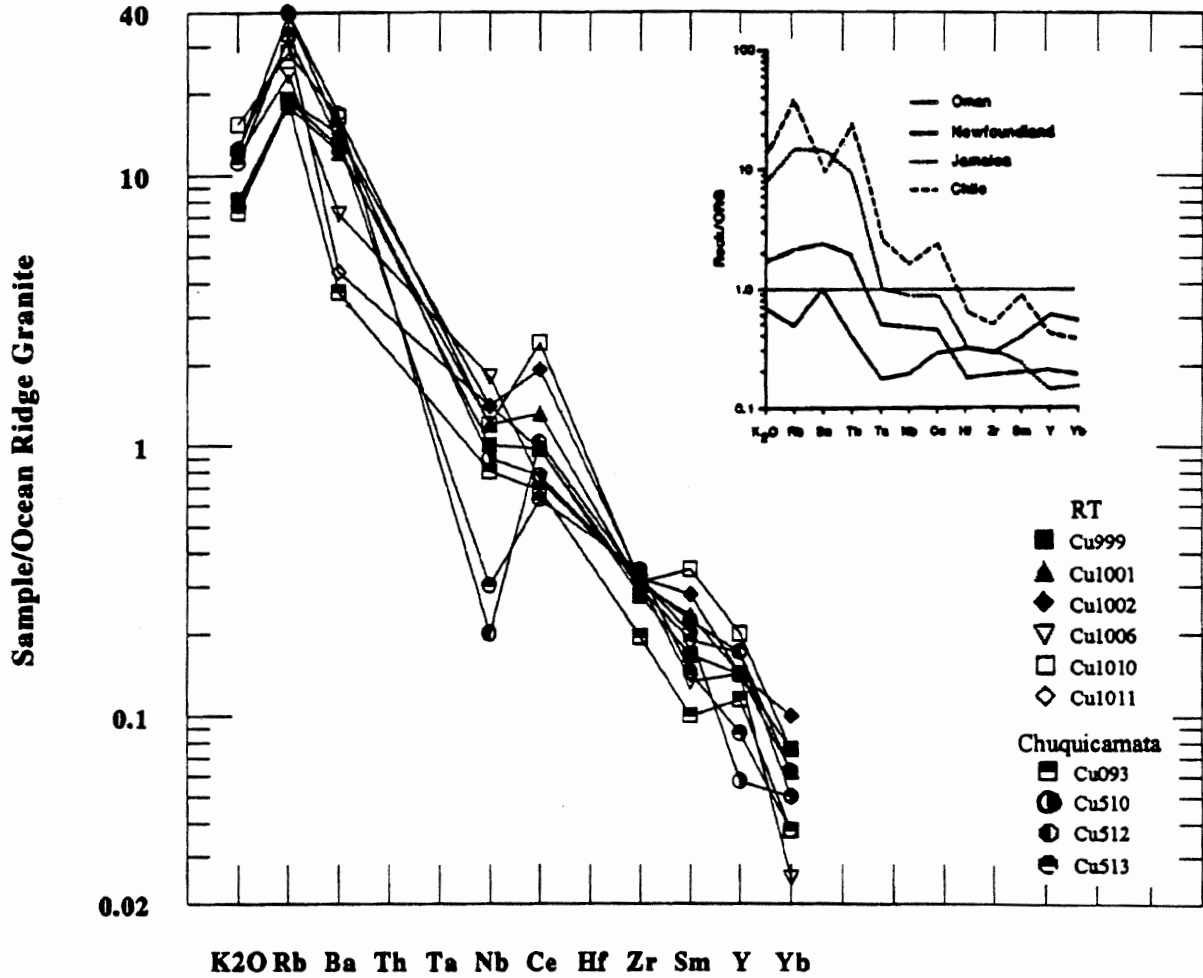


Figure 2.9 Volcanic arc granites are typically enriched in K, Rb, Ba, Th, Ce and Sm relative to Ta, Nb, Hf, Zr, Y and Yb. Pearce et al. (1984) use this diagram to identify tectonic setting based on element values normalized to a hypothetical ocean ridge granite. The resulting patterns are similar to those for a typical Chilean volcanic arc granite (see insert).

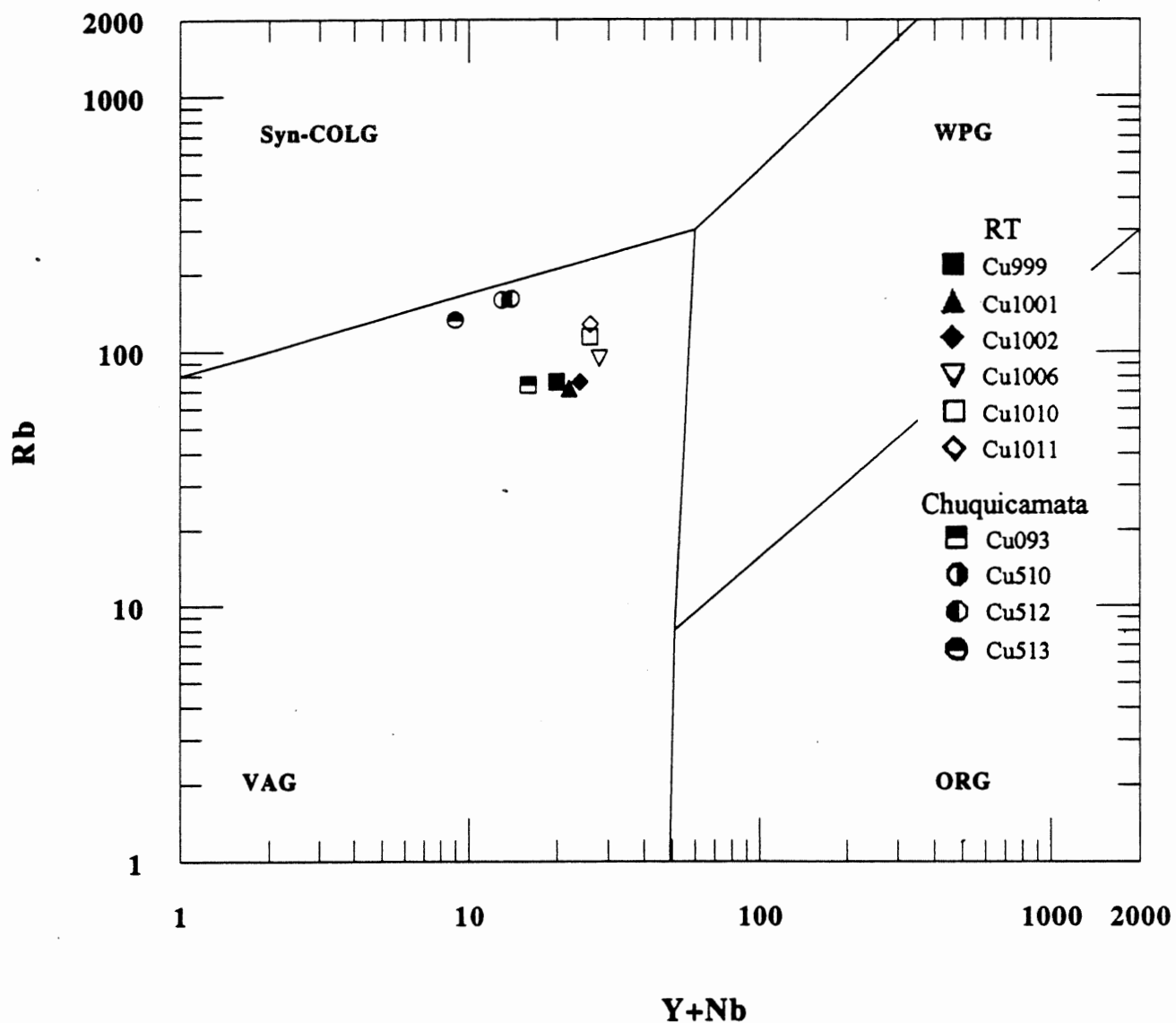


Figure 2.10 This discrimination diagram using Rb, Y and Nb (from Pearce et al., 1984), clearly defines the sample set as volcanic arc granites (VAG) as opposed to collision granites (syn-COLG), within-plate granites (WPG) or ocean ridge granites (ORG).

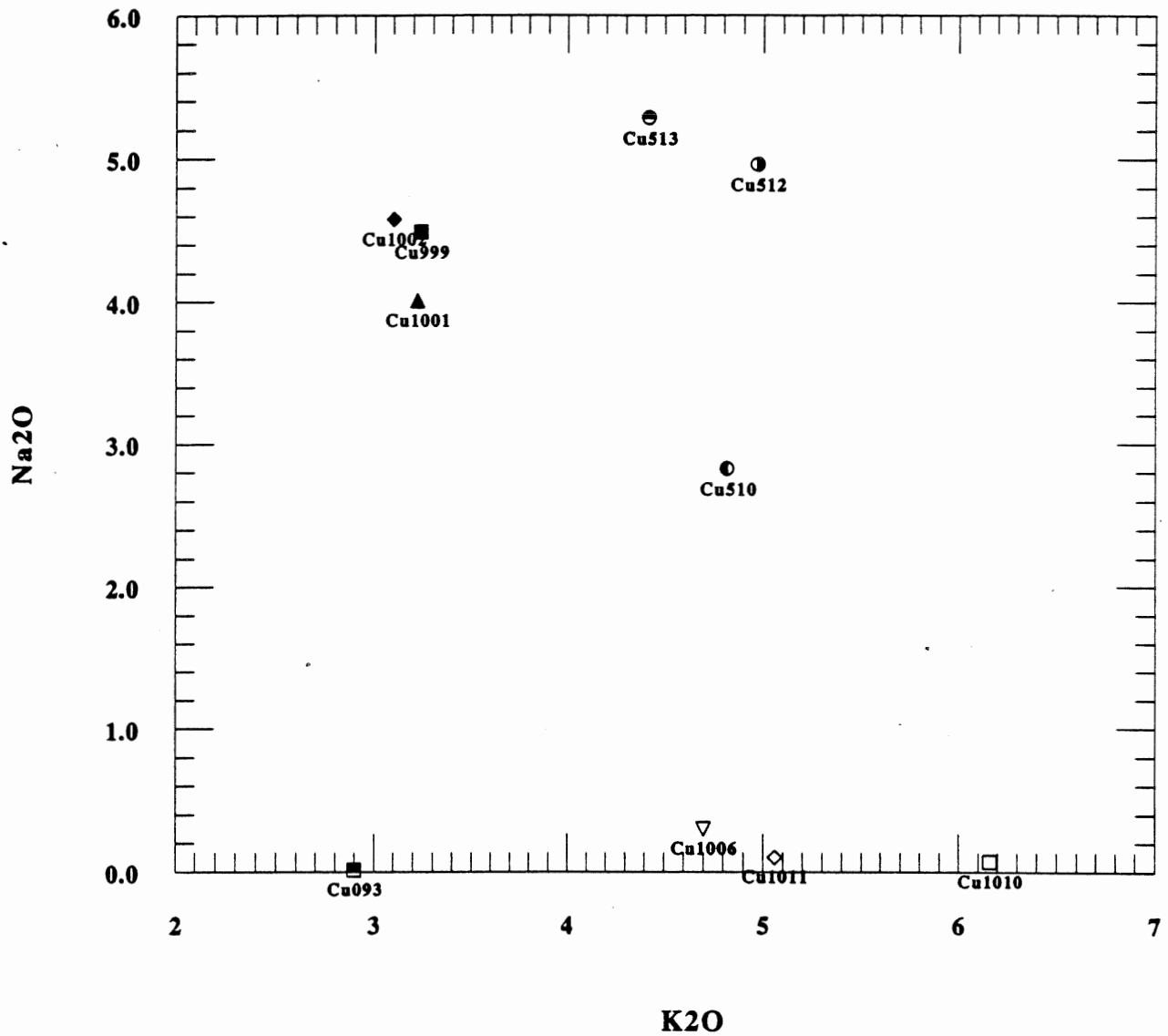


Figure 2.11 This diagram shows discrimination among the sample set according to the degree of alteration undergone by each sample. Cu-1006 and Cu-1010 are argillically altered, Cu-1011 and Cu-093 are quartz-sericitically altered and Cu-999, Cu-1001, Cu-1002 and Cu-512 are potassically altered. It may be concluded that Na depletion occurs with increasing alteration.

potassium content of both groups can be attributed to orthoclase content but the increased level of potassium in the more highly altered samples is likely due to the significant amounts of sericite (potassium bearing mica) present. The Chuquicamata samples show similar trends. Cu-093 from the quartz-sericite alteration zone is depleted in sodium. Cu-513 from the argillic alteration zone has potassium amounts similar to RT samples Cu-1006 and Cu-1010 of the same alteration zone.

2.3.3.4 Rare Earth Elements

Chondrite-normalized (La 0.367; Ce 0.957; Pr 0.137; Nd 0.711; Sm 0.231; Eu 0.087; Gd 0.306; Tb 0.058; Dy 0.381; Ho 0.0851; Er 0.249; Tm 0.0356; Yb 0.248; Lu 0.0381; Y 2.1; Evensen et al., 1978) rare earth patterns from RT show enrichment in light rare earth elements (LREE) and low values for heavy rare earth elements (HREE) (see Figure 2.12). This is similar to the pattern shown by the Chuquicamata samples. This trend of enriched LREE's and depleted HREE's is indicative of strong rare earth element fractionation between melt and a residual mineral phase that retained HREE's during magma genesis (Maksaev, 1990). In the case of Radomiro Tomic, the residual mineral phase retaining HREE's would likely have been amphibole. As well, hydrothermal alteration may also have the effect of enriching LREE's and depleting HREE's (Taylor and Fryer, 1982).

2.3.4 Productive vs Unproductive Porphyry Copper Deposits

The discrimination diagram of Baldwin and Pearce (1983) uses Y vs MnO_2 to distinguish

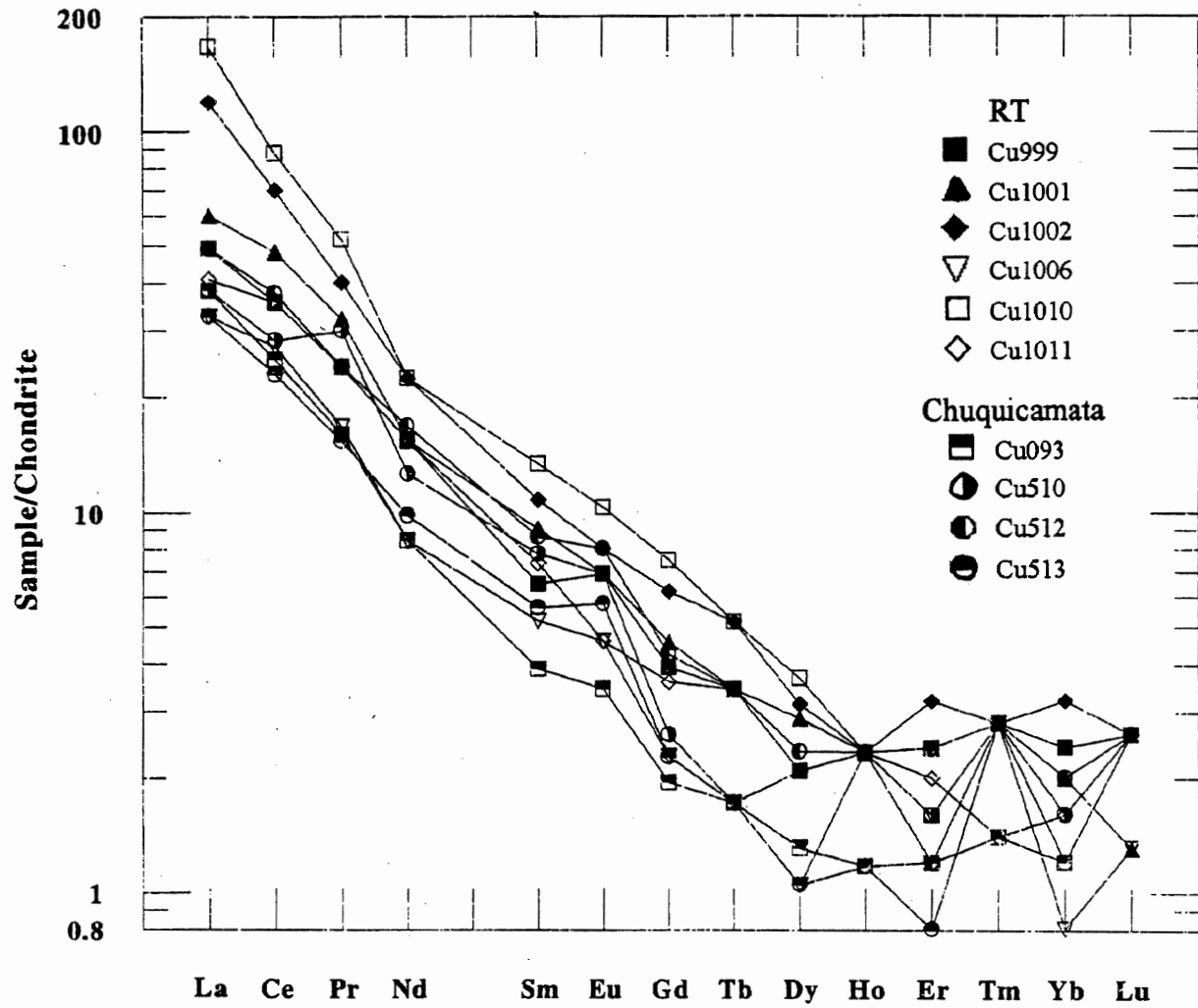


Figure 2.12 Chondrite-normalized (La 0.367; Ce 0.957; Pr 0.137; Nd 0.711; Sm 0.231; Eu 0.087; Gd 0.306; Tb 0.058; Dy 0.381; Ho 0.0851; Er 0.249; Tm 0.0356; Yb 0.248; Lu 0.0381; Y 2.1; Evensen et al., 1978) rare earth patterns from RT show enrichment in light rare earth elements (LREE) and low values for heavy rare earth elements (HREE). This is similar to the pattern shown by the Chuquicamata samples.

between productive and unproductive intrusions. The data generated the expected results when plotted on this diagram since it is already known that Radomiro Tomic is a productive deposit. This helps to demonstrate the possible value of this discrimination diagram as an exploration tool. The more highly altered samples (Cu-1006, Cu-1010, and Cu-1011) at Radomiro Tomic plot within the productive region of the diagram while the least altered samples (Cu-999, Cu-1001, and Cu-1002) plot in the sub-productive zone (see Figure 2.13). Although this diagram does show a good correlation between the samples with greater copper content and those with less copper, there is some controversy about whether or not the diagram really shows potential productivity or just the degree of alteration.

2.3.5 Conclusions

The original, pre-alteration rock type of the sample set from Radomiro Tomic is quartz monzodiorite as derived from the $Zr/TiO_2 * 0.0001$ vs Nb/Y discrimination diagram (Winchester and Floyd, 1977). Tectonic setting was determined by using a comparison of patterns made from certain trace element values normalized to a hypothetical ocean ridge granite and the Radomiro Tomic samples were determined to have had a volcanic arc setting. By plotting Na_2O vs K_2O the samples can be clearly divided into those that have undergone extensive alteration (Cu-1006, Cu-1010 and Cu-1011) and those that have not (Cu-999, Cu-1001, and Cu-1002). It is probable that rare earth element amounts were affected by amphibole crystallization in the magma, resulting in depletion of the heavy rare earth elements (HREE) and enrichment of light rare earth elements (LREE). As well, the Y vs MnO_2 diagram determines the more highly altered sections of the

Productive vs Unproductive Intrusions

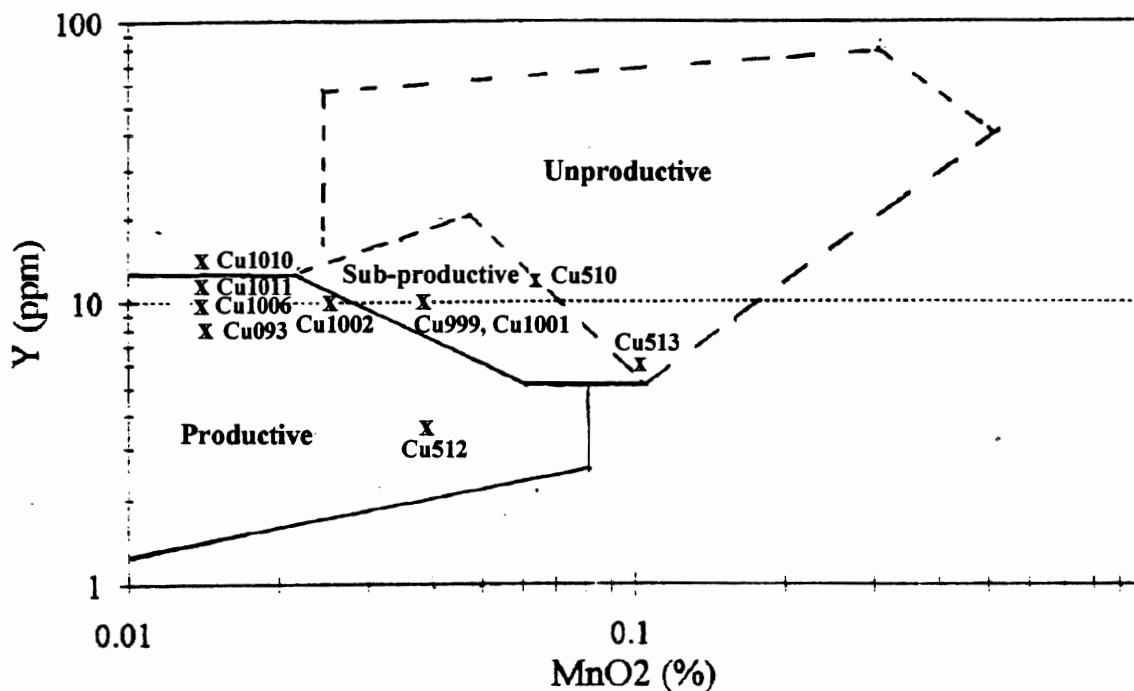


Figure 2.13 Discrimination diagram (after Baldwin and Pearce, 1983) separating productive and non-productive intrusions based on Y vs MnO₂. There is definite segregation of the more highly mineralized (and altered) samples which are classed as productive, from those of the potassic alteration zone that are classed as sub-productive. This correlation was confirmed with observations from ore microscopy.

Radomiro Tomic deposit to be productive while the least altered sections are sub-productive.

Overall, the results concur with those of similar analyses done on samples from
Chuquicamata.

Chapter 3

Dated Minerals and Methods

3.1 Introduction

This chapter deals specifically with the potassium-bearing minerals that were separated from each of the drill core samples. These sub-samples of potassium feldspar (orthoclase), biotite and sericite were mechanically separated for submission to $^{40}\text{Ar}/^{39}\text{Ar}$ dating analysis, X-ray diffraction analysis and electron microprobe analysis.

3.2 Mineral Separation

Mineral separation was done in order to provide individual samples for argon dating. In addition enough of each sample was separated to provide sub-samples for X-ray diffraction and electron microprobe analysis. In order to liberate the individual minerals, 2-4cm³ pieces of drillcore were manually crushed to the 40-60mesh level (\approx 1mm grain-size). The crushed sample was then washed in distilled water to remove the clay-sized fraction, and dried in an oven at 60°C for several hours. At this stage, I used a low-power, binocular microscope to identify grains of good quality and manually removed those grains for dating. For most samples, individual minerals were separated at a grainsize of approximately 2-3mm. For a sub-sample to be considered good quality the grains had to have few or no visible inclusions. The individual grains were then graded into three categories: (1) those with no inclusions, suitable for argon dating; (2) those with very

few inclusions which were used for X-ray diffraction analysis; (3) those with few inclusions which were used for electron microprobe analysis. Argon dating requires samples with no inclusions that might contaminate the analysis with spurious argon gas, but inclusions may be allowed as long as they are not potassium bearing minerals. X-ray diffraction was used to provide confirmation of the mineral composition.

3.3 Supporting X-ray Diffraction Analysis

X-ray diffraction analyses were done at the Fission Track Research Laboratory, Earth Sciences Department, Dalhousie University for the purpose of verifying the visual identification of the samples selected for argon dating. Analyses were performed on small sub-samples by standard powder diffraction. An automated Philips 100kV generator and diffractometer unit was used for mineral identification by powder diffractometry. The sub-samples were crushed to a very fine-grained granular consistency by hand in acetone using an agate mortar and pestle. The powdered sub-samples were placed on glass microscope slides and in the case of samples Cu-1001Bi and Cu-1010K, on amorphous silica mounts (to reduce the background response from the mount itself) and the acetone allowed to evaporate. The mounted sample was then placed in the diffractometer. The sample and X-ray detector are rotated at a known rate with respect to the $\text{CuK}\alpha$ X-ray source and the energy detected is recorded and processed automatically. The output consists of a peak list and energy response curve. Peak lists can be found in Appendix B.

Diffractograms were done to verify the compositions of minerals selected for argon dating, specifically K-feldspar, biotite and sericite. Diffractograms were also generated to apply the Triclinicity Test on all K-feldspar samples found. Triclinicity testing, which can provide a

measure of the rate of cooling of the potassium feldspar, is discussed in greater detail in Section 3.6.

3.4 XRD Results on Dated Minerals

Cu-999K: A very good match with orthoclase, albite and quartz was found with about 95% of all peaks identified including all major peaks (see Figure 3.1a). In thin section, the orthoclase crystals show perthitic texture with inclusions of plagioclase, quartz, minor biotite and apatite (see Figure 3.1b).

Cu-999Bi: A relatively good match for biotite was found with the possibility of some phlogopite content (see Figure 3.2a). In thin section, biotite occurs as good clean (few or no inclusions) crystals with only slight chloritization along the edges of some grains (see Figure 3.2b). Biotite grains without visible chlorite were selected for both argon dating and XRD analysis.

Cu-1001K: This sub-sample provided a very good match with orthoclase, albite and quartz accounting for almost 95% of all peaks generated including all major peaks (see Figure 3.3a). In thin section the orthoclase crystals showed perthitic texture with inclusions of quartz (see Figure 3.3c).

Cu-1001Bi: A very good match for biotite was determined which accounted for all major and minor peaks (see Figure 3.3b). In thin section, biotite grains were relatively free of chloritization (see Figure 3.3c).

Cu-1002K: A very good match with orthoclase, albite and quartz accounting for almost

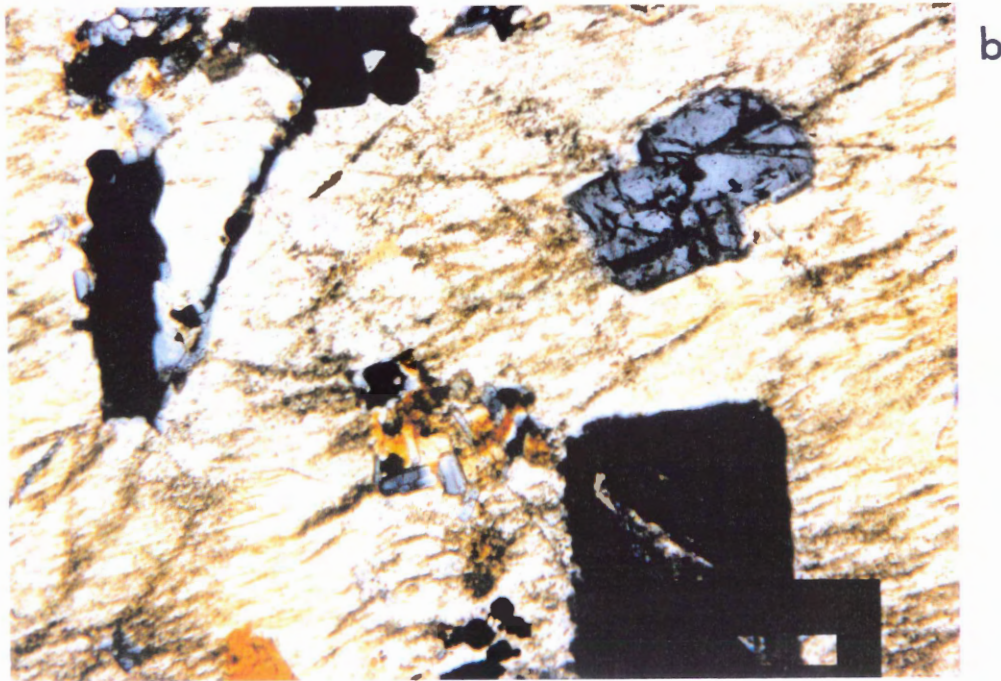
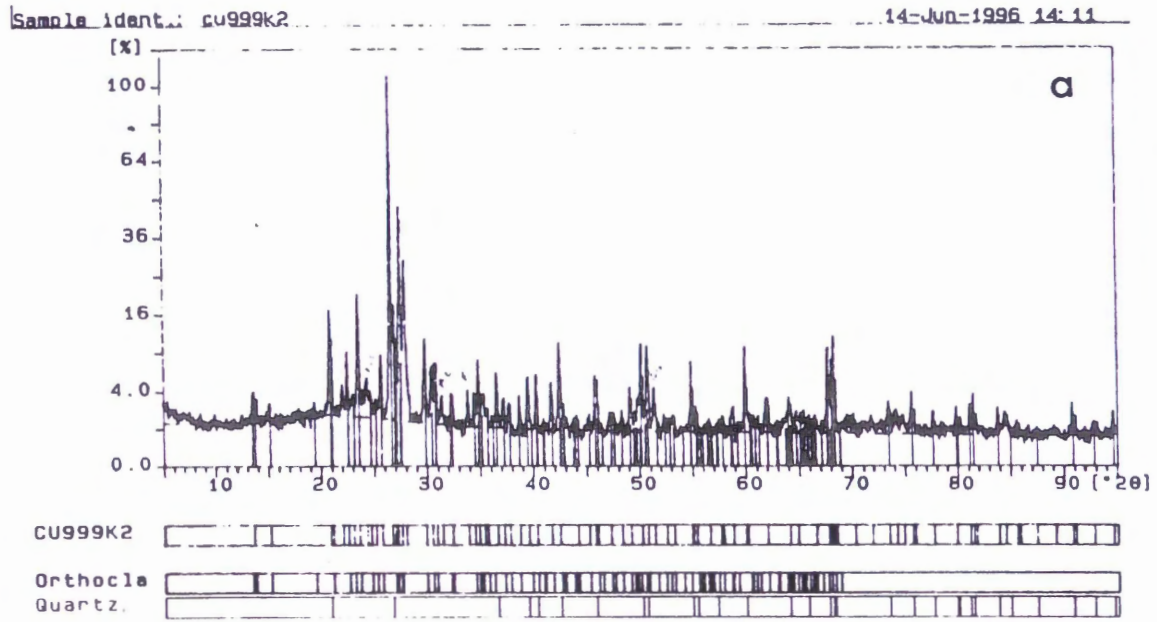


Figure 3.1a-b a) XRD identification of perthitic orthoclase and quartz in Cu-999K.
 c) Photomicrograph of Cu-999 showing perthitic orthoclase host grain with inclusions of plagioclase, apatite, biotite and opaque minerals. (magn. 5X; scale bar = 380mm; XPL)

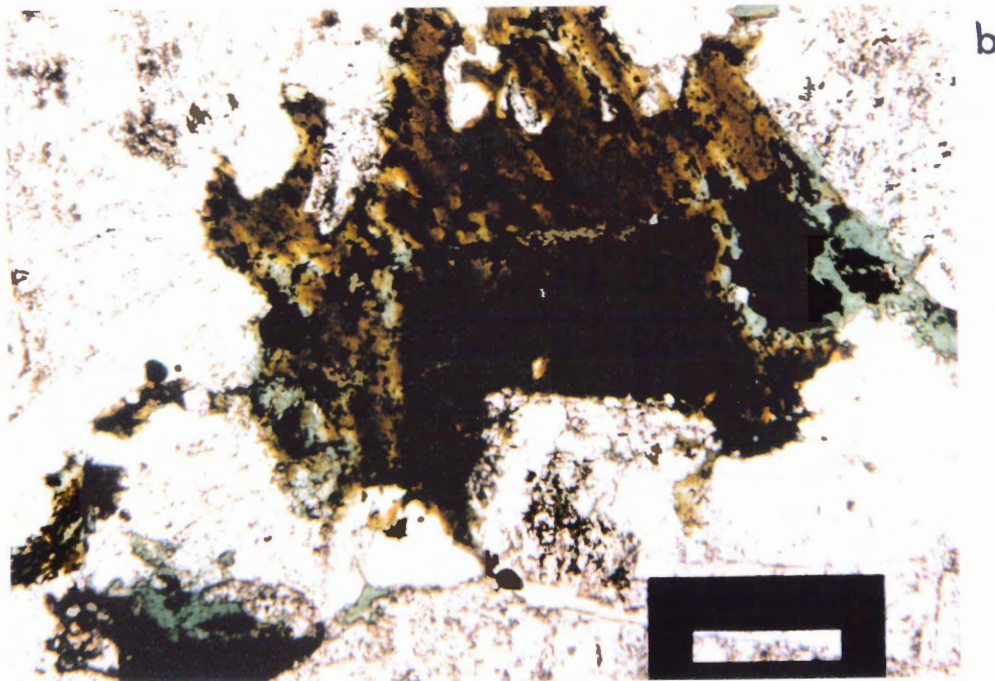
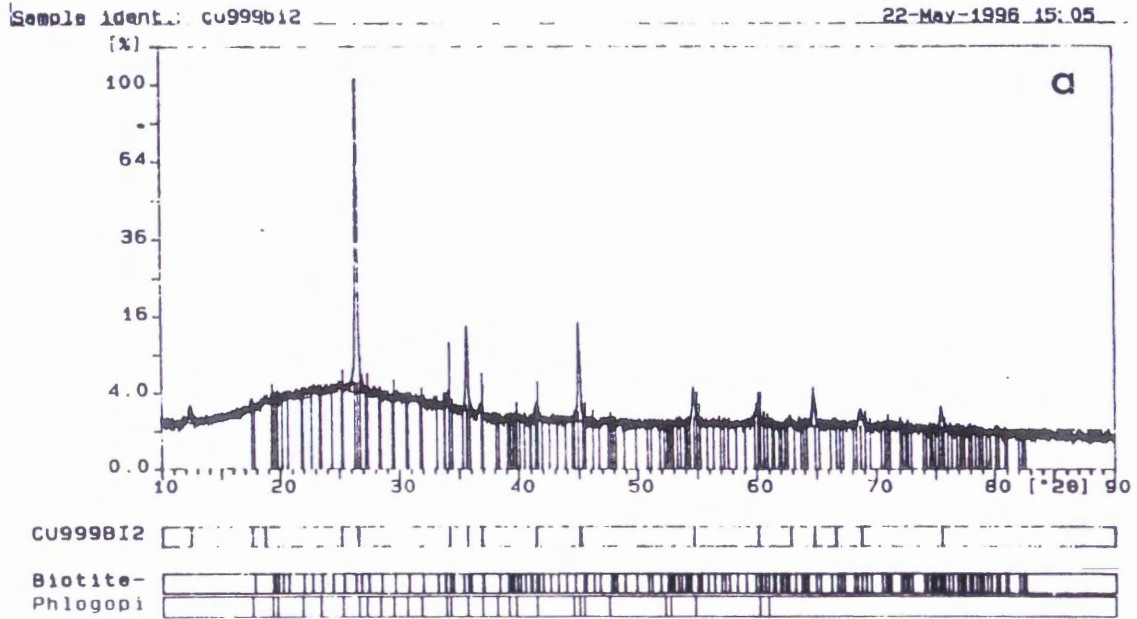


Figure 3.2a-b a) XRD identification of biotite in Cu-999Bi. b) Photomicrograph of Cu-999 showing biotite grain at centre with chlorite and opaque minerals at edges. (magn. 5X; scale bar = 380mm; PPL)

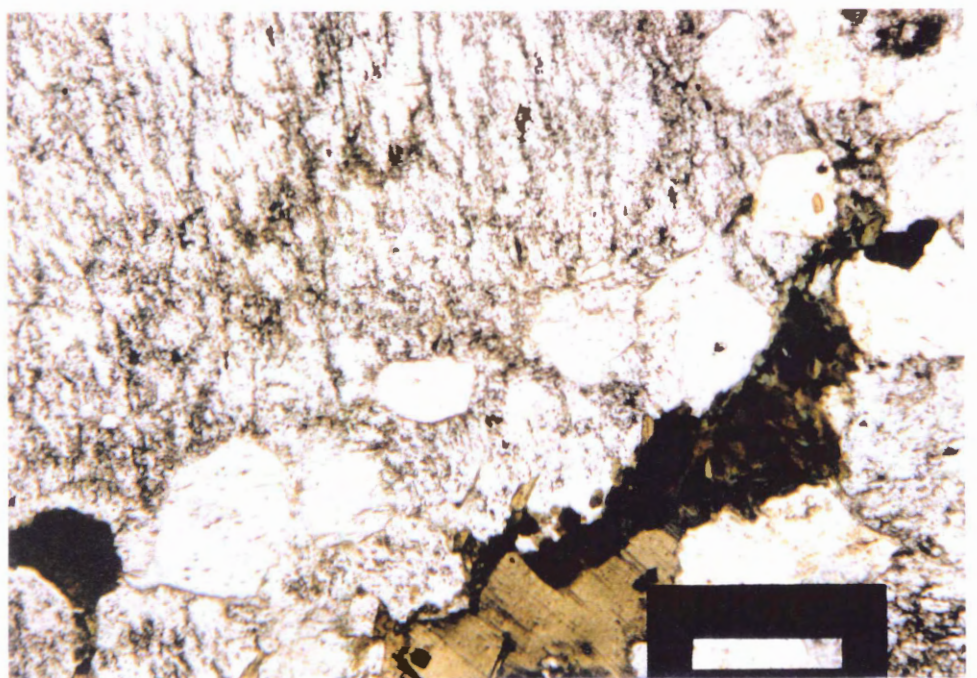
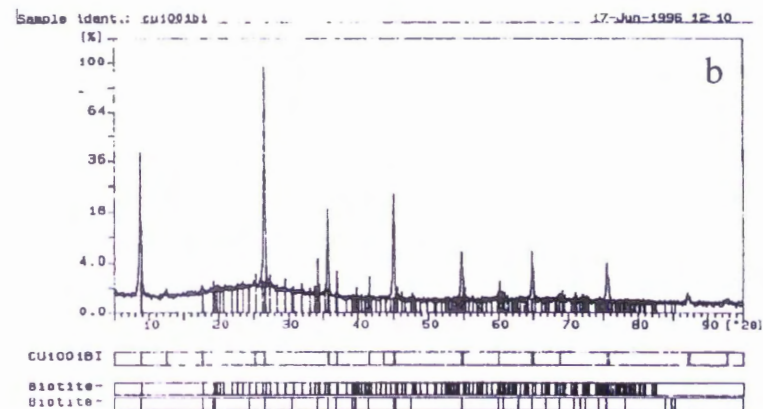
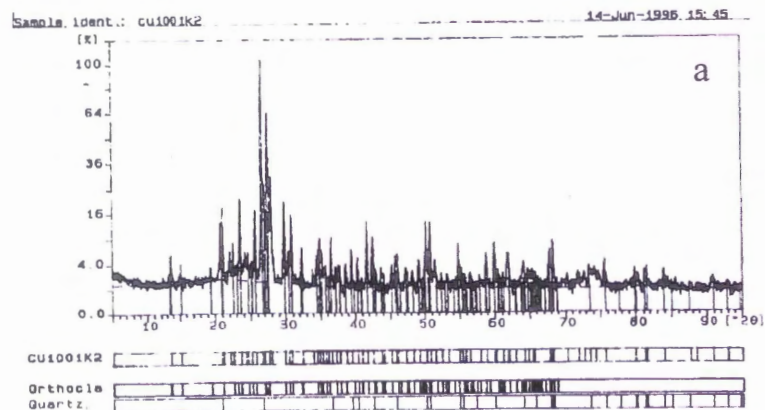


Figure 3.3a-c a) XRD identification of perthitic orthoclase and quartz in Cu-1001K. b) XRD identification of biotite in Cu-1001Bi. c) photomicrograph of Cu-1001 showing perthitic orthoclase in the upper left, slightly chloritized biotite at bottom-centre with quartz grains between. (magn. 5X; scale bar = 380mm; PPL)

95% of all peaks generated including all major peaks (see Figure 3.4a). In thin section the orthoclase crystals show perthitic texture with inclusions of quartz, minor biotite, opaques and apatite (see Figure 3.4c). Only grains without biotite inclusions were selected for argon dating.

Cu-1002Bi: A good match for biotite (see Figure 3.4b). In thin section biotite occurs as good clean crystals with only slight chloritization along the edges of some grains. Only biotite grains that were not chloritized were selected for argon dating and XRD analysis (see Figure 3.4c).

Cu-1006K: The pattern from this sample provided a perfect match for orthoclase (see Figure 3.5a). In thin section K-feldspar was difficult to identify visually since it usually was obscured by clays (see Figure 3.5b) but once the mineral is mechanically separated good pink K-feldspar crystals became apparent. Although inclusions were undetectable, it is likely that kaolinite was present as was found from electron microprobe analysis. Over 95% of the peaks were identified and were attributable to orthoclase.

Cu-1010K: The pattern from this sample was a perfect match for orthoclase (see Figure 3.6a). In thin section K-feldspar is difficult to identify visually since it usually was obscured by clays (see Figure 3.6b) but once the mineral is mechanically separated clean, pink K-feldspar crystals become apparent. Although no inclusions were identified, it is likely that kaolinite was present as was found from electron microprobe analysis. Over 95% of the peaks were identified and attributed to orthoclase.

Cu-1011SR: This sub-sample returned a perfect match for a combination of muscovite, illite and quartz (see Figure 3.7a) when combined with its light yellow-green colour and very fine grained nature, confirms this as a sericite. In thin section the very fine grained nature of sericite can be seen with fine grained quartz intermixed (see Figure 3.7b).

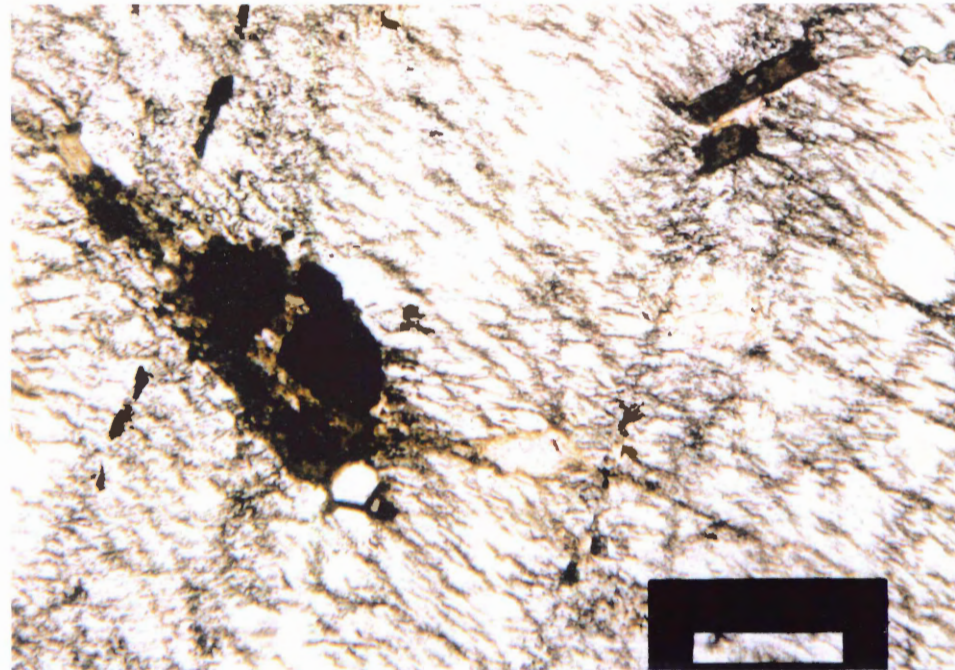
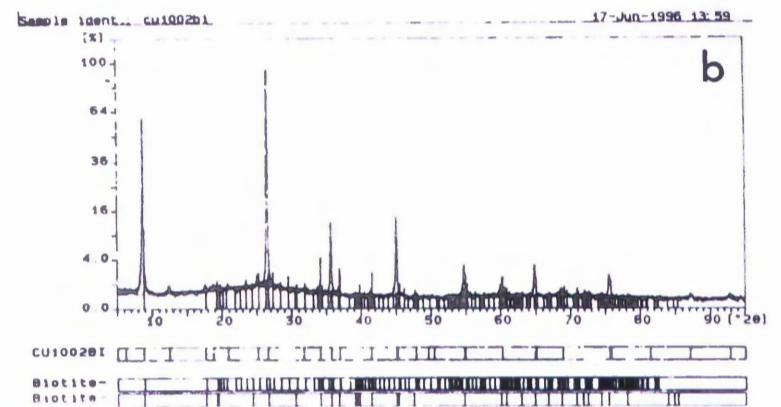
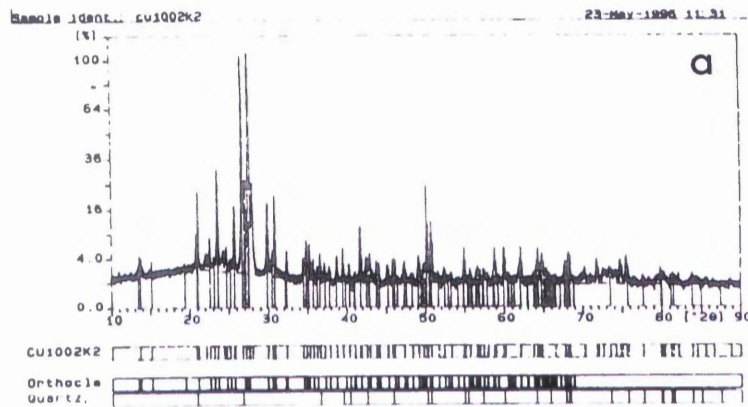


Figure 3.4a-c a) XRD identification of perthitic orthoclase and quartz in Cu-1002K. b) XRD identification of biotite in Cu-1002Bi. c) Photomicrograph of Cu-1002 showing K-feldspar phenocryst with minor inclusions of biotite and opaque minerals. (magn. 5X; scale bar = 380mm; PPL)

Sample ident.: cu1006k

14-May-1996 15:50

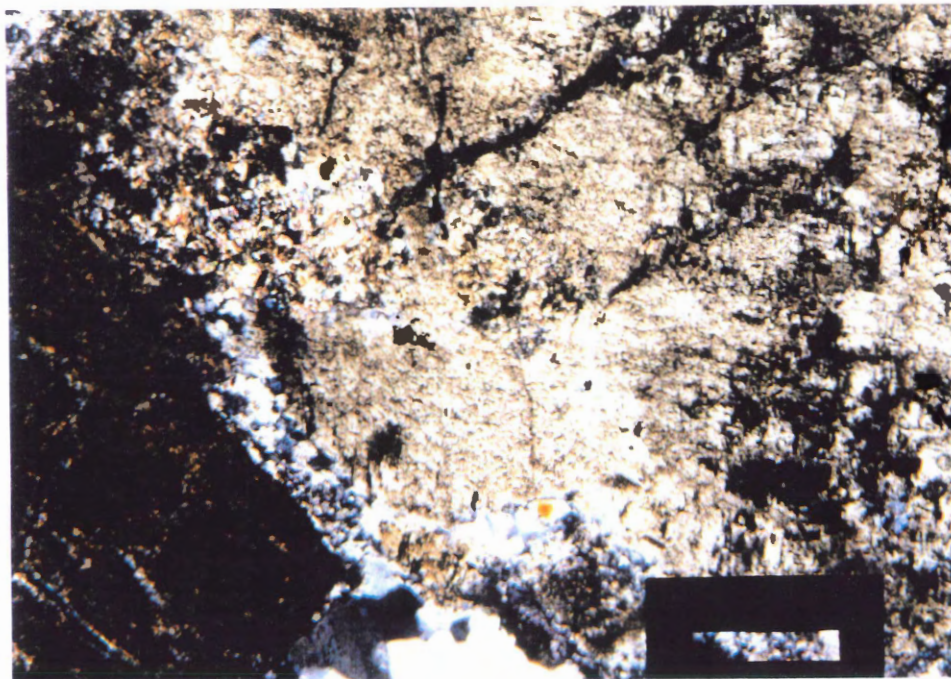
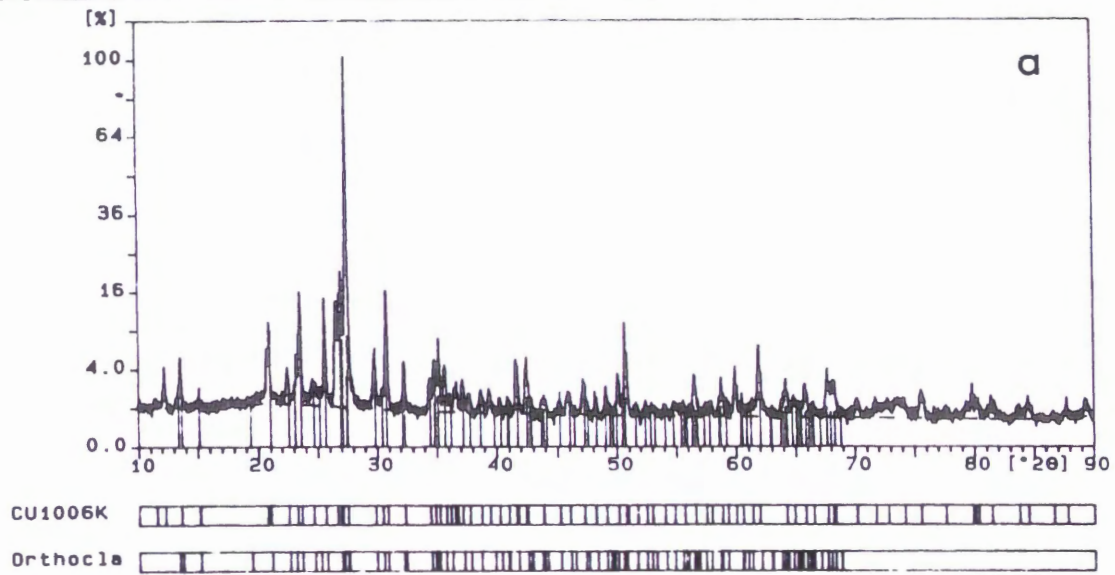


Figure 3.5a-b a) XRD identification of orthoclase and quartz in Cu-1006K. b) Photomicrograph of Cu-1006 showing orthoclase at centre with quartz and then kaolinite at bottom left. (magn. 5X; scale bar = 380mm; XPL)

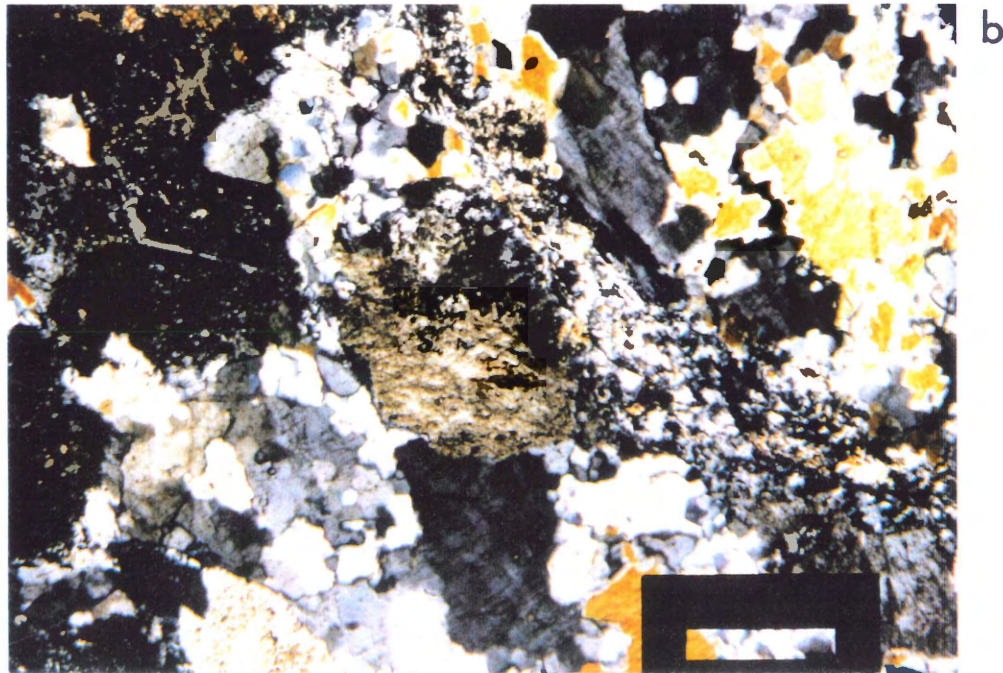
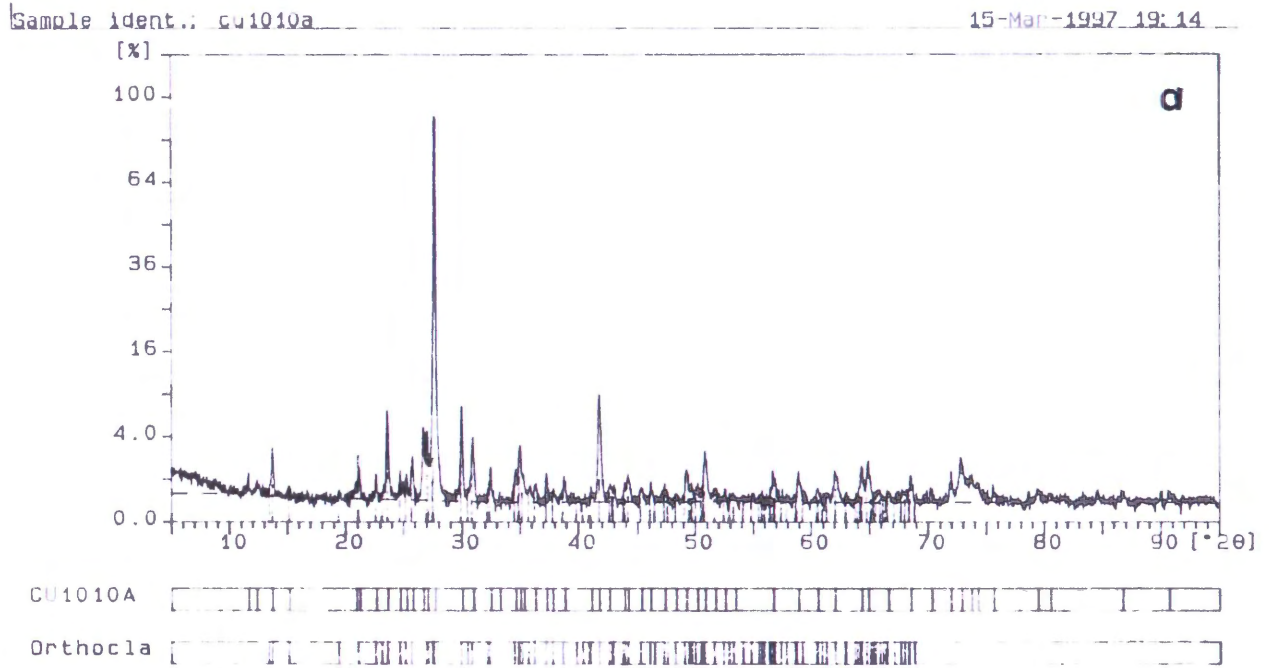


Figure 3.6a-b a) XRD identification of orthoclase and quartz in Cu-1010K. b) Photomicrograph of Cu-1010 showing orthoclase at centre surrounded by quartz grains. Kaolinite appears in the upper left. (magn. 5X; scale bar = 380mm; XPL)

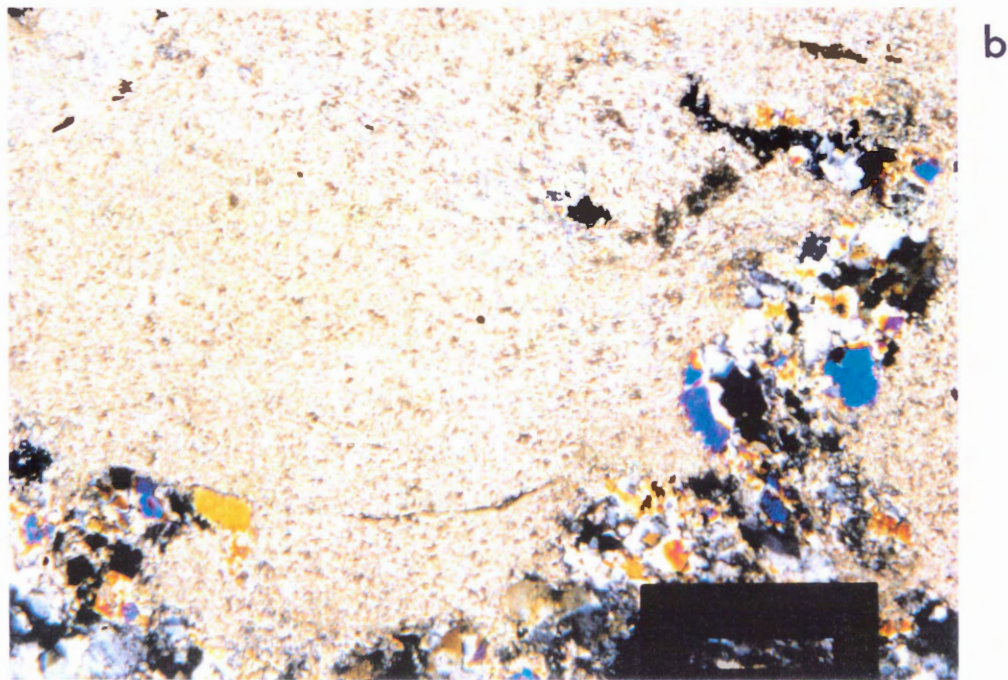
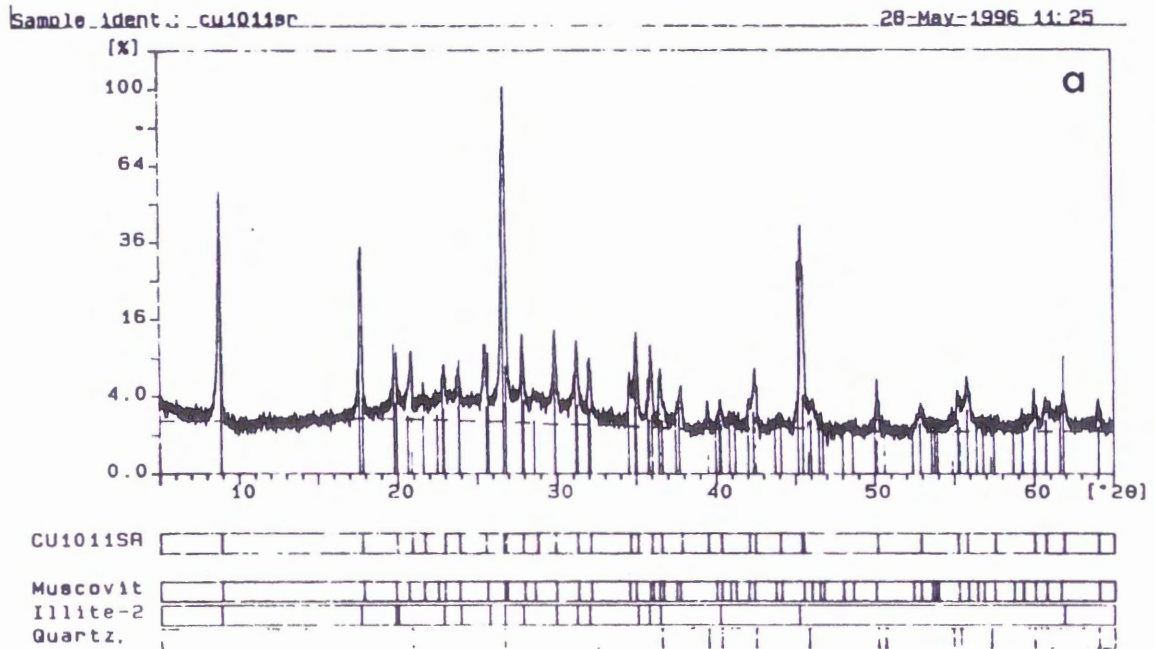


Figure 3.7a-b a) XRD identification of sericite in Cu-1011. b) Photomicrograph of Cu-1011 showing dominant fine-grained sericite throughout most of the field of view with coarser-grained, quartz as the only other mineral visible. (magn. 5X; scale bar = 380mm; XPL)

Cu-1011SK: This sub-sample was originally thought to be a potassium feldspar grain. This mineral separate was spotted with a white powdery mineral which, with only visual means of identification, may have been either sericite or kaolinite. Subsequent XRD analysis revealed only orthoclase. When sample Cu-1011SK was run through the step-wise degassing process, it was determined that this sample behaved as a sericite from the characteristic manner in which argon gas was evolved. Further examination of Cu-1011SK (XRD, electron microprobe and petrology) has resulted in the decision to reclassify this sub-sample as a sericite that is almost identical to sub-sample Cu-1011SR.

3.5 Perthitic Textures, K-Feldspar Origin and the Validity of Using K-feldspar for $^{40}\text{Ar}/^{39}\text{Ar}$ Dating

Cu-999, Cu-1001, Cu1002 all have perthitic textures (see Figure 3.8). Perthite textures have two possible origins: exsolution of the sodic phase as a primary magmatic potassium feldspar cooled, or a reaction with sodic-rich fluids acting on earlier-formed potassium feldspar. In either case, the presence of perthitic texture suggests that the potassium feldspar from DDH3439 was formed in late-magmatic conditions (Gates, 1953). These samples were specifically selected because of their location outside the main ore body in the hopes that these samples had been only minimally affected by alteration effects.

Perthitic textures have long been said to provide pathways for increased argon diffusion resulting in argon-loss (up to 40%) and an anomalously young age generated by $^{40}\text{Ar}/^{39}\text{Ar}$ dating (Sardarov, 1957; Berger, 1975). However, Parsons et al. (1988) state that it is incorrect to assume that perthite lamellar interfaces invariably provide a channel for argon-loss and that the

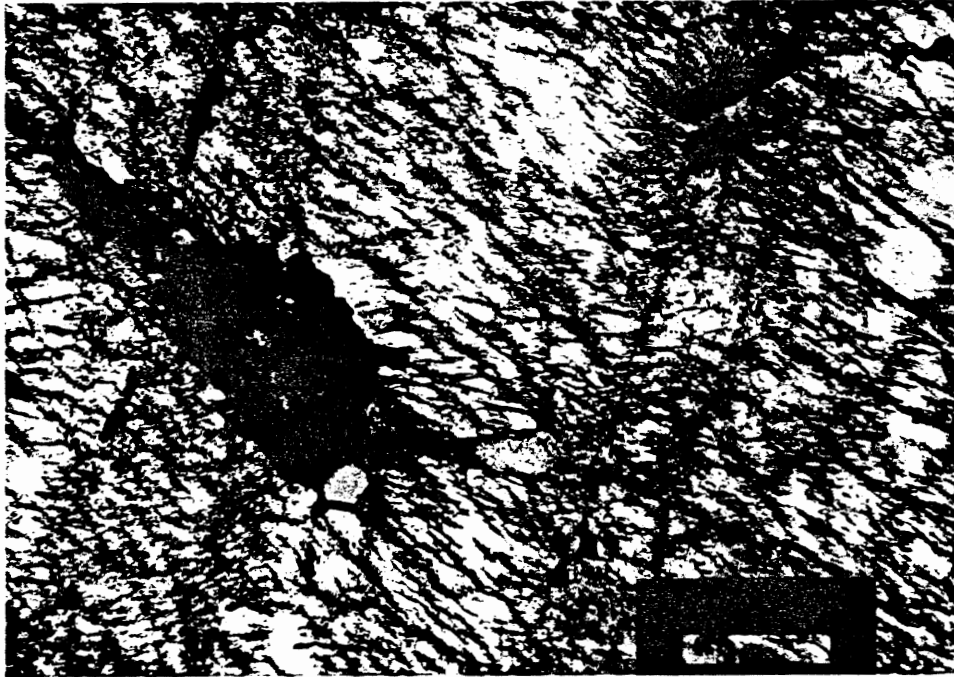


Figure 3.8 This photomicrograph of Cu-1002 shows narrow albite lamellae forming perthitic texture within the orthoclase host grain. The role of these lamellae as pathways that allow significant argon-loss is controversial (Sardarov, 1957; Parsons et al., 1988). Strong correlation of argon dates between biotite and K-feldspar grains from the same sample suggests that the lamellae do not result in significant argon-loss. (scale bar = 380 μ m; PPL)

great majority of perthites studied have been found to be fully coherent. Parsons et al. (1988) also observe that the coarseness of the exsolution texture has no correlation with argon retention. Therefore, it will be assumed that the perthitic K-feldspars found in the DDH3439 samples are valid for $^{40}\text{Ar}/^{39}\text{Ar}$ dating.

3.6 Triclinicity Tests and Cooling Rates of Potassium Feldspars

The potassium feldspar crystals may exist as triclinic or monoclinic structures. The time period over which a potassium feldspar crystal has to cool determines its structure. Microclines, which are plutonic in origin and have undergone slow cooling, have more time for their crystal structure to become ordered. Microcline crystals are triclinic as are some orthoclase crystals. On the other hand, sanidine and some orthoclase crystals are monoclinic as a result of fast cooling.

In the test for triclinicity, one examines the range of 29.5° to 30.2° 2θ $\text{CuK}\alpha$ in X-ray diffraction patterns of potassium feldspars and determines if a single high intensity peak exists or if two exist. Triclinic potassium feldspars will exhibit a double peak within this range of 2θ $\text{CuK}\alpha$ demonstrating greater ordering of the crystal structure. Monoclinic potassium feldspars having very little ordering in their crystal structure will exhibit only a single high intensity peak with this range.

Monoclinic potassium feldspars are 'expected to have cooled quickly and their presence would indicate a volcanic or high-level subvolcanic environment' whereas triclinic potassium feldspars are expected to have 'crystallized slowly under plutonic conditions in deep-seated granites and in most metamorphic rocks' (Hutchison, 1974).

In all cases, the potassium feldspars examined during this study exhibited a single, high-intensity peak within the range of 29.5° and 30.2° 2θ $\text{CuK}\alpha$ (see Figure 3.9). This is indicative of fast cooling and high-level subvolcanic emplacement which concurs with the porphyritic textures observed in hand specimen.

3.7 Electron Microprobe Methods

The electron microprobe at Dalhousie University's Earth Sciences Department was used to determine the potassium content and homogeneity of potassium distribution in the dated samples and among the entire sample set. The microprobe was also used to identify any potassium-bearing phases or inclusions that might contaminate the argon dating analysis. Grain mounts were made of each dated mineral. These were carbon coated before being mounted in the electron microprobe for analysis. The JEOL 733 electron microprobe is equipped with four wavelength-dispersive spectrometers and an Oxford Link eXL energy dispersive system, the latter of which was used for all elements analyzed. Resolution of the energy dispersive detector was 137eV at 5.9KeV. Each spectrum was acquired for 40 seconds with an accelerating voltage of 15Kv and a beam current of 15nA. The width of the microprobe beam was approximately 1 micron. Raw data correction was done using Link's ZAF matrix correction program.

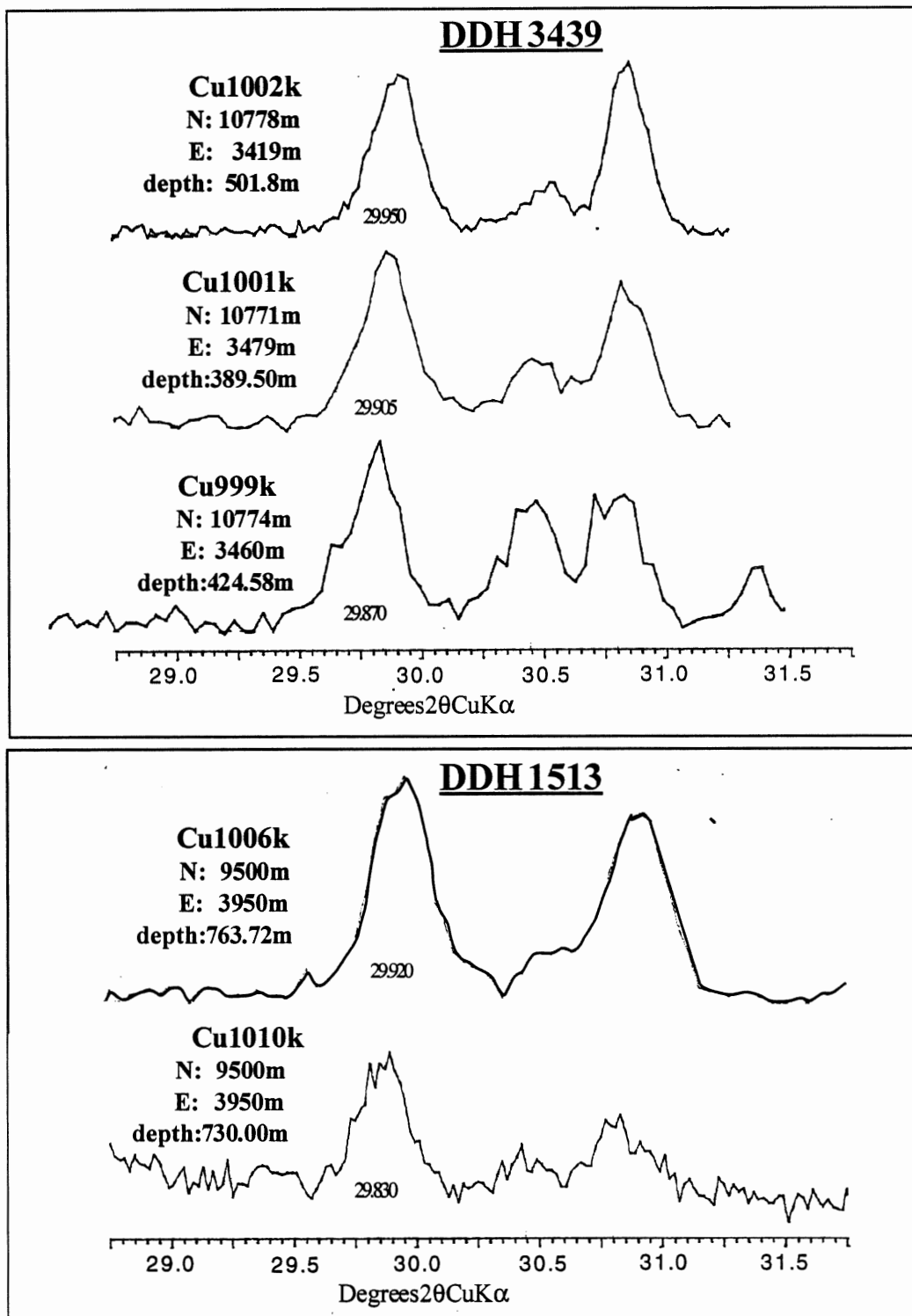


Figure 3.9 Alkali-feldspars with a single high intensity peak in the range of 29.82-29.97 degrees 2θ (Cu K α) are expected to have cooled rapidly and are indicative of volcanic or high-level sub-volcanic environments (Hutchison, 1974).

3.8 Electron Microprobe Results

Data and detection limits from electron microprobe analyses can be found in Appendix C. Two main conclusions were drawn from the results of electron microprobe analysis. First, few samples contained potassium-bearing inclusions that would result in anomalous ages from argon dating. These samples were all from DDH3439. The K-feldspar grains contained small amounts of biotite in some cases but these did not pose a problem since the inclusions were easily avoided during the mineral separation process through crushing and manual picking of inclusion-free grains. This is supported by X-ray diffraction analysis which did not identify these problematic inclusions.

The second conclusion was that potassium was homogeneously distributed throughout each dated mineral grain from edges to centres irrespective of mineral type (see Table 3.1a-c). Spot analyses on 144 grains which included K-feldspar, biotite and sericite also proved that potassium content is relatively constant among each of these minerals. These spot analyses can be seen for a sample grain from each dated mineral in Figures 3.10-3.19 on the following pages.

Table 3.1a Averaged K-feldspar Microprobe Data for RT Dated Samples - January 15-16, 1997

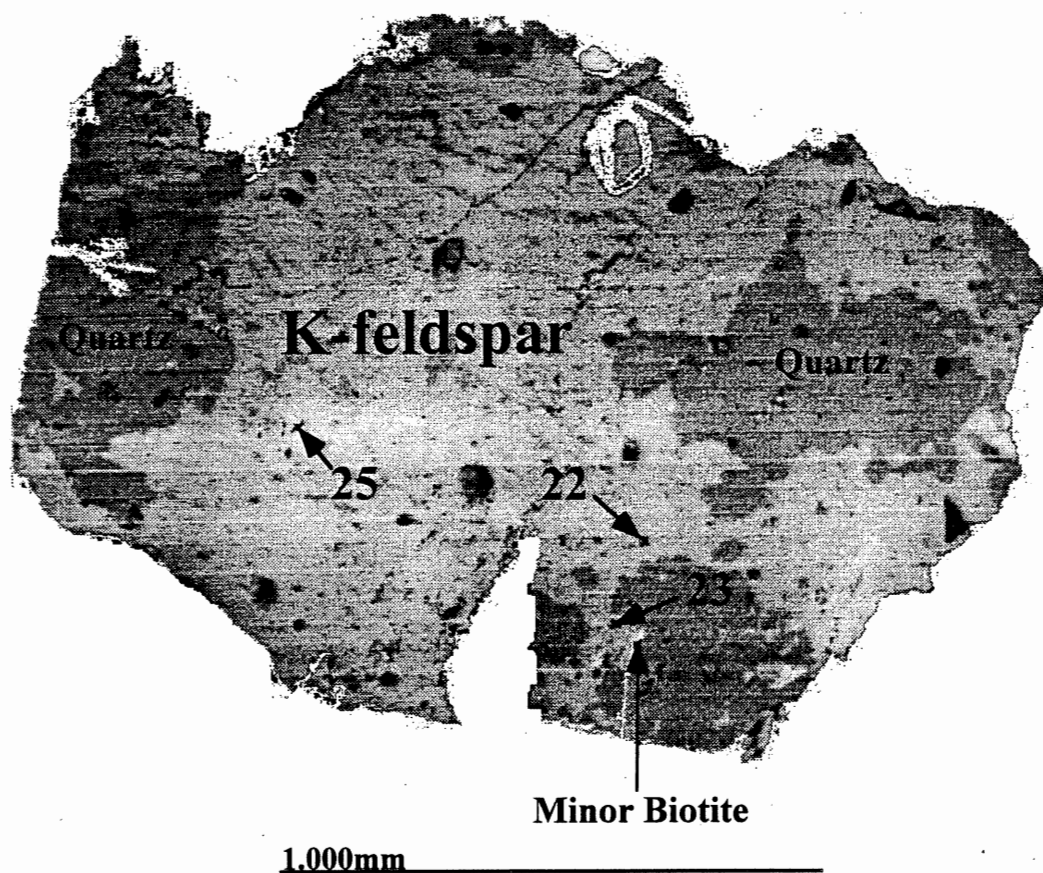
| Sample # | SiO ₂ | Al ₂ O ₃ | Na ₂ O | K₂O | BaO | Total |
|--------------------|------------------|--------------------------------|-------------------|-----------------------|------|-------|
| Cu1006 | 63.91 | 18.62 | 1.74 | 13.53 | 0.84 | 98.42 |
| Cu1010 | 63.25 | 18.45 | 1.58 | 13.56 | 1.08 | 97.77 |
| Cu999 | 63.12 | 18.45 | 1.03 | 14.69 | 1.27 | 98.38 |
| Cu1001 | 63.46 | 18.38 | 1.22 | 14.60 | 0.95 | 98.20 |
| Cu1002 | 62.96 | 18.61 | 1.62 | 13.78 | 1.44 | 98.42 |
| Average K-feldspar | 63.34 | 18.50 | 1.44 | 14.03 | 1.12 | 98.24 |

Table 3.1b Averaged Biotite Microprobe Data for RT Dated Samples - January 15-16, 1997

| Sample # | SiO ₂ | TiO ₂ | Al ₂ O ₃ | FeO | MnO | MgO | Na ₂ O | K₂O | Cl | Total |
|-----------------|------------------|------------------|--------------------------------|-------|------|-------|-------------------|-----------------------|------|-------|
| Cu999 | 34.96 | 3.42 | 13.09 | 13.86 | 0.45 | 14.15 | | 8.36 | | 88.51 |
| Cu1001 | 35.96 | 3.37 | 13.82 | 13.41 | 0.29 | 14.40 | 0.30 | 8.35 | 0.10 | 89.70 |
| Cu1002 | 37.21 | 3.39 | 14.43 | 14.04 | 0.35 | 14.95 | 0.34 | 8.32 | 0.11 | 93.13 |
| Average Biotite | 36.05 | 3.39 | 13.78 | 13.77 | 0.36 | 14.50 | 0.32 | 8.34 | 0.11 | 90.45 |

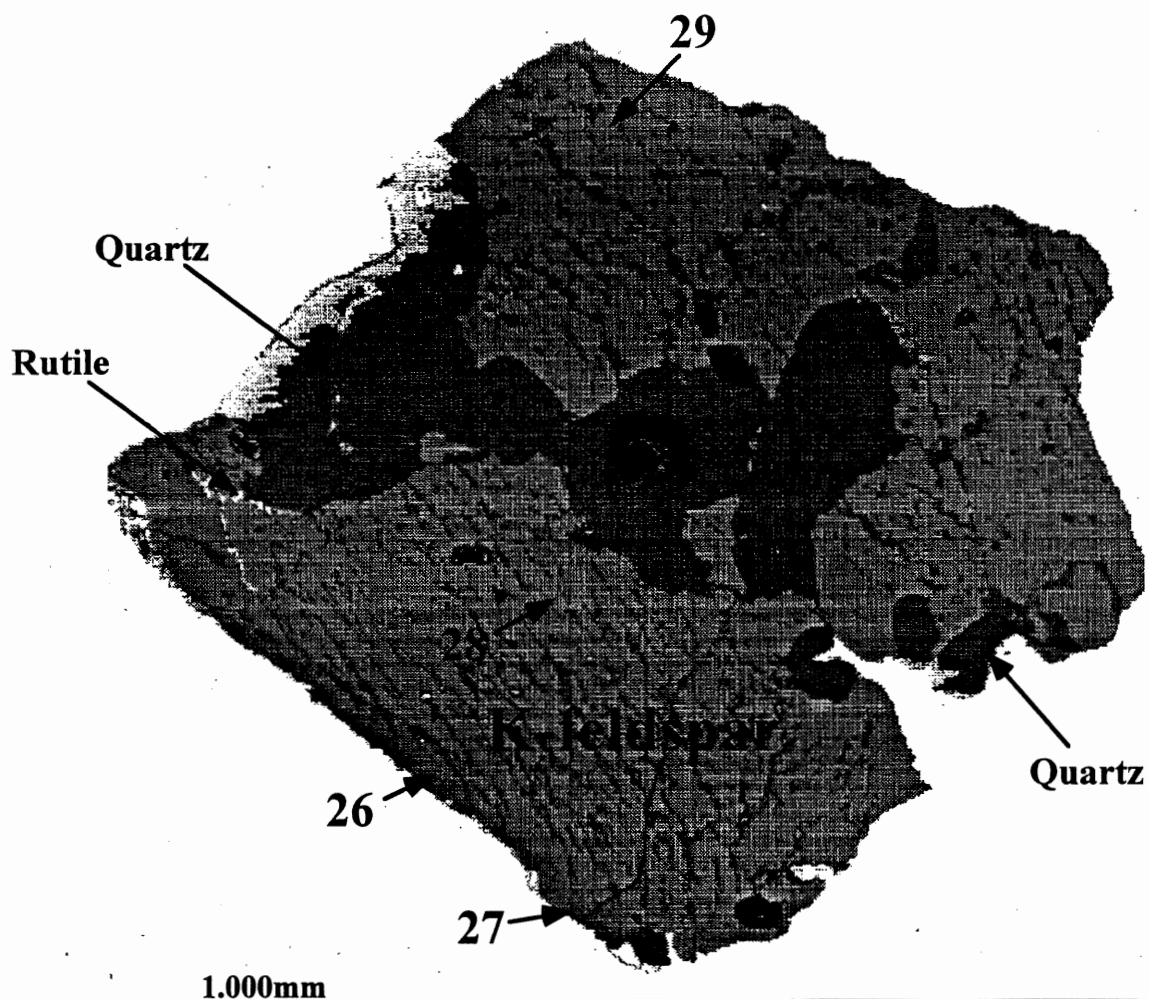
Table 3.1c Averaged Sericite Microprobe Data for RT Dated Samples - January 15-16, 1997

| Sample # | SiO ₂ | Al ₂ O ₃ | FeO | MgO | Na ₂ O | K₂O | Total |
|------------------|------------------|--------------------------------|------|------|-------------------|-----------------------|-------|
| Cu1011SK | 45.47 | 34.97 | 1.24 | 0.60 | 0.39 | 8.89 | 91.84 |
| Cu1011SR | 46.63 | 33.87 | 0.95 | 1.23 | 0.36 | 8.58 | 91.61 |
| Average Sericite | 46.05 | 34.42 | 1.09 | 0.91 | 0.38 | 8.74 | 91.72 |



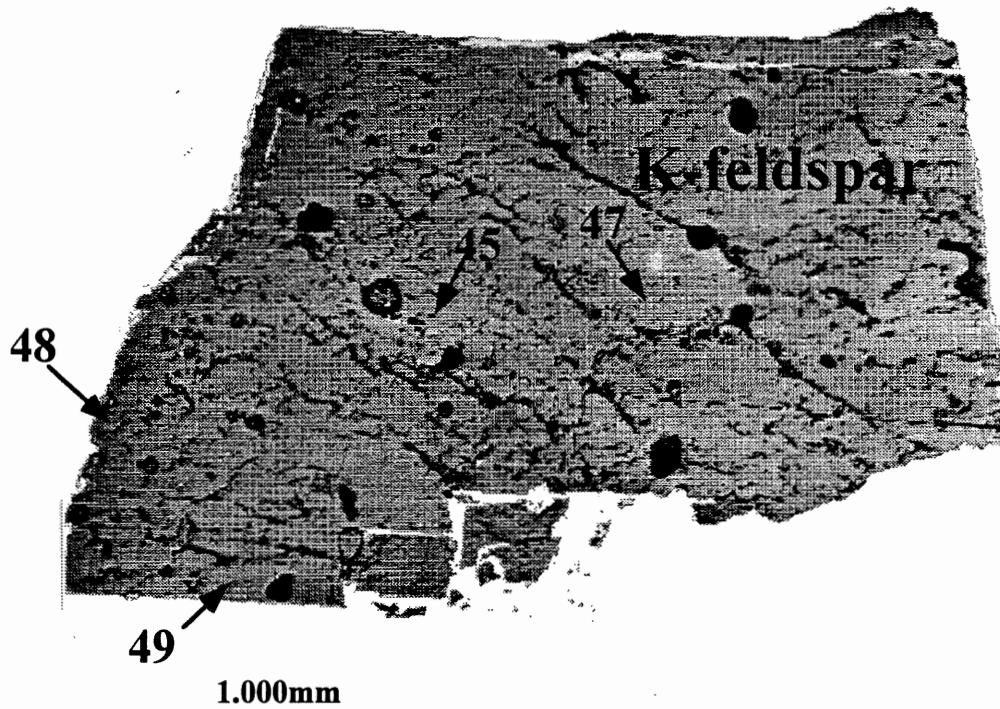
| Point | SiO ₂ | Al ₂ O ₃ | Na ₂ O | K ₂ O | BaO | Total |
|-------------------|------------------|--------------------------------|-------------------|------------------|------|-------|
| 22 | 63.46 | 18.30 | 0.63 | 15.63 | 0.59 | 98.61 |
| 23 | 63.71 | 18.20 | 0.97 | 15.29 | | 98.16 |
| 25 | 62.83 | 18.74 | 1.68 | 13.62 | 1.58 | 98.46 |
| avg | 63.33 | 18.42 | 1.09 | 14.85 | 1.09 | 98.41 |
| avg RT K-feldspar | 63.34 | 18.50 | 1.44 | 14.03 | 0.96 | 98.31 |

Figure 3.10 Electron microprobe image of Cu-999K. The numbered points on the image correspond to the table of analyses. Perthitic texture (best seen in upper-centre of image) in the crystal was due to unmixing of sodic-plagioclase from K-feldspar although the possibility exists that this texture may be the result of the exposure of K-feldspar to sodic-rich hydrothermal fluids (Gates, 1953). Other minerals within the Cu-999K grains were determined to be quartz and minor biotite. Biotite did not pose a problem, as it was easily eliminated through mechanical separation methods. No inclusions of biotite were visible in the samples submitted for $^{40}\text{Ar}/^{39}\text{Ar}$ dating and subsequent argon dating results did not indicate the presence of a second potassium-bearing phase within the K-feldspar.



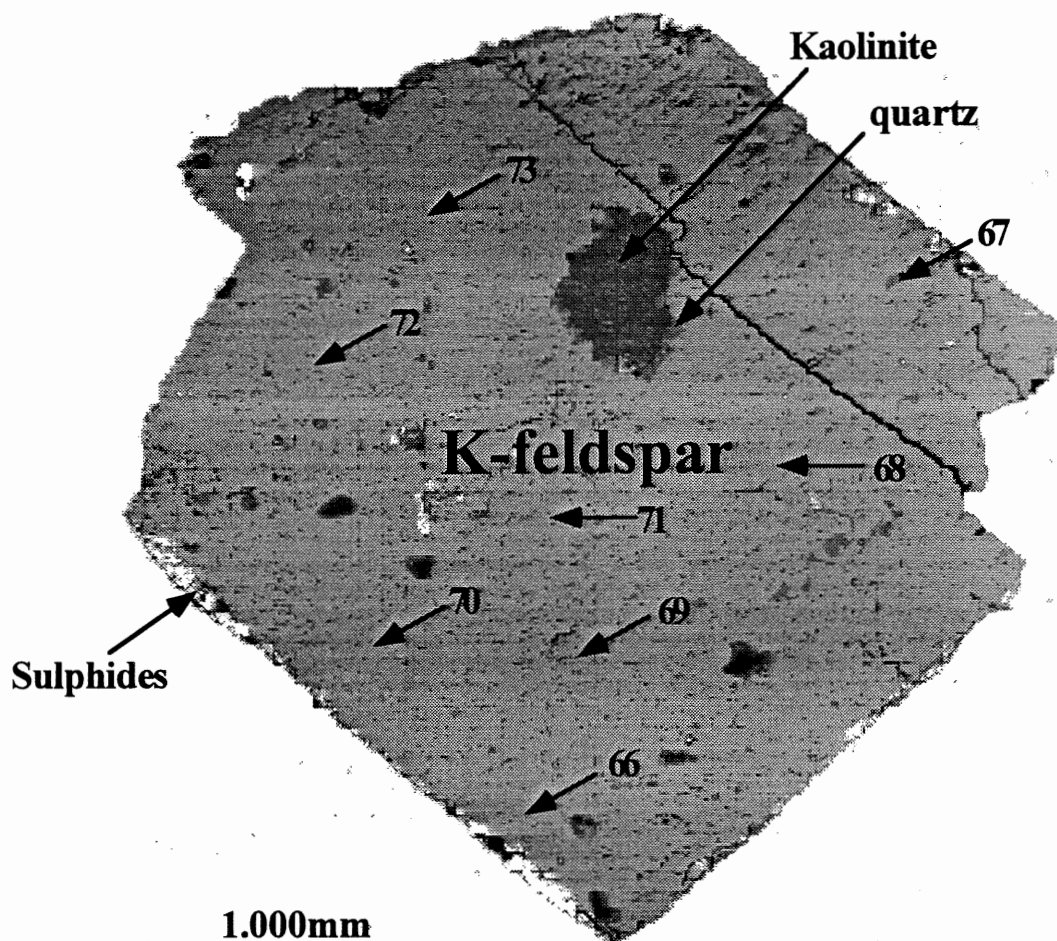
| Point | SiO ₂ | Al ₂ O ₃ | Na ₂ O | K ₂ O | BaO | Total |
|-------------------|------------------|--------------------------------|-------------------|------------------|------|-------|
| 26 | 64.22 | 18.21 | 1.36 | 14.78 | | 98.57 |
| 27 | 63.49 | 18.28 | 1.06 | 15.36 | | 98.18 |
| 28 | 63.29 | 18.73 | 1.62 | 13.53 | 1.51 | 98.66 |
| 29 | 63.71 | 18.13 | 0.88 | 14.48 | | 97.20 |
| avg | 63.68 | 18.34 | 1.23 | 14.54 | | 98.15 |
| avg RT K-feldspar | 63.34 | 18.50 | 1.44 | 14.03 | 0.96 | 98.31 |

Figure 3.11 Electron microprobe image of Cu-1001K. The numbered points on the image correspond to the table of analyses. Perthitic texture in the crystal was due to unmixing of sodic-plagioclase from K-feldspar although the possibility exists that this texture may be the result of the exposure of K-feldspar to sodic-rich hydrothermal fluids (Gates, 1953). Other minerals within the Cu-1001K grains were determined to be quartz and rutile.



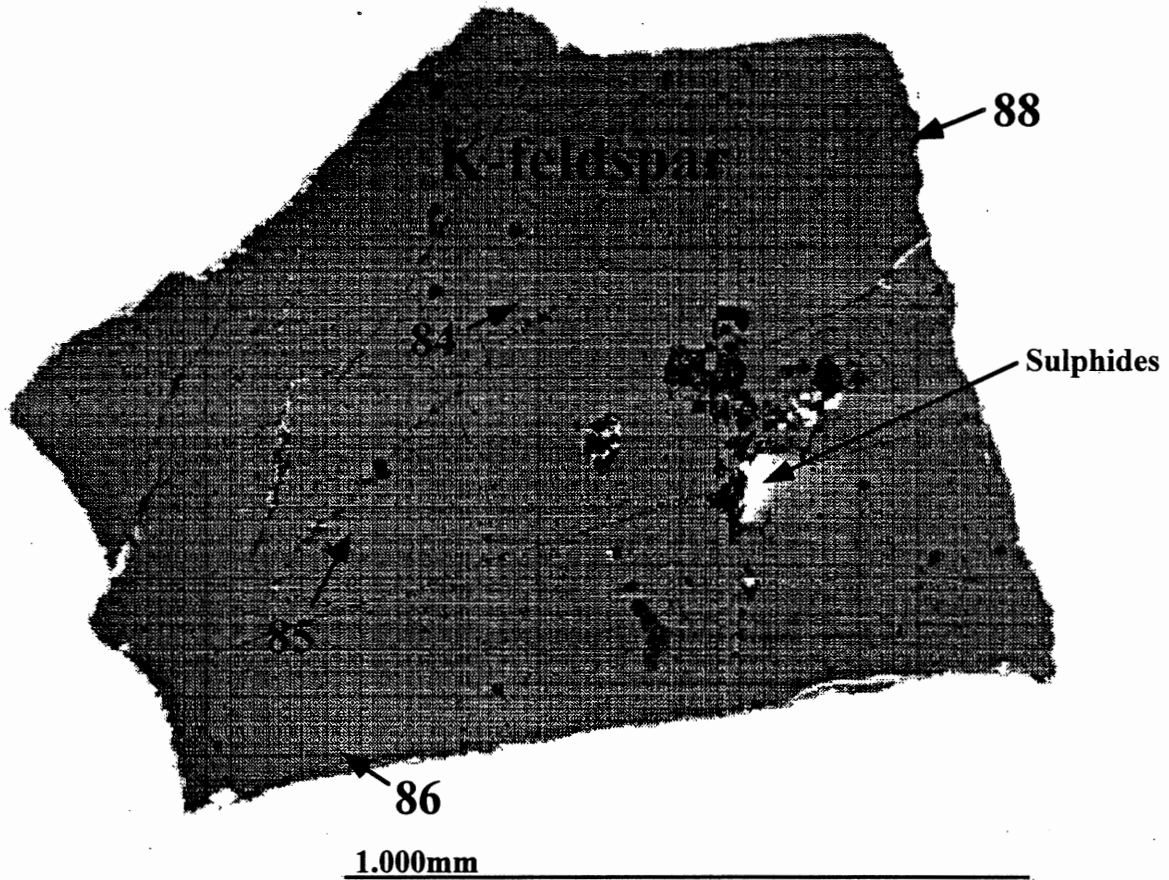
| Point | SiO ₂ | Al ₂ O ₃ | Na ₂ O | K ₂ O | BaO | Total |
|-------------------|------------------|--------------------------------|-------------------|------------------|------|-------|
| 45 | 62.90 | 18.62 | 1.71 | 13.58 | 1.39 | 98.20 |
| 47 | 63.09 | 18.76 | 1.46 | 14.16 | 1.65 | 99.12 |
| 48 | 62.85 | 18.60 | 1.44 | 14.10 | 1.69 | 98.68 |
| 49 | 62.57 | 18.73 | 1.63 | 13.56 | 1.59 | 98.08 |
| avg | 62.85 | 18.68 | 1.56 | 13.85 | 1.58 | 98.52 |
| avg RT K-feldspar | 63.34 | 18.50 | 1.44 | 14.03 | 0.96 | 98.31 |

Figure 3.12 Electron microprobe image of Cu-1002K. The numbered points on the image correspond to the table of analyses. Perthitic texture in the crystal was due to unmixing of sodic-plagioclase from K-feldspar although the possibility exists that this texture may be the result of the exposure of K-feldspar to sodic-rich hydrothermal fluids (Gates, 1953). Other minerals within the Cu-1002K grains were determined to be quartz, plagioclase phenocrysts and Fe-oxides.



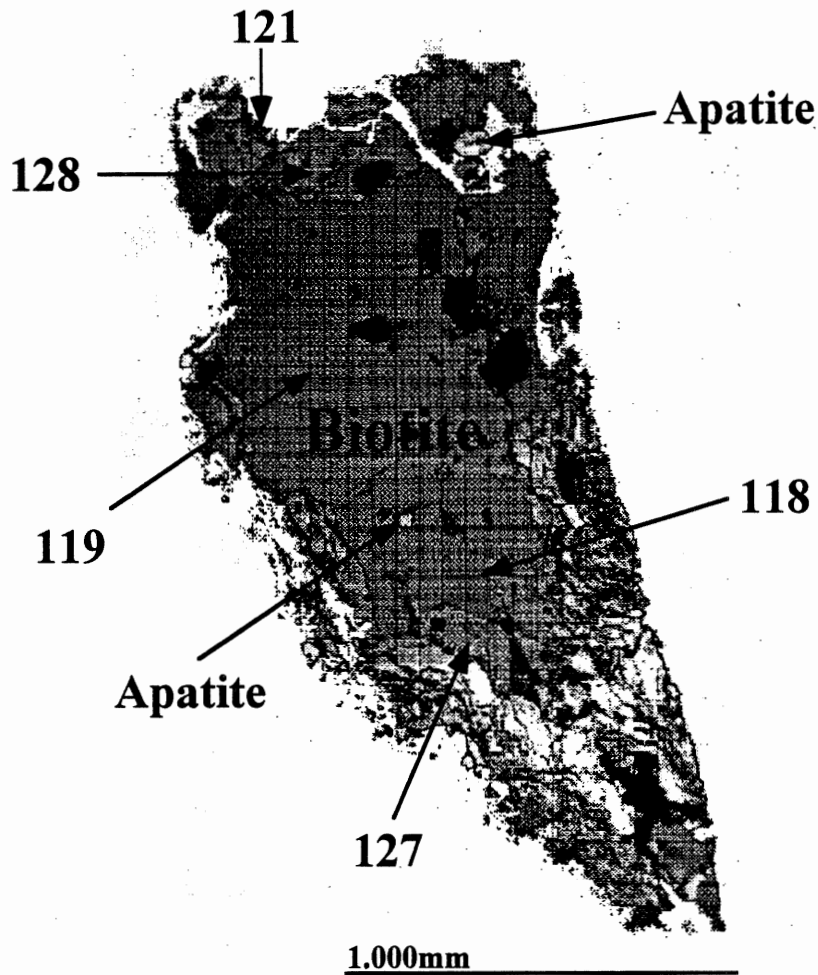
| Point | SiO ₂ | Al ₂ O ₃ | Na ₂ O | K ₂ O | Cl | BaO | Total |
|-------------------|------------------|--------------------------------|-------------------|------------------|------|------|-------|
| 66 | 63.65 | 18.36 | 1.23 | 14.36 | | 0.68 | 98.27 |
| 67 | 62.29 | 18.04 | 1.01 | 14.20 | | 0.74 | 96.27 |
| 68 | 63.53 | 18.09 | 1.01 | 14.46 | | | 97.08 |
| 69 | 53.68 | 15.55 | 0.85 | 12.95 | | | 83.03 |
| 70 | 63.40 | 18.44 | 1.19 | 14.60 | | 0.66 | 98.28 |
| 71 | 64.52 | 18.86 | 2.21 | 12.73 | | 0.80 | 99.12 |
| 72 | 63.15 | 18.54 | 2.30 | 13.12 | | 0.96 | 98.08 |
| 73 | 63.11 | 18.67 | 2.09 | 13.06 | 0.11 | 0.86 | 97.89 |
| avg | 62.17 | 18.03 | 1.52 | 13.59 | | 0.80 | 95.68 |
| avg RT K-feldspar | 63.34 | 18.50 | 1.44 | 14.03 | | 0.96 | 98.31 |

Figure 3.13 Electron microprobe image of Cu-1006K. The numbered points on the image correspond to the table of analyses. Inclusions in the K-feldspar crystal were determined to be quartz and kaolinite with sulphides at the edges of the grain.



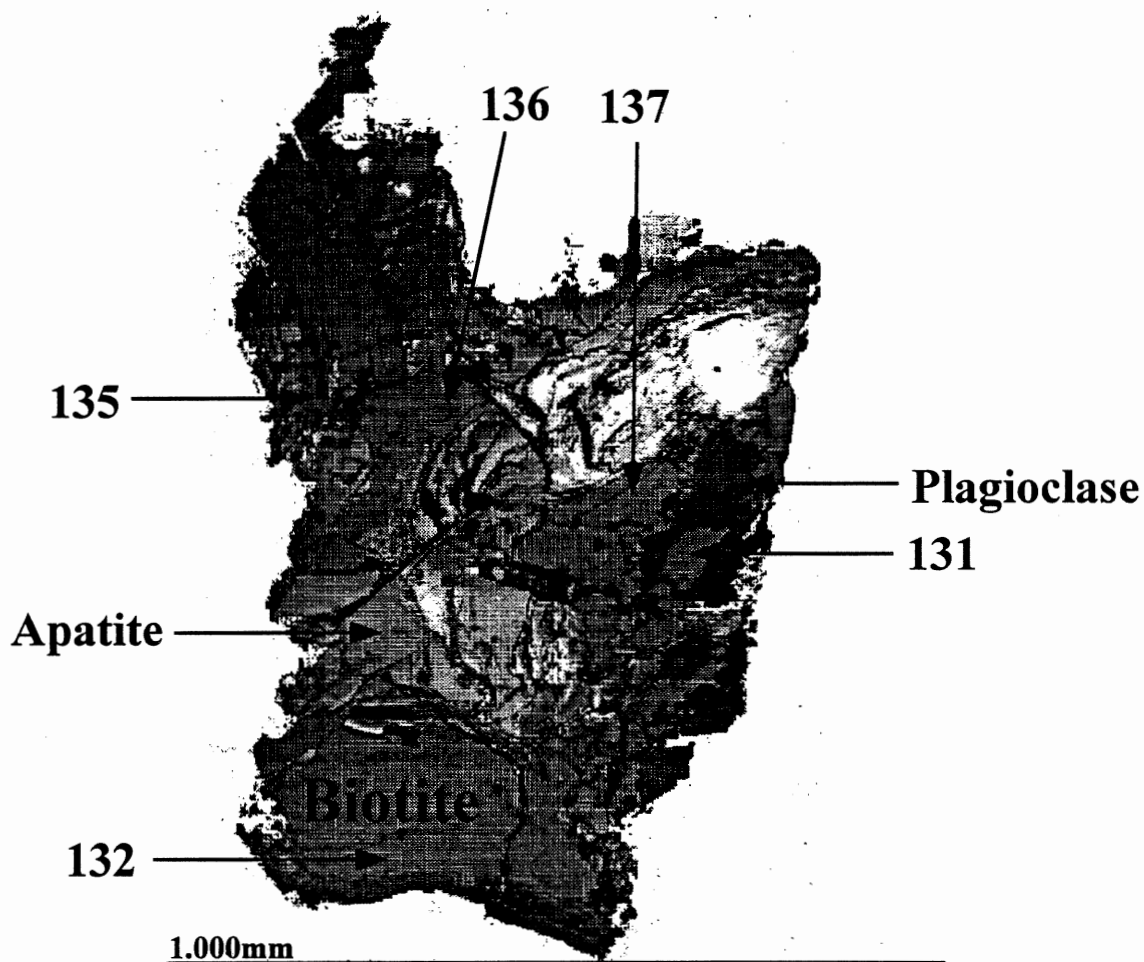
| Point | SiO ₂ | Al ₂ O ₃ | Na ₂ O | K₂O | BaO | Total |
|-------------------|------------------|--------------------------------|-------------------|-----------------------|------|-------|
| 84 | 61.90 | 18.48 | 1.34 | 13.86 | 1.79 | 97.37 |
| 85 | 63.01 | 18.71 | 2.33 | 12.84 | 1.65 | 98.53 |
| 86 | 63.32 | 19.02 | 2.22 | 12.74 | 1.16 | 98.46 |
| 88 | 63.55 | 18.65 | 1.15 | 14.46 | 0.81 | 98.62 |
| avg | 62.94 | 18.71 | 1.76 | 13.48 | 1.35 | 98.25 |
| avg RT K-feldspar | 63.34 | 18.50 | 1.44 | 14.03 | 0.96 | 98.31 |

Figure 3.14 Electron microprobe image of Cu-1010K. The numbered points on the image correspond to the table of analyses. Note the lack of perthitic texture in this crystal as compared to Cu-999K, Cu-1001K and Cu-1002K. Sulphides (seen as bright spots) represent the only mineral inclusion in this sample.



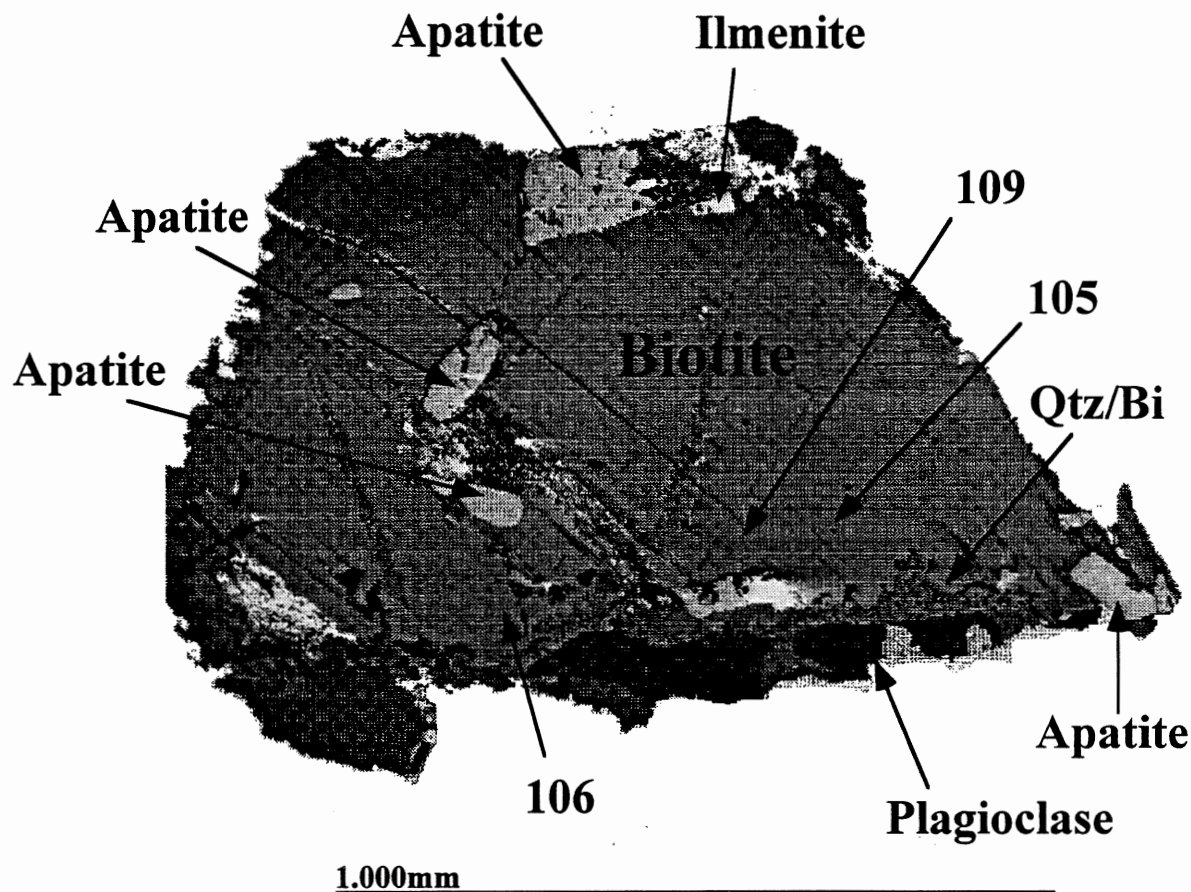
| Point | SiO ₂ | TiO ₂ | Al ₂ O ₃ | FeO | MnO | MgO | Na ₂ O | K ₂ O | Cl | BaO | Total |
|--------------------|------------------|------------------|--------------------------------|-------|------|-------|-------------------|------------------|------|------|-------|
| 118 | 36.63 | 3.79 | 13.59 | 14.69 | 0.54 | 14.86 | | 8.81 | | 0.74 | 93.65 |
| 119 | 36.10 | 3.73 | 13.37 | 14.68 | 0.58 | 14.51 | 0.28 | 8.72 | | | 91.97 |
| 121 | 35.80 | 3.28 | 13.70 | 15.08 | 0.31 | 14.19 | | 8.52 | 0.09 | | 90.96 |
| 127 | 34.30 | 3.31 | 12.76 | 13.66 | 0.41 | 13.82 | | 8.26 | | | 86.51 |
| 128 | 31.98 | 2.98 | 12.03 | 11.19 | 0.41 | 13.35 | | 7.49 | | | 79.44 |
| avg | 34.96 | 3.42 | 13.09 | 13.86 | 0.45 | 14.15 | | 8.36 | | | 88.51 |
| Average RT Biotite | 36.20 | 3.38 | 13.80 | 13.77 | 0.36 | 14.60 | 0.34 | 8.38 | 0.10 | 0.87 | 90.73 |

Figure 3.15 Electron microprobe image of Cu-999Bi. The numbered points on the image correspond to the table of analyses. There appears to be little variation in potassium content within individual grains, among the grains of one sample and as well, among the entire sample set. Two forms of biotite are present in this sample based on Fe content. Analysis points 127 and 128 show higher Fe amounts than in points 118-121. This compositional variation appears to be responsible for a slight difference in the colouring of the biotite in the image above. There are also inclusions of plagioclase and apatite within this sample.



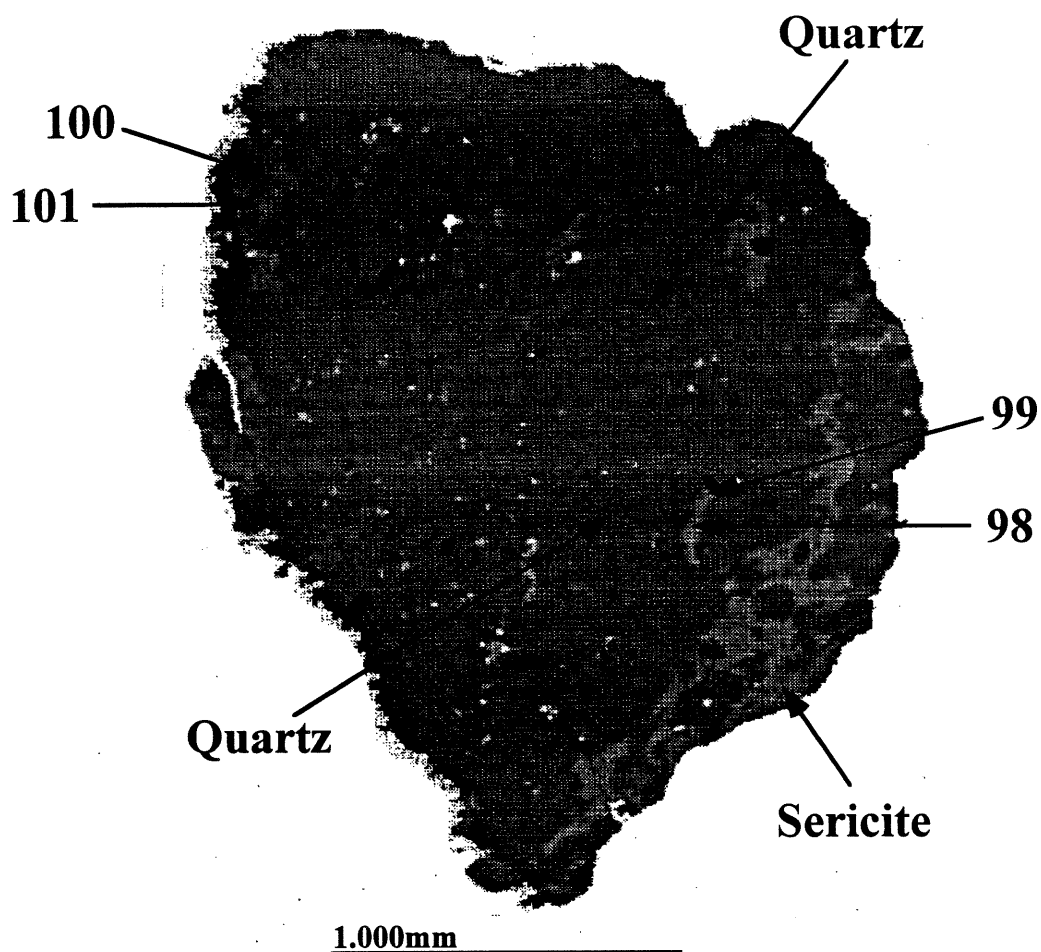
| Point | SiO ₂ | TiO ₂ | Al ₂ O ₃ | FeO | MnO | MgO | Na ₂ O | K ₂ O | Cl | BaO | Total |
|--------------------|------------------|------------------|--------------------------------|-------|------|-------|-------------------|------------------|------|------|-------|
| 131 | 37.15 | 3.53 | 14.15 | 14.78 | | 14.59 | 0.31 | 8.63 | 0.10 | | 93.23 |
| 132 | 35.35 | 3.79 | 13.88 | 15.17 | 0.29 | 13.56 | | 8.69 | | 1.01 | 91.73 |
| 135 | 33.72 | 2.89 | 13.12 | 11.99 | 0.27 | 13.38 | 0.25 | 7.70 | | | 83.33 |
| 136 | 36.16 | 3.15 | 14.10 | 12.37 | | 14.33 | 0.28 | 8.20 | 0.12 | | 88.70 |
| 137 | 37.40 | 3.86 | 14.30 | 15.09 | | 14.20 | | 8.81 | 0.09 | | 93.74 |
| avg | 35.95 | 3.44 | 13.91 | 13.88 | 0.28 | 14.01 | 0.28 | 8.40 | 0.10 | 1.01 | 90.14 |
| Average RT Biotite | 36.20 | 3.38 | 13.80 | 13.77 | 0.36 | 14.60 | 0.34 | 8.38 | 0.10 | 0.87 | 90.73 |

Figure 3.16 Electron microprobe image of Cu-1001Bi. The numbered points on the image correspond to the table of analyses. There appears to be little variation in potassium content within individual grains, among the grains of one sample and as well, among the entire sample set. There are inclusions of plagioclase and apatite in this sample as well.



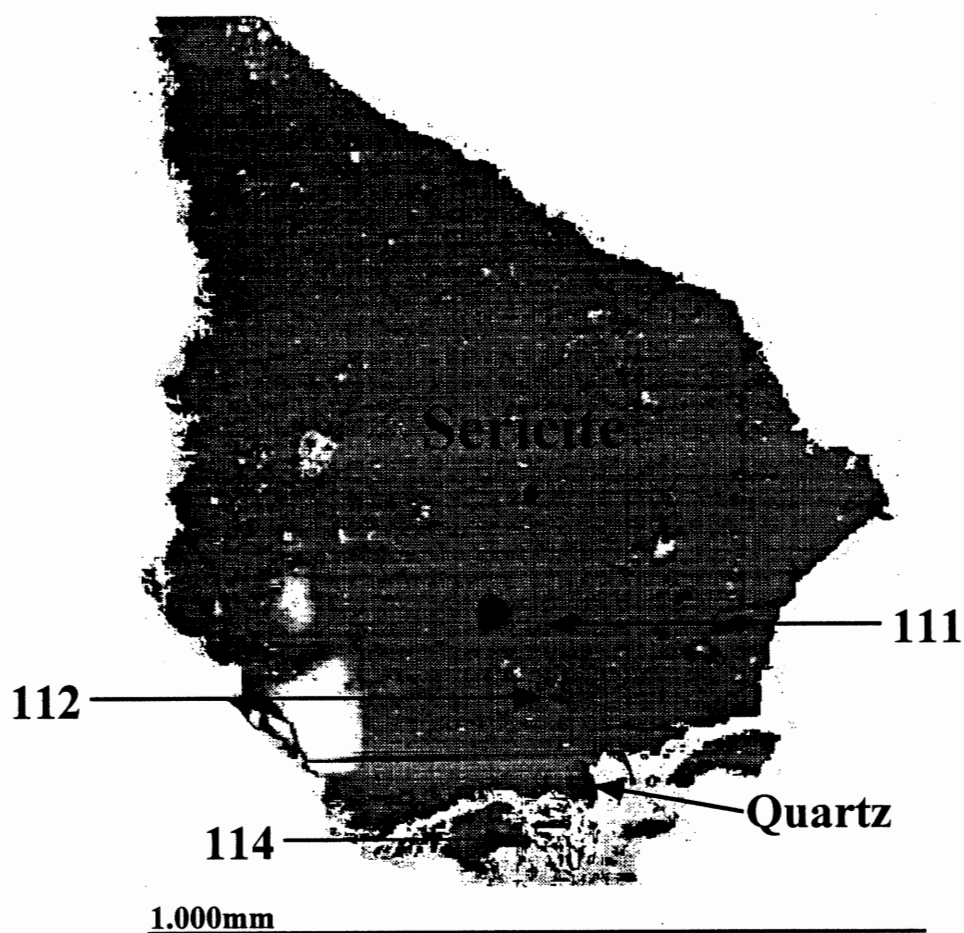
| Point | SiO ₂ | TiO ₂ | Al ₂ O ₃ | FeO | MnO | MgO | Na ₂ O | K ₂ O | Cl | BaO | Total |
|--------------------|------------------|------------------|--------------------------------|-------|------|-------|-------------------|------------------|------|------|-------|
| 105 | 36.59 | 4.00 | 14.25 | 14.48 | 0.36 | 13.99 | | 8.32 | 0.10 | | 92.09 |
| 106 | 37.17 | 2.57 | 14.90 | 14.28 | 0.38 | 14.88 | | 8.06 | | | 92.24 |
| 109 | 37.94 | 3.11 | 15.58 | 14.20 | 0.31 | 14.85 | 0.29 | 8.68 | | | 94.96 |
| avg | 37.23 | 3.23 | 14.91 | 14.32 | 0.35 | 14.57 | | 8.35 | | | 93.10 |
| Average RT Biotite | 36.20 | 3.38 | 13.80 | 13.77 | 0.36 | 14.60 | 0.34 | 8.38 | 0.10 | 0.87 | 90.73 |

Figure 3.17 Electron microprobe image of Cu-1002Bi. The numbered points on the image correspond to the table of analyses. There appears to be little variation in potassium content within individual grains, among the grains of one sample and as well, among the entire sample set. There are inclusions of plagioclase, ilmenite and apatite. As well there is a myrmekitic intergrowth of biotite and quartz (labelled Qtz/Bi).



| Point | SiO ₂ | TiO ₂ | Al ₂ O ₃ | FeO | MgO | Na ₂ O | K ₂ O | Cl | Total |
|---------------------|------------------|------------------|--------------------------------|------|------|-------------------|------------------|------|-------|
| 98 | 45.46 | | 35.48 | 1.03 | 0.46 | 0.36 | 9.24 | | 92.02 |
| 99 | 45.73 | | 35.51 | 0.81 | 0.62 | 0.41 | 9.04 | | 92.12 |
| 100 | 45.14 | 0.34 | 35.10 | 1.04 | 0.54 | 0.40 | 8.82 | | 91.38 |
| 101 | 45.55 | 0.32 | 33.79 | 2.08 | 0.78 | 0.41 | 8.48 | 0.43 | 91.85 |
| avg | 45.47 | 0.33 | 34.97 | 1.24 | 0.60 | 0.39 | 8.89 | | 91.84 |
| Average RT Sericite | 46.05 | 0.33 | 34.42 | 1.09 | 0.91 | 0.38 | 0.28 | | 92.13 |

Figure 3.18 Electron microprobe image of Cu-1011SK. The numbered points on the image correspond to the table of analyses. This sample is from a zone of quartz-sericite alteration. The only other mineral inclusions in this sample are digenite and covellite which were identified by reflected light microscopy.



| Point | SiO ₂ | TiO ₂ | Al ₂ O ₃ | FeO | MgO | Na ₂ O | K ₂ O | Total |
|---------------------|------------------|------------------|--------------------------------|------|------|-------------------|------------------|-------|
| 111 | 45.10 | | 34.45 | 0.94 | 0.83 | 0.26 | 8.27 | 89.85 |
| 112 | 46.02 | | 34.99 | 1.21 | 0.88 | 0.47 | 9.36 | 92.93 |
| 114 | 45.89 | | 34.56 | 1.31 | 1.01 | 0.37 | 9.40 | 92.54 |
| avg | 34.25 | | 26.00 | 0.86 | 0.68 | 0.28 | 6.76 | 91.77 |
| Average RT Sericite | 46.05 | 0.33 | 34.42 | 1.09 | 0.91 | 0.38 | 8.74 | 92.13 |

Figure 3.19 Electron microprobe image of Cu-1011SR. The numbered points on the image correspond to table of analyses. This sample is from a zone of quartz-sericite alteration and is mostly sericite with tiny quartz inclusions and veinlets. The only other mineral inclusions in this sample are digenite and covellite which were identified by reflected light microscopy .

Chapter 4

$^{40}\text{Ar}/^{39}\text{Ar}$ Dating

4.1 Argon Dating Theory

During the radioactive decay of the parent isotope ^{40}K , the daughter isotopes of ^{40}Ar and ^{40}Ca are produced. In argon dating, it is the production of ^{40}Ar that is important and 11.2% of ^{40}K atoms decay to ^{40}Ar with a decay constant of $4.962 \times 10^{-10}\text{yr}^{-1}$ (Steiger and Jäger, 1977). Under ideal conditions it is assumed that any ^{40}Ar present in a sample is the result of the decay of ^{40}K . Therefore, this type of argon is referred to as radiogenic argon, represented by the symbol $^{40}\text{Ar}^*$. Argon tends to remain in the gaseous phase as a magma cools and as an inert gas it does not combine with other elements to form compounds or minerals. However, the introduction of excess argon into the crystal structure through metamorphic or alteration processes may result in anomalously old apparent ages. In the case of hydrothermal systems, it is highly likely that argon is carried by the circulating fluids in the convection cell. Argon may therefore become incorporated in any newly forming hydrothermal minerals, in the low temperature domains of pre-existing or primary minerals as they undergo alteration, or within fluid inclusions. Domains are places in a crystal lattice that trap argon. Lower temperature domains require less energy to liberate or incorporate argon and are more likely to record lower temperature alteration processes such as quartz-sericite alteration which occurs at 200-350°C (Richards and McDougall, 1990). High temperature domains are less prone to the liberation or incorporation of argon and are

more likely to record higher temperature events such as primary cooling from a magma or potassic alteration (350-550°C, Rose and Burt, 1979). After taking excess argon into consideration, an accurate age for a mineral can be derived from the relative amounts of $^{40}\text{Ar}^*$ to ^{40}K present.

The amount of ^{40}K is measured indirectly by neutron activation analysis (McDougall and Harrison, 1988). Samples are irradiated with fast neutrons in a nuclear reactor, which converts a small proportion of ^{39}K to ^{39}Ar . For this process, the Radomiro Tomic samples were shipped to the reactor at McMaster University (Hamilton, Ontario).

After cooling and subsequent return to the Argon Lab at Dalhousie University, samples are then heated in an ultra-high vacuum and the gas produced is analyzed and measured by mass spectrometer to obtain the ratio of $^{40}\text{Ar}^*$ to ^{39}Ar . This step was completed at Dalhousie. ^{39}Ar is proportional to ^{39}K and the ratio of ^{39}K to ^{40}K is fixed, therefore the amount of ^{40}K can be derived from the amount of ^{39}Ar . Thus the ratio of $^{40}\text{Ar}^*/^{39}\text{Ar}$ is proportional to the ratio of $^{40}\text{Ar}^*/^{40}\text{K}$ and therefore to the age of the sample.

The age t comes from the equation:

$$t = 1/\lambda \ln[(^{40}\text{Ar}^*/^{39}\text{Ar})(J)+1], \text{ where}$$

λ is the decay constant. The value for J is obtained by simultaneously irradiating a flux monitor or standard of known K-Ar age, and then heating it and analysing the gas to obtain a $^{40}\text{Ar}^*/^{39}\text{Ar}$ ratio. J is calculated from the following equation:

$$J = (e^{\lambda t_m} - 1) / (^{40}\text{Ar}^*/^{39}\text{Ar})_s, \text{ where}$$

t_m is the age of the standard and $(^{40}\text{Ar}^*/^{39}\text{Ar})_s$ is the ratio measured for the standard sample.

The samples were individually wrapped in thin aluminum foil and placed in an aluminum capsule with flux monitors interspersed and similarly wrapped. The flux monitor used was the hornblende standard MMHb-1 (Alexander et al., 1978). The J values obtained from the standards were plotted with errors against their positions along the length of the capsule. A straight line fitted to the plotted points provided J values for the samples (York, 1969). The J value represents a unitless measure of the efficiency of conversion of ^{39}K to ^{39}Ar and is used to correct for differences in neutron flux that occur within the reactor during the irradiation phase. A J -value of 0.00232 was found for all the dated samples in this project.

For high precision $^{40}\text{Ar}/^{39}\text{Ar}$ dating, a step-wise degassing method is used which involves extracting gas at sequential temperature steps and measuring the isotope ratios at each step. The apparent age of each step is plotted against the percentage total ^{39}Ar released at each step, and the resulting graph is called an age spectrum. The amount of gas produced at each step determines the weight the corresponding apparent age carries in the calculation of the age of the sample (Hanes, 1991).

The ages should represent the point at which the rapid cooling of a pluton or heated hydrothermal fluids reach temperatures less than the closure temperatures of the minerals selected for dating. The closure temperature is the temperature at which the products of radioactive decay (in this case ^{40}Ar), become immobile due to a reduction in temperature which closes the crystal lattice of the rock or mineral during solidification. From the point at which a crystal reaches its closure temperature, daughter products from radioactive decay will accumulate and an age may be calculated from the ratio of the parent isotope to its daughter isotope. Closure temperatures vary according to mineralogy composition

(perthitic K-feldspar 150°C: Harrison and McDougall, 1982; biotite 300-350°C:

McDougall and Harrison, 1988; sericite ≈350°C: Purdy and Jäger, 1976 & Jäger, 1979). By comparing the ages generated from samples of differing closure temperatures, it may be possible to determine a cooling rate.

4.2 $^{40}\text{Ar}/^{39}\text{Ar}$ Results

A well-defined plateau as defined by Turner (1968) and Fitch et al. (1969) is one where several sequential steps (a minimum of three consecutive steps is generally required) in the heating schedule share a similar age (with overlapping 1σ error) in a plateau diagram. As well, any steps in the heating schedule that are dominated by atmospheric argon will be excluded from the calculation of the plateau age. This section will provide an interpretation of the argon plateau diagrams for each sample as well as an interpretation of mineral-pair comparisons.

The average age for all dated minerals is 32.6Ma. The average age for potassic alteration minerals (K-feldspar and biotite) is 32.7Ma. Average ages by mineral type were 32.6Ma for K-feldspar and 32.7Ma for biotite. The two sericite samples are thought to be two different types (replacement and vein sericite) and therefore an average of the two would be meaningless. The older sericite has an age of 33.0Ma while the younger sericite has an age of 31.8Ma. A summary of the results of argon dating is shown in Table 4.1 followed by a more detailed account of the results ordered by drillcore and mineral type.

The errors given are at the 1σ level and include the dominant uncertainty of the J factor (0.00232). Age spectra and datasheets are located in Appendix D.

Table 4.1 Summary of $^{40}\text{Ar}/^{39}\text{Ar}$ Dates for RT - February 17, 1997.

| Lab# | Field# | Drill Core | Depth (m) | Mineral Dated | Age (Ma) |
|-----------|----------|---------------|--------------|------------------|----------|
| Cu-999K | Z660-95 | dd3439 | 424.58 | K-feldspar | 32.2±0.3 |
| Cu-999Bi | Z660-95 | dd3439 | 424.58 | biotite | 32.6±0.3 |
| Cu-1001K | Z662-95 | dd3439 | 389.85 | K-feldspar | 32.8±0.3 |
| Cu-1001Bi | Z662-95 | dd3439 | 389.85 | biotite | 32.9±0.3 |
| Cu-1002K | Z663-95 | dd3439 | 501.08 | K-feldspar | 33.0±0.3 |
| Cu-1002Bi | Z663-95 | dd3439 | 501.08 | biotite | 32.6±0.3 |
| Cu-1006K | Z667-95 | dd1513 | 763.72 | K-feldspar | 32.7±0.3 |
| Cu-1010K | Z671A-95 | dd1513 | 730.00 | K-feldspar | 32.2±0.3 |
| Cu-1011SK | Z671B-95 | dd1513 | 428.80 | sericite | 33.0±0.3 |
| Cu-1011SR | Z671B-95 | dd1513 | 428.80 | sericite | 31.8±0.3 |

4.2.1 Potassium Feldspar Results

The crystal structure of potassium feldspar is divided into a low and a high domain with respect to argon retention. Domains are temperature-dependent sites within a crystal where argon gas may remain trapped. The low temperature domain corresponds to sites within the crystal that are sensitive to low temperature thermal events. In other words, argon-loss or introduction of excess argon may occur in these sites during low-temperature

thermal events.

Cu-999K1: The age spectra (see Figure 4.1a) for this sub-sample, a perthitic K-feldspar, can be divided into two domains, the low temperature domain which ranges from 750°C to 1025°C in the heating schedule, and a high temperature domain from 1025°C to 1250°C in the heating schedule. The high temperature domain was chosen for calculating the plateau age for its stability as was determined from the $^{37}\text{Ar}/^{39}\text{Ar}$ plot seen in Figure 4.2a. The $^{37}\text{Ar}/^{39}\text{Ar}$ plot shows that there is probable minor contribution of argon from some phase other than K-feldspar. This extraneous gas can be attributed to the albitic phase that defines the perthitic texture. The average plateau age from this sample, weighted by the percent gas release at each heating step, was calculated to be $32.2\pm 0.3\text{Ma}$.

Cu-1001K1: This sub-sample is a perthitic K-feldspar from outside the orebody and shows a well-defined plateau at $32.8\pm 0.3\text{Ma}$ between 1000°C and 1225°C (see Figure 4.1b). This corresponds to the high temperature domain and approximately 75% of the gas released by the sample. Some minor fluctuations occur in the low temperature domain, but a reasonably good plateau at the same approximate age can be interpolated between the heating schedule steps of 650°C and 1000°C. However, less than 25% of the gas is released in this interval so its importance is not significant.

Cu-1002K1: This perthitic K-feldspar sub-sample has an average age (weighted to percent gas release) of $33.0\pm 0.3\text{Ma}$ calculated from the high temperature domain (see Figure 4.1c). The high temperature domain used ranged from 1100°C to 1250°C in the

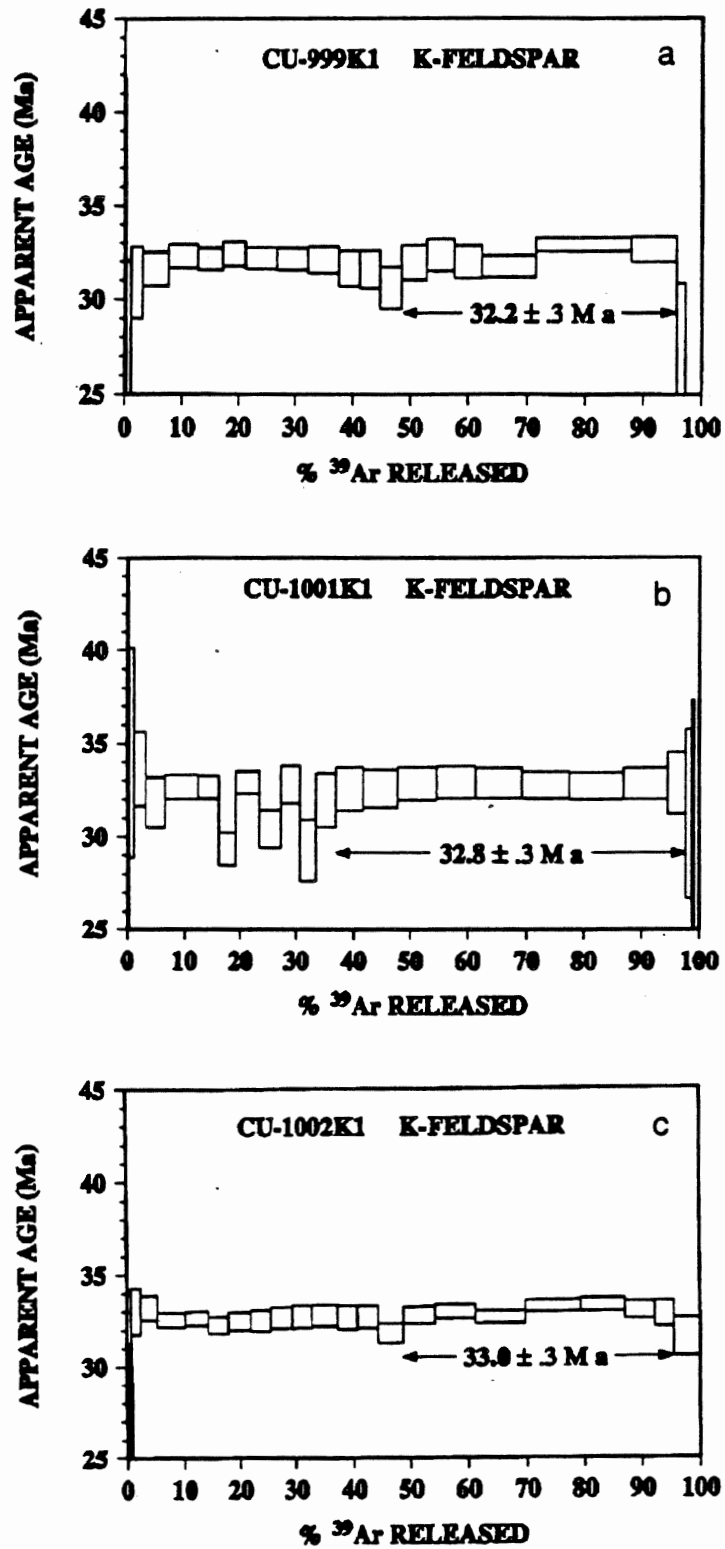


Figure 4.1a-c $^{40}\text{Ar}/^{39}\text{Ar}$ age spectra for potassium feldspar samples from DDH3439.

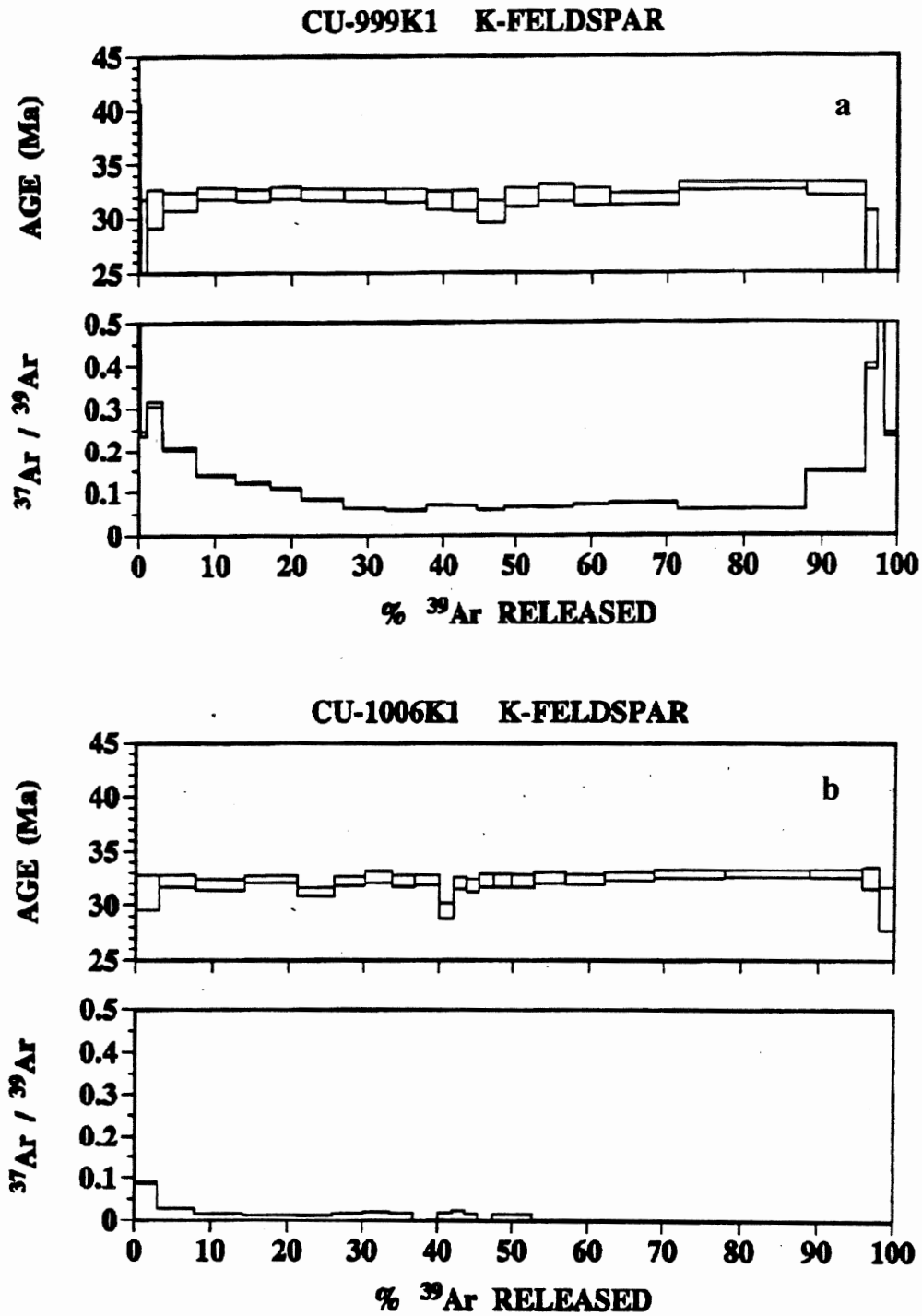


Figure 4.2a-b $^{37}\text{Ar}/^{39}\text{Ar}$ plots from K-feldspar samples Cu-999K1 and Cu-1006K1 representing the release of radiogenic argon generated from calcium during the irradiation phase of sample preparation. Peaks in the calcium plot are interpreted to represent the presence of Ca-bearing phases within the K-feldspar.

heating schedule and accounted for 46.2% of the gas released.

Cu-1006K1: This sub-sample is a K-feldspar with no perthitic texture. Its average age (weighted by percent gas release) was calculated from the high temperature domain (see Figure 4.3a) to be 32.7 ± 0.3 Ma. This is a very good plateau with only a few minor fluctuations in gas release. The $^{37}\text{Ar}/^{39}\text{Ar}$ plot clearly indicates that this is a single phase sub-sample (see Figure 4.2b).

Cu-1010K1: This sub-sample is also a clean K-feldspar with no perthitic textures. The $^{37}\text{Ar}/^{39}\text{Ar}$ values found in the data sheets (located in Appendix D) indicate that this is a single-phase mineral sample. A very good plateau exists in the high temperature domain from 1200°C to 1450°C in the heating schedule (see Figure 4.3b). This segment accounts for 61.5% of the total gas released. An average age (weighted by percent gas release) was calculated to 32.2 ± 0.3 Ma.

4.2.2 Biotite Results

Cu-999Bi1: This biotite sub-sample shows some signs of argon loss as the age gradually increases at the lower temperature heating steps (see Figure 4.4a). It is standard laboratory practice with biotite to use almost the entire spectrum to calculate the average age. This essentially mimics the total gas age but ignores the extreme low and high heating

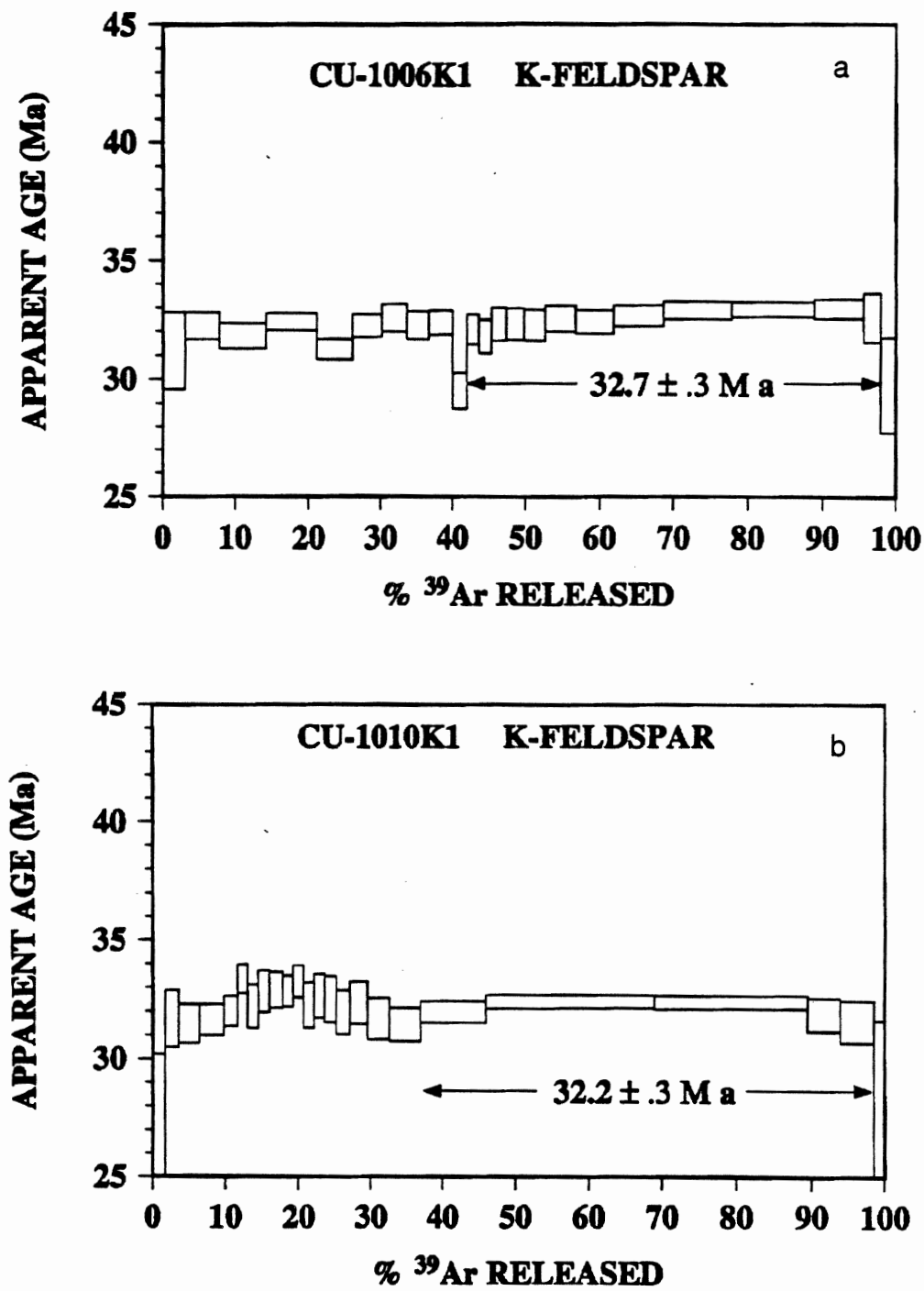


Figure 4.3a-b $^{40}\text{Ar}/^{39}\text{Ar}$ age spectra for potassium feldspar samples from DDH1513.

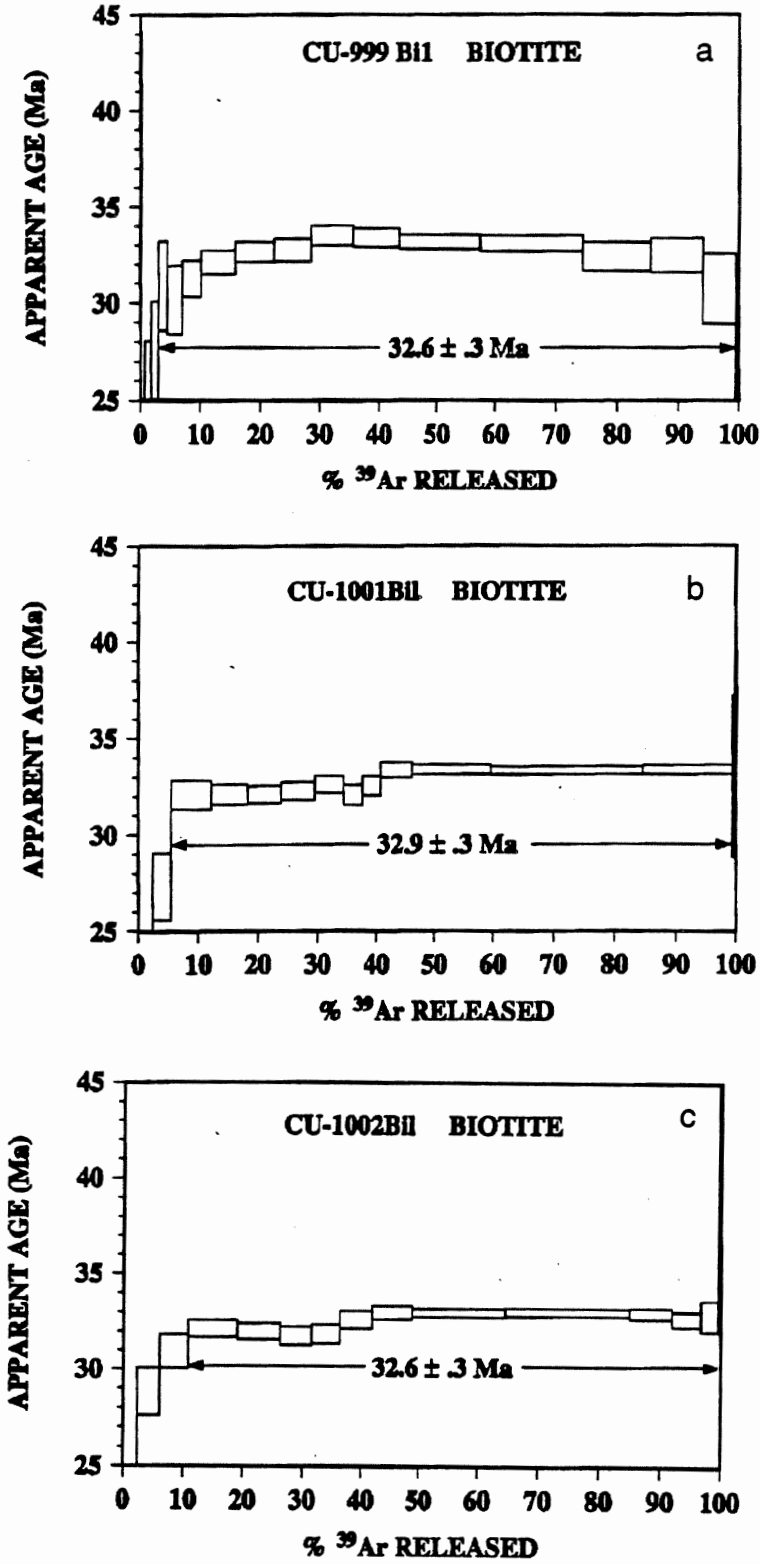


Figure 4.4a-c $^{40}\text{Ar}/^{39}\text{Ar}$ age spectra for biotite samples from DDH3439.

steps where the gas release is not reliable. This procedure attempts to negate the effects of possible argon recoil. Argon recoil involves the mobilization of argon from biotite into intercalated chlorite layers. However, it was determined from XRD analysis that the biotite used in this project was likely to be less than 1% chloritized. The calculated age is 32.6 ± 0.3 Ma.

Cu-1001Bi1: This sub-sample appears to have a two stage thermal history with a high temperature gas release pattern showing an age of about 33Ma and a low temperature age of approximately 32Ma (see Figure 4.4b). Again, for biotite, it is standard laboratory practice to calculate the average age based on almost the entire heating schedule to average the effects of argon recoil as discussed for sample Cu-999Bi1. This procedure approximates the total gas age while excluding the extreme high and low heating steps which are not considered reliable. Therefore the calculated average age (weighted by percent gas release) is 32.9 ± 0.3 Ma.

Cu-1002Bi1: This sub-sample of biotite shows a similar spectrum to those of Cu-999Bi and Cu-1001Bi with an age of 32.6 ± 0.3 Ma (see Figure 4.4c). The gradual increase in age with increasing percent ^{39}Ar released is indicative of minor argon loss, similar to the pattern seen in Cu-999Bi. As well, the two stage pattern seen in the spectra for Cu-1001Bi seems to be present with a low temperature plateau (age of ≈ 31.9 Ma) and a high temperature plateau (≈ 32.9 Ma). The low temperature plateau may correspond to the quartz-sericite alteration event (sericite date of 31.8Ma). This is not conclusive however as a

similar result may be attributed to argon recoil (see discussion for sample Cu-999Bi1).

4.2.3 Sericite Results

Cu-1011SK: This sub-sample, which has a very good plateau with an average age of 33.0 ± 0.3 Ma, is similar to K-feldspar and biotite ages and significantly older than the other sericite from Cu-1011SR which was dated to 31.8 Ma. Cu-1011SK shows no indications of excess argon problems as interpreted from the gas release pattern so the difference in age appears real. This sub-sample was originally picked as a K-feldspar sample from visual and X-ray diffraction observations; however the degassing pattern (see Figure 4.5a and gas release data found in Appendix D) exhibited by this sample revealed it as a sericite. The bulk of the gas (91.1%) was released between 700°C and 975°C in the heating schedule, similar to the release pattern in Cu-1011SR. This sample was subsequently reclassified as a sericite based upon the release pattern data combined with electron microprobe and further XRD analyses. It is thought that this may be a relic potassic alteration-related sericite which explains the much older age relative to sericite Cu-1011SR from the same sample.

Cu-1011SR: This sericite sample generated a very good plateau with an average age (weighted by percent gas release) of 31.8 ± 0.3 Ma (see Figure 4.5b). As with biotite, the age of the plateau approximates the total gas age excluding the extreme end steps of the

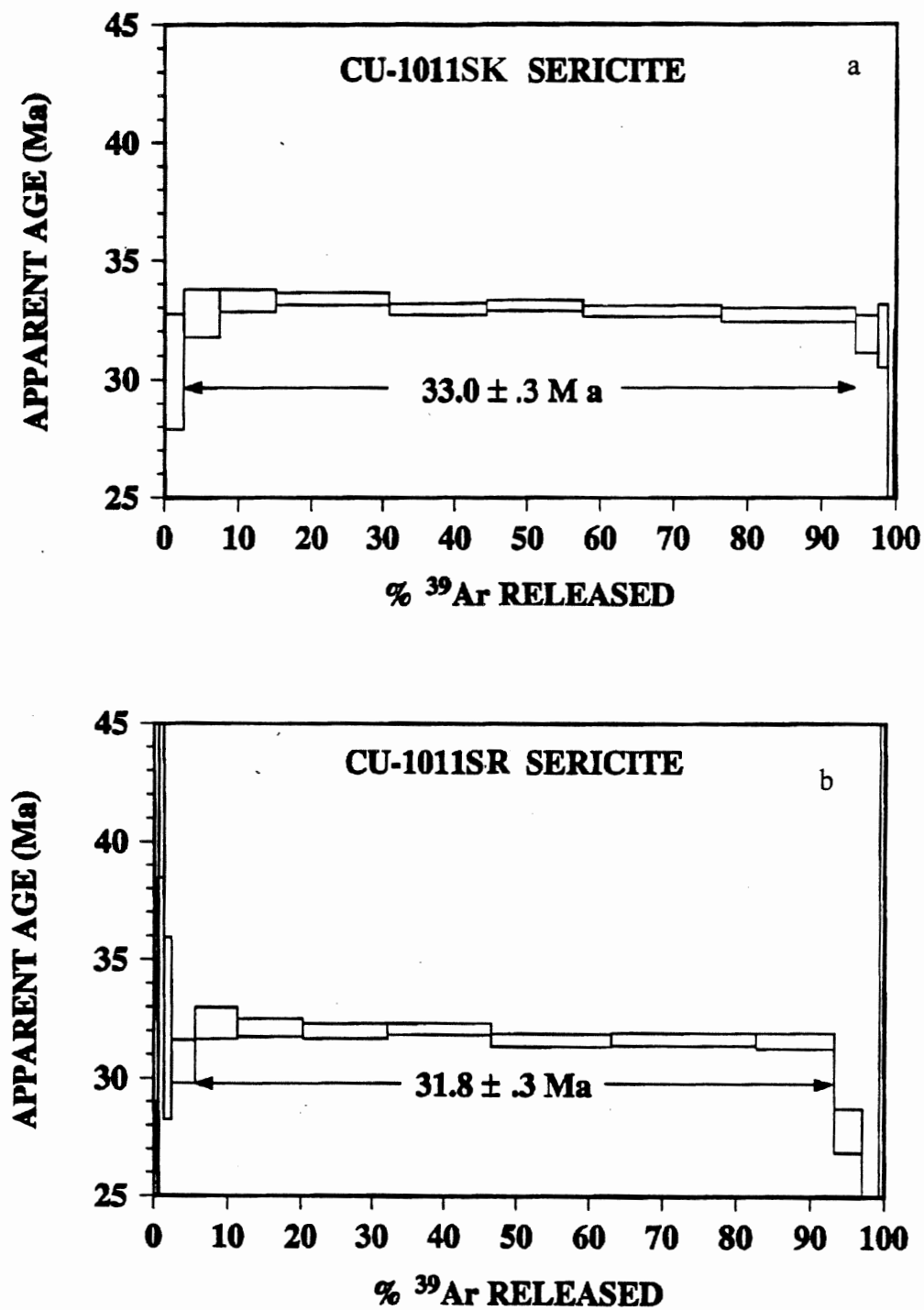


Figure 4.5a-b $^{40}\text{Ar}/^{39}\text{Ar}$ age spectra for sericite samples from DDH1513.

heating schedule where the atmospheric component of the gas released dominates the analysis. The bulk of the gas (87.5%) was released between 700°C and 1000°C in the heating schedule which is typical of a sericite.

4.3 Mineral Pairs from DDH3439 samples

Four of the samples provided mineral pairs for dating. K-feldspar and biotite grains were separated from each of the DDH3439 samples (Cu-1002, Cu-1001 and Cu-999) and two sericite grains were taken from sample Cu-1011 from DDH1513. The plateaus for each of these mineral pairs were combined in order to get a better comparison of the age data and possibly a more constrained age for the DDH3439 samples.

Cu-1002K1 + Cu-1002Bi1: The combined patterns from these two sub-samples again show good agreement in age in the high temperature domain region of the K-feldspar (see Figure 4.6). The K-feldspar sample has an age of 33.0 ± 0.3 Ma and the biotite has an age of 32.6 ± 0.3 Ma. If the calculation of the age of the biotite is limited to only the overlapping steps in the heating schedule of the K-feldspar the new age would be 32.9 ± 0.3 Ma. This new age combined with the K-feldspar age and the rapid cooling evidence again supports the theory of a high 32 Ma to low 33 Ma potassic event. There is good correlation of a possible low temperature plateau (weighted average age of 31.9 Ma) in the biotite spectrum to the age of the sericitic sub-sample (31.8 Ma). This low temperature plateau may be the result of argon recoil and not of a low temperature thermal event at RT.

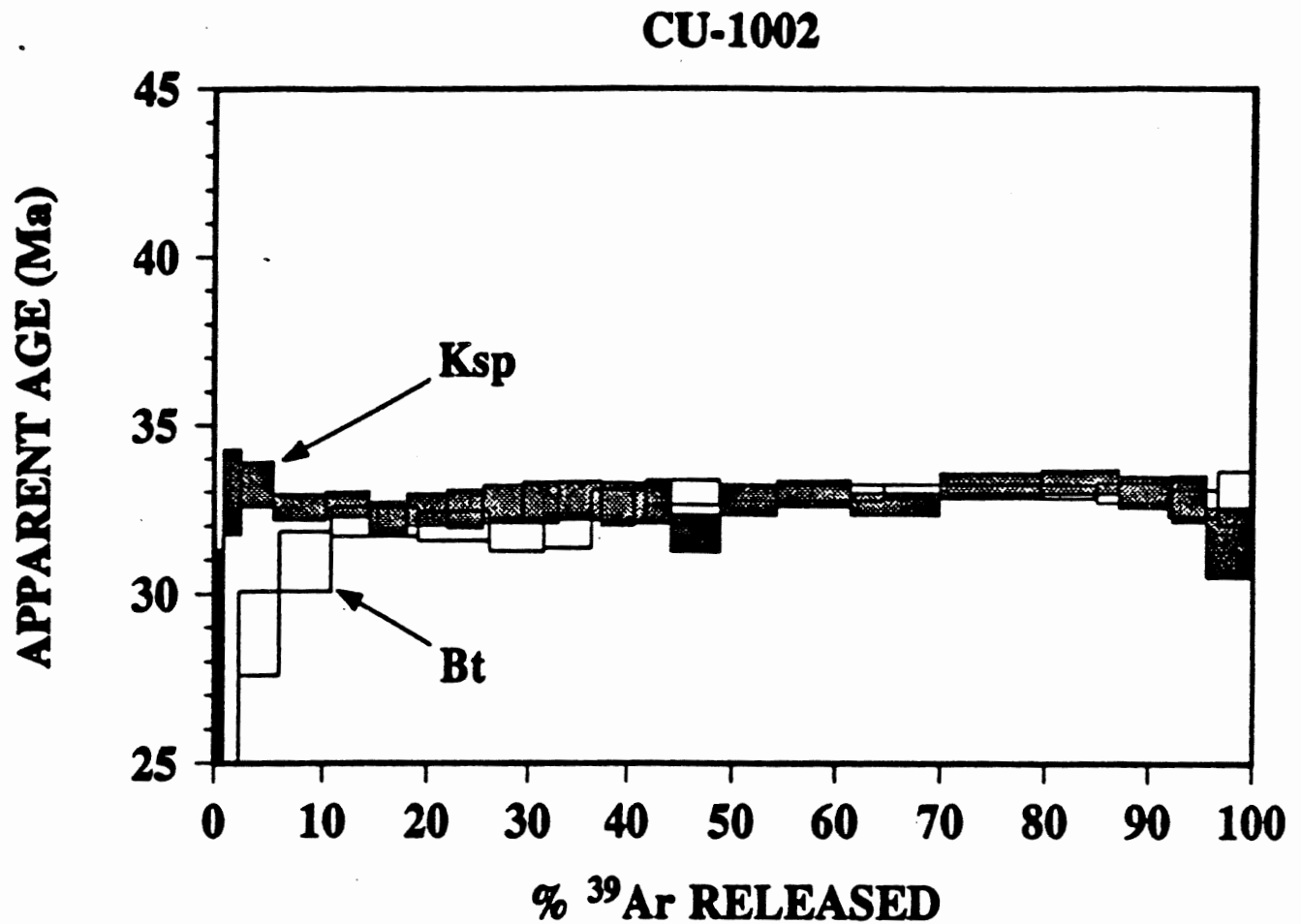


Figure 4.6 K-feldspar/biotite dated mineral pair from Cu-1002 showing excellent correlation in the high temperature domain in the range from 50% to 95% ^{39}Ar released. This region of overlap strengthens confidence in the calculated ages of each individual mineral (K-feldspar = $33.0 \pm 0.3\text{Ma}$ and biotite = $32.6 \pm 0.3\text{Ma}$).

The data combined with the lack of correlation between the K-feldspar low temperature domain and the sericite age may suggest that biotite is more susceptible to low temperature disturbances than K-feldspar when the two are subjected to the same conditions.

Cu-1001K1 + Cu-1001Bi1: The combined patterns from these two sub-samples show excellent agreement in age (see Figure 4.7). The K-feldspar sample has an age of 32.8 ± 0.3 Ma and the biotite has an age of 32.9 ± 0.3 Ma. This similarity in calculated ages combined with the similarity of the gas release pattern strengthen the confidence in constraining the age of the potassic event at Radomiro Tomic to a high 32 Ma to low 33 Ma window. Rapid cooling is implied by K-feldspar and biotite having congruent patterns though different closure temperatures.

Cu-999K1 + Cu-999Bi1: The age calculated for the K-feldspar sub-sample was 32.2 ± 0.3 Ma which was young compared to the ages generated from the other potassic alteration mineral separates. The overall average age for all samples was 32.6 Ma which includes the 31.8 Ma age for the sericite sample. However, when looking at the combination of the K-feldspar/biotite pair (see Figure 4.8), one can see that there is overlap of two high temperature steps in the heating schedule. The K-feldspar and biotite are assumed to have been the result of the same hydrothermal alteration event and because it has already been assumed that this is a rapidly cooled system from XRD evidence, we can also assume that the age of these two crystals should be the same within the resolution of the $^{40}\text{Ar}/^{39}\text{Ar}$ dating technique. Therefore, it should be possible to narrow down the age of these samples using

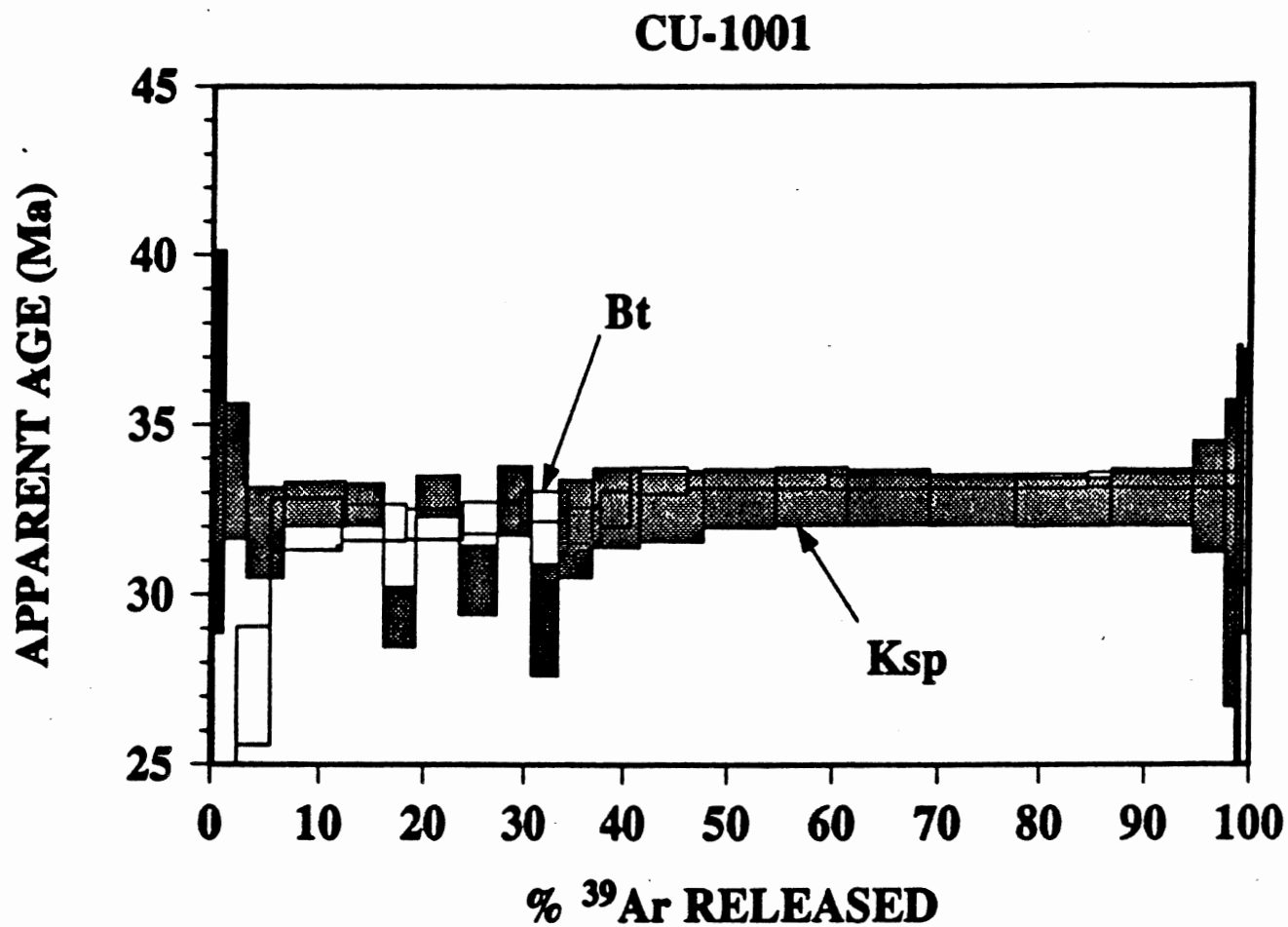


Figure 4.7 K-feldspar/biotite dated mineral pair from Cu-1001 showing excellent correlation in the high temperature domain in the range from 40% to 95% ³⁹Ar released. This region of overlap strengthens confidence in the calculated ages of each individual mineral (K-feldspar = 32.8 ± 0.3 Ma and biotite = 32.9 ± 0.3 Ma).

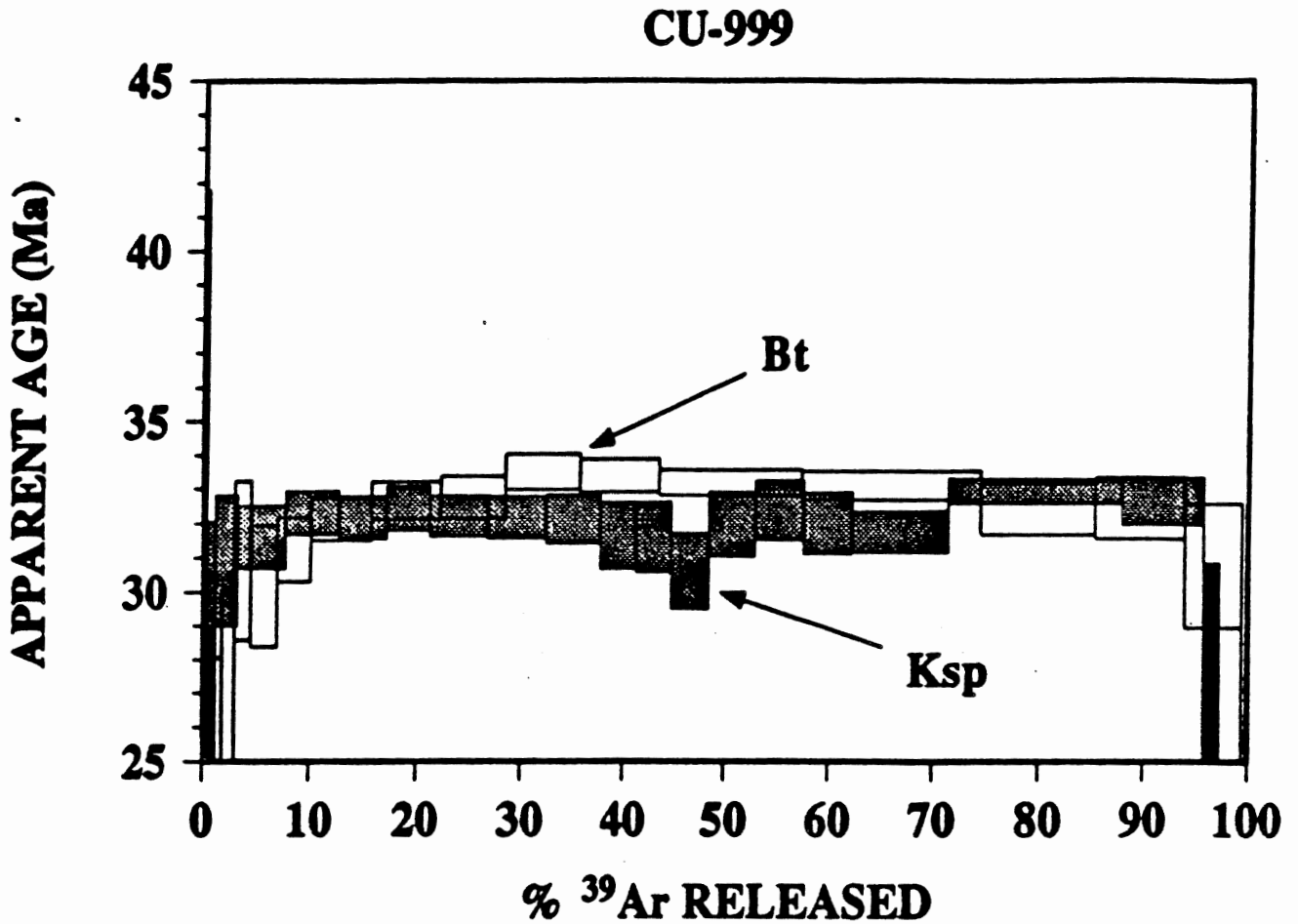


Figure 4.8 K-feldspar/biotite dated mineral pair from Cu-999 showing overlap in the high temperature domain in the range from 75% to 95% ³⁹Ar released. If an age were to be calculated based on this region of overlap, the K-feldspar age would be older at 32.8 ± 0.3 Ma which has a better correlation with the other K-feldspars from DDH3439.

these overlapping steps in the heating schedule. Calculations based only on the two overlapping steps from the K-feldspar sub-sample reveal a much older age 32.8 ± 0.3 Ma) more consistent with other similar samples. The new age calculated for the biotite separate from its two overlapping steps is 32.4 ± 0.3 Ma, which is now slightly younger but still overlapping within 1σ error of the new K-feldspar age.

Cu-1011SR + Cu-1011SK: No overlap is apparent (see Figure 4.9) between these two age spectra even though the shape of their age spectra and their degassing character has similar trends. The reason that this is important is because they are both sericites separated from Cu-1011, however, Cu-1011SR has an age of 31.8Ma and Cu-1011SK has an age of 33.0Ma. A working hypothesis is that, although the two samples are both sericite, Cu-1011SK is part of a younger quartz-sericite alteration assemblage dated to 31.8Ma. Cu-1011SK may have formed in the outer quartz-sericite alteration zone (see onion-skin model; Figure 1.4) as part of the earlier hydrothermal event recorded during the earlier hydrothermal event recorded by the potassic alteration minerals at about 33Ma. The quartz-sericite alteration effects were primarily chemical exchange and not merely a thermal effect, therefore the hydrothermal event failed to reset the previously formed sericite because the older sericite was in equilibrium with the circulating hydrothermal fluids. This may also explain why Cu-1011SK was not initially identified as a sericite. Cu-1011SK was older and formed under different conditions, possibly resulting in a different appearance than the younger Cu-1011SR sub-sample.

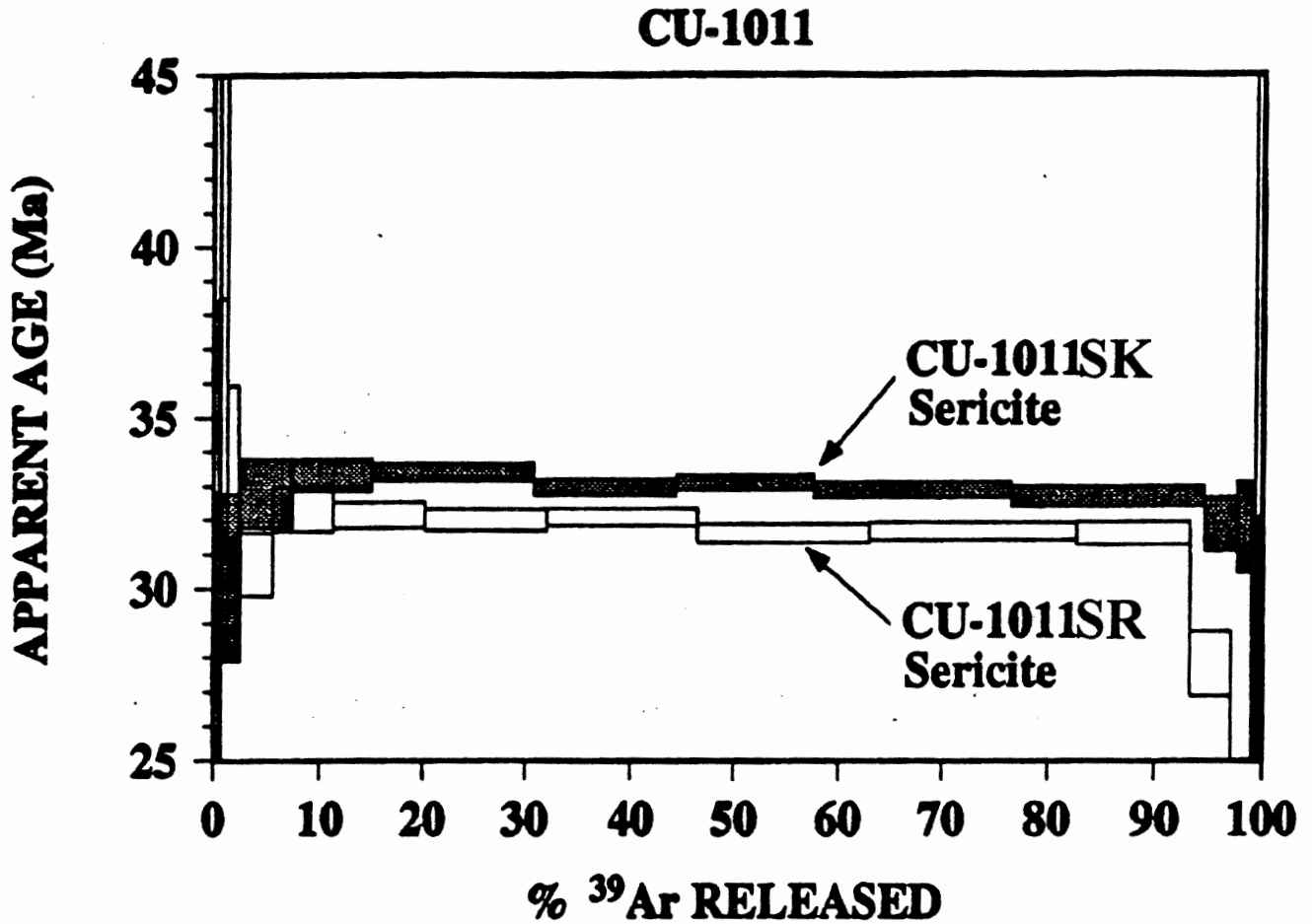


Figure 4.9 Two sericite argon release patterns from Cu-1011 showing no overlap but similar shape and degassing trends. It is suspected that the pair represents two generations of sericite, replacement sericite corresponding to the quartz-sericite alteration during the initial hydrothermal event (Cu-1011SK = 33.0 ± 0.3 Ma) and vein-sericite corresponding to quartz-sericite event at RT (Cu-1011SR = 31.8 ± 0.3 Ma).

Chapter 5

Conclusions and Future Work

5.1 Conclusions from Whole-Rock Chemistry and Mineralogy

Whole-rock geochemical data were used in a variety of discrimination diagrams which classified such things as original rock type, tectonic setting and magma source. The pre-alteration rock type at Radomiro Tomic can be inferred to be quartz monzodiorite when data were plotted on the Winchester and Floyd (1977) discrimination diagram that compares Zr/TiO_2 to Nb/Y . Tectonic setting was confirmed to be Chilean volcanic arc granite by using a spider diagram after Pearce et al. (1984) and also by plotting Rb against Y+Nb. Radomiro Tomic rare earth element patterns match those of the Chuquicamata sample set which suggests a similar magma source. The short distance between Radomiro Tomic and Chuquicamata combined with the REE data increases the probability that the intrusions associated with these deposits shared the same magma source at depth.

X-ray powder diffraction was used to conduct triclinicity tests on all potassium feldspars that were dated. This test is an indicator of cooling rates of these crystals which is based on how ordered the crystal lattice of a potassium feldspar becomes as it cools. All potassium feldspars (all orthoclase) showed similar results indicative of high level sub-volcanic emplacement.

Mineral chemistry results from electron microprobe analyses (144 data points) show that potassium content is consistent from edge to centres of K-feldspar, biotite and sericite grains, among grains within a sample and also among the sample set for each mineral type (5 K-feldspar,

3 biotite and 2 sericite). Therefore potassium content and distribution among each of the K-feldspars, biotites and sericites is essentially homogeneous. Also, no inclusions were found containing potassium in DDH1513 K-feldspar samples. Few inclusions were found in DDH3439 potassium feldspar samples that might affect age and those that were found were easily avoided in the mineral separation stage.

Perthitic textures were observed in the DDH3439 potassium feldspar separates which suggests that the K-feldspar was formed at or near magmatic temperatures and therefore suggests that the ages generated from these K-feldspars may be close to the emplacement age.

5.2 $^{40}\text{Ar}/^{39}\text{Ar}$ Dating

Two thermal events are recorded by argon geochronology at Radomiro Tomic. The older event (~33.0Ma) is associated with potassic, argillic and sericitic alteration while the younger event is associated with quartz-sericitic alteration (~31.8.0Ma). This is based on the interpretation of ten $^{40}\text{Ar}/^{39}\text{Ar}$ dates (see Figure 5.1) from six drillcore samples with an average age of 32.6Ma.

K-feldspar and biotite pairs (Cu-999K1/Cu-999Bi1, Cu-1001K1/Cu1001Bi1 and Cu-1002K1/Cu1002Bi1) all gave similar ages within the resolution of the $^{40}\text{Ar}/^{39}\text{Ar}$ dating technique. This suggests rapid cooling to temperatures below 150°C based on similar ages coming from minerals with different closure temperatures. The lack of any evidence, in the K-feldspar plateaus, of significant argon-loss leads to the conclusion that temperatures must have cooled rapidly to below 150°C. Had the K-feldspar crystals been held at temperatures greater than 150°C or

RT High Precision Argon Dates Final Data

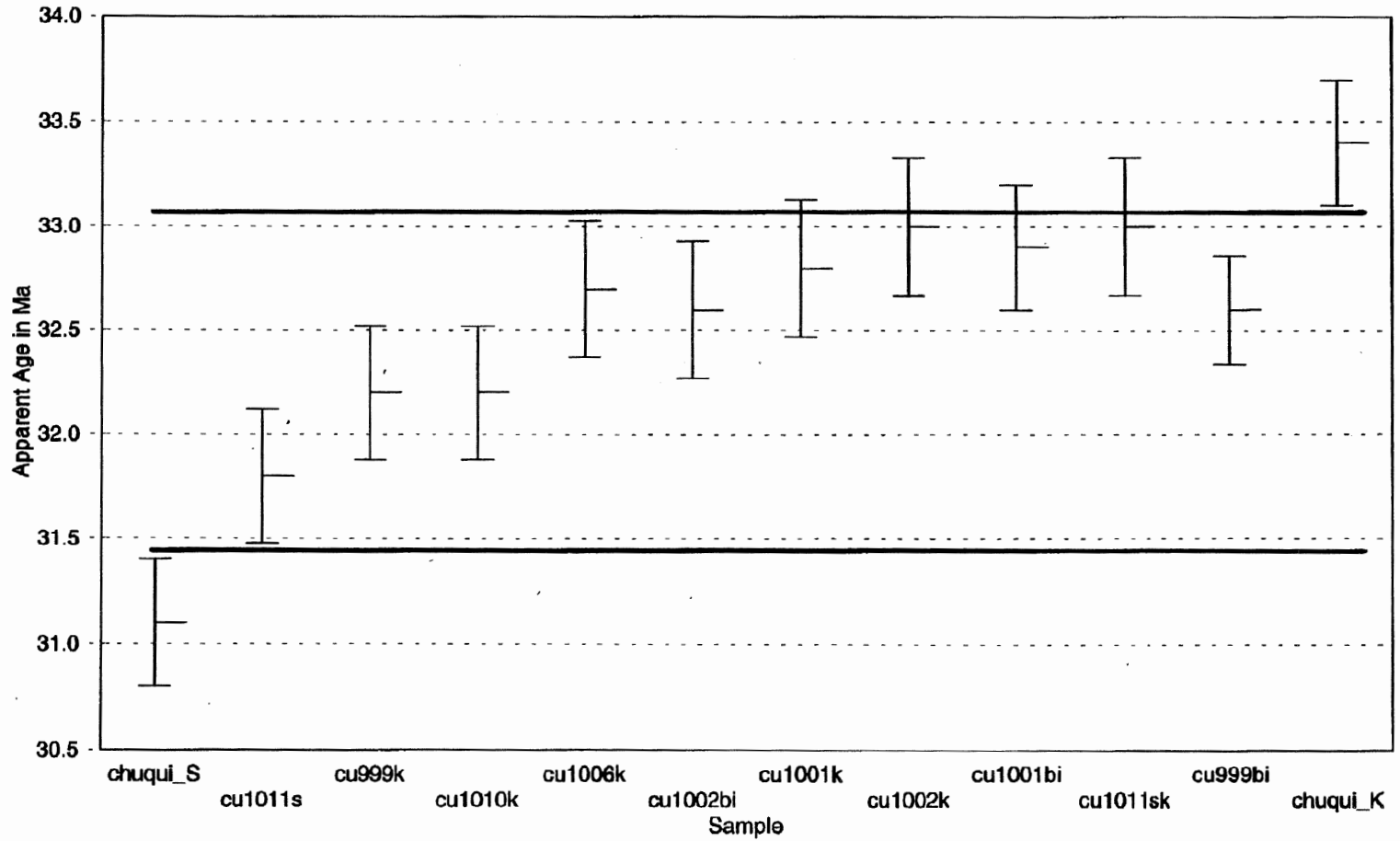


Figure 5.1 All RT ages with associated errors. Also shown are the average ages for the potassic alteration and quartz-sericite alteration at Chuquicamata (33.4Ma labelled Chuqui_K and 31.1Ma labelled Chuqui_S respectively; Reynolds et al., 1997).

greater, for periods of time ≥ 1 Ma, substantial argon-loss would have occurred (Foland, 1974).

The combined argon plateau diagrams from Cu-1002K1 and Cu-1002Bi1 show good agreement in age of the high temperature domain region of the K-feldspar (see Figure 4.6). Individually, the K-feldspar sample has an age of 33.0 ± 0.3 Ma and the biotite has an age of 32.6 ± 0.3 Ma. If the calculation of the age of the biotite is limited to only the overlapping steps in the heating schedule of the K-feldspar the new age of the biotite would be 32.9 ± 0.3 Ma. This age combined with the K-feldspar age and the rapid cooling evidence again supports the hypothesis of a high 32Ma to low 33Ma potassic alteration event. Overlap of a low-temperature plateau (weighted average of 31.9Ma) in the biotite spectra of Cu-1002Bi with the age generated from the younger sericite sample (31.8Ma) may suggest partial resetting of the biotite age as a result of the younger hydrothermal event. However, this low-temperature disturbance in the biotite spectra may only be the result of argon recoil.

There is a good agreement of a low temperature plateau (weighted average age of 31.9Ma) in the biotite spectra to the age of the sericite sub-sample (Cu-1011SR; 31.8Ma). This data combined with the lack of correlation between the K-feldspar low temperature domain of sample Cu-1002K1 and the sericite age suggests that biotite is more susceptible to low temperature disturbances than K-feldspar, when subjected to the same conditions. In other words, this may indicate that the closure temperature of the K-feldspar high temperature domain is greater than the closure temperature of biotite (300-350°C; McDougall and Harrison, 1988) and also greater than the temperatures attained during quartz-sericite alteration (200-350°C; Richards and McDougall, 1990).

The implication of similar low-30Ma quartz-sericite alteration ages at Radomiro Tomic and Chuquicamata is that the hydrothermal event responsible for the quartz-sericite alteration may actually be regional and unrelated specifically to Chuquicamata but more related to an episode of regional fault movement (M. Graves, pers comm).

A comparison of age spectra between two K-feldspar crystals, one from RT and the other from Chuquicamata, dated by $^{40}\text{Ar}/^{39}\text{Ar}$ techniques is shown in Figure 5.2. Both K-feldspar are from potassic alteration zones and have perthitic textures. Cu-1002 has a flat 'well-behaved' age spectrum which generates an age of $33.0\pm 0.3\text{Ma}$ while Cu-406 from Chuquicamata clearly records a different thermal history. There is a break in the plateau of Cu-406, dividing the high and low temperature domains of the K-feldspar crystal. Two events are recorded by Cu-406, an older event at $33.7\pm 0.2\text{Ma}$ in the high temperature domain and a younger event ($\sim 31\text{Ma}$) in the low temperature domain (Reynolds et al., 1997). This strongly suggests that Chuquicamata and Radomiro Tomic have experienced different thermal histories.

5.3 Evidence for Two Sericite Types

There are six factors which lead to the conclusion of the presence of two types of sericite within sample Cu-1011:

- 1) different appearance (Cu-1011SK was originally identified as a K-feldspar,
- 2) different ages (Cu-1011SK 33.0Ma; Cu-1011SR 31.8Ma),
 - a) the older age of Cu-1011SK is similar to age of the older hydrothermal event as

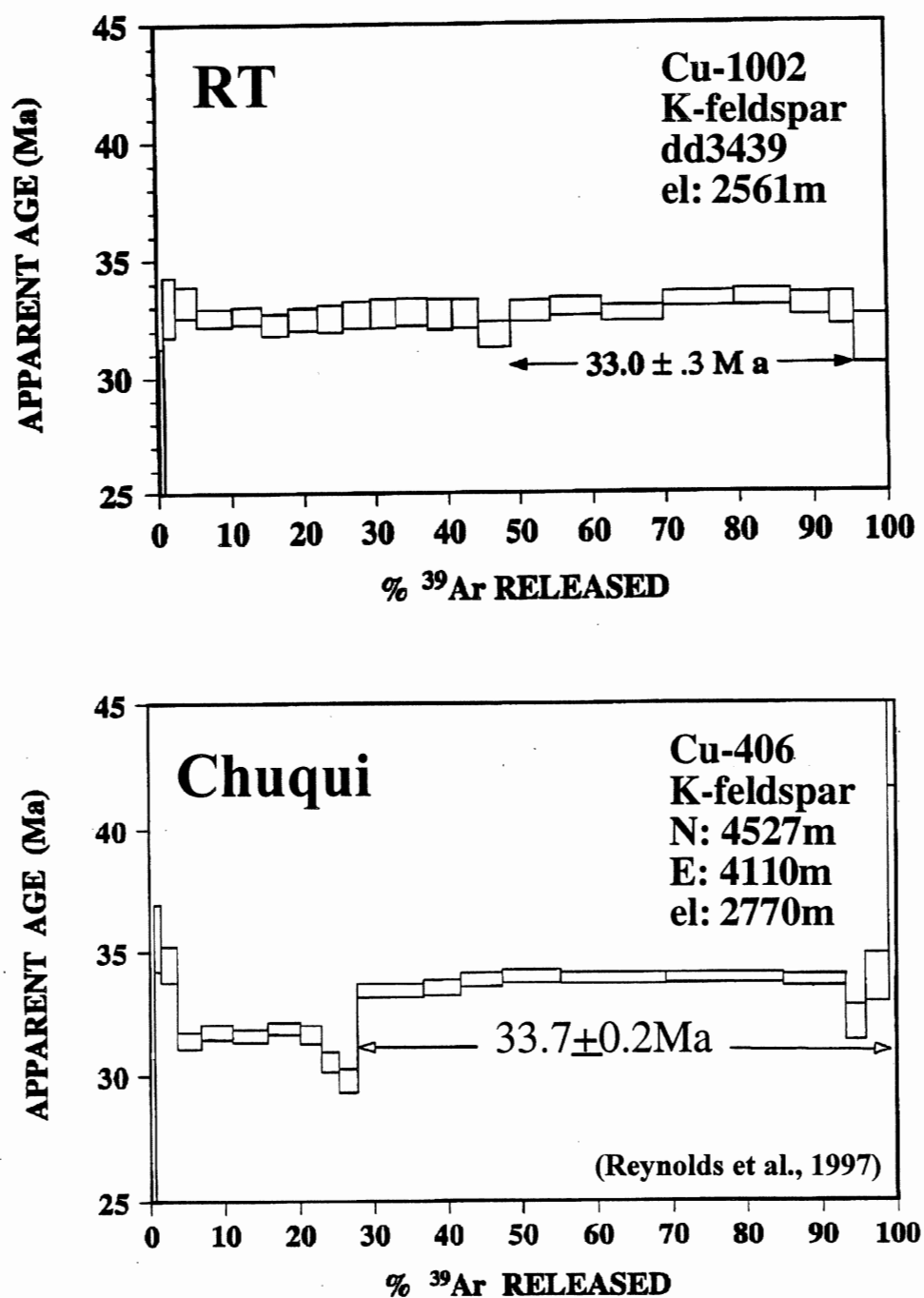


Figure 5.2 A comparison of K-feldspar plateau diagrams between samples from Chuquicamata and Radomiro Tomic. Note the distinctive break in the plateau for sample Cu-406 dividing a higher temperature, older plateau at 33.7Ma (the age of potassic alteration at Chuqui) and a younger, lower temperature plateau at about 31.1Ma that corresponds to the age of Chuqui sericitic alteration. No break appears in the RT K-feldspar clearly indicating a different thermal history at Radomiro Tomic.

seen from the ages of the other samples,

b) the younger sericite is somewhat similar in age to the second hydrothermal event recorded in quartz-sericite alteration assemblages at Chuquicamata suggesting a similar pattern in the type or intensity of thermal events at both deposits,

3) there are no signs of excess argon in the age spectra of the older sericite, and

4) there are no signs of argon-loss in the younger sericite sample.

5.4 Proposed Genesis (see Figure 5.3)

A sequence of events can be inferred from the dating results and from microscope analysis. At about 34Ma, dated from K-feldspar from the potassic alteration zone, a pluton was emplaced at Chuquicamata. About 1.0 million years later (33.0Ma) a second pluton or stock from the pluton at Chuquicamata was emplaced 8-10km north at Radomiro Tomic. Evidence of rapid cooling of the pluton comes from triclinicity tests and dating of mineral pairs of K-feldspar and biotite from single samples. At <32Ma regional-scale movement along the Domeyko Fault system generated fluids resulting in low temperature, quartz-sericitic alteration that formed new sericite at Radomiro Tomic (31.8Ma) and disturbed the low temperature domains of some of the K-feldspar and biotite crystals but left the potassium and argon content of Cu-1011SK unaffected.

As for addressing the three hypotheses put forth in Chapter 1 on the origin of Radomiro Tomic in relation to the Chuquicamata deposit, more sampling is required. The results of this

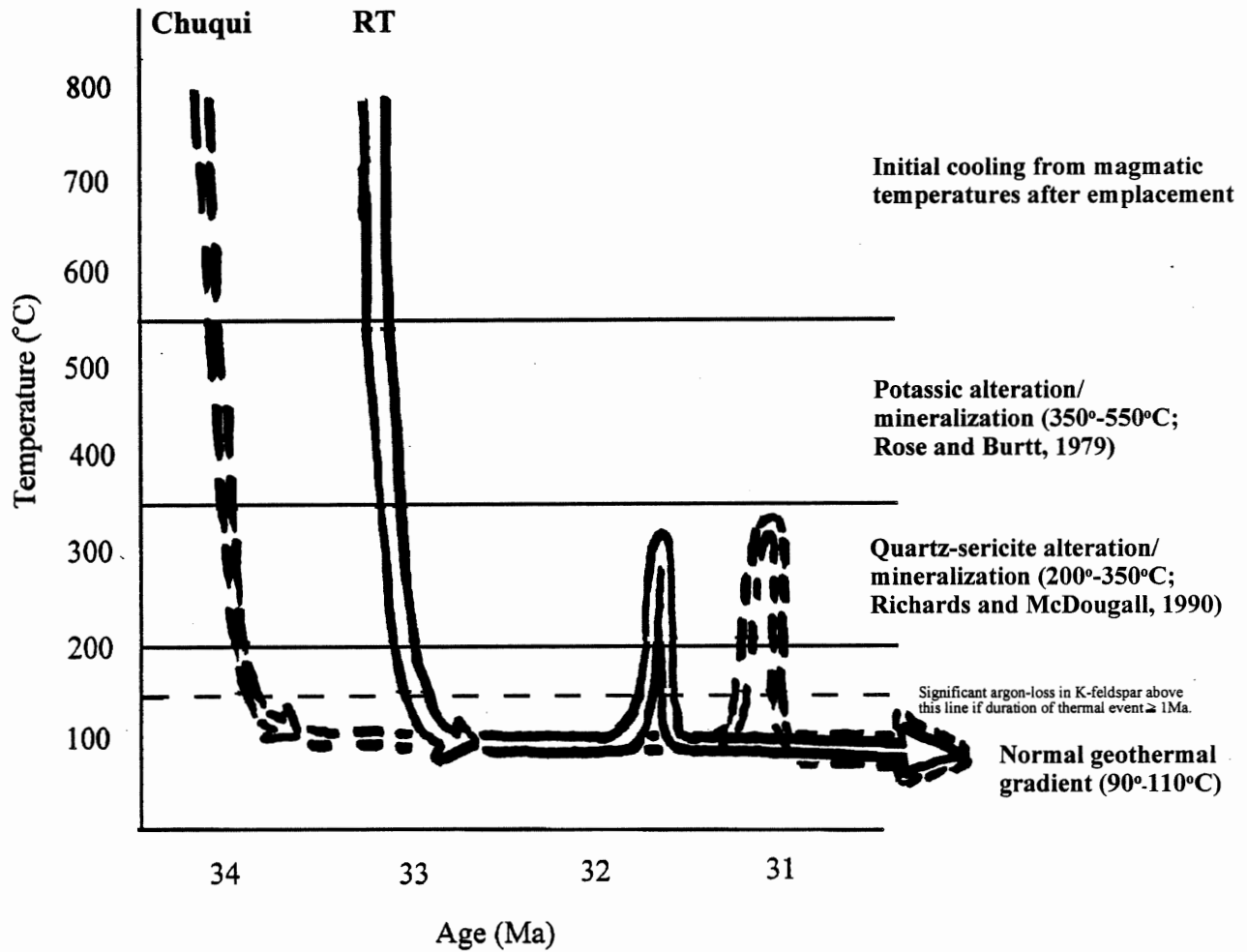


Figure 5.3 Hypothetical sequence of events at Radomiro Tomic and Chuquicamata showing the results of two hydrothermal events due to the emplacement of plutons at Chuquicamata (34Ma) RT (33Ma). Rapid cooling follows each event shown, to levels below 150°C within 1Ma (Roedder, 1976). If the temperature did not cool to below 150°C within this time period the K-feldspar plateau diagram would show evidence of significant argon-loss (Foland, 1974). As well, dating of mineral pairs with higher and lower closure temperatures (K-feldspar and biotite) from the same sample showed no detectable difference in age which is to be expected with rapid cooling. At 31.8Ma, quartz-sericite alteration minerals at RT record a younger hydrothermal event, while quartz-sericite alteration minerals at Chuquicamata record an even younger event at 31.1Ma.

study have only highlighted the need for more data. However, the most likely hypothesis for the origin of RT that is favoured by the author, is that proposed above which involves the emplacement of separate plutons from a similar source. This does not disprove the other hypotheses but this scenario does have the advantage of simplicity.

5.5 Future Work

Since the data generated from this project are based on a limited sample set (ten dated minerals from six drillcore samples) it should be considered a reconnaissance study of geochronology of the Radomiro Tomic deposit. Although the work has identified the possibility of two thermal events similar in ages to the two phases at Chuquicamata, more sampling is required (specifically, more sericite samples) in order to put greater confidence in these results. Both types of sericites, vein and replacement, are required in order to reproduce the old and young ages from this study and to prove that vein sericites are younger. Also samples are required to complete a transect between Radomiro Tomic and Chuquicamata in order to identify differences between local and regional scale hydrothermal effects.

References

- Alexander, E., Michelson, G. and M. Lanphere, 1978, 'MMHb-1: A new $^{40}\text{Ar}/^{39}\text{Ar}$ dating standard', USGS Open File Report 78-701, p6-8
- Alfaro, M., 1997, 'Relationship Between Volcanism and the Occurrence of Hydrothermal Ore Deposits in Young Cordilleran Environments', in Contributions to Latin American Ore Deposit Geology, abstract, MDD/GAC Symposium 4, Ottawa
- Alpers, C. and G. Brimhall, 1988, 'Middle Miocene climatic change in the Atacama in the Atacama Desert, northern Chile: evidence from supergene mineralization at La Escondida', GSA Bulletin, v100, p1640-1656
- Baldwin, A. and J. Pearce, 1982, 'Discrimination of productive and non-productive porphyritic intrusions in the Chilean Andes', Economic Geology, v77, 664-674
- Berger, G., 1975, ' $^{40}\text{Ar}/^{39}\text{Ar}$ Step Heating of Thermally Overprinted Biotite, Hornblende and Potassium Feldspar from Eldora, Colorado', Earth and Planetary Science Letters, v26, p387-408
- Berggren, W., Kent, D., Flynn, J., and J. van Couvering, 1985, 'Cenozoic geochronology', GSA Bulletin, v96, p1407-p1418
- Camus, F., 1997, 'Porphyry Copper Systems in the Chilean Andes', in Contributions to Latin American Ore Deposit Geology, GAC/MAC Symposium, May 19-21, Ottawa, abstract
- Cuadra, P., 1996, 'Proyecto Mina Radomiro Tomic: El Mayor Desafío de Codelco', Geoinformativo, Bulletin of the Colegio de Geólogos de Chile, Santiago, Summer, 1996/1997, 2p
- Cuadra, P., Grez, E., Gröpper, H. and V. Villarroel, 1994, 'Informe Preliminar Modelamiento Geológico Proyecto Radomiro Tomic, CODELCO', confidential internal company report
- Evensen, N., Hamilton, P. and R. O'niions, 1978, 'Rare-earth abundances in chondritic meteorites', Geochimica et Cosmochimica Acta, v42, p1199-1212
- Fitch, F., Miller, J., and J. Mitchell, 1969, 'A new approach to radioisotopic dating in orogenic belts', in Time and Place in Orogeny, Kent, Satherthwaite and Spencer (eds), Geological Society of London Special Publication No.3, 157p
- Foland, K., 1974, ' Ar^{40} diffusion in homogeneous orthoclase and an interpretation of Ar diffusion in K-feldspars', Geochimica et Cosmochimica Acta, v38, p151-166

- Gates, R., 1953, 'Petrogenic Significance of Perthite', in Selected Petrogenic Relationships of Plagioclase, Emmons (ed), GSA Memoir 52
- Hanes, J., 1991, 'K-Ar and $^{40}\text{Ar}/^{39}\text{Ar}$ geochronology: methods and applications', In Short Course Handbook on Applications of Radiogenic Isotope Systems to Problems in Geology, Heaman and Ludden (eds), Mineralogical Association of Canada Short Course Handbook, v19, p27-57
- Harrison, T. and I. McDougall, 1982, 'The thermal significance of potassium feldspar K-Ar ages inferred from $^{40}\text{Ar}/^{39}\text{Ar}$ age spectrum results', *Geochimica Cosmochimica Acta*, v46, p1811-1820
- Hutchison, C.S., 1974, 'Laboratory Handbook of Petrographic Techniques', John Wiley and Sons, Toronto, 527p
- Jäger, E., 1979, 'Introduction to geochronology', in *Isotope Geology*, Springer, p1-12
- Lowell, J. and J. Guilbert, 1970, 'Lateral and Vertical Alteration-Mineralization Zoning in Porphyry Ore Deposits', *Economic Geology*, v65, p373-408
- Maksaev, V., 1990, 'Metallogeny, geological evolution and thermochronology of the Chilean Andes between latitudes 21° and 26° South, and the origin of major porphyry copper deposits', PhD Thesis, Dalhousie University, Halifax, Canada, 554p
- Maksaev, V. and M. Zentilli, 1988, 'Marco metalogenico regional de los megadepositos de tipo porfido cuprifero del norte grande de Chile', V Congreso Geologico Chileno, Tomo I, pB181-B212
- McDougall, I. and T. Harrison, 1988, 'Geochronology and Thermochronology by the $^{40}\text{Ar}/^{39}\text{Ar}$ Method', Oxford University Press
- Parsons, I., Rex, D., Guise, P. and A. Halliday, 1988, 'Argon-loss by alkali feldspars', *Geochimica et Cosmochimica Acta*, v52, p1097-1112
- Pearce, J., Harris, B. and A. Tindle, 1984, 'Trace element discrimination diagrams for tectonic interpretation of granitic rocks', *J. Of Petrology*, v25, i4, p956-983
- Peña Y Lillo, O., 1927, 'Breve reseña sobre la minería en Chile', *Boletín de la Sociedad Nacional de Minería*, Santiago, v39, p702-722
- Phillips, W., 1973, 'Mechanical effects of retrograde boiling and its probable importance in the formation of some porphyry ore deposits', Institute of Mining and Metallurgy, pB90-B98

- Reynolds, P., Ravenhurst, C., Zentilli, M., and D.Lindsay, 1997, 'High-precision $^{40}\text{Ar}/^{39}\text{Ar}$ Dating of Two Consecutive Hydrothermal Events in the Chuquibambilla Porphyry Copper System, Chile', *Isotope Geoscience*, in press
- Richards and McDougall, 1990, 'Geochronology of the Porgera gold deposit, Papua, New Guinea: Resolving the effects of excess argon on K-Ar and $^{40}\text{Ar}/^{39}\text{Ar}$ age estimates for magmatism and mineralization', *Geochimica et Cosmochimica Acta*, v54, p1397-1415
- Roedder, E., 1976, 'Fluid inclusion evidence on the genesis of ores in sedimentary and volcanic rocks', In K.H.Wolf (ed), *Handbook of Stratiform and Stratiform Ore Deposits*, Elsevier, Amsterdam, v2, p67-110
- Rose, A. and D. Burt, 1979, 'Hydrothermal alteration', in Barnes (ed) *Geochemistry of hydrothermal ore deposits*, 2nd edition, Wiley-Interscience, p173-235
- Ruddiman, W., and J. Kutzbach, 1989, 'Forcing of late Cenozoic northern hemisphere climate by plateau uplift in southern Asia and the American West', *Journal of Geophysical Research*, v94, p18409-18427
- Sardarov, S., 1957, 'Retention of radiogenic argon in microcline', *Geochemistry*, v3, p233-237
- Sawkins, F., 1990, 'Metal deposits in relation to plate tectonics', second edition, Springer Verlag, 461p
- Sillitoe, R., 1973, 'The Tops and Bottoms of Porphyry Copper Deposits', *Economic Geology*, v68, p799-815
- Sondergeld, C. and D. Turcotte, 1979, 'A laboratory study of mineral deposition in a boiling environment', *Economic Geology*, v74, p109-115
- Steiger, R. and E. Jäger, 1977, 'Subcommission on Geochronology: Convention on the Use of Decay Constants in Geo- and Cosmochronology', *Earth and Planetary Science Letters*, v36, p359-362
- Titley, S. and Beane, R., 1981, 'Porphyry copper deposits. Part I. Geologic settings, petrology, and tectonogenesis', *Economic Geology*, 75th Anniversary Volume, p214-235
- Turner, G., 1968, 'The distribution of potassium and argon in chondrites', in Aherns, L.H. (ed), *Origin and distribution of the elements*, London, Pergamon, p387-398
- Winchester, J., and P. Floyd, 1977, 'Geochemical discrimination of different magma series and their differentiation products using immobile elements', *Chemical Geology*, v20, p325-343

York, D., 1969, 'Least squares fitting of a straight line with correlated errors', *Earth and Planetary Science Letters*, v5, 973-975

Zentilli, M., Leiva, G., Rojas de la R., J., and M. Graves, 1994, 'The Chuquicamata Porphyry Copper System Revisited', *Society of Economic Geologists (SEG) Symposium*, Concepcion, Chile, 17-21 October, 5p

Appendix A.

Whole-rock Geochemical Data

Radomiro Tomic and Chuquicamata Geochemical Data and Analytical Methods

| Sample | SiO2 % | TiO2 % | Al2O3 % | Fe2O3 % | FeO % | FeOT % | Fe2O3T % | MnO % | MgO % | CaO % | Na2O % | K2O % | P2O5 % | H2Op | H2Om | LOI % | Total |
|------------------------|--------|--------|---------|---------|-------------|--------|----------|-------|-------|-------|--------|-------|--------|--------------|--------------|-------|-------------|
| Cu999 | 70.06 | 0.24 | 15.59 | 1.84 | 1.06 | 2.72 | 3.02 | 0.03 | 0.46 | 2.39 | 4.49 | 3.24 | 0.10 | 0.19 | 0.03 | 0.50 | 98.94 |
| Cu1001 | 72.03 | 0.29 | 14.09 | 1.76 | 0.94 | 2.52 | 2.80 | 0.03 | 0.52 | 2.00 | 4.01 | 3.22 | 0.11 | 0.27 | 0.10 | 0.47 | 98.53 |
| Cu1002 | 69.14 | 0.28 | 15.92 | 1.69 | 1.16 | 2.68 | 2.98 | 0.02 | 0.51 | 2.45 | 4.58 | 3.10 | 0.12 | 0.35 | 0.22 | 0.78 | 98.59 |
| Cu1006 | 75.49 | 0.19 | 13.57 | 0.66 | 0.91 | 1.50 | 1.67 | 0.01 | 0.08 | 0.16 | 0.30 | 4.70 | 0.10 | 2.39 | 0.48 | 3.53 | 98.79 |
| Cu1010 | 70.06 | 0.27 | 15.94 | 1.13 | 0.81 | 1.83 | 2.03 | 0.01 | 0.20 | 0.16 | 0.07 | 6.16 | 0.10 | 2.64 | 0.45 | 3.94 | 98.04 |
| Cu1011 | 73.25 | 0.22 | 16.35 | 0.74 | 0.50 | 1.17 | 1.30 | 0.01 | 0.38 | 0.04 | 0.10 | 5.06 | 0.03 | 1.64 | 0.19 | 2.52 | 98.70 |
| Cu093 | 77.34 | 0.17 | 9.5 | 1.11 | 2.17 | 3.17 | 3.52 | 0.01 | 0.21 | 1.52 | 0.01 | 3.7 | 0.07 | 1.14 | 0.14 | 4.15 | 96.98 |
| Cu510 | 72.6 | 0.22 | 13.5 | 2.97 | 0.91 | 3.58 | 3.98 | 0.05 | 0.5 | 0.42 | 2.82 | 4.82 | 0.07 | 1.14 | 0.09 | 1.9 | 99.9 |
| Cu512 | 69.6 | 0.22 | 15.7 | 1.16 | 0.79 | 1.83 | 2.04 | 0.03 | 0.6 | 0.88 | 4.96 | 4.97 | 0.09 | 0.65 | 0.28 | 1.35 | 99.6 |
| Cu513 | 72 | 0.19 | 15.7 | 0.65 | 0.68 | 1.26 | 1.41 | 0.08 | 0.56 | 0.38 | 5.28 | 4.42 | 0.1 | 0.61 | 0.15 | 1.1 | 100.5 |
| Analytical Info | | | | | | | | | | | | | | | | | |
| Detection Limit | 0.01 | 0.01 | 0.01 | 0.01 | 0.01 | 0.01 | 0.01 | 0.01 | 0.01 | 0.01 | 0.01 | 0.01 | 0.01 | 0.01 | 0.01 | 0.01 | 0.01 |
| Upper Limit | 100 | 100 | 100 | 100 | 100 | 100 | 100 | 100 | 100 | 100 | 100 | 100 | 100 | 100 | 100 | 100 | 105 |
| Method | XRF | XRF | XRF | XRF | Titrimetric | XRF | XRF | XRF | XRF | XRF | XRF | XRF | XRF | Leico RMC100 | Leico RMC100 | XRF | Calculation |

Trace Element Data

| Sample | Ba (ppm) | Rb (ppm) | Sr (ppm) | Y (ppm) | Zr (ppm) | Nb (ppm) | Cu (%) | S (%) |
|------------------------|----------|----------|----------|---------|----------|----------|------------------|-------------------|
| Cu999 | 635.00 | 76.00 | 584.00 | 10.00 | 93.00 | 10.00 | 0.05 | 0.11 |
| Cu1001 | 610.00 | 72.00 | 508.00 | 10.00 | 102.00 | 12.00 | 0.01 | 0.04 |
| Cu1002 | 710.00 | 76.00 | 590.00 | 10.00 | 108.00 | 14.00 | 0.08 | 0.07 |
| Cu1006 | 360.00 | 94.00 | 128.00 | 10.00 | 105.00 | 18.00 | 0.46 | 0.58 |
| Cu1010 | 820.00 | 114.00 | 136.00 | 14.00 | 105.00 | 12.00 | 1.06 | 0.87 |
| Cu1011 | 220.00 | 128.00 | 10.00 | 12.00 | 99.00 | 14.00 | 0.11 | 0.04 |
| Cu093 | 185.00 | 74.00 | 188.00 | 8.00 | 66.00 | 8.00 | 1.86 | 1.86 |
| Cu510 | 840.00 | 160.00 | 190.00 | 12.00 | 106.00 | 2.00 | 0.02 | 0.02 |
| Cu512 | 721.00 | 158.00 | 346.00 | 4.00 | 108.00 | 9.00 | 0.45 | 0.45 |
| Cu513 | 661.00 | 132.00 | 253.00 | 6.00 | 116.00 | 3.00 | 0.19 | 0.19 |
| Analytical Info | | | | | | | | |
| Detection Limit | 5 | 2 | 2 | 2 | 3 | 2 | 0.01 | 0.01 |
| Upper Limit | 50000 | 50000 | 50000 | 50000 | 50000 | 50000 | 100 | 100 |
| Method | XRF | XRF | XRF | XRF | XRF | XRF | AAS | Leico-IR Detector |
| | | | | | | | Nitric-HCl dig'n | Leico furnace |

Rare Earth Element Data

| Sample | La (ppm) | Ce (ppm) | Pr (ppm) | Nd (ppm) | Sm (ppm) | Eu (ppm) | Gd (ppm) | Tb (ppm) | Dy (ppm) | Ho (ppm) | Er (ppm) | Tm (ppm) | Yb (ppm) | Lu (ppm) |
|------------------------|----------|----------|----------|----------|----------|----------|----------|----------|----------|----------|----------|----------|----------|----------|
| Cu999 | 18.00 | 34.00 | 3.30 | 11.00 | 1.50 | 0.60 | 1.20 | 0.20 | 0.80 | 0.20 | 0.60 | 0.10 | 0.60 | 0.10 |
| Cu1001 | 22.00 | 46.00 | 4.40 | 11.00 | 1.10 | 0.60 | 1.40 | 0.20 | 1.10 | 0.20 | 0.60 | 0.10 | 0.50 | 0.10 |
| Cu1002 | 44.00 | 67.00 | 5.50 | 16.00 | 2.50 | 0.70 | 1.90 | 0.30 | 1.20 | 0.20 | 0.80 | 0.10 | 0.80 | 0.10 |
| Cu1006 | 12.00 | 26.00 | 2.30 | 6.00 | 1.20 | 0.40 | 0.70 | 0.10 | 0.20 | 0.20 | 0.10 | 0.10 | 0.20 | 0.10 |
| Cu1010 | 61.00 | 84.00 | 7.10 | 16.00 | 3.10 | 0.90 | 2.30 | 0.30 | 1.40 | 0.20 | 0.10 | 0.10 | 0.60 | 0.10 |
| Cu1011 | 15.00 | 34.00 | 3.30 | 11.00 | 1.70 | 0.40 | 1.10 | 0.20 | 0.80 | 0.20 | 0.50 | 0.10 | 0.40 | 0.10 |
| Cu093 | 14.00 | 24.00 | 2.20 | 6.00 | 0.90 | 0.30 | 0.60 | 0.10 | 0.50 | 0.10 | 0.30 | 0.10 | 0.30 | 0.10 |
| Cu510 | 18.00 | 36.00 | 3.30 | 12.00 | 2.00 | 0.70 | 1.30 | 0.20 | 0.90 | 0.20 | 0.10 | 0.10 | 0.50 | 0.10 |
| Cu512 | 14.00 | 27.00 | 4.10 | 9.00 | 1.80 | 0.60 | 0.80 | 0.10 | 0.80 | 0.20 | 0.10 | 0.10 | 0.40 | 0.10 |
| Cu513 | 12.00 | 22.00 | 2.10 | 7.00 | 1.30 | 0.50 | 0.70 | 0.10 | 0.10 | 0.20 | 0.10 | 0.10 | 0.30 | 0.10 |
| Analytical Info | | | | | | | | | | | | | | |
| Detection Limit | 1 | 2 | 0.2 | 1 | 0.5 | 0.2 | 0.2 | 0.1 | 0.5 | 0.2 | 0.5 | 0.1 | 0.1 | 0.1 |
| Upper Limit | 10000 | 10000 | 1000 | 1000 | 500 | 100 | 500 | 100 | 500 | 1000 | 500 | 500 | 1000 | 500 |
| Method | ICP-MS | ICP-MS | ICP-MS | ICP-MS | ICP-MS | ICP-MS | ICP-MS | ICP-MS | ICP-MS | ICP-MS | ICP-MS | ICP-MS | ICP-MS | ICP-MS |



Chemex Labs Ltd.

Analytical Chemists * Geochemists * Registered Assayers
 5175 Timberlea Blvd., Mississauga
 Ontario, Canada L4W 2S3
 PHONE: 905-624-2808 FAX: 905-624-6163

To: CUESTA RESEARCH LTD.

154 VICTORIA RD.
 DARTMOUTH, NS
 B3A 1V8

A9626404

Comments: ATTN: MILTON GRAVES

CERTIFICATE **A9626404**

(LJB) - CUESTA RESEARCH LTD.

Project:

P.O. #:

Samples submitted to our lab in Mississauga, ON.
 This report was printed on 20-AUG-96.

| SAMPLE PREPARATION | | |
|--------------------|----------------|---------------------------------|
| CHEMEX CODE | NUMBER SAMPLES | DESCRIPTION |
| 205 | 10 | Geochem ring to approx 150 mesh |
| 226 | 10 | 0-3 Kg crush and split |

| ANALYTICAL PROCEDURES | | | | | |
|-----------------------|----------------|------------------------------|------------------|-----------------|-------------|
| CHEMEX CODE | NUMBER SAMPLES | DESCRIPTION | METHOD | DETECTION LIMIT | UPPER LIMIT |
| 902 | 10 | Al2O3 %: XRF | XRF | 0.01 | 100.00 |
| 906 | 10 | CaO %: XRF | XRF | 0.01 | 100.00 |
| 2590 | 10 | Cr2O3 %: XRF | XRF | 0.01 | 100.00 |
| 903 | 10 | Fe2O3 %: XRF | XRF | 0.01 | 100.00 |
| 908 | 10 | K2O %: XRF | XRF | 0.01 | 100.00 |
| 905 | 10 | MgO %: XRF | XRF | 0.01 | 100.00 |
| 1989 | 10 | MnO %: XRF | XRF | 0.01 | 100.00 |
| 907 | 10 | Na2O %: XRF | XRF | 0.01 | 100.00 |
| 909 | 10 | P2O5 %: XRF | XRF | 0.01 | 100.00 |
| 901 | 10 | SiO2 %: XRF | XRF | 0.01 | 100.00 |
| 904 | 10 | TiO2 %: XRF | XRF | 0.01 | 100.00 |
| 910 | 10 | LOI %: XRF | XRF | 0.01 | 100.00 |
| 2540 | 10 | Total % | CALCULATION | 0.01 | 105.00 |
| 2091 | 10 | Ba ppm: XRF | XRF | 5 | 50000 |
| 2067 | 10 | Bb ppm: XRF | XRF | 2 | 50000 |
| 2098 | 10 | Bx ppm: XRF | XRF | 2 | 50000 |
| 2973 | 10 | Hb ppm: XRF | XRF | 2 | 50000 |
| 2978 | 10 | Ix ppm: XRF | XRF | 3 | 50000 |
| 2974 | 10 | Y ppm: XRF | XRF | 2 | 50000 |
| 451 | 10 | FeO %: Acid decomposition | TITRATION | 0.01 | 100.0 |
| 818 | 10 | Crystalline water | Leoc EMC100 | 0.01 | 100.0 |
| 819 | 10 | Surface moisture | Leoc EMC100 | 0.01 | 100.0 |
| 1380 | 10 | S %: Leoc furnace | LECO-IR DETECTOR | 0.01 | 100.0 |
| 301 | 10 | Cu %: Conc. Nitric-HCL dig'n | AAS | 0.01 | 100.0 |

3



Chemex Labs Ltd.

Analytical Chemists * Geochemists * Registered Assayers
 5175 Timberlea Blvd., Mississauga
 Ontario, Canada L4W 2S3
 PHONE: 905-624-2808 FAX: 905-624-6183

To: CUESTA RESEARCH LTD.

154 VICTORIA RD.
 DARTMOUTH, NS
 B3A 1V8

A9626405

Comments: ATTN: MILTON GRAVES

CERTIFICATE **A9626405**

(LJB) - CUESTA RESEARCH LTD.

Project:
 P.O.#:

Samples submitted to our lab in Mississauga, ON.
 This report was printed on 3-SEP-96.

| SAMPLE PREPARATION | | |
|--------------------|----------------|---|
| CHEMEX CODE | NUMBER SAMPLES | DESCRIPTION |
| 299 | 10 | Pulp, prepped on other workorder Meta-borate fusion charge |
| 297 | 10 | |

| ANALYTICAL PROCEDURES | | | | | |
|-----------------------|----------------|----------------|--------|-----------------|-------------|
| CHEMEX CODE | NUMBER SAMPLES | DESCRIPTION | METHOD | DETECTION LIMIT | UPPER LIMIT |
| 2501 | 10 | Ce ppm: ICP-MS | ICP-MS | 2 | 10000 |
| 2502 | 10 | Dy ppm: ICP-MS | ICP-MS | 0.5 | 500 |
| 2503 | 10 | Er ppm: ICP-MS | ICP-MS | 0.5 | 500 |
| 2504 | 10 | Hf ppm: ICP-MS | ICP-MS | 0.2 | 100.0 |
| 2505 | 10 | Gd ppm: ICP-MS | ICP-MS | 0.2 | 500 |
| 2506 | 10 | Mo ppm: ICP-MS | ICP-MS | 0.2 | 1000 |
| 2507 | 10 | La ppm: ICP-MS | ICP-MS | 1 | 10000 |
| 2508 | 10 | Lu ppm: ICP-MS | ICP-MS | 0.1 | 500 |
| 2509 | 10 | Md ppm: ICP-MS | ICP-MS | 1 | 1000 |
| 2510 | 10 | Pr ppm: ICP-MS | ICP-MS | 0.2 | 1000 |
| 2511 | 10 | Sm ppm: ICP-MS | ICP-MS | 0.5 | 500 |
| 2512 | 10 | Tb ppm: ICP-MS | ICP-MS | 0.1 | 100.0 |
| 2513 | 10 | Tm ppm: ICP-MS | ICP-MS | 0.1 | 500 |
| 2514 | 10 | Yb ppm: ICP-MS | ICP-MS | 0.1 | 1000 |



Chemex Labs Ltd.

Analytical Chemists * Geochemists * Registered Assayers
 6175 Timberlea Blvd., Mississauga
 Ontario, Canada L4W 2S3
 PHONE: 905-824-2908 FAX: 905-824-8183

To: CUESTA RESEARCH LTD.

154 VICTORIA RD.
 DARTMOUTH, NS
 B3A 1V8

Project:
 Comments: ATTN: MILTON GRAVES

Page Number : 1
 Total Pages : 1
 Certificate Date : 03-SEP-98
 Invoice No. : 19826405
 P.O. Number :
 Account : LJB

CERTIFICATE OF ANALYSIS A9626405

| SAMPLE | PREP CODE | Ca ppm | Dy ppm | Kr ppm | Ru ppm | Od ppm | Mo ppm | La ppm | Lu ppm | Md ppm | Pr ppm | Sr ppm | Tb ppm | Ta ppm | Yb ppm |
|-------------------|--------------------|---------------|----------------|----------------|----------------|----------------|----------------|---------------|----------------|--------------|----------------|----------------|----------------|---------------------|----------------|
| CU 093 | 299 297 | 24 | 0.5 | 0.3 | 0.3 | 0.6 | 0.1 | 14 | 0.1 | 6 | 2.2 | 0.9 | 0.1 | < 0.1 | 0.3 |
| CU 093 | 299 297 | 24 | 0.5 | 0.3 | 0.3 | 0.6 | 0.1 | 14 | 0.1 | 6 | 2.2 | 0.9 | 0.1 | < 0.1 | 0.3 |
| CU 093 | 299 297 | 24 | 0.5 | 0.3 | 0.3 | 0.6 | 0.1 | 14 | 0.1 | 6 | 2.2 | 0.9 | 0.1 | < 0.1 | 0.3 |
| CU 999 | 299 297 | 34 | 0.8 | 0.6 | 0.6 | 1.2 | 0.2 | 18 | 0.1 | 11 | 3.3 | 1.5 | 0.2 | 0.1 | 0.6 |
| CU 1001 | 299 297 | 46 | 1.1 | 0.6 | 0.6 | 1.4 | 0.2 | 22 | < 0.1 | 11 | 4.4 | 2.1 | 0.2 | 0.1 | 0.5 |
| CU 1002 | 299 297 | 67 | 1.2 | 0.8 | 0.7 | 1.9 | 0.2 | 44 | 0.1 | 16 | 5.8 | 2.8 | 0.3 | 0.1 | 0.8 |
| CU 1006 | 299 297 | 26 | 0.6 | 0.4 | 0.4 | 0.7 | 0.2 | 12 | < 0.1 | 6 | 2.3 | 1.2 | 0.1 | 0.1 | 0.2 |
| CU 1010 | 299 297 | 84 | 1.4 | 0.4 | 0.9 | 2.3 | 0.2 | 61 | 0.1 | 16 | 7.1 | 3.1 | 0.3 | 0.1 | 0.6 |
| CU 1011 | 299 297 | 34 | 0.8 | 0.8 | 0.4 | 1.1 | 0.2 | 15 | 0.1 | 11 | 3.3 | 1.7 | 0.2 | < 0.1 | 0.4 |

AS

CERTIFICATION: 



Chemex Labs Ltd.

Analytical Chemists * Geochemists * Registered Assayers
 5175 Timberlea Blvd., Mississauga
 Ontario, Canada L4W 2S3
 PHONE: 905-624-2808 FAX: 905-624-8163

To: CUESTA RESEARCH LTD.

164 VICTORIA RD.
 DARTMOUTH, NS
 B3A 1V8

Project:
 Comments: ATTN: MILTON GRAVES

Page Number : 1-A
 Total Pages : 1
 Certificate Date: 20-AUG-96
 Invoice No. : 19626404
 P.O. Number :
 Account : LJB

CERTIFICATE OF ANALYSIS A9626404

| SAMPLE | PREP CODE | Al2O3 % XRF | CaO % XRF | Cr2O3 % XRF | Fe2O3 % XRF | K2O % XRF | MgO % XRF | MnO % XRF | Na2O % XRF | P2O5 % XRF | SiO2 % XRF | TiO2 % XRF | LOI % XRF | TOTAL % | Ba ppm |
|---|--|--|---|--|---|---|---|---|--|---|--|---|---|--|--|
| CU 993 CU 993 CU 993 CU 993 CU 999 | 205 226 205 226 205 226 205 226 205 226 | 9.50 9.50 9.50 9.50 15.55 | 1.52 1.52 1.52 1.52 2.39 | < 0.01 < 0.01 < 0.01 < 0.01 < 0.01 | 1.11 1.11 1.11 1.11 1.84 | 2.90 2.90 2.90 2.90 3.24 | 0.21 0.21 0.21 0.21 0.46 | 0.03 0.03 0.03 0.03 0.03 | < 0.01 < 0.01 < 0.01 < 0.01 4.49 | 0.07 0.07 0.07 0.07 0.10 | 77.34 77.34 77.34 77.34 70.06 | 0.17 0.17 0.17 0.17 0.24 | 4.15 4.15 4.15 4.15 0.50 | 96.98 96.98 96.98 96.98 98.94 | 185 185 185 185 635 |
| CU 1001 CU 1002 CU 1006 CU 1010 CU 1011 | 205 226 205 226 205 226 205 226 205 226 | 14.09 15.92 13.57 15.94 16.35 | 2.00 2.45 0.16 0.16 0.04 | < 0.01 < 0.01 < 0.01 < 0.01 < 0.01 | 1.76 1.69 0.66 1.13 0.74 | 3.22 3.10 4.70 4.16 3.06 | 0.52 0.51 0.08 0.20 0.30 | 0.03 0.02 0.01 0.01 0.01 | 4.01 4.50 0.30 0.97 0.10 | 0.11 0.12 0.10 0.10 0.03 | 72.03 69.14 75.49 70.06 73.25 | 0.29 0.20 0.19 0.27 0.22 | 0.47 0.70 3.53 1.94 2.52 | 98.53 98.59 98.79 98.04 98.70 | 610 710 360 820 220 |

A6

CERTIFICATION: Heidi Bickler



Chemex Labs Ltd.

Analytical Chemists * Geochemists * Registered Assayers
 5175 Timberlea Blvd., Mississauga
 Ontario, Canada L4W 2S3
 PHONE: 905-624-2806 FAX: 905-624-6183

To: CUESTA RESEARCH LTD.

164 VICTORIA RD.
 DARTMOUTH, NS
 B3A 1V8

Project:
 Comments: ATTN: MILTON GRAVES

Page Number : 1-8
 Total Pages : 1
 Certificate Date: 20-AUG-96
 Invoice No. : 19626404
 P.O. Number :
 Account : LJB

CERTIFICATE OF ANALYSIS A9626404

| SAMPLE | PREP CODE | Rb ppm | Sr ppm | Nb ppm | Zr ppm | Y ppm | FeO % | +H2O % | -H2O % | S % Total | Cu % | | | | |
|-------------------|--------------------|---------------|----------------|--------------|---------------|--------------|-----------------|-----------------|-----------------|-----------------|-----------------|--|--|--|--|
| CU 993 | 205 226 | 74 | 188 | 8 | 66 | 8 | 2.17 | 1.14 | 0.14 | 1.83 | 1.86 | | | | |
| CU 993 | 205 226 | 74 | 188 | 8 | 66 | 8 | 2.17 | 1.14 | 0.14 | 1.83 | 1.86 | | | | |
| CU 999 | 205 226 | 76 | 584 | 10 | 93 | 10 | 1.06 | 0.19 | 0.03 | 0.11 | 0.05 | | | | |
| CU 1001 | 205 226 | 72 | 508 | 12 | 102 | 10 | 0.94 | 0.27 | 0.10 | 0.04 | 0.09 | | | | |
| CU 1002 | 205 226 | 76 | 590 | 14 | 108 | 10 | 1.16 | 0.35 | 0.22 | 0.07 | 0.08 | | | | |
| CU 1006 | 205 226 | 94 | 128 | 18 | 105 | 10 | 0.91 | 2.39 | 0.48 | 0.58 | 0.46 | | | | |
| CU 1010 | 205 226 | 114 | 136 | 12 | 105 | 14 | 0.81 | 2.64 | 0.45 | 0.87 | 1.06 | | | | |
| CU 1011 | 205 226 | 128 | 10 | 14 | 99 | 12 | 0.50 | 1.64 | 0.19 | 0.04 | 0.11 | | | | |
| | | | | | | | | | | | | | | | |

A7

CERTIFICATION: Milton Graves



Chemex Labs Ltd.

Analytical Chemists * Geochemists * Registered Assayers
5175 Timberlea Blvd., Mississauga,
Ontario, Canada L4W 2S3
PHONE: 416-624-2606

CUESTA RESEARCH LTD.

154 VICTORIA RD.
DARTMOUTH, NS
B3A 1V6

Project :
Comments: ATTN: MILTON C. GRAVES

Page N : 1
Total Pages : 1
Certificate Date: 15-DEC-99
Invoice No.: 19325722
P.O. Number
Account : LJB

CERTIFICATE OF ANALYSIS A9325722

| SAMPLE | PREP CODE | Al2O3 % | CaO % | Cr2O3 % | Fe2O3 % | K2O % | MgO % | MnO % | Na2O % | P2O5 % | SiO2 % | TiO2 % | LOI % | TOTAL % | Ba ppm | Rb ppm | Sr ppm | Mb ppm | Zr ppm | Y ppm |
|----------|-----------|---------|-------|---------|---------|-------|-------|-------|--------|--------|--------|--------|-------|---------|--------|--------|--------|--------|--------|-------|
| | | XRF | XRF | XRF | XRF | XRF | XRF | XRF | XRF | XRF | XRF | XRF | XRF | XRF | % | | | | | |
| CU93-510 | 214 -- | 13.50 | 0.42 | < 0.01 | 2.97 | 4.62 | 0.50 | 0.05 | 2.82 | 0.07 | 72.60 | 0.22 | 1.90 | 99.90 | 840 | 160 | 190 | < 2 | 106 | 12 |
| CU93-512 | 214 -- | 15.70 | 0.88 | < 0.01 | 1.16 | 4.97 | 0.60 | 0.03 | 4.96 | 0.09 | 69.60 | 0.22 | 1.35 | 99.60 | 721 | 158 | 346 | 9 | 108 | 4 |
| CU93-513 | 214 -- | 15.70 | 0.38 | < 0.01 | 0.65 | 4.42 | 0.56 | 0.08 | 5.28 | 0.10 | 72.00 | 0.19 | 1.10 | 100.50 | 661 | 132 | 253 | 3 | 116 | 6 |
| | | | | | | | | | | | | | | | | | | | | |
| | | | | | | | | | | | | | | | | | | | | |
| | | | | | | | | | | | | | | | | | | | | |

CERTIFICATION *[Signature]*



Chemex Labs Ltd.

Analytical Chemists * Geochemists * Registered Assayers
212 Brookbank Ave., North Vancouver
British Columbia, Canada V7J 2C1
PHONE: 604-964-0221

Client: CUESTA RESEARCH LTD.

154 VICTORIA RD.
DARTMOUTH, NS
B3A 1V8

Project:
Comments: ATTN: MILTON C. GRAVES

Page Number: 1
Total Pages: 1
Certificate Date: 13-DEC-98
Invoice No.: 19325723
P.O. Number:
Account: LJB

CERTIFICATE OF ANALYSIS A9325723

| SAMPLE | PREP CODE | S % Total | +H2O % | -H2O % | FeO % | | | | | | |
|-----------------------|-----------------------|-----------------------|-----------------------|-----------------------|-----------------------|--|--|--|--|--|--|
| CU93-510 | 299 -- | 0.019 | 1.14 | 0.09 | 0.91 | | | | | | |
| CU93-512 | 299 -- | 0.449 | 0.65 | 0.28 | 0.79 | | | | | | |
| CU93-513 | 299 -- | 0.191 | 0.61 | 0.15 | 0.68 | | | | | | |
| | | | | | | | | | | | |
| | | | | | | | | | | | |
| | | | | | | | | | | | |

CERTIFICATION: Albosta



Chemex Labs Ltd.

Analytical Chemists * Geochemists * Registered Assayers
5175 Timberlea Blvd., Mississauga,
Ontario, Canada L4W 2S3
PHONE: 416-624-2806

to: CUESTA RESEARCH LTD.

154 VICTORIA RD.
DARTMOUTH, NS
B3A 1V8

Project :
Comments: ATTN: MILTON C. GRAVES

Page Number : 1
Total Pages : 1
Certificate Date : 18-DEC-93
Invoice No. : 19325724
P.O. Number :
Account : LJB

CERTIFICATE OF ANALYSIS A9325724

| SAMPLE | PREP CODE | Ce ppm | Dy ppm | Er ppm | Eu ppm | Gd ppm | Ho ppm | La ppm | Lu ppm | Nd ppm | Pr ppm | Sm ppm | Tb ppm | Ta ppm | Tb ppm |
|----------|-----------|--------|--------|--------|--------|--------|--------|--------|--------|--------|--------|--------|--------|--------|--------|
| CUS3-510 | 299 297 | 36 | 0.9 | 0.3 | 0.7 | 1.3 | 0.2 | 18 | 0.1 | 12 | 3.3 | 2.0 | 0.2 | 0.1 | 0.5 |
| CUS3-512 | 299 297 | 27 | 0.8 | 0.4 | 0.6 | 0.8 | 0.2 | 14 | 0.1 | 9 | 2.4 | 1.8 | 0.1 | 0.1 | 0.4 |
| CUS3-513 | 299 297 | 22 | 0.4 | 0.2 | 0.5 | 0.7 | 0.1 | 12 | 0.1 | 7 | 2.1 | 1.3 | 0.1 | 0.1 | 0.3 |
| | | | | | | | | | | | | | | | |
| | | | | | | | | | | | | | | | |
| | | | | | | | | | | | | | | | |
| | | | | | | | | | | | | | | | |

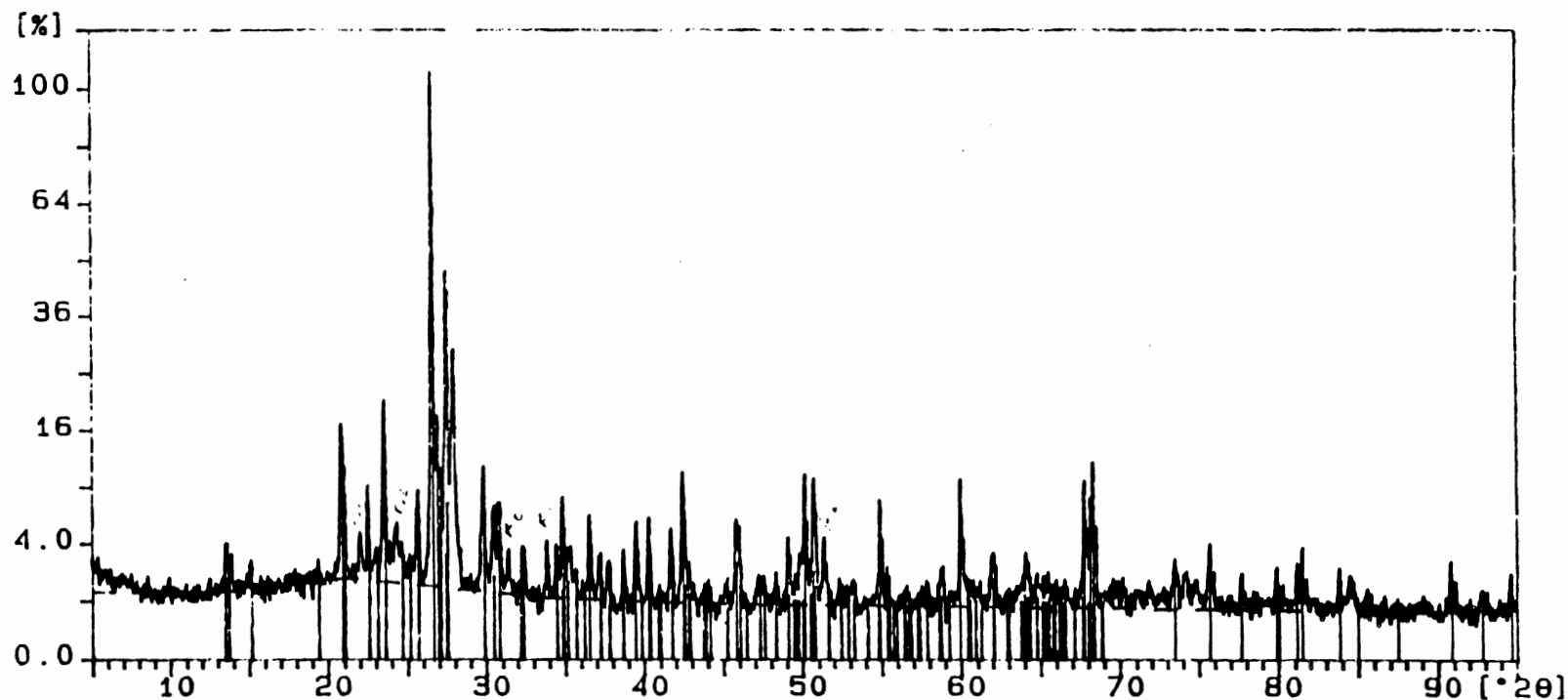
CERTIFICATION:

Appendix B.

X-ray Powder Diffractograms and Peak Lists

Sample ident.: cu999k2

14-Jun-1996 14:11



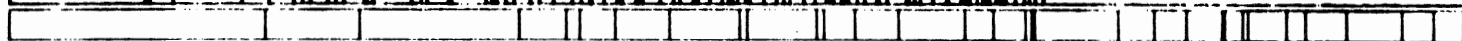
CU999K2



Orthoclase



Quartz,



Sample identification: cu999k2

Data measured at: 14-Jun-1996 13:08:00

Diffractometer type: PW3710 BASED

Tube anode: Cu

Generator tension [kV]: 40

Generator current [mA]: 45

Wavelength Alpha1 []: 1.54060

Wavelength Alpha2 []: 1.54439

Intensity ratio (alpha2/alpha1): 0.500

Divergence slit: 1x

Receiving slit: 0.1

Monochromator used: YES

Start angle [x2i]: 5.000

End angle [x2i]: 95.000

Step size [x2i]: 0.020

Maximum intensity: 2284.840

Time per step [s]: 0.500

Type of scan: CONTINUOUS

Minimum peak tip width: 0.00

Maximum peak tip width: 1.00

Peak base width: 2.00

Minimum significance: 0.75

Number of peaks: 87

| Angle [x2i] | d-value '1 [] | d-value '2 [] | Peak width [x2i] | Peak int [counts] | Back. int [counts] | Rel. int [%] | Signif. |
|----------------|------------------|------------------|---------------------|----------------------|-----------------------|-----------------|---------|
| 13.570 | 6.5200 | 6.5360 | 0.100 | 59 | 31 | 2.6 | 0.96 |
| 15.165 | 5.8377 | 5.8520 | 0.080 | 36 | 34 | 1.6 | 0.85 |
| 20.875 | 4.2520 | 4.2624 | 0.080 | 286 | 45 | 12.5 | 1.17 |
| 21.110 | 4.2052 | 4.2155 | 0.060 | 159 | 45 | 6.9 | 1.51 |
| 22.050 | 4.0280 | 4.0379 | 0.100 | 67 | 44 | 2.9 | 0.93 |
| 22.570 | 3.9363 | 3.9460 | 0.100 | 169 | 42 | 7.4 | 2.91 |
| 23.050 | 3.8554 | 3.8649 | 0.160 | 35 | 41 | 1.5 | 0.96 |
| 23.605 | 3.7660 | 3.7753 | 0.180 | 437 | 41 | 19.1 | 12.92 |
| 24.305 | 3.6591 | 3.6681 | 0.160 | 77 | 40 | 3.4 | 1.12 |
| 24.680 | 3.6044 | 3.6132 | 0.120 | 50 | 40 | 2.2 | 1.62 |
| 25.135 | 3.5402 | 3.5489 | 0.200 | 26 | 38 | 1.1 | 0.96 |
| 25.730 | 3.4596 | 3.4681 | 0.120 | 164 | 37 | 7.2 | 2.84 |
| 26.665 | 3.3404 | 3.3486 | 0.100 | 2285 | 36 | 100.0 | 11.52 |
| 26.980 | 3.3021 | 3.3102 | 0.100 | 392 | 36 | 17.2 | 3.48 |
| 27.175 | 3.2788 | 3.2869 | 0.080 | 231 | 36 | 10.1 | 1.63 |
| 27.565 | 3.2333 | 3.2413 | 0.120 | 894 | 35 | 39.1 | 9.24 |
| 27.990 | 3.1852 | 3.1930 | 0.140 | 708 | 34 | 31.0 | 7.70 |
| →29.870 | 2.9889 | 2.9962 | 0.100 | 219 | 31 | 9.6 | 2.33 |
| 30.475 | 2.9309 | 2.9381 | 0.080 | 144 | 30 | 6.3 | 0.80 |
| 30.900 | 2.8915 | 2.8987 | 0.080 | 149 | 29 | 6.5 | 1.28 |
| 31.430 | 2.8440 | 2.8510 | 0.120 | 48 | 29 | 2.1 | 1.63 |
| 32.365 | 2.7639 | 2.7707 | 0.200 | 58 | 27 | 2.5 | 2.48 |

File: CU999K2.DI

14-Jun-1996 13:46

=====

Phillips Analytical X-Ray 8. V.

PC-APD, Diffraction software

| Angle [2θ] | d-value '1 [Å] | d-value '2 [Å] | Peak width [2θ] | Peak int [counts] | Back. int [counts] | Rel. int [%] | Signif. |
|------------------------|-------------------|-------------------|-----------------------------|----------------------|-----------------------|-----------------|---------|
| 33.860 | 2.6452 | 2.6517 | 0.040 | 76 | 25 | 3.3 | 3.38 |
| 34.455 | 2.6009 | 2.6073 | 0.080 | 71 | 25 | 3.1 | 1.02 |
| 34.870 | 2.5709 | 2.5772 | 0.080 | 174 | 25 | 7.6 | 1.67 |
| 35.395 | 2.5340 | 2.5402 | 0.120 | 56 | 25 | 2.5 | 1.29 |
| 35.685 | 2.5140 | 2.5202 | 0.120 | 32 | 25 | 1.4 | 1.68 |
| 36.585 | 2.4542 | 2.4603 | 0.100 | 151 | 24 | 6.6 | 1.94 |
| 37.235 | 2.4129 | 2.4188 | 0.200 | 46 | 24 | 2.0 | 2.85 |
| 37.805 | 2.3778 | 2.3836 | 0.200 | 45 | 23 | 2.0 | 2.54 |
| 38.730 | 2.3231 | 2.3288 | 0.080 | 59 | 23 | 2.6 | 0.91 |
| 39.545 | 2.2771 | 2.2827 | 0.100 | 96 | 22 | 4.2 | 1.51 |
| 40.340 | 2.2340 | 2.2395 | 0.080 | 114 | 22 | 5.0 | 1.36 |
| 41.695 | 2.1645 | 2.1698 | 0.140 | 85 | 21 | 3.7 | 3.29 |
| 42.470 | 2.1268 | 2.1320 | 0.060 | 250 | 21 | 10.9 | 0.95 |
| 44.145 | 2.0499 | 2.0549 | 0.200 | 16 | 20 | 0.7 | 1.43 |
| 45.180 | 2.0053 | 2.0102 | 0.120 | 20 | 20 | 0.9 | 0.87 |
| 45.835 | 1.9781 | 1.9830 | 0.060 | 112 | 20 | 4.9 | 0.76 |
| 46.045 | 1.9696 | 1.9745 | 0.060 | 102 | 20 | 4.5 | 1.30 |
| 47.270 | 1.9214 | 1.9261 | 0.120 | 28 | 19 | 1.2 | 0.98 |
| 48.325 | 1.8819 | 1.8865 | 0.200 | 21 | 19 | 0.9 | 1.23 |
| 49.155 | 1.8520 | 1.8566 | 0.160 | 66 | 19 | 2.9 | 1.93 |
| 50.190 | 1.8162 | 1.8207 | 0.080 | 234 | 19 | 10.2 | 2.22 |
| 50.755 | 1.7973 | 1.8018 | 0.080 | 213 | 19 | 9.3 | 1.78 |
| 51.395 | 1.7764 | 1.7808 | 0.100 | 71 | 19 | 3.1 | 1.42 |
| 52.545 | 1.7402 | 1.7445 | 0.240 | 14 | 19 | 0.6 | 1.07 |
| 53.240 | 1.7191 | 1.7234 | 0.280 | 17 | 19 | 0.7 | 0.80 |
| 54.910 | 1.6707 | 1.6749 | 0.080 | 174 | 18 | 7.6 | 3.12 |
| 55.065 | 1.6664 | 1.6705 | 0.060 | 71 | 18 | 3.1 | 0.75 |
| 55.365 | 1.6581 | 1.6622 | 0.060 | 41 | 18 | 1.8 | 1.77 |
| 56.605 | 1.6247 | 1.6287 | 0.240 | 14 | 18 | 0.6 | 1.33 |
| 57.650 | 1.5977 | 1.6016 | 0.480 | 7 | 18 | 0.3 | 1.92 |
| 57.890 | 1.5916 | 1.5955 | 0.200 | 15 | 18 | 0.7 | 0.87 |
| 58.815 | 1.5688 | 1.5726 | 0.200 | 42 | 18 | 1.8 | 0.88 |
| 60.000 | 1.5406 | 1.5444 | 0.080 | 207 | 18 | 9.1 | 2.85 |
| 60.170 | 1.5367 | 1.5404 | 0.060 | 79 | 18 | 3.5 | 2.28 |
| 62.010 | 1.4954 | 1.4991 | 0.160 | 55 | 18 | 2.4 | 1.25 |
| 64.090 | 1.4518 | 1.4554 | 0.060 | 59 | 18 | 2.6 | 0.95 |
| 64.830 | 1.4370 | 1.4405 | 0.240 | 25 | 18 | 1.1 | 1.44 |
| 66.565 | 1.4037 | 1.4071 | 0.240 | 19 | 18 | 0.8 | 0.99 |
| 67.785 | 1.3814 | 1.3848 | 0.080 | 210 | 18 | 9.2 | 2.50 |
| 67.990 | 1.3777 | 1.3811 | 0.060 | 112 | 18 | 4.9 | 1.77 |
| 68.180 | 1.3743 | 1.3777 | 0.060 | 172 | 18 | 7.5 | 1.00 |
| 68.350 | 1.3713 | 1.3747 | 0.080 | 246 | 18 | 10.8 | 3.56 |
| 68.540 | 1.3680 | 1.3713 | 0.060 | 110 | 18 | 4.8 | 1.01 |
| 70.285 | 1.3382 | 1.3415 | 0.160 | 14 | 18 | 0.6 | 1.11 |
| 71.895 | 1.3122 | 1.3154 | 0.240 | 17 | 17 | 0.7 | 1.20 |
| 73.470 | 1.2879 | 1.2910 | 0.120 | 45 | 17 | 2.0 | 1.69 |
| 74.205 | 1.2769 | 1.2801 | 0.240 | 29 | 17 | 1.3 | 1.68 |
| 74.865 | 1.2673 | 1.2704 | 0.240 | 23 | 17 | 1.0 | 0.78 |
| 75.705 | 1.2553 | 1.2584 | 0.080 | 62 | 17 | 2.7 | 0.90 |
| 75.930 | 1.2522 | 1.2552 | 0.080 | 31 | 17 | 1.4 | 1.62 |
| 77.705 | 1.2279 | 1.2309 | 0.080 | 31 | 17 | 1.4 | 0.88 |

File: CU999X2.D1

14-Jun-1996 13:46

=====

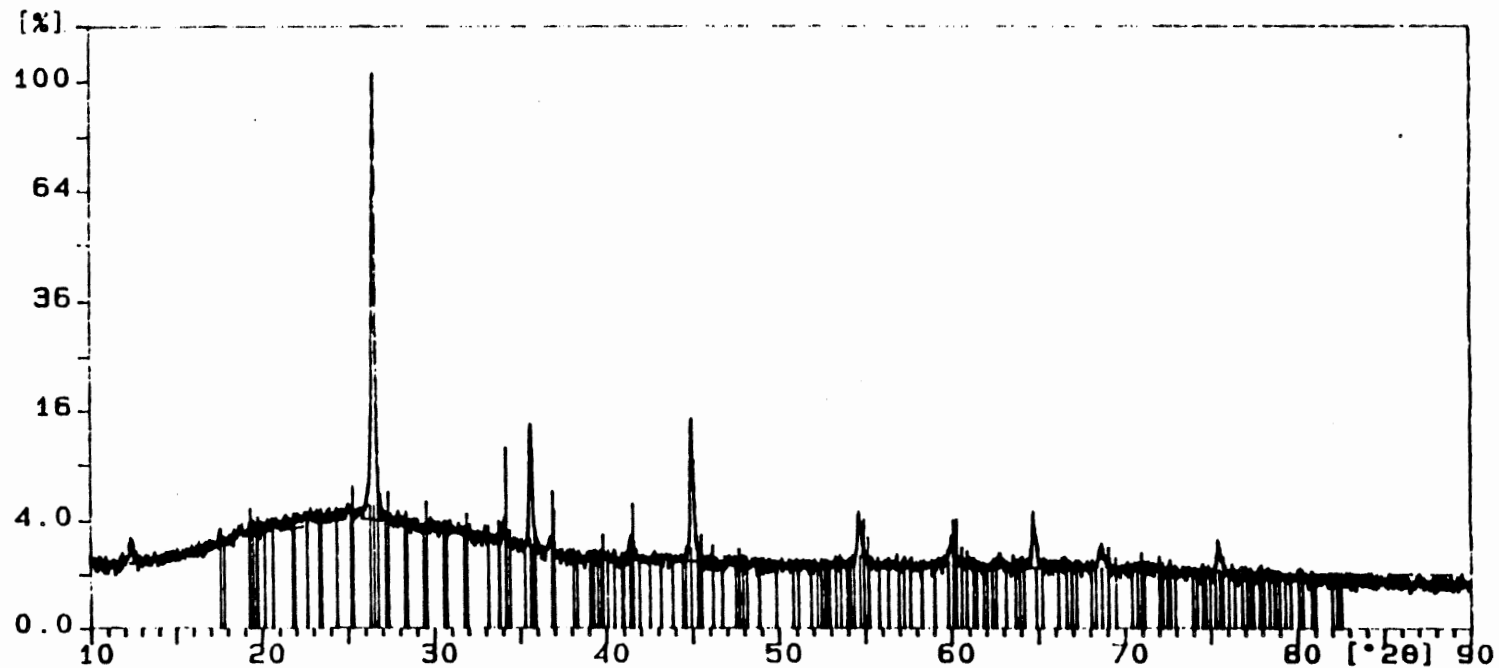
Phillips Analytical X-Ray B. V.

PC-APD, Diffraction software

| Angle [2θ] | d-value '1 [Å] | d-value '2 [Å] | Peak width [2θ] | Peak int [counts] | Back. int [counts] | Rel. int [%] | Signif. |
|------------------------|-------------------|-------------------|-----------------------------|----------------------|-----------------------|-----------------|---------|
| 79.900 | 1.1996 | 1.2026 | 0.120 | 37 | 16 | 1.6 | 2.05 |
| 81.190 | 1.1838 | 1.1867 | 0.100 | 62 | 16 | 2.7 | 2.15 |
| 81.530 | 1.1797 | 1.1826 | 0.060 | 71 | 16 | 3.1 | 1.59 |
| 81.805 | 1.1764 | 1.1793 | 0.080 | 30 | 16 | 1.3 | 1.13 |
| 83.885 | 1.1525 | 1.1553 | 0.100 | 26 | 16 | 1.1 | 1.01 |
| 84.530 | 1.1453 | 1.1481 | 0.160 | 26 | 16 | 1.1 | 0.89 |
| 95.595 | 1.1338 | 1.1366 | 0.120 | 18 | 16 | 0.8 | 1.57 |
| 85.845 | 1.1311 | 1.1339 | 0.100 | 13 | 15 | 0.6 | 0.84 |
| 87.445 | 1.1145 | 1.1172 | 0.200 | 6 | 15 | 0.3 | 0.76 |
| 89.215 | 1.0969 | 1.0996 | 0.480 | 7 | 15 | 0.3 | 0.89 |
| 90.865 | 1.0812 | 1.0839 | 0.120 | 48 | 15 | 2.1 | 1.21 |
| 91.135 | 1.0787 | 1.0814 | 0.100 | 26 | 15 | 1.1 | 1.26 |
| 92.830 | 1.0634 | 1.0660 | 0.120 | 15 | 15 | 0.7 | 0.83 |
| 94.650 | 1.0477 | 1.0503 | 0.120 | 29 | 15 | 1.3 | 3.18 |

Sample ident.: cu999bi2

22-May-1996 15:05



File: CU999812.D1

22-May-1996 14:37

Phillips Analytical X-Ray B. V.

PC-AP0, Diffraction software

Sample identification: cu999812

Data measured at: 22-May-1996 13:43:00

Diffractometer type: PM3710 BASED

Tube anode: Cu

Generator tension [kV]: 40

Generator current [mA]: 45

Wavelength Alpha1 [Å]: 1.54060

Wavelength Alpha2 [Å]: 1.54439

Intensity ratio (alpha2/alpha1): 0.500

Divergence slit: 1x

Receiving slit: 0.1

Monochromator used: YES

Start angle [x2i]: 10.000

End angle [x2i]: 90.000

Step size [x2i]: 0.020

Maximum intensity: 4761.000

Time per step [s]: 0.800

Type of scan: CONTINUOUS

Minimum peak tip width: 0.00

Maximum peak tip width: 1.00

Peak base width: 2.00

Minimum significance: 0.75

Number of peaks: 18

| Angle [x2i] | d-value '1 [Å] | d-value '2 [Å] | Peak width [x2i] | Peak int [counts] | Back. int [counts] | Rel. int [%] | Signif. |
|-------------|----------------|----------------|------------------|-------------------|--------------------|--------------|---------|
| 12.465 | 7.0954 | 7.1129 | 0.160 | 58 | 71 | 1.2 | 1.35 |
| 17.585 | 5.0394 | 5.0518 | 0.060 | 49 | 117 | 1.0 | 0.77 |
| 18.675 | 4.7476 | 4.7593 | 0.480 | 17 | 137 | 0.4 | 0.76 |
| 25.105 | 3.5443 | 3.5530 | 0.240 | 37 | 202 | 0.8 | 0.91 |
| 26.520 | 3.3583 | 3.3666 | 0.140 | 4761 | 196 | 100.0 | 33.34 |
| 34.145 | 2.6238 | 2.6303 | 0.200 | 74 | 125 | 1.6 | 2.03 |
| 35.630 | 2.5178 | 2.5240 | 0.160 | 552 | 110 | 11.6 | 10.38 |
| 36.850 | 2.4372 | 2.4432 | 0.240 | 41 | 92 | 0.9 | 0.86 |
| 41.420 | 2.1782 | 2.1836 | 0.160 | 53 | 77 | 1.1 | 0.94 |
| 44.975 | 2.0140 | 2.0189 | 0.080 | 635 | 74 | 13.3 | 3.16 |
| 45.105 | 2.0084 | 2.0134 | 0.040 | 335 | 74 | 7.0 | 1.29 |
| 54.645 | 1.6782 | 1.6823 | 0.120 | 130 | 67 | 2.7 | 2.28 |
| 60.080 | 1.5387 | 1.5425 | 0.200 | 64 | 64 | 1.3 | 1.38 |
| 62.770 | 1.4791 | 1.4827 | 0.480 | 14 | 62 | 0.3 | 1.14 |
| 64.750 | 1.4386 | 1.4421 | 0.080 | 161 | 61 | 3.4 | 0.83 |
| 66.540 | 1.4042 | 1.4076 | 0.060 | 29 | 59 | 0.6 | 0.76 |
| 68.695 | 1.3653 | 1.3686 | 0.200 | 50 | 58 | 1.1 | 0.79 |
| 75.470 | 1.2586 | 1.2617 | 0.060 | 71 | 50 | 1.5 | 0.75 |

File: CU1001K2.D1

14-Jun-1996 15:23

=====

Phillips Analytical X-Ray 8. V.

PC-APD, Diffraction software

Sample identification: cu1001k2

Data measured at: 14-Jun-1996 14:45:00

Diffractometer type: PW3710 BASED

Tube anode: Cu

Generator tension (kV): 40

Generator current (mA): 45

Wavelength Alpha1 (Å): 1.54060

Wavelength Alpha2 (Å): 1.54439

Intensity ratio (alpha2/alpha1): 0.500

Divergence slit: 1x

Receiving slit: 0.1

Monochromator used: YES

Start angle [x2i]: 5.000

End angle [x2i]: 95.000

Step size [x2i]: 0.020

Maximum intensity: 1814.760

Time per step (s): 0.500

Type of scan: CONTINUOUS

Minimum peak tip width: 0.00

Maximum peak tip width: 1.00

Peak base width: 2.00

Minimum significance: 0.75

Number of peaks: 82

| Angle [x2i] | d-value '1 [Å] | d-value '2 [Å] | Peak width [x2i] | Peak int [counts] | Back. int [counts] | Rel. int [%] | Signif. |
|-------------|----------------|----------------|------------------|-------------------|--------------------|--------------|---------|
| 13.690 | 6.4631 | 6.4790 | 0.060 | 76 | 26 | 4.2 | 0.86 |
| 15.165 | 5.8377 | 5.8520 | 0.240 | 20 | 28 | 1.1 | 1.33 |
| 20.935 | 4.2399 | 4.2504 | 0.140 | 210 | 37 | 11.6 | 3.00 |
| 21.205 | 4.1865 | 4.1968 | 0.060 | 199 | 37 | 11.0 | 0.77 |
| 22.065 | 4.0253 | 4.0352 | 0.240 | 55 | 36 | 3.0 | 3.49 |
| 22.540 | 3.9415 | 3.9512 | 0.060 | 135 | 36 | 7.4 | 1.01 |
| 22.645 | 3.9235 | 3.9331 | 0.080 | 94 | 36 | 5.2 | 1.12 |
| 23.655 | 3.7582 | 3.7674 | 0.180 | 317 | 35 | 17.5 | 9.80 |
| 24.290 | 3.6614 | 3.6704 | 0.240 | 53 | 34 | 2.9 | 1.59 |
| 24.635 | 3.6109 | 3.6197 | 0.120 | 66 | 34 | 3.6 | 1.42 |
| 25.180 | 3.5339 | 3.5426 | 0.240 | 41 | 32 | 2.3 | 2.27 |
| 25.765 | 3.4550 | 3.4635 | 0.140 | 269 | 31 | 14.8 | 5.59 |
| 26.630 | 3.3447 | 3.3529 | 0.080 | 1376 | 31 | 75.8 | 3.52 |
| 26.735 | 3.3318 | 3.3400 | 0.080 | 1815 | 31 | 100.0 | 3.53 |
| 26.990 | 3.3009 | 3.3090 | 0.080 | 416 | 30 | 22.9 | 1.74 |
| 27.640 | 3.2247 | 3.2327 | 0.200 | 992 | 30 | 54.7 | 21.59 |
| 28.020 | 3.1819 | 3.1897 | 0.140 | 493 | 29 | 27.2 | 7.07 |
| →29.905 | 2.9854 | 2.9928 | 0.180 | 317 | 27 | 17.5 | 10.94 |
| →30.485 | 2.9300 | 2.9372 | 0.080 | 90 | 27 | 5.0 | 0.94 |
| 30.825 | 2.8984 | 2.9055 | 0.100 | 210 | 26 | 11.6 | 1.63 |
| 32.410 | 2.7602 | 2.7670 | 0.080 | 106 | 24 | 5.8 | 0.93 |
| 33.990 | 2.6354 | 2.6419 | 0.160 | 12 | 23 | 0.7 | 0.76 |

File: CU1001K2.D1

14-Jun-1996 15:23

Phillips Analytical X-Ray 8. V.

PC-APD, Diffraction software

| Angle [2θ] | d-value '1 [Å] | d-value '2 [Å] | Peak width [2θ] | Peak int [counts] | Back. int [counts] | Rel. int [%] | Signif. |
|------------------------|-------------------|-------------------|-----------------------------|----------------------|-----------------------|-----------------|---------|
| 34.495 | 2.5980 | 2.6044 | 0.200 | 49 | 23 | 2.7 | 2.38 |
| 34.895 | 2.5691 | 2.5754 | 0.200 | 132 | 22 | 7.3 | 3.52 |
| 35.260 | 2.5433 | 2.5496 | 0.140 | 86 | 22 | 4.8 | 2.31 |
| 35.705 | 2.5127 | 2.5188 | 0.160 | 45 | 22 | 2.5 | 0.98 |
| 36.175 | 2.4811 | 2.4872 | 0.160 | 15 | 21 | 0.8 | 0.88 |
| 36.645 | 2.4503 | 2.4564 | 0.060 | 149 | 21 | 8.2 | 0.76 |
| 37.260 | 2.4113 | 2.4172 | 0.240 | 44 | 21 | 2.4 | 2.60 |
| 37.770 | 2.3799 | 2.3857 | 0.240 | 36 | 20 | 2.0 | 2.80 |
| 38.765 | 2.3211 | 2.3268 | 0.160 | 48 | 20 | 2.6 | 1.73 |
| 39.505 | 2.2793 | 2.2849 | 0.060 | 106 | 19 | 5.8 | 2.77 |
| 40.350 | 2.2335 | 2.2390 | 0.160 | 58 | 19 | 3.2 | 2.07 |
| 41.025 | 2.1983 | 2.2037 | 0.160 | 18 | 19 | 1.0 | 0.76 |
| 41.730 | 2.1627 | 2.1681 | 0.080 | 225 | 19 | 12.4 | 1.89 |
| 42.515 | 2.1246 | 2.1298 | 0.060 | 130 | 19 | 7.2 | 1.66 |
| 43.815 | 2.0645 | 2.0696 | 0.160 | 29 | 19 | 1.6 | 1.14 |
| 44.140 | 2.0501 | 2.0551 | 0.200 | 29 | 19 | 1.6 | 1.35 |
| 45.210 | 2.0040 | 2.0090 | 0.280 | 36 | 19 | 2.0 | 3.37 |
| 45.820 | 1.9788 | 1.9836 | 0.080 | 52 | 19 | 2.9 | 0.86 |
| 46.095 | 1.9676 | 1.9724 | 0.160 | 81 | 19 | 4.5 | 1.74 |
| 47.230 | 1.9229 | 1.9276 | 0.160 | 40 | 19 | 2.2 | 1.01 |
| 48.355 | 1.8808 | 1.8854 | 0.200 | 28 | 19 | 1.5 | 1.15 |
| 49.145 | 1.8524 | 1.8569 | 0.100 | 67 | 19 | 3.7 | 0.89 |
| 50.230 | 1.8149 | 1.8193 | 0.100 | 256 | 19 | 14.1 | 2.70 |
| 50.810 | 1.7955 | 1.7999 | 0.080 | 216 | 19 | 11.9 | 0.85 |
| 51.485 | 1.7735 | 1.7779 | 0.060 | 66 | 19 | 3.6 | 1.56 |
| 52.460 | 1.7429 | 1.7471 | 0.200 | 23 | 19 | 1.3 | 1.03 |
| 53.340 | 1.7162 | 1.7204 | 0.160 | 14 | 18 | 0.8 | 0.80 |
| 54.915 | 1.6706 | 1.6747 | 0.120 | 92 | 18 | 5.1 | 2.77 |
| 55.350 | 1.6585 | 1.6626 | 0.060 | 45 | 18 | 2.5 | 1.32 |
| 55.800 | 1.6462 | 1.6502 | 0.160 | 14 | 18 | 0.8 | 0.94 |
| 56.415 | 1.6297 | 1.6337 | 0.200 | 19 | 18 | 1.1 | 0.79 |
| 57.955 | 1.5900 | 1.5939 | 0.240 | 14 | 18 | 0.8 | 1.52 |
| 58.875 | 1.5673 | 1.5712 | 0.060 | 85 | 18 | 4.7 | 1.21 |
| 59.990 | 1.5408 | 1.5446 | 0.140 | 117 | 18 | 6.4 | 4.56 |
| 60.210 | 1.5357 | 1.5395 | 0.060 | 62 | 18 | 3.4 | 1.25 |
| 61.290 | 1.5112 | 1.5149 | 0.240 | 22 | 18 | 1.2 | 1.76 |
| 61.905 | 1.4977 | 1.5014 | 0.160 | 66 | 18 | 3.6 | 0.86 |
| 62.095 | 1.4936 | 1.4972 | 0.120 | 76 | 18 | 4.2 | 1.40 |
| 62.950 | 1.4753 | 1.4789 | 0.240 | 14 | 18 | 0.8 | 0.78 |
| 64.245 | 1.4487 | 1.4522 | 0.200 | 55 | 18 | 3.0 | 1.64 |
| 64.820 | 1.4372 | 1.4407 | 0.120 | 38 | 18 | 2.1 | 1.22 |
| 65.405 | 1.4258 | 1.4293 | 0.100 | 37 | 18 | 2.1 | 0.89 |
| 65.605 | 1.4219 | 1.4254 | 0.100 | 30 | 18 | 1.7 | 0.77 |
| 67.790 | 1.3813 | 1.3847 | 0.120 | 96 | 18 | 5.3 | 1.11 |
| 68.215 | 1.3737 | 1.3771 | 0.060 | 135 | 18 | 7.4 | 0.82 |
| 68.385 | 1.3707 | 1.3741 | 0.100 | 132 | 18 | 7.3 | 1.93 |
| 70.330 | 1.3375 | 1.3408 | 0.240 | 13 | 18 | 0.7 | 1.80 |
| 71.920 | 1.3118 | 1.3150 | 0.240 | 29 | 18 | 1.6 | 2.47 |
| 72.775 | 1.2985 | 1.3016 | 0.400 | 23 | 18 | 1.3 | 1.73 |
| 73.500 | 1.2874 | 1.2906 | 0.120 | 45 | 18 | 2.5 | 1.96 |
| 74.265 | 1.2760 | 1.2792 | 0.240 | 34 | 18 | 1.9 | 1.54 |

File: CU1001K2.D1

14-Jun-1996 15:24

=====

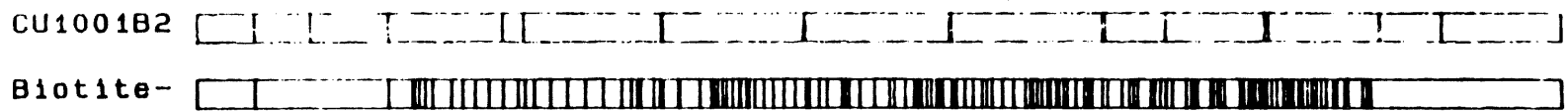
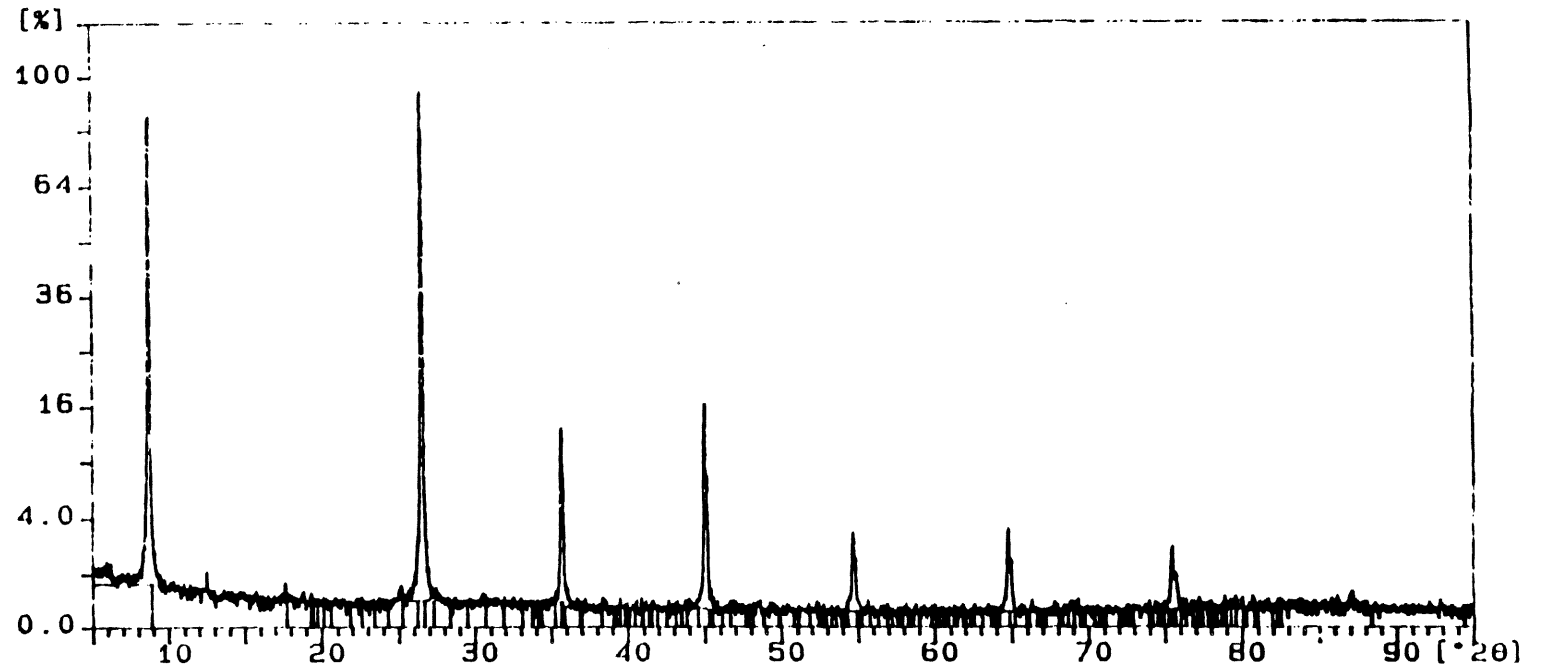
Phillips Analytical X-Ray 8. V.

PC-APD, Diffraction software

| Angle [2θ] | d-value '1 [Å] | d-value '2 [Å] | Peak width [2θ] | Peak int [counts] | Back. int [counts] | Rel. int [%] | Signif. |
|------------------------|-------------------|-------------------|-----------------------------|----------------------|-----------------------|-----------------|---------|
| 75.690 | 1.2555 | 1.2586 | 0.200 | 45 | 18 | 2.5 | 2.03 |
| 79.945 | 1.1991 | 1.2020 | 0.100 | 44 | 19 | 2.4 | 1.39 |
| 81.245 | 1.1831 | 1.1860 | 0.080 | 37 | 18 | 2.2 | 0.86 |
| 81.495 | 1.1801 | 1.1830 | 0.060 | 37 | 18 | 2.1 | 1.46 |
| 83.930 | 1.1520 | 1.1548 | 0.080 | 35 | 18 | 1.9 | 1.87 |
| 87.675 | 1.1122 | 1.1149 | 0.240 | 10 | 14 | 0.5 | 1.27 |
| 88.475 | 1.1042 | 1.1069 | 0.480 | 6 | 14 | 0.3 | 0.90 |
| 90.870 | 1.0812 | 1.0839 | 0.120 | 29 | 15 | 1.6 | 1.26 |
| 92.965 | 1.0622 | 1.0649 | 0.640 | 5 | 15 | 0.3 | 0.94 |

Sample ident.: cu1001b2

20-Jun-1996 13:08



File: CU100182.01

20-Jun-1996 12:49

=====

Phillips Analytical X-Ray 8. V.

PC-APD, Diffraction software

Sample identification: cu1001b2

Data measured at: 20-Jun-1996 12:11:00

Diffractometer type: PW3710 BASED

Tube anode: Cu

Generator tension [kv]: 40

Generator current [mA]: 45

Wavelength Alpha1 [Å]: 1.54060

Wavelength Alpha2 [Å]: 1.54439

Intensity ratio (alpha2/alpha1): 0.500

Divergence slit: 1x

Receiving slit: 0.1

Monochromator used: YES

Start angle [x2i]: 5.000

End angle [x2i]: 95.000

Step size [x2i]: 0.020

Maximum intensity: 4108.810

Time per step [s]: 0.500

Type of scan: CONTINUOUS

Minimum peak tip width: 0.00

Maximum peak tip width: 1.00

Peak base width: 2.00

Minimum significance: 0.75

Number of peaks: 18

| Angle [x2i] | d-value '1 [Å] | d-value '2 [Å] | Peak width [x2i] | Peak int [counts] | Back. int [counts] | Rel. int [%] | Signif. |
|----------------|-------------------|-------------------|---------------------|----------------------|-----------------------|-----------------|---------|
| 8.835 | 10.0008 | 10.0254 | 0.080 | 4070 | 28 | 99.1 | 15.63 |
| 12.550 | 7.0475 | 7.0649 | 0.060 | 23 | 16 | 0.6 | 0.79 |
| 17.690 | 5.0097 | 5.0220 | 0.100 | 21 | 10 | 0.5 | 1.29 |
| 25.210 | 3.5298 | 3.5385 | 0.160 | 16 | 10 | 0.4 | 0.88 |
| 26.620 | 3.3459 | 3.3542 | 0.120 | 4109 | 11 | 100.0 | 22.36 |
| 35.725 | 2.5113 | 2.5175 | 0.060 | 529 | 7 | 12.9 | 1.83 |
| 35.845 | 2.5032 | 2.5093 | 0.040 | 276 | 6 | 6.7 | 3.04 |
| 45.075 | 2.0097 | 2.0147 | 0.080 | 655 | 5 | 16.0 | 4.96 |
| 45.200 | 2.0044 | 2.0094 | 0.040 | 335 | 5 | 8.2 | 5.39 |
| 54.725 | 1.6760 | 1.6801 | 0.080 | 125 | 3 | 3.1 | 1.88 |
| 54.870 | 1.6719 | 1.6760 | 0.060 | 66 | 3 | 1.6 | 1.51 |
| 64.825 | 1.4371 | 1.4406 | 0.080 | 128 | 3 | 3.1 | 1.75 |
| 65.015 | 1.4334 | 1.4369 | 0.060 | 67 | 3 | 1.6 | 2.28 |
| 68.980 | 1.3603 | 1.3637 | 0.480 | 4 | 4 | 0.1 | 1.63 |
| 75.530 | 1.2578 | 1.2609 | 0.120 | 90 | 4 | 2.2 | 2.82 |
| 75.775 | 1.2543 | 1.2574 | 0.080 | 40 | 5 | 1.0 | 2.61 |
| 83.070 | 1.1617 | 1.1646 | 0.060 | 7 | 6 | 0.2 | 0.76 |
| 87.125 | 1.1178 | 1.1205 | 0.120 | 15 | 5 | 0.4 | 1.07 |

File: CU1002K2.DI

23-May-1996 11:16

=====

Phillips Analytical X-Ray B. V.

PC-APD, Diffraction software

Sample identification: cu1002k2

Data measured at: 23-May-1996 10:23:00

Diffractometer type: PW3710 BASED

Tube anode: Cu

Generator tension [kV]: 40

Generator current [mA]: 45

Wavelength Alpha1 [Å]: 1.54060

Wavelength Alpha2 [Å]: 1.54439

Intensity ratio (alpha2/alpha1): 0.500

Divergence slit: 1x

Receiving slit: 0.1

Monochromator used: YES

Start angle [x2i]: 10.000

End angle [x2i]: 90.000

Step size [x2i]: 0.020

Maximum intensity: 3249.000

Time per step [s]: 0.800

Type of scan: CONTINUOUS

Minimum peak tip width: 0.00

Maximum peak tip width: 1.00

Peak base width: 2.00

Minimum significance: 0.75

Number of peaks: 95

| Angle [x2i] | d-value '1 [Å] | d-value '2 [Å] | Peak width [x2i] | Peak int [counts] | Back. int [counts] | Rel. int [%] | Signif. |
|-------------|----------------|----------------|------------------|-------------------|--------------------|--------------|---------|
| 13.650 | 6.4820 | 6.4979 | 0.200 | 85 | 53 | 2.6 | 1.63 |
| 15.110 | 5.8588 | 5.8732 | 0.160 | 20 | 58 | 0.6 | 0.95 |
| 20.880 | 4.2510 | 4.2614 | 0.080 | 159 | 81 | 4.9 | 1.13 |
| 21.125 | 4.2022 | 4.2126 | 0.080 | 660 | 81 | 20.3 | 5.08 |
| 22.105 | 4.0181 | 4.0280 | 0.080 | 85 | 77 | 2.6 | 0.76 |
| 22.595 | 3.9320 | 3.9417 | 0.120 | 199 | 76 | 6.1 | 3.27 |
| 23.130 | 3.8423 | 3.8517 | 0.120 | 64 | 74 | 2.0 | 1.19 |
| 23.585 | 3.7692 | 3.7785 | 0.100 | 942 | 72 | 29.0 | 5.58 |
| 24.350 | 3.6525 | 3.6615 | 0.120 | 79 | 69 | 2.4 | 1.22 |
| 24.675 | 3.6051 | 3.6140 | 0.100 | 135 | 69 | 4.1 | 1.92 |
| 25.130 | 3.5408 | 3.5496 | 0.200 | 49 | 67 | 1.5 | 1.14 |
| 25.630 | 3.4729 | 3.4814 | 0.040 | 282 | 67 | 8.7 | 0.97 |
| 25.760 | 3.4557 | 3.4642 | 0.140 | 449 | 66 | 13.8 | 7.29 |
| 26.730 | 3.3324 | 3.3406 | 0.120 | 3249 | 64 | 100.0 | 20.23 |
| 27.145 | 3.2824 | 3.2905 | 0.060 | 762 | 62 | 23.4 | 5.08 |
| 27.540 | 3.2362 | 3.2442 | 0.060 | 2767 | 61 | 85.2 | 1.16 |
| 27.645 | 3.2242 | 3.2321 | 0.060 | 3069 | 61 | 94.5 | 3.25 |
| 28.010 | 3.1830 | 3.1908 | 0.140 | 767 | 59 | 23.6 | 6.37 |
| 29.950 | 2.9811 | 2.9884 | 0.200 | 538 | 53 | 16.6 | 14.83 |
| 30.580 | 2.9211 | 2.9283 | 0.080 | 108 | 52 | 3.3 | 1.35 |
| 30.850 | 2.8961 | 2.9032 | 0.160 | 571 | 50 | 17.6 | 14.76 |
| 32.360 | 2.7643 | 2.7711 | 0.060 | 112 | 45 | 3.5 | 2.20 |

File: CU1002K2.D1

23-May-1996 11:16

=====

Phillips Analytical X-Ray B. V.

PC-APD, Diffraction software

| Angle [2θ] | d-value '1 [Å] | d-value '2 [Å] | Peak width [2θ] | Peak int [counts] | Back. int [counts] | Rel. int [%] | Signif. |
|------------------------|-------------------|-------------------|-----------------------------|----------------------|-----------------------|-----------------|---------|
| 34.440 | 2.6020 | 2.6084 | 0.120 | 61 | 41 | 1.9 | 1.78 |
| 34.890 | 2.5695 | 2.5758 | 0.080 | 204 | 41 | 6.3 | 1.19 |
| 35.285 | 2.5416 | 2.5479 | 0.060 | 172 | 41 | 5.3 | 1.60 |
| 35.740 | 2.5103 | 2.5165 | 0.080 | 74 | 41 | 2.3 | 0.76 |
| 36.210 | 2.4788 | 2.4849 | 0.080 | 38 | 40 | 1.2 | 0.81 |
| 36.600 | 2.4532 | 2.4593 | 0.060 | 114 | 40 | 3.5 | 2.05 |
| 37.205 | 2.4147 | 2.4207 | 0.080 | 72 | 38 | 2.2 | 0.83 |
| 37.870 | 2.3738 | 2.3797 | 0.200 | 38 | 38 | 1.2 | 2.02 |
| 38.740 | 2.3225 | 2.3282 | 0.080 | 94 | 37 | 2.9 | 1.02 |
| 39.520 | 2.2784 | 2.2841 | 0.060 | 146 | 36 | 4.5 | 1.18 |
| 40.315 | 2.2353 | 2.2408 | 0.100 | 69 | 36 | 2.1 | 1.36 |
| 41.045 | 2.1972 | 2.2027 | 0.160 | 28 | 35 | 0.9 | 1.01 |
| 41.695 | 2.1645 | 2.1698 | 0.060 | 272 | 35 | 8.4 | 1.16 |
| 41.815 | 2.1585 | 2.1639 | 0.040 | 317 | 34 | 9.8 | 4.20 |
| 42.550 | 2.1229 | 2.1282 | 0.080 | 104 | 34 | 3.2 | 0.78 |
| 42.945 | 2.1043 | 2.1095 | 0.080 | 110 | 34 | 3.4 | 0.86 |
| 43.775 | 2.0663 | 2.0714 | 0.060 | 86 | 32 | 2.7 | 2.44 |
| 44.115 | 2.0512 | 2.0562 | 0.060 | 49 | 32 | 1.5 | 1.41 |
| 45.190 | 2.0049 | 2.0098 | 0.200 | 52 | 31 | 1.6 | 2.22 |
| 45.830 | 1.9783 | 1.9832 | 0.120 | 74 | 31 | 2.3 | 2.00 |
| 46.035 | 1.9700 | 1.9749 | 0.200 | 90 | 31 | 2.8 | 1.90 |
| 47.325 | 1.9193 | 1.9240 | 0.060 | 90 | 31 | 2.8 | 1.29 |
| 48.355 | 1.8808 | 1.8854 | 0.200 | 29 | 31 | 0.9 | 1.01 |
| 49.135 | 1.8527 | 1.8573 | 0.080 | 108 | 31 | 3.3 | 1.10 |
| 49.790 | 1.8299 | 1.8344 | 0.060 | 71 | 30 | 2.2 | 1.27 |
| 50.185 | 1.8164 | 1.8209 | 0.060 | 762 | 30 | 23.4 | 3.25 |
| 50.320 | 1.8118 | 1.8163 | 0.060 | 361 | 30 | 11.1 | 2.38 |
| 50.765 | 1.7970 | 1.8014 | 0.100 | 372 | 30 | 11.5 | 2.38 |
| 51.710 | 1.7664 | 1.7707 | 0.240 | 21 | 30 | 0.7 | 1.14 |
| 52.375 | 1.7455 | 1.7498 | 0.200 | 49 | 30 | 1.5 | 1.44 |
| 53.350 | 1.7159 | 1.7201 | 0.140 | 32 | 30 | 1.0 | 1.24 |
| 54.930 | 1.6702 | 1.6743 | 0.080 | 161 | 30 | 5.0 | 1.45 |
| 55.100 | 1.6654 | 1.6695 | 0.060 | 76 | 30 | 2.3 | 1.97 |
| 55.710 | 1.6486 | 1.6527 | 0.060 | 53 | 30 | 1.6 | 1.77 |
| 56.620 | 1.6243 | 1.6283 | 0.120 | 45 | 29 | 1.4 | 0.79 |
| 56.955 | 1.6155 | 1.6195 | 0.060 | 46 | 29 | 1.4 | 1.16 |
| 57.445 | 1.6029 | 1.6068 | 0.240 | 45 | 29 | 1.4 | 2.63 |
| 57.990 | 1.5891 | 1.5930 | 0.160 | 19 | 29 | 0.6 | 1.30 |
| 58.810 | 1.5689 | 1.5728 | 0.060 | 164 | 29 | 5.0 | 0.80 |
| 58.985 | 1.5647 | 1.5685 | 0.060 | 76 | 29 | 2.3 | 1.13 |
| 60.000 | 1.5406 | 1.5444 | 0.100 | 166 | 29 | 5.1 | 3.15 |
| 60.165 | 1.5368 | 1.5405 | 0.060 | 77 | 29 | 2.4 | 0.75 |
| 62.120 | 1.4930 | 1.4967 | 0.080 | 151 | 29 | 4.7 | 1.45 |
| 63.760 | 1.4585 | 1.4621 | 0.120 | 34 | 28 | 1.0 | 0.84 |
| 64.300 | 1.4476 | 1.4511 | 0.060 | 156 | 28 | 4.8 | 3.88 |
| 64.485 | 1.4439 | 1.4474 | 0.060 | 69 | 28 | 2.1 | 1.62 |
| 64.825 | 1.4371 | 1.4406 | 0.080 | 130 | 28 | 4.0 | 1.12 |
| 66.550 | 1.4040 | 1.4074 | 0.240 | 22 | 28 | 0.7 | 1.02 |
| 67.795 | 1.3812 | 1.3846 | 0.100 | 77 | 28 | 2.4 | 0.98 |
| 68.225 | 1.3735 | 1.3769 | 0.060 | 144 | 28 | 4.4 | 2.24 |
| 68.420 | 1.3701 | 1.3735 | 0.100 | 121 | 27 | 3.7 | 1.43 |

File: CU1002K2.D1

23-May-1996 11:17

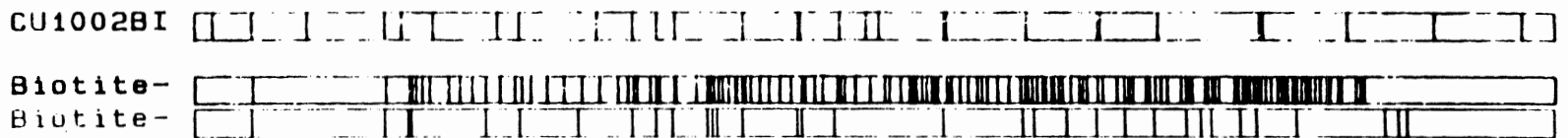
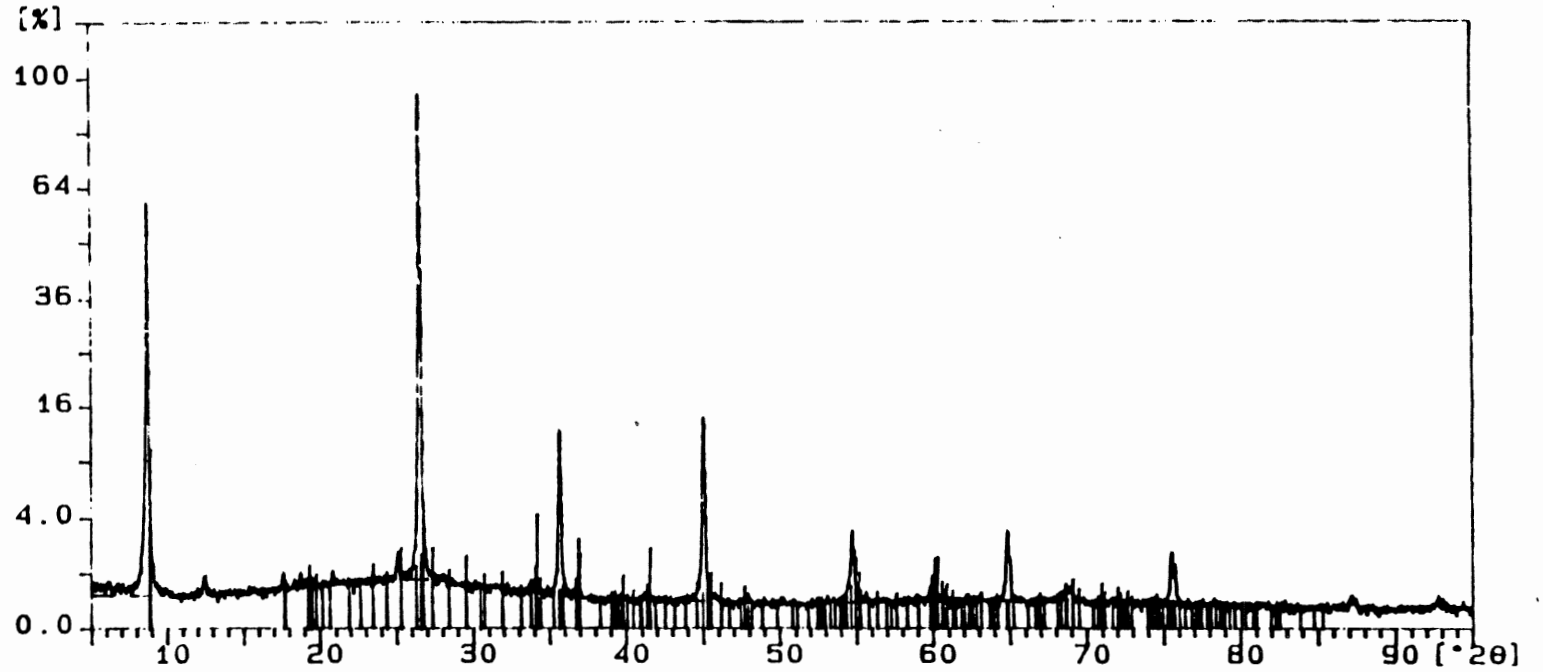
Phillips Analytical X-Ray 8. V.

PC-APD, Diffraction software

| Angle [x2i] | d-value '1 [] | d-value '2 [] | Peak width [x2i] | Peak int [counts] | Back. int [counts] | Rel. int [%] | Signif. |
|----------------|------------------|------------------|---------------------|----------------------|-----------------------|-----------------|---------|
| 70.275 | 1.3384 | 1.3417 | 0.120 | 52 | 27 | 1.6 | 1.83 |
| 71.845 | 1.3130 | 1.3162 | 0.080 | 90 | 27 | 2.8 | 1.37 |
| 72.045 | 1.3098 | 1.3130 | 0.080 | 45 | 27 | 1.4 | 0.79 |
| 72.655 | 1.3003 | 1.3035 | 0.120 | 49 | 27 | 1.5 | 1.09 |
| 73.525 | 1.2871 | 1.2902 | 0.200 | 53 | 27 | 1.6 | 1.16 |
| 74.220 | 1.2767 | 1.2799 | 0.240 | 40 | 27 | 1.2 | 2.04 |
| 74.845 | 1.2676 | 1.2707 | 0.060 | 98 | 26 | 3.0 | 2.22 |
| 75.050 | 1.2646 | 1.2677 | 0.060 | 66 | 26 | 2.0 | 0.75 |
| 75.600 | 1.2568 | 1.2599 | 0.080 | 117 | 26 | 3.6 | 1.57 |
| 75.835 | 1.2535 | 1.2566 | 0.080 | 59 | 26 | 1.8 | 0.85 |
| 77.685 | 1.2282 | 1.2312 | 0.100 | 23 | 26 | 0.7 | 0.92 |
| 79.925 | 1.1993 | 1.2023 | 0.060 | 55 | 26 | 1.7 | 1.55 |
| 80.130 | 1.1968 | 1.1997 | 0.100 | 38 | 26 | 1.2 | 0.84 |
| 80.385 | 1.1936 | 1.1965 | 0.120 | 36 | 26 | 1.1 | 1.02 |
| 81.215 | 1.1835 | 1.1864 | 0.060 | 29 | 25 | 0.9 | 1.10 |
| 81.470 | 1.1804 | 1.1833 | 0.120 | 38 | 25 | 1.2 | 1.06 |
| 82.145 | 1.1724 | 1.1753 | 0.120 | 18 | 25 | 0.6 | 1.29 |
| 83.900 | 1.1523 | 1.1551 | 0.120 | 35 | 25 | 1.1 | 0.90 |
| 84.495 | 1.1457 | 1.1485 | 0.140 | 26 | 25 | 0.8 | 1.28 |
| 85.580 | 1.1339 | 1.1367 | 0.120 | 18 | 25 | 0.5 | 0.75 |
| 86.625 | 1.1229 | 1.1257 | 0.240 | 8 | 25 | 0.2 | 0.84 |
| 88.780 | 1.1012 | 1.1039 | 0.320 | 8 | 24 | 0.3 | 0.82 |

Sample ident.: cu1002b1

17-Jun-1996 13:59



File: CU1002BI.D1

17-Jun-1996 12:58

=====

Phillips Analytical X-Ray B. V.

PC-APD, Diffraction software

Sample identification: cu1002bi

Data measured at: 17-Jun-1996 12:20:00

Diffractometer type: PW3710 BASED

Tube anode: Cu

Generator tension [kV]: 40

Generator current [mA]: 45

Wavelength Alpha1 [Å]: 1.54060

Wavelength Alpha2 [Å]: 1.54439

Intensity ratio (alpha2/alpha1): 0.500

Divergence slit: 1x

Receiving slit: 0.1

Monochromator used: YES

Start angle [x2i]: 5.000

End angle [x2i]: 95.000

Step size [x2i]: 0.020

Maximum intensity: 9331.560

Time per step [s]: 0.500

Type of scan: CONTINUOUS

Minimum peak tip width: 0.00

Maximum peak tip width: 1.00

Peak base width: 2.00

Minimum significance: 0.75

- Number of peaks: 29

| Angle [x2i] | d-value '1 [Å] | d-value '2 [Å] | Peak width [x2i] | Peak int [counts] | Back. int [counts] | Rel. int [%] | Signif. |
|----------------|-------------------|-------------------|---------------------|----------------------|-----------------------|-----------------|---------|
| 6.255 | 14.1189 | 14.1536 | 0.240 | 27 | 35 | 0.3 | 0.81 |
| 8.830 | 10.0065 | 10.0311 | 0.100 | 5791 | 35 | 62.1 | 23.11 |
| 12.505 | 7.0728 | 7.0902 | 0.140 | 61 | 35 | 0.7 | 2.23 |
| 17.670 | 5.0153 | 5.0277 | 0.080 | 45 | 49 | 0.5 | 1.23 |
| 18.780 | 4.7213 | 4.7329 | 0.120 | 42 | 53 | 0.5 | 1.95 |
| 20.885 | 4.2500 | 4.2604 | 0.240 | 25 | 61 | 0.3 | 1.18 |
| 25.130 | 3.5408 | 3.5496 | 0.080 | 108 | 74 | 1.2 | 0.84 |
| 26.585 | 3.3503 | 3.3585 | 0.140 | 9332 | 77 | 100.0 | 51.00 |
| 31.745 | 2.8165 | 2.8234 | 0.960 | 5 | 50 | 0.1 | 1.10 |
| 34.115 | 2.6260 | 2.6325 | 0.240 | 40 | 40 | 0.4 | 1.80 |
| 35.705 | 2.5127 | 2.5188 | 0.080 | 1282 | 35 | 13.7 | 4.61 |
| 36.925 | 2.4324 | 2.4384 | 0.480 | 20 | 29 | 0.2 | 1.69 |
| 41.435 | 2.1775 | 2.1828 | 0.320 | 18 | 26 | 0.2 | 0.92 |
| 45.065 | 2.0101 | 2.0151 | 0.080 | 1459 | 23 | 15.6 | 4.77 |
| 45.195 | 2.0047 | 2.0096 | 0.040 | 671 | 23 | 7.2 | 6.68 |
| 47.800 | 1.9013 | 1.9060 | 0.640 | 8 | 19 | 0.1 | 1.39 |
| 49.555 | 1.8380 | 1.8425 | 0.100 | 5 | 18 | 0.1 | 0.83 |
| 50.420 | 1.8085 | 1.8129 | 0.960 | 5 | 18 | 0.1 | 1.00 |
| 54.745 | 1.6754 | 1.6795 | 0.080 | 296 | 22 | 3.2 | 1.98 |
| 54.910 | 1.6707 | 1.6749 | 0.060 | 151 | 22 | 1.6 | 1.63 |
| 60.175 | 1.5365 | 1.5403 | 0.200 | 38 | 24 | 0.4 | 0.81 |
| 64.870 | 1.4362 | 1.4397 | 0.100 | 262 | 25 | 2.8 | 3.61 |

=====

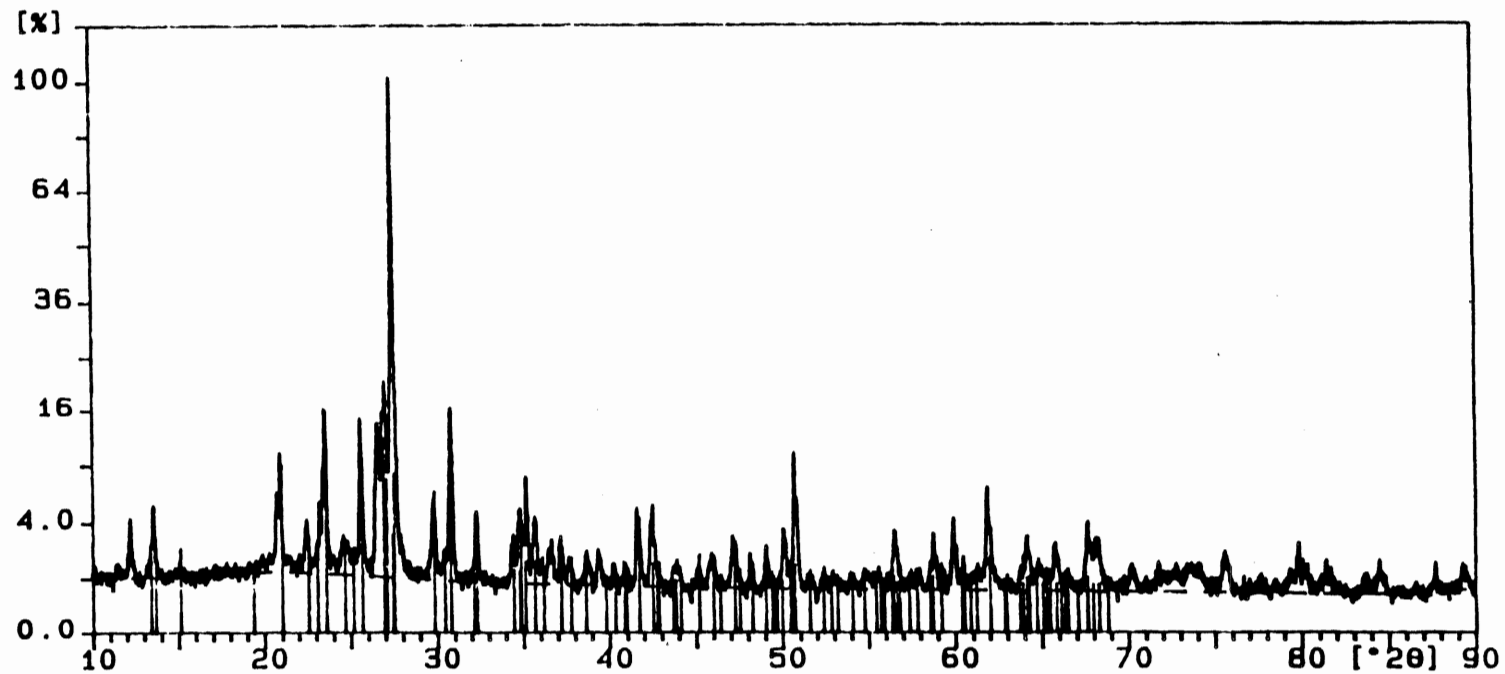
Phillips Analytical X-Ray B. V.


PC-APD, Diffraction software

| Angle [2θ] | d-value '1 [Å] | d-value '2 [Å] | Peak width [2θ] | Peak int [counts] | Bact. int [counts] | Rel. int [%] | Signif. |
|------------------------|-------------------|-------------------|-----------------------------|----------------------|-----------------------|-----------------|---------|
| 65.050 | 1.4327 | 1.4362 | 0.080 | 112 | 25 | 1.2 | 0.95 |
| 68.860 | 1.3624 | 1.3658 | 0.480 | 26 | 23 | 0.3 | 2.14 |
| 75.605 | 1.2567 | 1.2598 | 0.140 | 164 | 19 | 1.8 | 4.92 |
| 75.815 | 1.2538 | 1.2569 | 0.100 | 104 | 19 | 1.1 | 1.33 |
| 81.435 | 1.1808 | 1.1837 | 0.640 | 5 | 14 | 0.1 | 1.13 |
| 87.130 | 1.1177 | 1.1205 | 0.120 | 23 | 14 | 0.2 | 1.50 |
| 92.870 | 1.0631 | 1.0657 | 0.640 | 10 | 14 | 0.1 | 1.53 |

Sample ident.: cu1006k

14-May-1996 15:50



CU1006K 

Orthocla 

Phillips Analytical X-Ray B. V.

PC-APD, Diffraction software

Sample identification: cu1006k

Data measured at: 14-May-1996 14:34:00

Diffractometer type: PW3710 BASED

Tube anode: Cu

Generator tension [kV]: 40

Generator current [mA]: 45

Wavelength Alpha1 [Å]: 1.54060

Wavelength Alpha2 [Å]: 1.54439

Intensity ratio (alpha2/alpha1): 0.500

Divergence slit: 1x

Receiving slit: 0.1

Monochromator used: YES

Start angle [x2i]: 10.000

End angle [x2i]: 90.000

Step size [x2i]: 0.020

Maximum intensity: 4502.410

Time per step [s]: 0.800

Type of scan: CONTINUOUS

Minimum peak tip width: 0.00

Maximum peak tip width: 1.00

Peak base width: 2.00

Minimum significance: 0.75

Number of peaks: 81

| Angle [x2i] | d-value '1 [Å] | d-value '2 [Å] | Peak width [x2i] | Peak int [counts] | Back. int [counts] | Rel. int [%] | Signif. |
|-------------|----------------|----------------|------------------|-------------------|--------------------|--------------|---------|
| 11.520 | 7.6752 | 7.6941 | 0.120 | 22 | 48 | 0.5 | 0.95 |
| 12.235 | 7.2283 | 7.2460 | 0.080 | 125 | 48 | 2.8 | 1.42 |
| 13.575 | 6.5176 | 6.5337 | 0.100 | 199 | 48 | 4.4 | 2.87 |
| 15.110 | 5.8588 | 5.8732 | 0.240 | 19 | 48 | 0.4 | 1.16 |
| 20.745 | 4.2783 | 4.2889 | 0.100 | 174 | 58 | 3.9 | 1.70 |
| 20.985 | 4.2299 | 4.2403 | 0.080 | 303 | 56 | 6.7 | 2.72 |
| 22.480 | 3.9519 | 3.9616 | 0.160 | 121 | 55 | 2.7 | 1.91 |
| 23.230 | 3.8260 | 3.8354 | 0.060 | 156 | 53 | 3.5 | 2.88 |
| 23.575 | 3.7708 | 3.7800 | 0.100 | 650 | 53 | 14.4 | 4.94 |
| 24.580 | 3.6188 | 3.6277 | 0.160 | 76 | 52 | 1.7 | 0.94 |
| 25.610 | 3.4756 | 3.4841 | 0.100 | 620 | 50 | 13.8 | 5.06 |
| 26.590 | 3.3496 | 3.3579 | 0.120 | 595 | 49 | 13.2 | 3.88 |
| 26.880 | 3.3142 | 3.3223 | 0.060 | 660 | 48 | 14.7 | 2.90 |
| 27.040 | 3.2949 | 3.3030 | 0.100 | 864 | 48 | 19.2 | 3.30 |
| 27.485 | 3.2426 | 3.2505 | 0.100 | 4502 | 46 | 100.0 | 14.51 |
| → 29.830 | 2.9928 | 3.0001 | 0.140 | 219 | 44 | 4.9 | 2.91 |
| → 30.440 | 2.9342 | 2.9414 | 0.120 | 58 | 42 | 1.3 | 1.02 |
| 30.855 | 2.8957 | 2.9028 | 0.120 | 702 | 41 | 15.6 | 7.71 |
| 32.305 | 2.7689 | 2.7757 | 0.080 | 177 | 40 | 3.9 | 1.24 |
| 34.430 | 2.6027 | 2.6091 | 0.060 | 104 | 37 | 2.3 | 1.31 |
| 34.850 | 2.5723 | 2.5786 | 0.080 | 190 | 37 | 4.2 | 0.99 |
| 35.215 | 2.5465 | 2.5528 | 0.060 | 324 | 37 | 7.2 | 1.23 |

A = 0.7331

File: CU1006K.DI

14-May-1996 15:28

=====

Phillips Analytical X-Ray 8. V.

PC-APD, Diffraction software

| Angle [2θ] | d-value '1 [Å] | d-value '2 [Å] | Peak width [2θ] | Peak int [counts] | Back. int [counts] | Rel. int [%] | Signif. |
|------------------------|-------------------|-------------------|-----------------------------|----------------------|-----------------------|-----------------|---------|
| 35.750 | 2.5096 | 2.5158 | 0.140 | 151 | 36 | 3.4 | 2.68 |
| 36.120 | 2.4847 | 2.4908 | 0.120 | 37 | 36 | 0.8 | 1.19 |
| 36.495 | 2.4601 | 2.4661 | 0.080 | 58 | 36 | 1.3 | 1.07 |
| 36.725 | 2.4452 | 2.4512 | 0.120 | 46 | 36 | 1.0 | 1.44 |
| 37.135 | 2.4191 | 2.4251 | 0.100 | 81 | 36 | 1.8 | 1.33 |
| 37.735 | 2.3820 | 2.3879 | 0.280 | 36 | 35 | 0.8 | 2.31 |
| 38.700 | 2.3248 | 2.3305 | 0.100 | 61 | 35 | 1.4 | 0.88 |
| 39.405 | 2.2848 | 2.2905 | 0.060 | 64 | 34 | 1.4 | 0.79 |
| 40.225 | 2.2401 | 2.2456 | 0.060 | 40 | 34 | 0.9 | 0.79 |
| 40.980 | 2.2006 | 2.2060 | 0.320 | 26 | 32 | 0.6 | 1.94 |
| 41.615 | 2.1685 | 2.1738 | 0.100 | 156 | 32 | 3.5 | 1.72 |
| 41.760 | 2.1613 | 2.1666 | 0.060 | 169 | 32 | 3.8 | 0.82 |
| 42.420 | 2.1292 | 2.1344 | 0.060 | 128 | 32 | 2.8 | 1.05 |
| 42.545 | 2.1232 | 2.1284 | 0.040 | 213 | 32 | 4.7 | 3.45 |
| 43.825 | 2.0641 | 2.0692 | 0.480 | 31 | 31 | 0.7 | 4.30 |
| 45.185 | 2.0051 | 2.0100 | 0.320 | 18 | 31 | 0.4 | 1.40 |
| 46.000 | 1.9714 | 1.9763 | 0.240 | 56 | 30 | 1.2 | 2.27 |
| 47.200 | 1.9241 | 1.9288 | 0.320 | 98 | 30 | 2.2 | 7.43 |
| 48.160 | 1.8879 | 1.8926 | 0.060 | 56 | 30 | 1.2 | 1.55 |
| 49.090 | 1.8543 | 1.8589 | 0.080 | 81 | 30 | 1.8 | 0.94 |
| 50.105 | 1.8191 | 1.8236 | 0.080 | 112 | 29 | 2.5 | 1.00 |
| 50.735 | 1.7980 | 1.8024 | 0.080 | 433 | 29 | 9.6 | 3.44 |
| 50.875 | 1.7934 | 1.7978 | 0.060 | 222 | 29 | 4.9 | 1.80 |
| 51.685 | 1.7672 | 1.7715 | 0.320 | 15 | 29 | 0.3 | 1.41 |
| 52.430 | 1.7438 | 1.7481 | 0.120 | 24 | 29 | 0.5 | 0.81 |
| 52.935 | 1.7283 | 1.7326 | 0.120 | 24 | 29 | 0.5 | 0.84 |
| 53.995 | 1.6969 | 1.7011 | 0.240 | 18 | 29 | 0.4 | 1.28 |
| 54.800 | 1.6738 | 1.6780 | 0.320 | 27 | 28 | 0.6 | 1.55 |
| 55.665 | 1.6499 | 1.6539 | 0.240 | 26 | 28 | 0.6 | 0.84 |
| 56.570 | 1.6256 | 1.6296 | 0.120 | 121 | 28 | 2.7 | 2.05 |
| 57.465 | 1.6024 | 1.6063 | 0.240 | 15 | 28 | 0.3 | 0.86 |
| 57.925 | 1.5907 | 1.5947 | 0.240 | 27 | 28 | 0.6 | 2.80 |
| 58.790 | 1.5694 | 1.5733 | 0.080 | 119 | 28 | 2.6 | 1.70 |
| 59.285 | 1.5575 | 1.5613 | 0.120 | 34 | 27 | 0.7 | 1.32 |
| 59.955 | 1.5416 | 1.5454 | 0.100 | 164 | 27 | 3.6 | 2.64 |
| 60.530 | 1.5284 | 1.5321 | 0.060 | 59 | 27 | 1.3 | 0.75 |
| 61.335 | 1.5102 | 1.5139 | 0.200 | 36 | 27 | 0.8 | 0.83 |
| 61.915 | 1.4975 | 1.5012 | 0.080 | 282 | 27 | 6.3 | 2.25 |
| 64.195 | 1.4497 | 1.4532 | 0.100 | 114 | 26 | 2.5 | 1.62 |
| 64.860 | 1.4364 | 1.4399 | 0.240 | 38 | 26 | 0.9 | 1.88 |
| 65.800 | 1.4181 | 1.4216 | 0.160 | 88 | 26 | 2.0 | 2.05 |
| 66.515 | 1.4046 | 1.4081 | 0.240 | 28 | 26 | 0.6 | 1.27 |
| 67.705 | 1.3828 | 1.3862 | 0.060 | 146 | 26 | 3.3 | 2.34 |
| 68.170 | 1.3745 | 1.3779 | 0.080 | 94 | 25 | 2.1 | 1.11 |
| 68.355 | 1.3712 | 1.3746 | 0.120 | 77 | 25 | 1.7 | 1.39 |
| 70.175 | 1.3401 | 1.3434 | 0.160 | 37 | 25 | 0.8 | 1.22 |
| 71.780 | 1.3140 | 1.3172 | 0.160 | 38 | 25 | 0.9 | 0.84 |
| 72.820 | 1.2978 | 1.3010 | 0.320 | 34 | 24 | 0.7 | 0.79 |
| 74.215 | 1.2768 | 1.2799 | 0.240 | 37 | 24 | 0.8 | 1.54 |
| 75.570 | 1.2572 | 1.2603 | 0.280 | 56 | 24 | 1.2 | 3.39 |
| 77.640 | 1.2288 | 1.2318 | 0.480 | 18 | 23 | 0.4 | 2.06 |

File: CU1006K.D1

14-May-1996 15:28

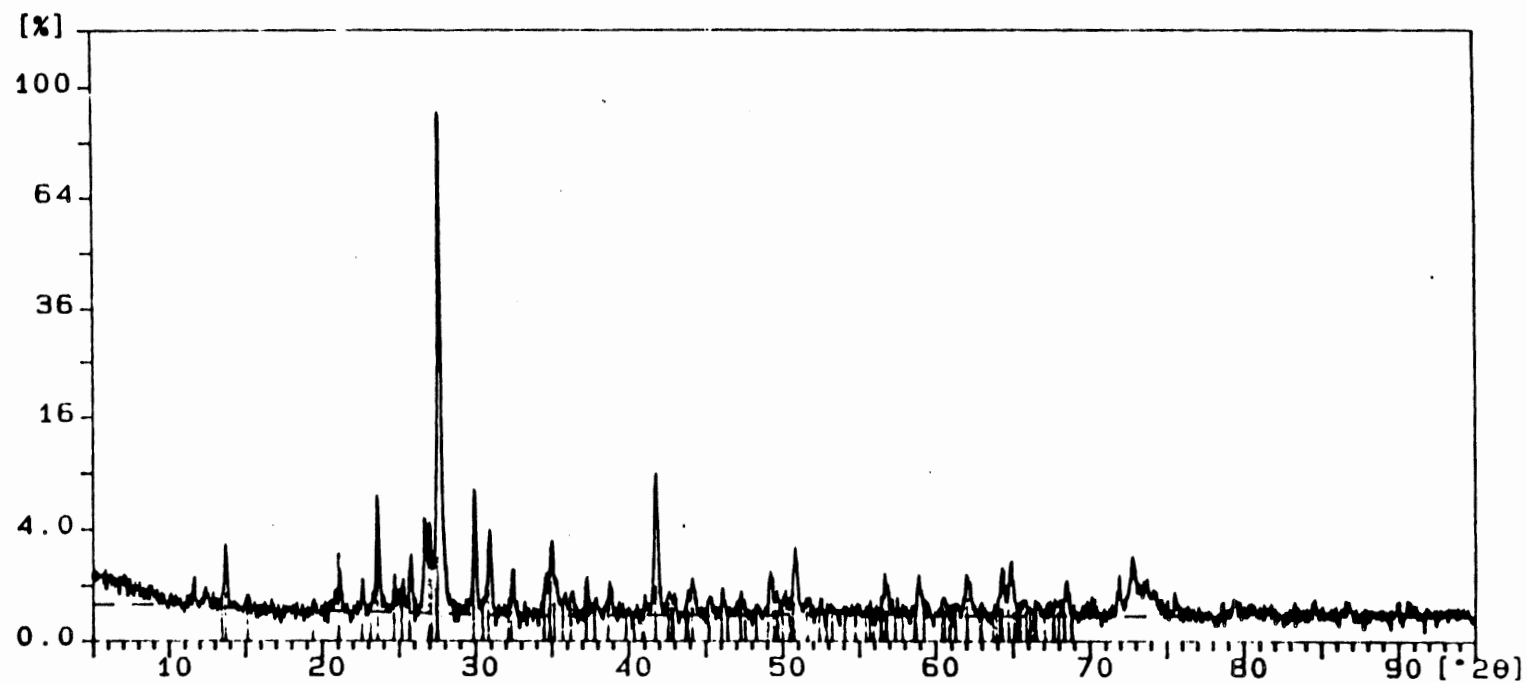
=====

Phillips Analytical X-Ray 8. V. PC-APD, Diffraction software

| Angle [x2i] | d-value '1 [] | d-value '2 [] | Peak width [x2i] | Peak int [counts] | Back. int [counts] | Rel. int [%] | Signif. |
|----------------|------------------|------------------|---------------------|----------------------|-----------------------|-----------------|---------|
| 79.880 | 1.1999 | 1.2028 | 0.060 | 102 | 23 | 2.3 | 2.19 |
| 80.095 | 1.1972 | 1.2001 | 0.060 | 59 | 23 | 1.3 | 0.97 |
| 80.350 | 1.1940 | 1.1970 | 0.120 | 40 | 22 | 0.9 | 1.02 |
| 81.445 | 1.1807 | 1.1836 | 0.100 | 58 | 22 | 1.3 | 1.47 |
| 83.730 | 1.1542 | 1.1571 | 0.320 | 17 | 22 | 0.4 | 1.08 |
| 84.485 | 1.1458 | 1.1486 | 0.120 | 42 | 22 | 0.9 | 0.91 |
| 86.600 | 1.1232 | 1.1259 | 0.480 | 7 | 22 | 0.2 | 1.01 |
| 87.760 | 1.1113 | 1.1140 | 0.080 | 37 | 27 | 0.8 | 0.82 |

Sample ident.: cu1010a

15-Mar-1997 19:14



File: CU1010A.C1

15-Mar-1997 16:00

Philips Analytical

PC-APD, Diffraction software

Sample identification: CU1010a

Data measured at: 15-Mar-1997 16:16:00

Diffractometer type: PW3710 BASED

Tube anode: Cu

Generator voltage (KV): 40

Generator current (mA): 45

Wavelength Alpha1 (Å): 1.54060

Wavelength Alpha2 (Å): 1.54439

Intensity ratio (alpha2/alpha1): 0.500

Divergence slit: 1x

Receiving slit: 0.1

Monochromator used: YES

Start angle (x2θ): 5.000

End angle (x2θ): 95.000

Step size (x2θ): 0.020

Maximum intensity: 3745.440

Time per step (s): 10.000

Type of scan: CONTINUOUS

Minimum peak tip width: 0.00

Maximum peak tip width: 1.00

Peak base width: 1.00

Minimum significance: 0.75

Number of peaks: 58

| Angle (x2θ) | d-value (Å) | d-value (Å) | Peak width (x2θ) | Peak Int (counts) | Back. Int (counts) | Rel. Int (%) | Signif. |
|-------------|-------------|-------------|------------------|-------------------|--------------------|--------------|---------|
| 11.700 | 7.6576 | 7.5762 | 0.120 | 16 | 17 | 0.5 | 1.35 |
| 12.415 | 7.1239 | 7.1414 | 0.200 | 12 | 15 | 0.3 | 0.78 |
| 13.740 | 6.4397 | 6.4556 | 0.120 | 94 | 14 | 2.5 | 2.32 |
| 15.015 | 5.8186 | 5.8329 | 0.480 | 7 | 12 | 0.2 | 1.10 |
| 20.360 | 4.2349 | 4.2453 | 0.120 | 34 | 11 | 0.9 | 1.34 |
| 21.025 | 4.1826 | 4.1929 | 0.260 | 46 | 11 | 1.2 | 1.13 |
| 22.675 | 3.9183 | 3.9280 | 0.080 | 28 | 10 | 0.7 | 1.21 |
| 23.665 | 3.7566 | 3.7659 | 0.120 | 143 | 10 | 6.5 | 5.29 |
| 24.745 | 3.5951 | 3.6039 | 0.120 | 34 | 10 | 0.9 | 0.76 |
| 25.020 | 3.5147 | 3.5230 | 0.120 | 34 | 10 | 0.9 | 0.75 |
| 25.650 | 3.4475 | 3.4523 | 0.160 | 69 | 10 | 1.9 | 2.33 |
| 26.735 | 3.3319 | 3.3400 | 0.120 | 143 | 10 | 5.2 | 2.87 |
| 27.090 | 3.2939 | 3.2970 | 0.180 | 159 | 9 | 4.2 | 7.26 |
| 27.705 | 3.2173 | 3.2252 | 0.100 | 1745 | 9 | 100.0 | 14.62 |
| 30.015 | 2.9733 | 2.9811 | 0.140 | 146 | 8 | 6.6 | 7.38 |
| 31.010 | 2.8615 | 2.8686 | 0.160 | 139 | 8 | 3.7 | 4.52 |
| 32.510 | 2.7519 | 2.7587 | 0.160 | 43 | 8 | 1.3 | 3.57 |
| 33.260 | 2.6900 | 2.6966 | 0.120 | 7 | 8 | 0.2 | 0.85 |
| 34.660 | 2.5865 | 2.5923 | 0.120 | 45 | 8 | 1.3 | 3.39 |
| 35.030 | 2.5581 | 2.5644 | 0.100 | 112 | 8 | 3.0 | 1.47 |
| 35.365 | 2.5365 | 2.5423 | 0.120 | 41 | 8 | 1.1 | 0.88 |
| 36.040 | 2.4701 | 2.4763 | 0.240 | 19 | 8 | 0.5 | 2.29 |

File: CU1010A.01

15-Mar-1997 18:54

Philips Analytical

PC-APD, Diffraction software

| Angle [2θ] | d-value [\AA] | d-value [\AA] | Peak width [2θ] | Peak int [counts] | Back. int [counts] | Rel. int [%] | Signif. |
|------------------------|-----------------------------|-----------------------------|-----------------------------|----------------------|-----------------------|-----------------|---------|
| 37.320 | 2.4069 | 2.4129 | 0.140 | 42 | 8 | 1.1 | 1.94 |
| 37.360 | 2.3744 | 2.3803 | 0.200 | 9 | 3 | 0.2 | 0.33 |
| 39.300 | 2.3133 | 2.3190 | 0.160 | 15 | 3 | 0.3 | 1.35 |
| 41.145 | 2.1921 | 2.1975 | 0.160 | 20 | 3 | 0.5 | 1.04 |
| 41.305 | 2.1590 | 2.1644 | 0.120 | 289 | 9 | 7.7 | 4.51 |
| 41.645 | 2.1184 | 2.1236 | 0.240 | 17 | 3 | 0.4 | 1.10 |
| 43.915 | 2.0601 | 2.0651 | 0.240 | 17 | 3 | 0.4 | 0.95 |
| 44.220 | 2.0466 | 2.0516 | 0.160 | 38 | 8 | 1.0 | 0.91 |
| 45.355 | 1.9960 | 2.0029 | 0.240 | 14 | 3 | 0.4 | 0.75 |
| 46.160 | 1.9650 | 1.9698 | 0.160 | 13 | 3 | 0.5 | 1.06 |
| 47.410 | 1.9150 | 1.9208 | 0.320 | 12 | 8 | 0.3 | 1.21 |
| 49.400 | 1.8791 | 1.8838 | 0.240 | 5 | 8 | 0.1 | 1.01 |
| 49.275 | 1.8478 | 1.8523 | 0.080 | 59 | 8 | 1.6 | 0.77 |
| 50.245 | 1.8144 | 1.8188 | 0.160 | 19 | 9 | 0.5 | 0.82 |
| 51.320 | 1.7731 | 1.7776 | 0.280 | 75 | 9 | 2.1 | 6.88 |
| 51.760 | 1.7643 | 1.7691 | 0.320 | 11 | 3 | 0.3 | 1.16 |
| 51.635 | 1.7384 | 1.7427 | 0.200 | 10 | 3 | 0.3 | 1.37 |
| 53.470 | 1.7123 | 1.7165 | 0.480 | 4 | 3 | 0.1 | 1.89 |
| 55.760 | 1.6206 | 1.6246 | 0.120 | 15 | 9 | 0.4 | 1.19 |
| 58.365 | 1.5651 | 1.5690 | 0.160 | 38 | 8 | 1.0 | 1.35 |
| 60.605 | 1.5267 | 1.5304 | 0.320 | 12 | 8 | 0.3 | 1.26 |
| 62.080 | 1.4933 | 1.4976 | 0.160 | 43 | 6 | 1.3 | 1.27 |
| 64.370 | 1.4462 | 1.4497 | 0.200 | 50 | 3 | 1.4 | 2.73 |
| 64.950 | 1.4346 | 1.4382 | 0.060 | 64 | 3 | 1.7 | 0.39 |
| 66.670 | 1.4017 | 1.4052 | 0.320 | 13 | 8 | 0.3 | 1.05 |
| 68.545 | 1.3679 | 1.3713 | 0.120 | 34 | 3 | 0.9 | 2.17 |
| 70.345 | 1.3372 | 1.3405 | 0.320 | 10 | 3 | 0.3 | 1.17 |
| 71.975 | 1.3109 | 1.3141 | 0.160 | 16 | 8 | 0.7 | 0.92 |
| 72.390 | 1.2967 | 1.2999 | 0.120 | 63 | 9 | 1.9 | 1.27 |
| 73.755 | 1.2836 | 1.2868 | 0.240 | 28 | 8 | 0.7 | 0.76 |
| 74.320 | 1.2752 | 1.2784 | 0.240 | 21 | 9 | 0.6 | 1.15 |
| 75.685 | 1.2556 | 1.2587 | 0.240 | 12 | 3 | 0.3 | 1.76 |
| 76.485 | 1.2048 | 1.2078 | 0.240 | 10 | 3 | 0.3 | 1.23 |
| 80.565 | 1.1914 | 1.1943 | 0.240 | 10 | 10 | 0.3 | 1.43 |
| 86.745 | 1.1217 | 1.1244 | 0.640 | 5 | 8 | 0.1 | 1.47 |
| 90.750 | 1.0323 | 1.0350 | 0.400 | 7 | 3 | 0.2 | 1.16 |

File: CU1011SR.DI

28-May-1996 11:14

=====

=====

Phillips Analytical X-Ray B. V.

PC-APD, Diffraction software

Sample identification: cu1011sr

Data measured at: 28-May-1996 10:49:00

Diffractometer type: PW3710 BASED

Tube anode: Cu

Generator tension [kV]: 40

Generator current [mA]: 45

Wavelength Alpha1 []: 1.54060

Wavelength Alpha2 []: 1.54439

Intensity ratio (alpha2/alpha1): 0.500

Divergence slit: 1r

Receiving slit: 0.1

Monochromator used: YES

Start angle [x2i]: 5.000

End angle [x2i]: 65.000

Step size [x2i]: 0.020

Maximum intensity: 1980.250

Time per step [s]: 0.500

Type of scan: CONTINUOUS

Minimum peak tip width: 0.00

Maximum peak tip width: 1.00

Peak base width: 2.00

Minimum significance: 0.75

Number of peaks: 36

| Angle [x2i] | d-value '1 [] | d-value '2 [] | Peak width [x2i] | Peak int [counts] | Back. int [counts] | Rel. int [%] | Signif. |
|----------------|------------------|------------------|---------------------|----------------------|-----------------------|-----------------|---------|
| 8.905 | 9.9224 | 9.9468 | 0.100 | 936 | 37 | 47.3 | 8.86 |
| 17.800 | 4.9790 | 4.9912 | 0.120 | 660 | 41 | 33.4 | 8.76 |
| 19.970 | 4.4426 | 4.4535 | 0.060 | 146 | 40 | 7.4 | 1.95 |
| 20.905 | 4.2459 | 4.2564 | 0.080 | 164 | 40 | 8.3 | 1.18 |
| 21.710 | 4.0903 | 4.1004 | 0.320 | 40 | 38 | 2.0 | 0.83 |
| 22.965 | 3.8695 | 3.8790 | 0.060 | 121 | 38 | 6.1 | 1.20 |
| 23.875 | 3.7241 | 3.7332 | 0.080 | 112 | 37 | 5.7 | 1.02 |
| 25.535 | 3.4856 | 3.4942 | 0.100 | 161 | 36 | 8.1 | 1.84 |
| 26.655 | 3.3416 | 3.3498 | 0.060 | 1136 | 36 | 57.4 | 1.04 |
| 26.810 | 3.3227 | 3.3308 | 0.120 | 1980 | 35 | 100.0 | 10.18 |
| 27.900 | 3.1953 | 3.2031 | 0.100 | 196 | 35 | 9.9 | 2.52 |
| 28.815 | 3.0959 | 3.1035 | 0.320 | 45 | 34 | 2.3 | 0.99 |
| 29.895 | 2.9864 | 2.9938 | 0.120 | 216 | 32 | 10.9 | 3.60 |
| 31.275 | 2.8577 | 2.8648 | 0.120 | 177 | 32 | 8.9 | 2.84 |
| 32.085 | 2.7874 | 2.7943 | 0.080 | 151 | 31 | 7.6 | 1.69 |
| 34.645 | 2.5871 | 2.5934 | 0.080 | 108 | 30 | 5.5 | 0.85 |
| 35.100 | 2.5546 | 2.5609 | 0.140 | 228 | 29 | 11.5 | 3.83 |
| 35.980 | 2.4941 | 2.5002 | 0.100 | 196 | 29 | 9.9 | 1.95 |
| 36.590 | 2.4539 | 2.4599 | 0.120 | 121 | 28 | 6.1 | 2.39 |
| 37.835 | 2.3760 | 2.3818 | 0.160 | 66 | 27 | 3.3 | 1.37 |
| 39.495 | 2.2798 | 2.2854 | 0.080 | 45 | 27 | 2.3 | 0.84 |
| 40.335 | 2.2343 | 2.2398 | 0.160 | 36 | 27 | 1.8 | 0.79 |

File: CU1011SR.D1

28-May-1996 11:15

=====

=====

Phillips Analytical X-Ray B. V.

PC-APD, Diffraction software

| Angle [x2i] | d-value '1 [] | d-value '2 [] | Peak width [x2i] | Peak int [counts] | Back. int [counts] | Rel. int [%] | Signif. |
|----------------|-------------------|-------------------|---------------------|----------------------|-----------------------|-----------------|---------|
| 42.085 | 2.1453 | 2.1506 | 0.120 | 37 | 27 | 1.9 | 0.75 |
| 42.470 | 2.1268 | 2.1320 | 0.040 | 104 | 27 | 5.3 | 1.22 |
| 44.035 | 2.0547 | 2.0598 | 0.640 | 11 | 28 | 0.5 | 0.98 |
| 45.395 | 1.9963 | 2.0012 | 0.080 | 790 | 28 | 39.9 | 3.14 |
| 45.525 | 1.9909 | 1.9958 | 0.060 | 506 | 28 | 25.6 | 0.80 |
| 50.165 | 1.8171 | 1.8215 | 0.120 | 81 | 24 | 4.1 | 6.58 |
| 52.905 | 1.7292 | 1.7335 | 0.200 | 30 | 24 | 1.5 | 1.04 |
| 55.225 | 1.6620 | 1.6660 | 0.080 | 71 | 24 | 3.6 | 0.87 |
| 55.800 | 1.6462 | 1.6502 | 0.080 | 85 | 24 | 4.3 | 1.09 |
| 57.535 | 1.6006 | 1.6045 | 0.480 | 10 | 24 | 0.5 | 0.78 |
| 60.000 | 1.5406 | 1.5444 | 0.100 | 74 | 24 | 3.7 | 1.66 |
| 60.725 | 1.5239 | 1.5277 | 0.400 | 42 | 24 | 2.1 | 2.24 |
| 61.865 | 1.4986 | 1.5022 | 0.200 | 58 | 24 | 2.9 | 1.77 |
| 64.030 | 1.4530 | 1.4566 | 0.120 | 42 | 24 | 2.1 | 0.81 |

Appendix C.

Electron Microprobe Data

K-feldspar Microprobe Data for RT Dated Samples (DDH3439) - January 15-16, 1997

| Sample # | Grain | Point | SiO2 | Al2O3 | Na2O | K2O | BaO | Total |
|----------|-------|-------|-------|-------|------|-------|------|-------|
| Cu999 | 1 | 4 | 63.23 | 18.02 | 1.00 | 15.12 | | 97.37 |
| Cu999 | 1 | 5 | 63.21 | 18.51 | 1.59 | 14.27 | 0.75 | 98.32 |
| Cu999 | 1 | 7 | 62.89 | 18.56 | 1.53 | 14.15 | 0.94 | 98.07 |
| Cu999 | 1 | 10 | 62.09 | 18.09 | 1.15 | 14.47 | 0.52 | 96.32 |
| Cu999 | 1 | 11 | 63.13 | 18.27 | 1.46 | 14.72 | | 97.59 |
| Cu999 | 2 | 13 | 62.45 | 18.42 | 1.36 | 14.20 | 1.21 | 97.64 |
| Cu999 | 2 | 14 | 62.53 | 18.21 | 1.09 | 14.68 | 1.10 | 97.62 |
| Cu999 | 2 | 17 | 63.18 | 18.62 | 0.89 | 14.53 | 1.34 | 98.56 |
| Cu999 | 2 | 18 | 62.81 | 18.37 | 0.96 | 14.43 | 1.16 | 97.73 |
| Cu999 | 2 | 19 | 62.61 | 18.48 | 1.10 | 14.38 | 2.08 | 98.66 |
| Cu999 | 3 | 20 | 63.22 | 18.44 | 1.00 | 14.95 | 0.87 | 98.48 |
| Cu999 | 4 | 22 | 63.46 | 18.30 | 0.63 | 15.63 | 0.59 | 98.61 |
| Cu999 | 4 | 23 | 63.71 | 18.20 | 0.97 | 15.29 | | 98.16 |
| Cu999 | 4 | 25 | 62.83 | 18.74 | 1.68 | 13.62 | 1.58 | 98.46 |
| | | avg | 63.12 | 18.45 | 1.03 | 14.69 | 1.27 | 98.38 |
| | | std | 0.36 | 0.17 | 0.30 | 0.61 | 0.48 | 0.30 |

| Sample # | Grain | Point | SiO2 | Al2O3 | Na2O | K2O | BaO | Total |
|----------|-------|-------|-------|-------|------|-------|------|-------|
| Cu1001 | 5 | 26 | 64.22 | 18.21 | 1.36 | 14.78 | | 98.57 |
| Cu1001 | 5 | 27 | 63.49 | 18.28 | 1.06 | 15.36 | | 98.18 |
| Cu1001 | 5 | 28 | 63.29 | 18.73 | 1.62 | 13.53 | 1.51 | 98.66 |
| Cu1001 | 5 | 29 | 63.71 | 18.13 | 0.88 | 14.48 | | 97.20 |
| Cu1001 | 6 | 33 | 63.74 | 18.13 | 0.91 | 15.23 | | 98.01 |
| Cu1001 | 6 | 34 | 63.75 | 18.27 | 0.83 | 15.37 | | 98.22 |
| Cu1001 | 6 | 35 | 63.84 | 18.35 | 0.99 | 15.15 | | 98.32 |
| Cu1001 | 6 | 36 | 62.42 | 18.62 | 1.71 | 13.64 | 1.35 | 97.75 |
| Cu1001 | 7 | 39 | 63.32 | 18.27 | 1.35 | 14.47 | 0.79 | 98.19 |
| Cu1001 | 7 | 40 | 63.98 | 18.37 | 0.91 | 14.55 | 0.52 | 98.34 |
| Cu1001 | 7 | 41 | 63.18 | 18.63 | 1.82 | 13.79 | 1.15 | 98.57 |
| | | avg | 63.46 | 18.38 | 1.22 | 14.60 | 0.95 | 98.20 |
| | | std | 0.50 | 0.17 | 0.38 | 0.64 | 0.32 | 0.24 |

| Sample # | Grain | Point | SiO2 | Al2O3 | Na2O | K2O | BaO | Total |
|----------|-------|-------|-------|-------|------|-------|------|-------|
| Cu1002 | 8 | 45 | 62.90 | 18.62 | 1.71 | 13.58 | 1.39 | 98.20 |
| Cu1002 | 8 | 47 | 63.09 | 18.76 | 1.46 | 14.16 | 1.65 | 99.12 |
| Cu1002 | 8 | 48 | 62.85 | 18.60 | 1.44 | 14.10 | 1.69 | 98.68 |
| Cu1002 | 8 | 49 | 62.57 | 18.73 | 1.63 | 13.56 | 1.59 | 98.08 |
| Cu1002 | 9 | 50 | 63.54 | 18.43 | 1.40 | 13.70 | 1.10 | 98.17 |
| Cu1002 | 9 | 51 | 63.16 | 18.57 | 1.21 | 14.35 | 1.41 | 98.71 |
| Cu1002 | 9 | 53 | 63.05 | 18.41 | 1.61 | 13.82 | 1.31 | 98.19 |
| Cu1002 | 9 | 54 | 63.50 | 18.43 | 0.96 | 14.82 | 1.16 | 98.86 |
| Cu1002 | 10 | 57 | 63.64 | 18.68 | 1.34 | 14.34 | 0.80 | 98.80 |
| Cu1002 | 10 | 60 | 62.97 | 18.56 | 1.28 | 14.18 | 1.00 | 98.00 |
| Cu1002 | 10 | 61 | 63.42 | 18.48 | 2.16 | 13.20 | 1.29 | 98.55 |
| Cu1002 | 10 | 62 | 60.99 | 19.13 | 2.81 | 11.77 | 3.14 | 97.84 |
| | | avg | 62.96 | 18.61 | 1.62 | 13.78 | 1.44 | 98.42 |
| | | std | 0.83 | 0.23 | 0.60 | 0.94 | 0.72 | 0.38 |

K-feldspar Microprobe Data for RT Dated Samples (DDH1513) - January 15-16, 1997

| Sample # | Grain | Point | SiO2 | Al2O3 | Na2O | K2O | Cl | BaO | Total |
|----------|-------|-------|-------|-------|------|--------------|------|------|-------|
| Cu1006 | 11 | 66 | 63.65 | 18.36 | 1.23 | 14.36 | | 0.68 | 98.27 |
| Cu1006 | 11 | 67 | 62.29 | 18.04 | 1.01 | 14.20 | | 0.74 | 96.27 |
| Cu1006 | 11 | 68 | 63.53 | 18.09 | 1.01 | 14.46 | | | 97.08 |
| Cu1006 | 11 | 69 | 53.68 | 15.55 | 0.85 | 12.95 | | | 83.03 |
| Cu1006 | 11 | 70 | 63.40 | 18.44 | 1.19 | 14.60 | | 0.66 | 98.28 |
| Cu1006 | 11 | 71 | 64.52 | 18.86 | 2.21 | 12.73 | | 0.80 | 99.12 |
| Cu1006 | 11 | 72 | 63.15 | 18.54 | 2.30 | 13.12 | | 0.96 | 98.08 |
| Cu1006 | 11 | 73 | 63.11 | 18.67 | 2.09 | 13.06 | 0.11 | 0.86 | 97.89 |
| Cu1006 | 12 | 74 | 64.13 | 18.44 | 1.97 | 13.64 | | | 98.18 |
| Cu1006 | 12 | 76 | 64.47 | 18.57 | 0.77 | 14.48 | | 0.55 | 98.84 |
| Cu1006 | 12 | 78 | 64.01 | 18.38 | 0.55 | 15.16 | | | 98.10 |
| Cu1006 | 13 | 80 | 63.97 | 18.89 | 2.31 | 12.51 | | 1.03 | 98.70 |
| | | avg | 63.91 | 18.62 | 1.74 | 13.53 | | 0.84 | 98.42 |
| | | std | 0.53 | 0.18 | 0.70 | 0.90 | | 0.17 | 0.43 |

| Sample # | Grain | Point | SiO2 | Al2O3 | FeO | Na2O | K2O | Cl | BaO | Total |
|----------|-------|-------|-------|-------|------|-------------|--------------|------|------|-------|
| Cu1010 | 14 | 84 | 61.90 | 18.48 | | 1.34 | 13.86 | | 1.79 | 97.37 |
| Cu1010 | 14 | 85 | 63.01 | 18.71 | | 2.33 | 12.84 | | 1.65 | 98.53 |
| Cu1010 | 14 | 86 | 63.32 | 19.02 | | 2.22 | 12.74 | | 1.16 | 98.46 |
| Cu1010 | 14 | 88 | 63.55 | 18.65 | | 1.15 | 14.46 | | 0.81 | 98.62 |
| Cu1010 | 15 | 89 | 63.89 | 18.15 | | 1.70 | 14.29 | | | 98.03 |
| Cu1010 | 15 | 90 | 62.66 | 17.74 | | 0.75 | 14.73 | | | 95.88 |
| Cu1010 | 15 | 91 | 63.51 | 18.36 | 0.42 | 2.07 | 12.01 | 0.12 | 0.77 | 97.26 |
| Cu1010 | 15 | 92 | 64.34 | 18.59 | | 2.24 | 12.52 | | 1.11 | 98.80 |
| Cu1010 | 16 | 94 | 63.72 | 18.69 | | 1.40 | 13.84 | | 0.71 | 98.36 |
| Cu1010 | 16 | 95 | 62.65 | 18.14 | | 0.62 | 14.29 | | 0.66 | 96.37 |
| | | avg | 63.25 | 18.45 | | 1.58 | 13.56 | | 1.08 | 97.77 |
| | | std | 0.68 | 0.35 | | 0.60 | 0.90 | | 0.41 | 0.96 |

Biotite Microprobe Data for RT Dated Samples - January 15-16, 1997

| Sample # | Grain | Point | SiO2 | TiO2 | Al2O3 | FeO | MnO | MgO | Na2O | K2O | Cl | BaO | Total |
|----------|-------|-------|-------|------|-------|-------|------|-------|------|-------------|------|------|-------|
| Cu999 | 22 | 118 | 36.63 | 3.79 | 13.59 | 14.69 | 0.54 | 14.86 | | 8.81 | | 0.74 | 93.65 |
| Cu999 | 22 | 119 | 36.10 | 3.73 | 13.37 | 14.68 | 0.58 | 14.51 | 0.28 | 8.72 | | | 91.97 |
| Cu999 | 22 | 121 | 35.80 | 3.28 | 13.70 | 15.08 | 0.31 | 14.19 | | 8.52 | 0.09 | | 90.96 |
| Cu999 | 22 | 127 | 34.30 | 3.31 | 12.76 | 13.66 | 0.41 | 13.82 | | 8.26 | | | 86.51 |
| Cu999 | 22 | 128 | 31.98 | 2.98 | 12.03 | 11.19 | 0.41 | 13.35 | | 7.49 | | | 79.44 |
| | | avg | 34.96 | 3.42 | 13.09 | 13.86 | 0.45 | 14.15 | | 8.36 | | | 88.51 |
| | | std | 1.68 | 0.30 | 0.62 | 1.42 | 0.10 | 0.53 | | 0.47 | | | 5.11 |

| Sample # | Grain | Point | SiO2 | TiO2 | Al2O3 | FeO | MnO | MgO | Na2O | K2O | Cl | BaO | Total |
|----------|-------|-------|-------|------|-------|-------|------|-------|------|-------------|------|------|-------|
| Cu1001 | 24 | 131 | 37.15 | 3.53 | 14.15 | 14.78 | | 14.59 | 0.31 | 8.63 | 0.10 | | 93.23 |
| Cu1001 | 24 | 132 | 35.35 | 3.79 | 13.88 | 15.17 | 0.29 | 13.56 | | 8.69 | | 1.01 | 91.73 |
| Cu1001 | 24 | 135 | 33.72 | 2.89 | 13.12 | 11.99 | 0.27 | 13.38 | 0.25 | 7.70 | | | 83.33 |
| Cu1001 | 24 | 136 | 36.16 | 3.15 | 14.10 | 12.37 | | 14.33 | 0.28 | 8.20 | 0.12 | | 88.70 |
| Cu1001 | 24 | 137 | 37.40 | 3.86 | 14.30 | 15.09 | | 14.20 | | 8.81 | 0.09 | | 93.74 |
| Cu1001 | 25 | 138 | 36.72 | 3.91 | 14.08 | 14.50 | 0.27 | 14.36 | | 8.53 | | | 92.38 |
| Cu1001 | 25 | 140 | 33.47 | 2.82 | 12.56 | 11.13 | | 13.67 | | 7.98 | | | 81.63 |
| Cu1001 | 25 | 141 | 37.39 | 3.38 | 14.04 | 13.84 | 0.33 | 15.58 | 0.41 | 8.51 | | | 93.49 |
| Cu1001 | 25 | 143 | 37.47 | 3.56 | 14.20 | 14.43 | | 15.29 | 0.28 | 8.84 | | | 94.07 |
| Cu1001 | 25 | 144 | 34.82 | 2.78 | 13.74 | 10.83 | | 15.00 | | 7.58 | | | 84.76 |
| | | avg | 35.96 | 3.37 | 13.82 | 13.41 | 0.29 | 14.40 | 0.30 | 8.35 | 0.10 | | 89.70 |
| | | std | 1.46 | 0.41 | 0.53 | 1.59 | 0.02 | 0.70 | 0.06 | 0.43 | 0.01 | | 4.52 |

| Sample # | Grain | Point | SiO2 | TiO2 | Al2O3 | FeO | MnO | MgO | Na2O | K2O | Cl | Total |
|----------|-------|-------|-------|------|-------|-------|------|-------|------|-------------|------|-------|
| Cu1002 | 18 | 102 | 37.58 | 3.75 | 14.00 | 13.68 | | 15.80 | | 8.47 | | 93.27 |
| Cu1002 | 18 | 103 | 38.36 | 3.67 | 14.48 | 14.33 | | 16.03 | 0.39 | 8.50 | | 95.75 |
| Cu1002 | 18 | 104 | 35.63 | 3.23 | 13.34 | 13.30 | | 14.12 | | 7.90 | 0.12 | 87.63 |
| Cu1002 | 19 | 105 | 36.59 | 4.00 | 14.25 | 14.48 | 0.36 | 13.99 | | 8.32 | 0.10 | 92.09 |
| Cu1002 | 19 | 106 | 37.17 | 2.57 | 14.90 | 14.28 | 0.38 | 14.88 | | 8.06 | | 92.24 |
| Cu1002 | 19 | 109 | 37.94 | 3.11 | 15.58 | 14.20 | 0.31 | 14.85 | 0.29 | 8.68 | | 94.96 |
| | | avg | 37.21 | 3.39 | 14.43 | 14.04 | 0.35 | 14.95 | 0.34 | 8.32 | 0.11 | 93.13 |
| | | std | 0.90 | 0.47 | 0.70 | 0.42 | 0.03 | 0.77 | 0.05 | 0.27 | 0.01 | 3.62 |

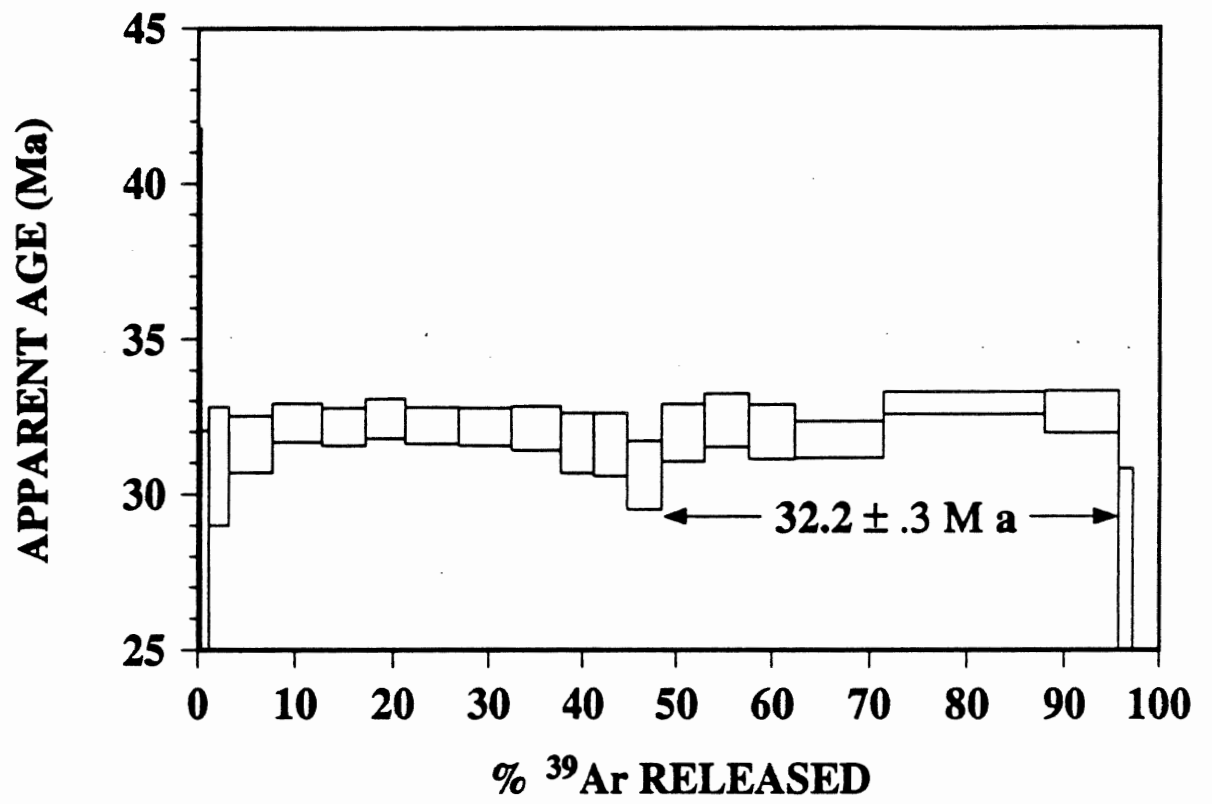
Sericite Microprobe Data for RT Dated Samples - January 15-16, 1997

| Sample # | Grain | Point | SiO2 | TiO2 | Al2O3 | FeO | MgO | Na2O | K2O | Cl | Total |
|----------|-------|-------|-------|------|-------|------|------|------|-------------|------|-------|
| Cu1011SK | 17 | 98 | 45.46 | | 35.48 | 1.03 | 0.46 | 0.36 | 9.24 | | 92.02 |
| Cu1011SK | 17 | 99 | 45.73 | | 35.51 | 0.81 | 0.62 | 0.41 | 9.04 | | 92.12 |
| Cu1011SK | 17 | 100 | 45.14 | 0.34 | 35.10 | 1.04 | 0.54 | 0.40 | 8.82 | | 91.38 |
| Cu1011SK | 17 | 101 | 45.55 | 0.32 | 33.79 | 2.08 | 0.78 | 0.41 | 8.48 | 0.43 | 91.85 |
| | | avg | 45.47 | 0.33 | 34.97 | 1.24 | 0.60 | 0.39 | 8.89 | | 91.84 |
| | | std | 0.21 | 0.01 | 0.70 | 0.49 | 0.12 | 0.02 | 0.28 | | 0.28 |

| Sample # | Grain | Point | SiO2 | TiO2 | Al2O3 | FeO | MgO | Na2O | K2O | Total |
|----------|-------|-------|-------|------|-------|------|------|------|-------------|-------|
| Cu1011SR | 20 | 111 | 45.10 | | 34.45 | 0.94 | 0.83 | 0.26 | 8.27 | 89.85 |
| Cu1011SR | 20 | 112 | 46.02 | | 34.99 | 1.21 | 0.88 | 0.47 | 9.36 | 92.93 |
| Cu1011SR | 20 | 114 | 45.89 | | 34.56 | 1.31 | 1.01 | 0.37 | 9.40 | 92.54 |
| Cu1011SR | 21 | 115 | 48.34 | 0.33 | 32.69 | 0.60 | 1.78 | | 8.02 | 91.75 |
| Cu1011SR | 21 | 116 | 47.77 | | 32.66 | 0.68 | 1.66 | 0.32 | 7.86 | 90.96 |
| | | avg | 46.63 | | 33.87 | 0.95 | 1.23 | 0.36 | 8.58 | 91.61 |
| | | std | 1.22 | | 0.99 | 0.28 | 0.41 | 0.08 | 0.67 | 1.11 |

Appendix D.

Argon Plateaus and Datasheets

CU-999K1 K-FELDSPAR

CU-999K1 K-FELDSPAR SUMMARY

D3

| oC | mV 39 | % 39 | AGE (Ma) | % ATM 37/39 | 36/40 | 39/40 | % IIC |
|------|-------|------|-----------------|-------------|---------|---------|-------|
| 500 | 1.1 | 0 | -48.7 +/- -98.9 | 103 .12 | .003497 | .002742 | .07 |
| 550 | 3.4 | .2 | 22.1 +/- 19.6 | 91.2 .48 | .003105 | .017188 | .7 |
| 600 | 12.4 | .8 | 27.4 +/- 4.6 | 67.2 .24 | .002286 | .051508 | .28 |
| 650 | 30 | 2 | 30.9 +/- 1.8 | 42.8 .31 | .001455 | .079281 | .33 |
| 700 | 65.9 | 4.4 | 31.5 +/- .9 | 26.2 .2 | .000889 | .099818 | .21 |
| 750 | 73.9 | 5 | 32.2 +/- .6 | 11.3 .13 | .000385 | .117365 | .14 |
| 775 | 66.4 | 4.5 | 32.1 +/- .6 | 9.1 .11 | .000311 | .120842 | .12 |
| 800 | 59 | 4 | 32.4 +/- .6 | 9 .1 | .000308 | .120067 | .11 |
| 850 | 82.1 | 5.5 | 32.1 +/- .5 | 10.7 .08 | .000364 | .118486 | .08 |
| 900 | 82 | 5.5 | 32.1 +/- .6 | 13.2 .06 | .00045 | .115249 | .06 |
| 950 | 77.2 | 5.2 | 32.1 +/- .7 | 15.7 .05 | .000534 | .112137 | .05 |
| 975 | 52.1 | 3.5 | 31.6 +/- .9 | 20 .06 | .000681 | .108158 | .07 |
| 1000 | 51.6 | 3.5 | 31.5 +/- 1 | 23.9 .06 | .000811 | .103087 | .07 |
| 1025 | 55.1 | 3.7 | 30.6 +/- 1 | 27.5 .05 | .000935 | .101285 | .06 |
| 1050 | 65.1 | 4.4 | 31.9 +/- .9 | 25.6 .06 | .000871 | .099339 | .06 |
| 1075 | 69.3 | 4.7 | 32.3 +/- .8 | 24.7 .06 | .000838 | .099372 | .06 |
| 1100 | 69.3 | 4.7 | 31.9 +/- .8 | 26.5 .07 | .000899 | .098151 | .07 |
| 1150 | 134.6 | 9.1 | 31.7 +/- .5 | 26.9 .07 | .000914 | .098115 | .07 |
| 1200 | 242 | 16.4 | 32.9 +/- .3 | 17.3 .05 | .000587 | .107007 | .05 |
| 1250 | 114.5 | 7.7 | 32.6 +/- .6 | 27.9 .14 | .000945 | .094202 | .15 |
| 1300 | 22.8 | 1.5 | 27.5 +/- 3.3 | 73.9 .39 | .002506 | .040621 | .47 |
| 1350 | 13.3 | .9 | 17.3 +/- 6.8 | 92.2 .5 | .003128 | .019067 | .94 |
| 1450 | 27 | 1.8 | 17.8 +/- 5.7 | 94 .23 | .003185 | .014238 | .43 |

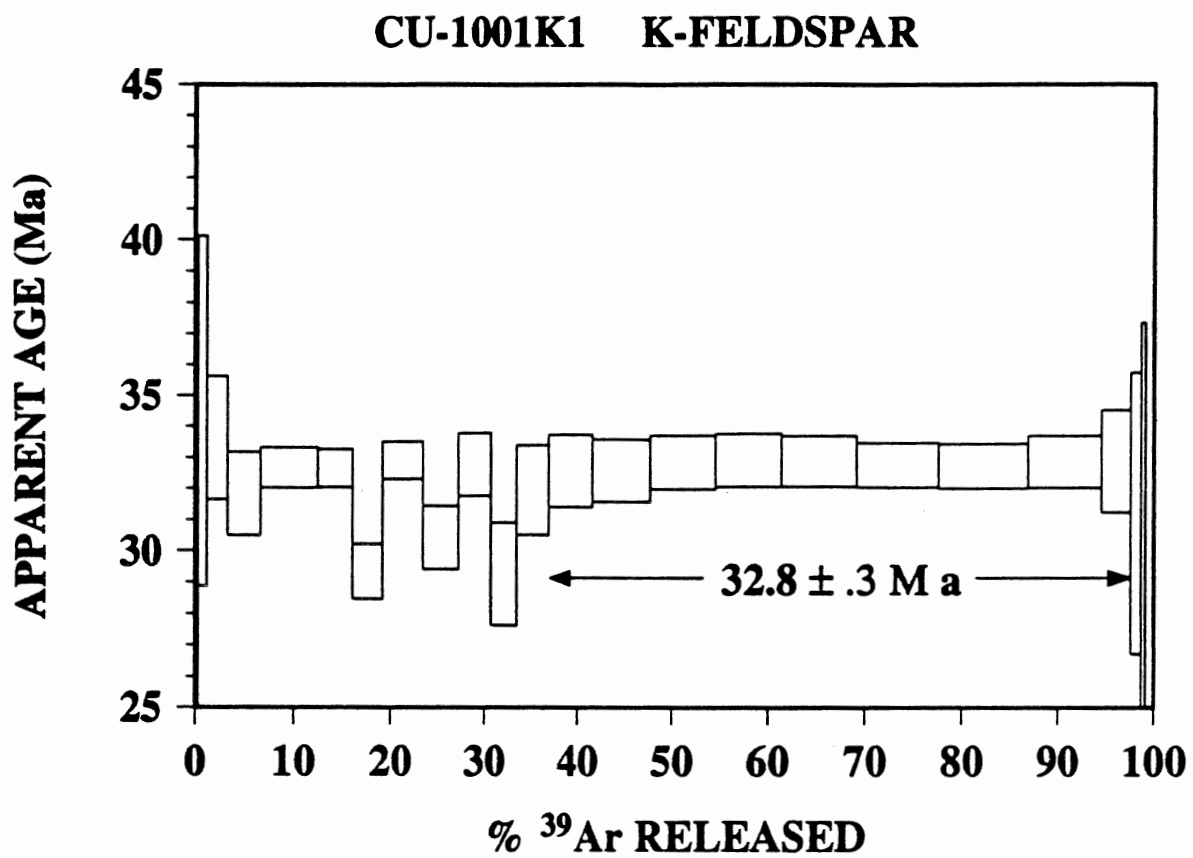
TOTAL GAS AGE = 31.5 Ma

J = .00232

ERROR ESTIMATES AT ONE SIGMA LEVEL

37/39, 36/40 AND 39/40 Ar RATIOS ARE CORRECTED FOR INTERFERING ISOTOPES

% IIC - INTERFERING ISOTOPES CORRECTION



CU-1001K1 K-FELDSPAR SUMMARY

D5

| OC | mV 39 | ‡ 39 | AGE (Ma) | ‡ ATM 37/39 | 36/40 | 39/40 | ‡ IIC |
|------|-------|------|---------------|-------------|---------|---------|-------|
| 550 | 3.9 | .3 | 12.8 +/- 21 | 93.1 .78 | .003188 | .023195 | 1.97 |
| 600 | 11.4 | .9 | 34.5 +/- 5.6 | 52 .13 | .001777 | .060331 | .13 |
| 650 | 25.8 | 2 | 33.6 +/- 1.9 | 23.3 .06 | .000795 | .098401 | .06 |
| 700 | 42.4 | 3.3 | 31.8 +/- 1.3 | 20.9 .04 | .000712 | .106741 | .04 |
| 750 | 72.9 | 5.8 | 32.6 +/- .6 | 7.3 .02 | .000251 | .121431 | .02 |
| 775 | 45.4 | 3.6 | 32.6 +/- .6 | .4 .02 | .000017 | .131056 | .03 |
| 800 | 38.7 | 3 | 29.3 +/- .8 | 7.8 .02 | .000269 | .135552 | .02 |
| 850 | 53.1 | 4.2 | 32.9 +/- .6 | 2.6 0 | .000088 | .12713 | 0 |
| 900 | 47.4 | 3.7 | 30.4 +/- 1 | 13 .02 | .000444 | .122891 | .02 |
| 950 | 43.2 | 3.4 | 32.7 +/- 1 | 10.8 .02 | .000368 | .117019 | .02 |
| 975 | 35.4 | 2.8 | 29.2 +/- 1.6 | 25.8 .02 | .000881 | .112075 | .02 |
| 1000 | 42.8 | 3.4 | 31.9 +/- 1.4 | 21.5 0 | .000732 | .105523 | 0 |
| 1025 | 59 | 4.7 | 32.5 +/- 1.1 | 21.6 .02 | .000735 | .10309 | .02 |
| 1050 | 76.7 | 6.1 | 32.5 +/- .9 | 20.6 .02 | .000702 | .104158 | .02 |
| 1075 | 85.6 | 6.8 | 32.8 +/- .8 | 18.2 .01 | .00062 | .106397 | .01 |
| 1100 | 85.6 | 6.8 | 32.9 +/- .8 | 16.8 .02 | .00057 | .108117 | .02 |
| 1125 | 97 | 7.7 | 32.8 +/- .8 | 16.7 .01 | .000569 | .108186 | .01 |
| 1150 | 106.3 | 8.4 | 32.7 +/- .7 | 16.6 .01 | .000563 | .108766 | .01 |
| 1175 | 116.4 | 9.2 | 32.7 +/- .7 | 17.9 .01 | .000609 | .107087 | .01 |
| 1200 | 96.1 | 7.6 | 32.8 +/- .8 | 18.3 .01 | .000622 | .106231 | .01 |
| 1225 | 38.7 | 3 | 32.8 +/- 1.6 | 25 .01 | .000852 | .097952 | .01 |
| 1250 | 13.5 | 1 | 31.2 +/- 4.5 | 50.2 .1 | .001717 | .06913 | .11 |
| 1350 | 5.6 | .4 | 18.2 +/- 19.1 | 93.1 .34 | .003168 | .016271 | .6 |
| 1450 | 10.4 | .8 | 8.8 +/- 14.7 | 98 0 | .003323 | .009447 | 0 |

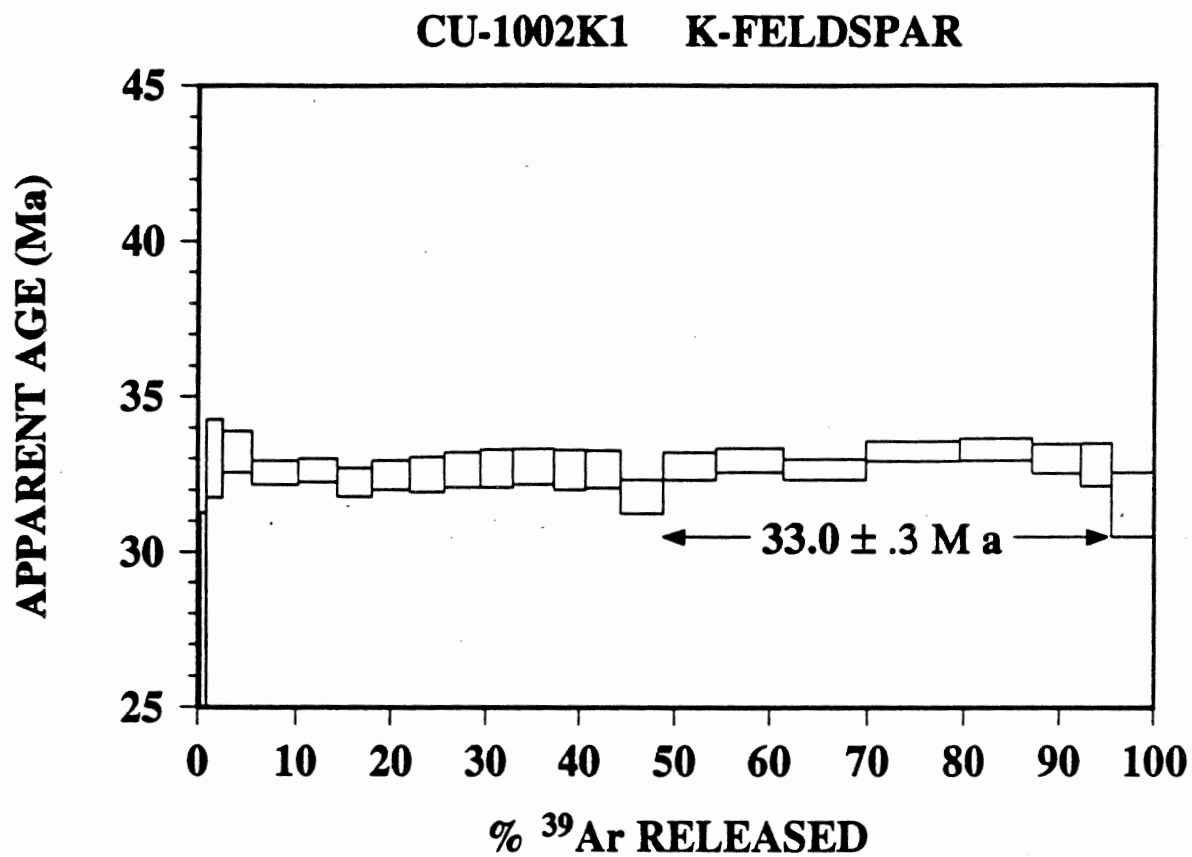
TOTAL GAS AGE = 32.1 Ma

J = .00232

ERROR ESTIMATES AT ONE SIGMA LEVEL

37/39,36/40 AND 39/40 Ar RATIOS ARE CORRECTED FOR INTERFERING ISOTOPES

‡ IIC - INTERFERING ISOTOPES CORRECTION



CU-1002K1 K-FELDSPAR SUMMARY

D7

| oC | mV 39 | % 39 | AGE (Ma) | % ATM 37/39 | 36/40 | 39/40 | % IIC |
|------|-------|------|--------------|-------------|---------|---------|-------|
| 550 | 8.2 | .3 | 9 +/- 8.7 | 94.6 .69 | .003217 | .025325 | 2.46 |
| 600 | 16.8 | .6 | 28 +/- 3.2 | 56.2 .18 | .001912 | .067314 | .21 |
| 650 | 42.9 | 1.5 | 32.9 +/- 1.2 | 27.4 .12 | .000931 | .094122 | .12 |
| 700 | 79.9 | 2.9 | 33.2 +/- .6 | 12.5 .08 | .000426 | .112414 | .08 |
| 750 | 129.3 | 4.7 | 32.5 +/- .3 | 6.8 .02 | .000232 | .122152 | .02 |
| 775 | 111.6 | 4.1 | 32.6 +/- .3 | 5.2 .01 | .000178 | .123949 | .01 |
| 800 | 99.9 | 3.6 | 32.2 +/- .4 | 7.9 .01 | .00027 | .121864 | .01 |
| 850 | 105.8 | 3.9 | 32.4 +/- .4 | 8.8 .01 | .000299 | .119819 | .01 |
| 900 | 97.4 | 3.5 | 32.4 +/- .5 | 11.1 0 | .000378 | .116748 | 0 |
| 950 | 104.3 | 3.8 | 32.6 +/- .5 | 14.8 .01 | .000503 | .111351 | .01 |
| 975 | 95.7 | 3.5 | 32.6 +/- .6 | 15.1 .01 | .000515 | .110739 | .01 |
| 1000 | 118 | 4.3 | 32.7 +/- .5 | 17.2 .01 | .000584 | .107799 | .01 |
| 1025 | 92 | 3.3 | 32.6 +/- .6 | 16.7 .01 | .000566 | .108927 | .01 |
| 1050 | 99.2 | 3.6 | 32.6 +/- .6 | 16 .02 | .000545 | .109674 | .02 |
| 1075 | 122.1 | 4.5 | 31.7 +/- .5 | 16.3 .01 | .000552 | .11236 | .01 |
| 1100 | 148.4 | 5.4 | 32.7 +/- .4 | 12.8 .01 | .000433 | .113495 | .01 |
| 1125 | 190.8 | 7 | 32.9 +/- .3 | 11.7 .01 | .000399 | .114118 | .01 |
| 1150 | 229.7 | 8.4 | 32.6 +/- .3 | 12 .01 | .000408 | .114831 | .01 |
| 1175 | 262.4 | 9.6 | 33.2 +/- .3 | 10.3 .01 | .00035 | .11491 | .01 |
| 1200 | 205 | 7.5 | 33.3 +/- .3 | 11.4 .01 | .000389 | .113301 | .01 |
| 1225 | 139.2 | 5.1 | 33 +/- .4 | 14.2 .01 | .000483 | .110782 | .01 |
| 1250 | 89.2 | 3.2 | 32.8 +/- .6 | 20.9 .01 | .00071 | .102854 | .01 |
| 1450 | 122.1 | 4.5 | 31.5 +/- 1 | 57.6 .01 | .001953 | .057239 | .01 |

TOTAL GAS AGE = 32.6 Ma

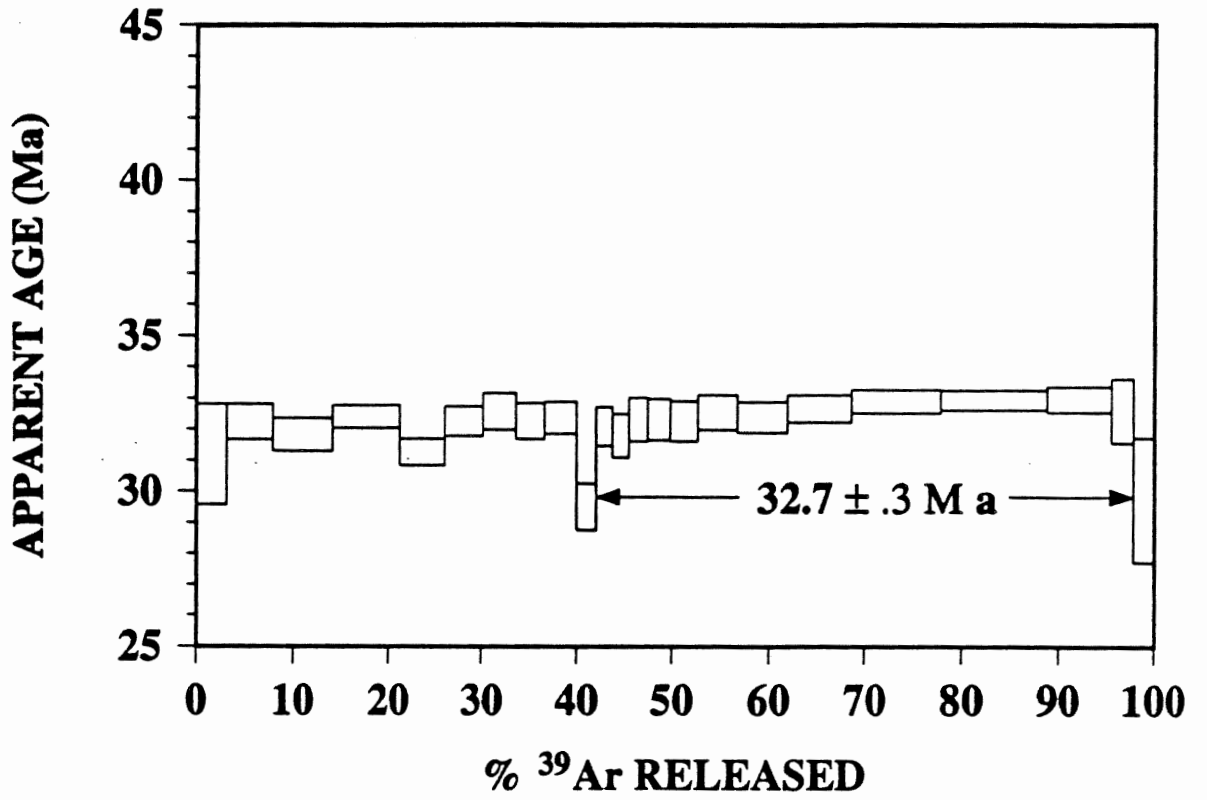
J = .00232

ERROR ESTIMATES AT ONE SIGMA LEVEL

37/39,36/40 AND 39/40 Ar RATIOS ARE CORRECTED FOR INTERFERING ISOTOPES

% IIC - INTERFERING ISOTOPES CORRECTION

CU-1006K1 K-FELDSPAR



CU-1006K1 K-FELDSPAR SUMMARY

D9

| OC | mV 39 | ‡ 39 | AGE (Ma) | ‡ ATM 37/39 | 36/40 | 39/40 | ‡ IIC |
|------|-------|------|--------------|-------------|---------|---------|-------|
| 600 | 95.3 | 3.1 | 31.1 +/- 1.6 | 71.9 .08 | .002434 | .038416 | .09 |
| 650 | 145.2 | 4.7 | 32.2 +/- .5 | 30.8 .02 | .001044 | .091473 | .02 |
| 700 | 191.9 | 6.2 | 31.8 +/- .5 | 21.3 .01 | .000722 | .105352 | .01 |
| 750 | 212.1 | 6.9 | 32.4 +/- .3 | 14.5 .01 | .000491 | .112455 | .01 |
| 775 | 148.6 | 4.8 | 31.2 +/- .4 | 12.4 .01 | .00042 | .11957 | .01 |
| 800 | 125.2 | 4.1 | 32.2 +/- .4 | 13.8 .01 | .000468 | .113984 | .01 |
| 850 | 106.2 | 3.4 | 32.5 +/- .5 | 14.2 .01 | .000483 | .112338 | .01 |
| 900 | 92.6 | 3 | 32.2 +/- .5 | 13.3 .01 | .00045 | .114719 | .01 |
| 950 | 102.3 | 3.3 | 32.3 +/- .5 | 11.4 0 | .000388 | .116758 | 0 |
| 975 | 59.8 | 1.9 | 29.4 +/- .7 | 15.6 .01 | .000531 | .122367 | .01 |
| 1000 | 50.8 | 1.6 | 32 +/- .6 | 7.7 .02 | .000264 | .123042 | .02 |
| 1025 | 53.7 | 1.7 | 31.7 +/- .6 | 10.4 .01 | .000353 | .120623 | .01 |
| 1050 | 60.6 | 1.9 | 32.3 +/- .7 | 11.2 0 | .000379 | .117509 | 0 |
| 1075 | 72.7 | 2.3 | 32.3 +/- .6 | 14.3 .01 | .000485 | .113338 | .01 |
| 1100 | 86.9 | 2.8 | 32.2 +/- .6 | 17.3 .01 | .000586 | .109482 | .01 |
| 1125 | 124.9 | 4.1 | 32.5 +/- .5 | 19.3 0 | .000655 | .105696 | 0 |
| 1150 | 158.3 | 5.1 | 32.3 +/- .4 | 23.3 0 | .000791 | .100858 | 0 |
| 1175 | 202.8 | 6.6 | 32.6 +/- .4 | 24.2 0 | .000822 | .098792 | 0 |
| 1200 | 282.3 | 9.2 | 32.8 +/- .3 | 22 0 | .000746 | .100943 | 0 |
| 1225 | 334.5 | 10.9 | 32.9 +/- .3 | 18.2 0 | .000619 | .105675 | 0 |
| 1250 | 207.8 | 6.8 | 32.9 +/- .4 | 20.7 0 | .000702 | .102484 | 0 |
| 1300 | 68.8 | 2.2 | 32.5 +/- 1 | 38.8 0 | .001316 | .080114 | 0 |
| 1450 | 63.2 | 2 | 29.7 +/- 1.9 | 74.8 0 | .002534 | .036099 | 0 |

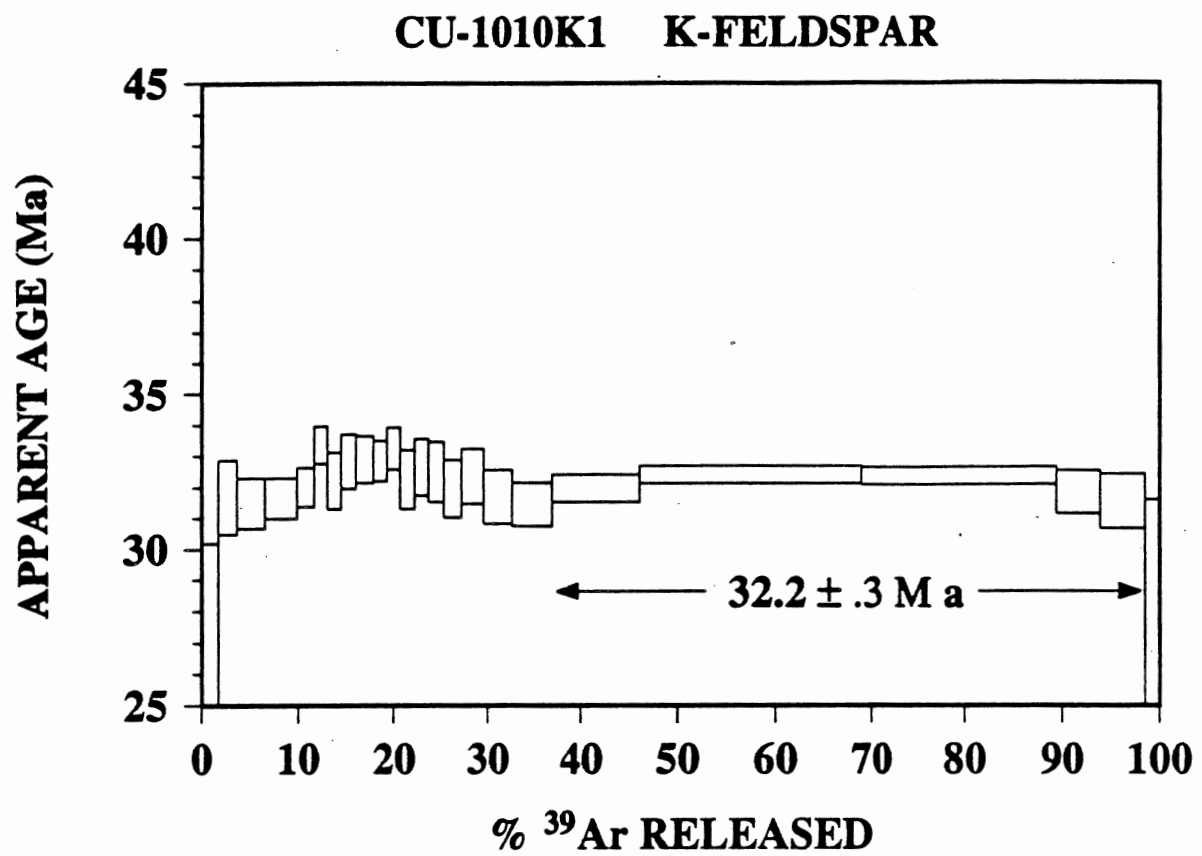
TOTAL GAS AGE = 32.2 Ma

J = .00232

ERROR ESTIMATES AT ONE SIGMA LEVEL

37/39, 36/40 AND 39/40 Ar RATIOS ARE CORRECTED FOR INTERFERING ISOTOPES

‡ IIC - INTERFERING ISOTOPES CORRECTION



CU-1010K1 K-FELDSPAR SUMMARY

D11

| oC | mV 39 | ‡ 39 | AGE (Ma) | ‡ ATM 37/39 | 36/40 | 39/40 | ‡ IIC |
|------|-------|------|--------------|-------------|---------|---------|-------|
| 600 | 44.2 | 1.7 | 26.5 +/- 3.6 | 87.3 0 | .002958 | .020284 | 0 |
| 650 | 47.1 | 1.8 | 31.6 +/- 1.1 | 30.4 0 | .001032 | .093902 | 0 |
| 700 | 71.8 | 2.8 | 31.4 +/- .8 | 22.7 .01 | .000772 | .104804 | .01 |
| 750 | 81.8 | 3.2 | 31.6 +/- .6 | 16 .01 | .000542 | .113406 | .01 |
| 775 | 45.7 | 1.8 | 32 +/- .6 | 6.7 0 | .00023 | .124742 | 0 |
| 800 | 33 | 1.3 | 33.3 +/- .5 | 3.4 0 | .000117 | .124189 | 0 |
| 850 | 36.4 | 1.4 | 32.2 +/- .9 | 11.6 0 | .000397 | .11754 | 0 |
| 900 | 38.4 | 1.5 | 32.8 +/- .8 | 10.9 0 | .000371 | .116258 | 0 |
| 950 | 45.6 | 1.8 | 32.8 +/- .7 | 9.1 0 | .00031 | .118235 | 0 |
| 975 | 36.7 | 1.4 | 32.8 +/- .6 | 5.8 .01 | .000198 | .122883 | .01 |
| 1000 | 33.4 | 1.3 | 33.2 +/- .6 | 4.8 0 | .000165 | .122773 | 0 |
| 1025 | 37.7 | 1.5 | 32.2 +/- .9 | 13.3 0 | .000453 | .115131 | 0 |
| 1050 | 35 | 1.4 | 32.6 +/- .8 | 10.9 0 | .000373 | .116921 | 0 |
| 1075 | 40.4 | 1.6 | 32.5 +/- .9 | 13.4 0 | .000455 | .114086 | 0 |
| 1100 | 48 | 1.9 | 31.9 +/- .9 | 16.6 0 | .000565 | .111602 | 0 |
| 1125 | 59.7 | 2.4 | 32.3 +/- .8 | 19.7 0 | .000668 | .106091 | 0 |
| 1150 | 75.4 | 3 | 31.6 +/- .8 | 25.4 0 | .000862 | .100497 | 0 |
| 1175 | 107.8 | 4.3 | 31.4 +/- .6 | 30.8 0 | .001043 | .093876 | 0 |
| 1200 | 226.6 | 9.1 | 31.9 +/- .4 | 29.3 0 | .000992 | .09423 | 0 |
| 1225 | 568.2 | 22.8 | 32.4 +/- .2 | 21.3 0 | .000721 | .103457 | 0 |
| 1250 | 510 | 20.5 | 32.3 +/- .2 | 19.1 0 | .000647 | .106421 | 0 |
| 1350 | 113.2 | 4.5 | 31.8 +/- .6 | 32.8 .01 | .001111 | .090004 | .01 |
| 1450 | 114.4 | 4.6 | 31.5 +/- .8 | 51.3 .01 | .001738 | .065745 | .01 |
| 1500 | 35.4 | 1.4 | 28.1 +/- 3.4 | 84.1 0 | .002849 | .024078 | 0 |

TOTAL GAS AGE = 32 Ma

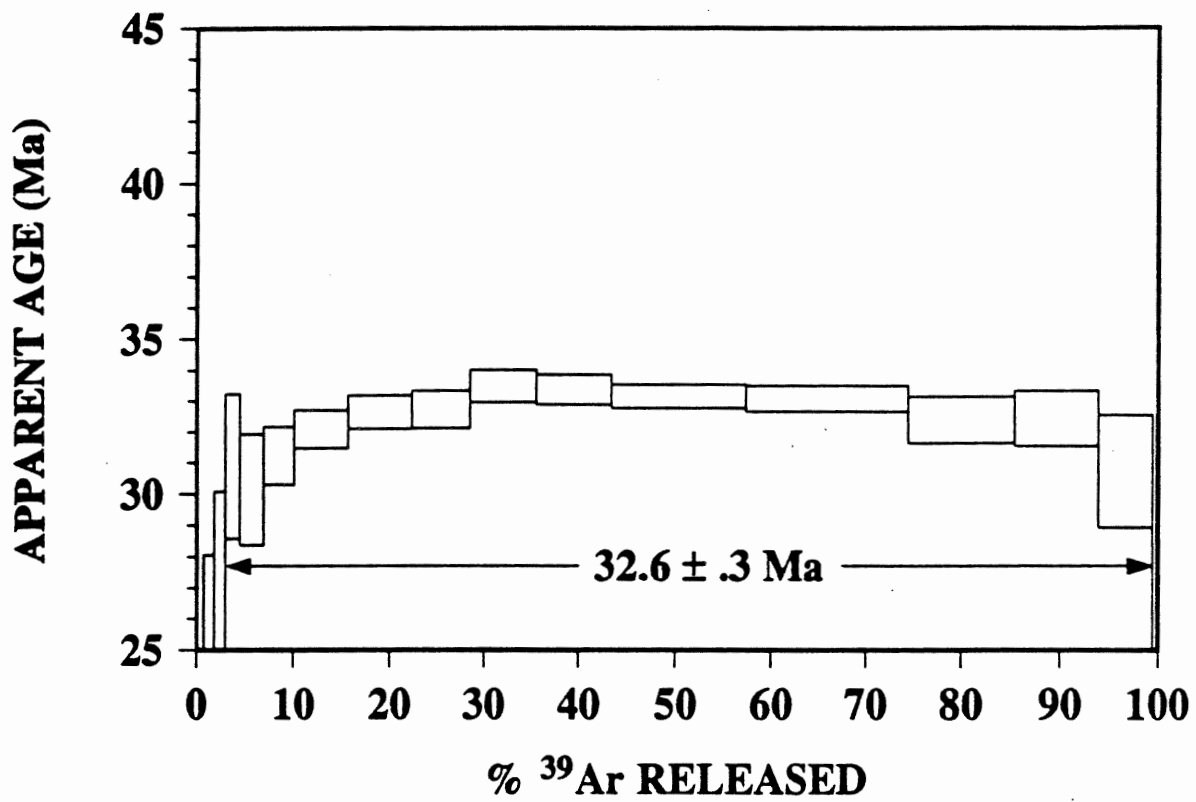
J = .00232

ERROR ESTIMATES AT ONE SIGMA LEVEL

37/39,36/40 AND 39/40 Ar RATIOS ARE CORRECTED FOR INTERFERING ISOTOPES

‡ IIC - INTERFERING ISOTOPES CORRECTION

CU-999 Bi1 BIOTITE



CU-999Bil BIOTITE SUMMARY

D13

| oC | mV 39 | ‡ 39 | AGE (Ma) | ‡ ATM 37/39 | 36/40 | 39/40 | ‡ IIC |
|------|-------|------|-----------------|-------------|---------|---------|-------|
| 600 | 10.4 | .7 | 3.7 +/- 7.1 | 92.7 .06 | .003211 | .088333 | .58 |
| 650 | 14.4 | 1 | 23.6 +/- 4.4 | 52.2 .03 | .001797 | .089526 | .05 |
| 675 | 15.6 | 1.1 | 26.5 +/- 3.5 | 37.4 -.03 | .00129 | .104467 | .02 |
| 700 | 20.2 | 1.4 | 30.9 +/- 2.3 | 22 0 | .000756 | .110903 | 0 |
| 725 | 33.1 | 2.4 | 30.1 +/- 1.7 | 21.2 0 | .000725 | .113553 | .01 |
| 750 | 42.8 | 3.1 | 31.2 +/- .9 | 4.3 0 | .000148 | .132824 | 0 |
| 800 | 76.9 | 5.6 | 32.1 +/- .6 | 3.6 0 | .000124 | .129054 | 0 |
| 850 | 89.7 | 6.6 | 32.6 +/- .5 | 2.6 0 | .000089 | .128019 | 0 |
| 900 | 83.2 | 6.1 | 32.7 +/- .6 | 4.2 0 | .000144 | .125594 | 0 |
| 950 | 97 | 7.1 | 33.4 +/- .5 | 3 .01 | .000104 | .124089 | .01 |
| 975 | 106.2 | 7.8 | 33.3 +/- .4 | 2.8 0 | .000095 | .124764 | 0 |
| 1000 | 189.2 | 13.9 | 33.1 +/- .3 | 3.6 0 | .000122 | .124175 | 0 |
| 1025 | 231.1 | 17 | 33 +/- .4 | 7.4 .01 | .000254 | .119389 | .01 |
| 1050 | 148.3 | 10.9 | 32.4 +/- .7 | 19.2 .02 | .000651 | .106609 | .02 |
| 1100 | 116.4 | 8.5 | 32.4 +/- .8 | 21.4 .03 | .000727 | .103647 | .03 |
| 1200 | 74.8 | 5.5 | 30.7 +/- 1.8 | 54.9 .24 | .001864 | .0627 | .26 |
| 1450 | 7.5 | .5 | -82.1 +/- -63.9 | 102.7 1 | .00348 | .001497 | .32 |

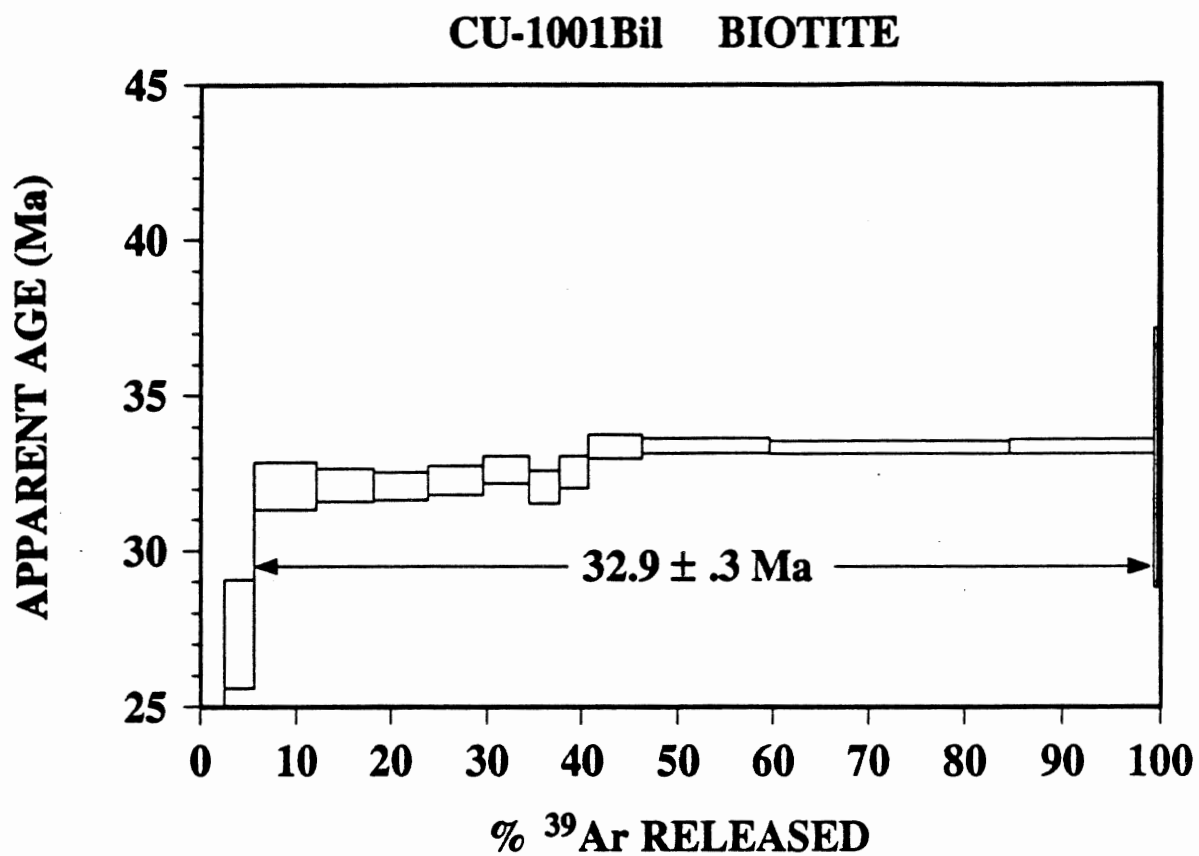
TOTAL GAS AGE = 31.6 Ma

J = .00232

ERROR ESTIMATES AT ONE SIGMA LEVEL

37/39,36/40 AND 39/40 Ar RATIOS ARE CORRECTED FOR INTERFERING ISOTOPES

‡ IIC - INTERFERING ISOTOPES CORRECTION



1001Bil BIOTITE SUMMARY

D15

| oC | mV 39 | % 39 | AGE (Ma) | % ATM 37/39 | 36/40 | 39/40 | % IIC | |
|------|-------|------|----------------|-------------|-------|---------|---------|---------|
| 600 | 15.7 | 1 | -61.9 +/- 6.3 | 295.5 | 18.79 | .009883 | .13225 | 8.48 |
| 650 | 20 | 1.3 | -.3 +/- 4.1 | 100.4 | 7.89 | .003392 | .078923 | 1005.29 |
| 700 | 44.5 | 3 | 27.3 +/- 1.7 | 47.4 | 1.93 | .0016 | .079842 | 2.33 |
| 750 | 96.9 | 6.6 | 32 +/- .7 | 24 | .6 | .000811 | .098161 | .62 |
| 775 | 89.6 | 6.1 | 32.1 +/- .5 | 8.4 | .52 | .00029 | .118031 | .54 |
| 800 | 81.9 | 5.5 | 32 +/- .4 | 4.5 | .47 | .00016 | .123127 | .49 |
| 850 | 84.2 | 5.7 | 32.2 +/- .4 | 5.7 | .44 | .000197 | .121001 | .45 |
| 900 | 71.1 | 4.8 | 32.6 +/- .4 | 3.7 | .5 | .000135 | .122051 | .51 |
| 925 | 47.2 | 3.2 | 32 +/- .5 | 3.4 | .7 | .000129 | .124424 | .73 |
| 950 | 44.4 | 3 | 32.5 +/- .5 | 2.5 | .73 | .000101 | .123642 | .75 |
| 1000 | 80.6 | 5.5 | 33.3 +/- .3 | 3 | .37 | .000109 | .12024 | .37 |
| 1050 | 196.1 | 13.3 | 33.4 +/- .2 | 2.2 | .16 | .000077 | .121312 | .16 |
| 1100 | 366.1 | 25 | 33.3 +/- .2 | 1.5 | .09 | .000053 | .122481 | .09 |
| 1150 | 215.9 | 14.7 | 33.3 +/- .2 | 1.5 | .14 | .000054 | .122331 | .14 |
| 1250 | 6.2 | .4 | 33 +/- 4.1 | 30 | 5.22 | .001054 | .085686 | 5.26 |
| 1450 | 3.3 | .2 | 138.7 +/- 35.8 | 74.4 | 9.28 | .002506 | .007393 | 2.62 |

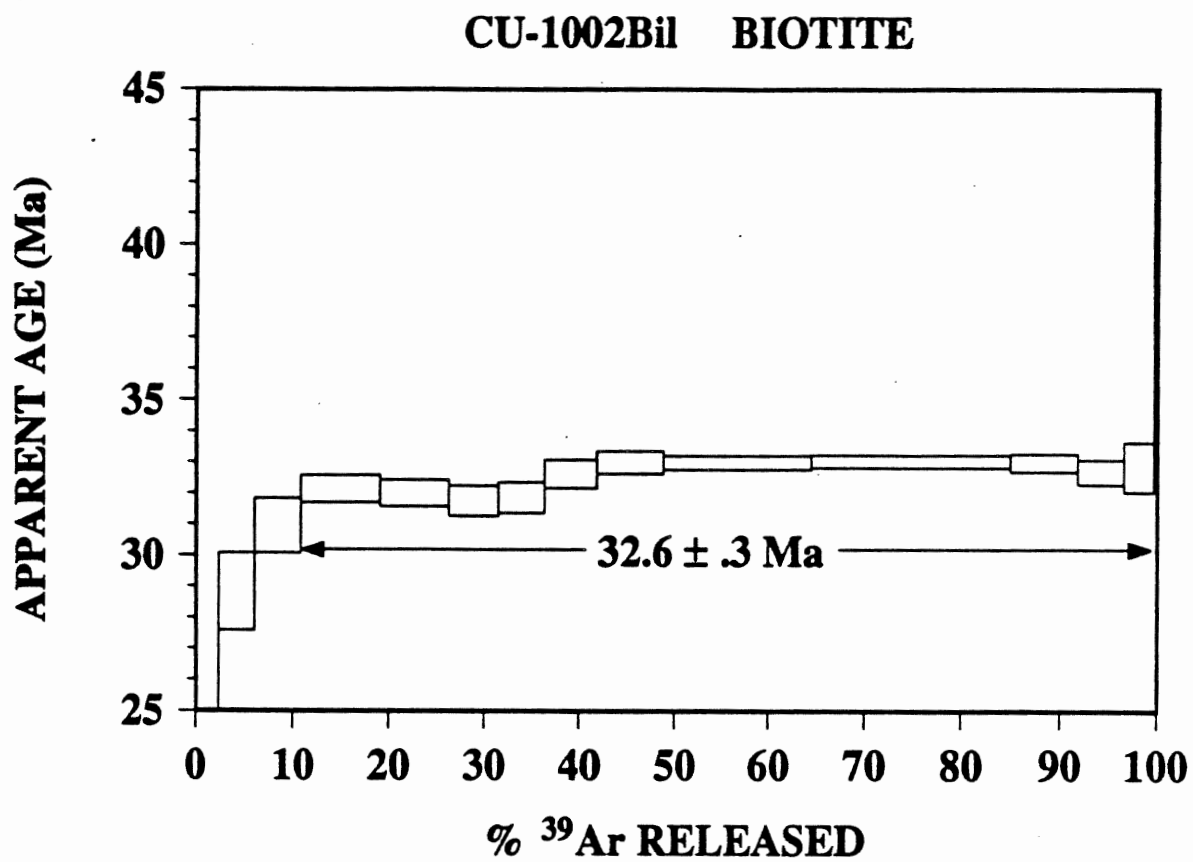
TOTAL GAS AGE = 31.5 Ma

J = .00232

ERROR ESTIMATES AT ONE SIGMA LEVEL

37/39,36/40 AND 39/40 Ar RATIOS ARE CORRECTED FOR INTERFERING ISOTOPES

% IIC - INTERFERING ISOTOPES CORRECTION



CU-1002B11 BIOTITE SUMMARY

D17

| oC | mV 39 | ‡ 39 | AGE (Ma) | ‡ ATM 37/39 | 36/40 | 39/40 | ‡ IIC | |
|------|-------|------|----------------|-------------|-------|---------|---------|-------|
| 600 | 12.6 | .9 | -62.3 +/- -6.6 | 218.8 | | | | |
| | | | | | 19.74 | .007377 | .08047 | 8.85 |
| 650 | 20.2 | 1.4 | 2.9 +/- 3.5 | 94.9 | 7.52 | .003222 | .07119 | 80.64 |
| 700 | 50.3 | 3.6 | 28.8 +/- 1.2 | 37.5 | 1.9 | .001276 | .089893 | 2.17 |
| 750 | 66.5 | 4.7 | 30.9 +/- .8 | 24.6 | 1.16 | .00084 | .100947 | 1.24 |
| 800 | 115.6 | 8.3 | 32.1 +/- .4 | 8.5 | .58 | .000295 | .118001 | .59 |
| 850 | 99 | 7.1 | 31.9 +/- .4 | 6.4 | .6 | .000227 | .121159 | .62 |
| 900 | 72.7 | 5.2 | 31.7 +/- .4 | 5.7 | .79 | .000208 | .122884 | .83 |
| 950 | 67.6 | 4.8 | 31.8 +/- .5 | 5.3 | .88 | .000198 | .122886 | .91 |
| 1000 | 76.4 | 5.5 | 32.6 +/- .4 | 4.9 | .72 | .000182 | .120545 | .73 |
| 1025 | 96 | 6.9 | 32.9 +/- .3 | 3 | .58 | .000116 | .1216 | .58 |
| 1050 | 219.1 | 15.7 | 32.9 +/- .2 | 1.7 | .25 | .000065 | .123433 | .25 |
| 1075 | 283.5 | 20.4 | 33 +/- .2 | 1.2 | .18 | .000047 | .123987 | .18 |
| 1100 | 95.9 | 6.9 | 32.9 +/- .2 | 1.1 | .45 | .00005 | .124135 | .45 |
| 1150 | 66.6 | 4.7 | 32.6 +/- .3 | 2.5 | .63 | .000102 | .123392 | .64 |
| 1250 | 42.1 | 3 | 32.8 +/- .8 | 9.6 | 1.44 | .000349 | .113642 | 1.46 |
| 1350 | 3.2 | .2 | 91 +/- 14.1 | 44.9 | 13.84 | .001552 | .024528 | 5.55 |
| 1450 | 1 | 0 | 207.3 +/- 83.9 | 74.7 | 45.72 | .002536 | .004863 | 9.51 |

TOTAL GAS AGE = 31.4 Ma

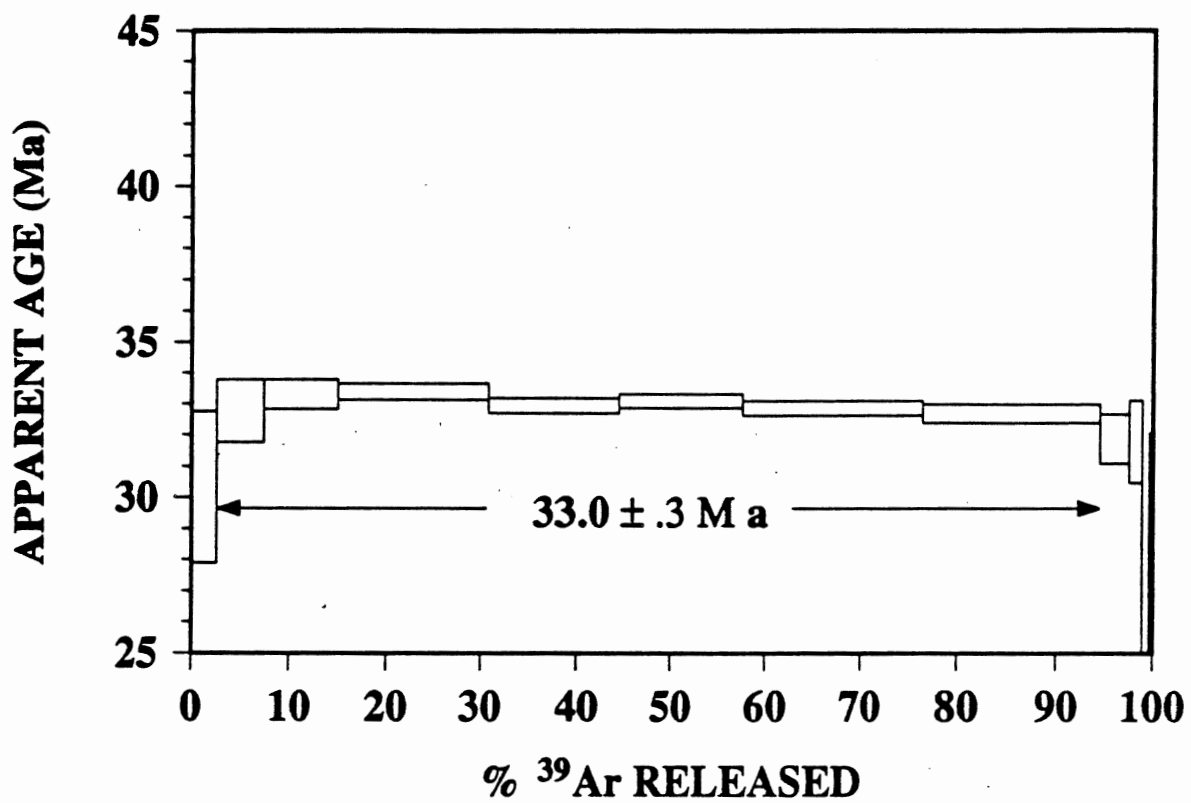
J = .00232

ERROR ESTIMATES AT ONE SIGMA LEVEL

37/39,36/40 AND 39/40 Ar RATIOS ARE CORRECTED FOR INTERFERING ISOTOPES

‡ IIC - INTERFERING ISOTOPES CORRECTION

CU-1011SK K-FELDSPAR



CU-1011^{SK} K-FELDSPAR SUMMARY

| oC | mV 39 | % 39 | AGE (Ma) | % ATM 37/39 | 36/40 | 39/40 | % IIC |
|------|-------|------|--------------|-------------|---------|---------|-------|
| 600 | 30.4 | 2.5 | 30.3 +/- 2.4 | 64.5 .08 | .002189 | .050049 | .09 |
| 659 | 57.4 | 4.8 | 32.7 +/- 1 | 25.1 .02 | .000854 | .09765 | .02 |
| 700 | 90.7 | 7.6 | 33.2 +/- .4 | 6.9 0 | .000236 | .119366 | 0 |
| 750 | 187.9 | 15.8 | 33.3 +/- .2 | 2.5 0 | .000087 | .124472 | 0 |
| 775 | 160.9 | 13.5 | 32.9 +/- .2 | 1.4 0 | .000047 | .127715 | 0 |
| 800 | 157.3 | 13.2 | 33 +/- .2 | .6 0 | .000021 | .128111 | 0 |
| 850 | 224.1 | 18.8 | 32.8 +/- .2 | 1.8 0 | .000062 | .12737 | 0 |
| 900 | 213.7 | 17.9 | 32.6 +/- .2 | 4.6 0 | .000156 | .124458 | 0 |
| 950 | 36 | 3 | 31.8 +/- .7 | 7.1 0 | .000244 | .125133 | 0 |
| 975 | 16.4 | 1.3 | 31.7 +/- 1.3 | 9.3 0 | .000318 | .123912 | 0 |
| 1000 | 8.4 | .7 | 14.2 +/- 4.1 | 61.2 .08 | .002112 | .120923 | .19 |
| 1025 | 3.9 | .3 | 29.5 +/- 2.5 | 10.7 0 | .000381 | .140982 | 0 |

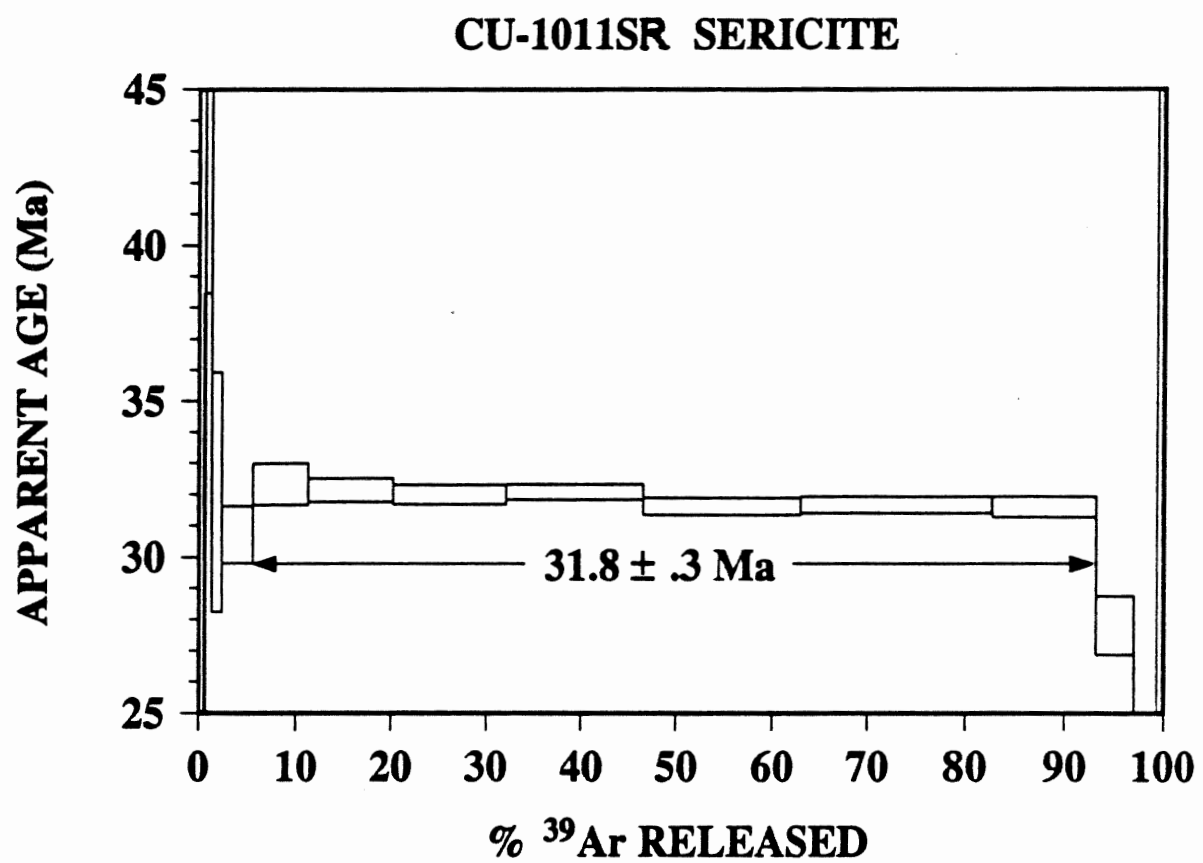
TOTAL GAS AGE = 32.7 Ma

J = .00232

ERROR ESTIMATES AT ONE SIGMA LEVEL

37/39, 36/40 AND 39/40 Ar RATIOS ARE CORRECTED FOR INTERFERING ISOTOPES

% IIC - INTERFERING ISOTOPES CORRECTION



SERICITE SUMMARY

| OC | mV 39 | ‡ 39 | AGE (Ma) | ‡ ATM 37/39 | 36/40 | 39/40 | ‡ IIC | |
|------|-------|------|----------------|-------------|---------|---------|---------|-------|
| 450 | 6.4 | .5 | -34 +/- -17.3 | 134.8 | | | | |
| | | | | 2.46 | .004602 | .045145 | 2.14 | |
| 500 | 1.7 | .1 | 26 +/- 12.3 | 39.1 | 11.44 | .001552 | .103071 | 14.43 |
| 550 | 6.7 | .6 | 44.2 +/- 5.7 | 24.7 | 2.66 | .000869 | .072675 | 2.04 |
| 600 | 11.5 | 1 | 32 +/- 3.8 | 33.2 | 1.34 | .001151 | .089851 | 1.39 |
| 650 | 35.8 | 3.1 | 30.7 +/- .9 | 6.9 | .59 | .000251 | .129736 | .64 |
| 700 | 64.7 | 5.7 | 32.3 +/- .6 | 7.1 | .3 | .000248 | .122687 | .31 |
| 750 | 100.9 | 8.9 | 32.1 +/- .3 | 2.5 | .19 | .000092 | .12937 | .2 |
| 800 | 133.4 | 11.8 | 31.9 +/- .3 | 1.8 | .15 | .000068 | .130772 | .16 |
| 850 | 161.9 | 14.3 | 32 +/- .2 | .4 | .13 | .00002 | .13231 | .14 |
| 900 | 186.2 | 16.5 | 31.6 +/- .2 | 2.3 | .12 | .000082 | .131707 | .12 |
| 950 | 221 | 19.6 | 31.6 +/- .2 | 2.6 | .1 | .00009 | .131149 | .11 |
| 1000 | 118.7 | 10.5 | 31.5 +/- .3 | 1.9 | .18 | .000069 | .132427 | .19 |
| 1050 | 42.7 | 3.7 | 27.8 +/- .9 | 10.5 | .52 | .000369 | .137836 | .61 |
| 1100 | 17.8 | 1.5 | 14.4 +/- 2.7 | 49 | 1.39 | .001696 | .153618 | 3.12 |
| 1200 | 8.1 | .7 | 3.4 +/- 8.7 | 93.7 | 3.61 | .00322 | .078848 | 33.02 |
| 1450 | 7.5 | .6 | 180.4 +/- 22.1 | 52.3 | 4.63 | .001776 | .01082 | 1.06 |

TOTAL GAS AGE = 31.9 Ma

J = .00232

ERROR ESTIMATES AT ONE SIGMA LEVEL

37/39, 36/40 AND 39/40 Ar RATIOS ARE CORRECTED FOR INTERFERING ISOTOPES

‡ IIC - INTERFERING ISOTOPES CORRECTION